



**UNIVERSITY OF MESSINA**  
**Department of Chemical, Biological, Pharmaceutical**  
**and Environmental Sciences**  
**Doctorate School in Chemical Sciences (XXX cycle)**  
**S.S.D. CHIM/08**

---

**Design, synthesis and biological  
evaluation of novel inhibitors of  
rhodesain, cysteine protease of  
*Trypanosoma brucei rhodesiense*, as  
antitrypanosomal agents**

**PhD student:**

**Santo PREVITI**

**Supervisor:**

**Prof. Silvana GRASSO**

**Co-Supervisor:**

**Prof. Roberta ETTARI**

**PhD Coordinator:**

**Prof. Sebastiano CAMPAGNA**

---

**2016/17 ACADEMIC YEAR**

# CONTENTS

<b>ACKNOWLEDGEMENTS.</b>	<b>.1</b>
<b>LIST OF USED ACRONYMS.</b>	<b>.2</b>
<b>1. AIM OF THE RESEARCH.</b>	<b>.5</b>
<b>2. HUMAN AFRICAN TRYPANOSOMIASIS.</b>	<b>.13</b>
2.1 Introduction.	.13
2.2 The parasites.	.13
2.3 HAT forms: symptoms and progression of the disease.	.15
2.4 Diagnostic methods.	.17
2.5 Pharmacological treatment.	.18
<b>3. CYSTEINE PROTEASES: ALTERNATIVE AND VALID TARGETS.</b>	<b>.25</b>
3.1 The ideal drug.	.25
3.2 Potential targets.	.26
3.3 Rhodesain: structure and functions.	.29
3.4 TbCatB: structure and functions.	.31
<b>4. RHODESAIN INHIBITORS.</b>	<b>.34</b>
4.1 Peptide-based inhibitors.	.34
4.1.1 Vinyl sulfones.	.35
4.1.2 Azadipeptide nitriles.	.38
4.1.3 Aziridine-2,3-dicarboxylates.	.40
4.1.4 Peptidyl aldehydes and ketones.	.41
4.2 Peptidomimetics.	.43
4.2.1 BDZ derivatives with aldehyde warhead.	.44
4.2.2 BDZ derivatives bearing vinyl ester portion as warhead.	.44
4.2.3 3-Bromo isoxazoline inhibitors.	.45
4.3 Non peptide inhibitors.	.47
4.3.1 Triazine nitriles.	.47
4.3.2 Purine nitriles.	.51
4.3.3 Thiosemicarbazones.	.53
4.3.4 Other non-peptide inhibitors.	.55
<b>5. RESULTS AND DISCUSSIONS.</b>	<b>.57</b>
5.1 Series A.	.57
5.2 Series B.	.62

5.3 Series C. . . . .	65
5.4 Series D. . . . .	68
5.5 Series E. . . . .	77
5.6 Series F. . . . .	80
<b>6. EXPERIMENTAL SECTION. . . . .</b>	<b>82</b>
6.1 Chemistry. . . . .	82
6.2 Biology. . . . .	146
6.3 Docking studies, molecular dynamics and computational chemistry. . . . .	150
<b>7. SUPPLEMENT. . . . .</b>	<b>153</b>
7.1 Introduction. . . . .	153
7.2 Aim of the research and results and discussions. . . . .	158
7.3 Experimental section. . . . .	163
<b>8. REFERENCES. . . . .</b>	<b>175</b>

## ACKNOWLEDGEMENTS

First of all, I want to thank my supervisor Prof. Silvana Grasso, for providing me her expertise, her suggestions and all that was necessary to carry out my research project. In addition, I would like thank her for giving me the opportunity to work in Paris for three months and for the participations to the European School Medicinal Chemistry.

I would like to thank my co-supervisor, Prof. Roberta Ettari, who has always been present during these three years and always available to give me her precious opinions and advices, both professional and non-professional. I thank her for conveying to me her professionalism, work ethic and love for research, elements that has helped me to grow up both scientifically and humanly.

I want to thank Prof. Maria Zappalà, which with her experience helped me in my professional growth, encouraging me to constantly do better.

I want to thank Prof. Sandrine Ongerì, Prof. Julia Kaffy, Jean-Louis Soulier, Nicolò, Faustine and Yao-Chun for the time spent in Paris, very important for my grow up professional.

I would like to thank Prof. Tanja Schirmeister (University of Mainz) and all her research group, for the biological assays against *Trypanosoma*, macrophages and HeLa cells.

I would like to thank Prof. Philip J. Rosenthal (University of California), for the biological evaluation of our molecules against falcipain-2 and *Plasmodium falciparum*.

I want to thank Dr. Sandro Cosconati (University of Campania Luigi Vanvitelli), for his important contribution by means docking and computational studies.

I want to thank Prof. Carlo De Micheli (University of Milan) and all his research group, for their contribution to obtain enantiomerically pure synthesis intermediates.

I want to thank Prof. Ettore Novellino and Prof. Luciana Marinelli (University of Naples) for the computational studies.

I would like to thank the PhDs Manuela and Milad and PhD student Santina for the time spent together in laboratories.

I want to thank my PhD colleague Fausta, always available to exchange information useful about PhD, deadlines, documents to be surrendered and reservations to use NMR instruments.

I want to thank all people who believed in me and supported me, during these three years with a message, a call, a walk in bicycle, a football match, a pizza together and in every way possible.

I would like to thank Melania, about everything that she has been for me over the last two years.

I would like to thank my sister Milena, for the continued affection and moral support, together with her boyfriend Domenico.

Lastly, I would like to thank my parents, who always supported me from the first to the last day. I owe them my good manners and without them I would not be the person I am today.

## LIST OF USED ACRONYMS

Ac: Acetyl

AFC: amino-4-trifluoromethylcoumarin

Ala (or A): alanine

Alloc : Allyloxycarbonyl

AMC: 7-amino-methyl-coumarin

Arg (or R): arginine

Asn (or N): Asparagine

Asp (or D): aspartic acid

BBB: Blood-Brain Barrier

BDZ: 1,4-benzodiazepine

Bn: Benzyl

Boc: tert-Butyloxycarbonyl

BSF: Bloodstream Form

CATT: Card Agglutination Test for Trypanosomiasis

Cbz (or Z): Carbobenzyloxy

ChT-L: chymotrypsin-like

C-L: caspase-like

CM: Cross-Methatesis

CNS: Central Nervous System

CSF: Cerebrospinal Fluid

Cys (or C): Cysteine

DAG: diacylglycerol

DBF: dibromoformaldoxime

DFMO: Difluoromethylornithine

DIPEA: N,N-Diisopropylethylamine

DNDi: Drug for Neglected Diseases initiative

EC<sub>50</sub>: Half maximal effective concentration

EDCI: 1-Ethyl-3-(3-dimethylaminopropyl)carbodiimide

EDG: Electron-Donating Group

EWG: Electron-Withdrawing Group

FABS: Fluorine Atoms for Biochemical Screening

FP-2: falcipain-2

FP-3: falcipan-3  
Gln (or Q): Glutamine  
Glu (or E): Glutamic Acid  
Gly (or G): glycine  
GPCRs: G<sub>q</sub> Protein Coupled Receptors  
GPI: glycosylphosphatidylinositol  
HAT: Human African Trypanosomiasis  
hCatB: human cathepsin B  
hCatL: human cathepsin L  
His (or H): Histidine  
HOBt: Hydroxybenzotriazole  
hPhe: Homophenylalanine  
IC<sub>50</sub>: half maximal inhibitory concentration  
IFN- $\gamma$ : interferon-gamma  
IP3: inositol-1,4,5-triphosphate  
K<sub>i</sub>: dissociation constant  
k<sub>2nd</sub>: second order rate constant  
Leu (or L): Leucine  
LMP: low-molecular weight protein  
MD: Molecular Dynamics  
MECL-1: multicatalytic endopeptidase complex  
Mel Ox: Melarsen oxide  
Mel T: Melarsen oxide-trypanothione  
Met (or M): Methionine  
MHC: Major Histocompatibility Complex  
MLCK: Myosin Light Chain Kinase  
MW: microwave  
NECT: Nifurtimox-Eflornithine Combination Therapy  
NTDs: Neglected Tropical Diseases  
ODC: ornithine decarboxylase  
PARs: Protease Activated Receptors  
PCF: Procyclic Form  
PCR: Polymerase chain reaction

PDB: Protein Data Bank  
PIP2: phosphatidylinositol-4,5-bisphosphate  
PLC: phospholipase C  
PLP: pyridoxal 5'-phosphate  
Phe (or F): Phenylalanine  
Pro (or P): Proline  
RCM: Ring-Closing Metathesis  
SAR: Structure-Activity Relationship  
SD: Standard deviation  
SI: Selectivity Index  
TAC: Tripartite Attachment Complex  
TbCatB: Trypanosoma brucei Cathepsin B  
TbCatL: Trypanosoma brucei Cathepsin L  
TC<sub>50</sub>: toxic concentration in 50% of the cell population  
TFA: Trifluoroacetic acid  
Thr (or T): threonine  
T-L: trypsin-like  
TNF- $\alpha$ : tumour necrosis factor  
Trp (or W): Tryptophan  
Tyr (or Y): tyrosine  
UPS: Ubiquitin-Proteasome System  
Val (or V): valine  
VSGs: Variant Surface Glycoproteins  
WHO: World Health Organization  
3FA: 3-trifluoromethyl-aniline  
4FA: 4-trifluoromethyl-aniline

## 1. AIM OF THE RESEARCH

Human African Trypanosomiasis (HAT), also known as sleeping sickness, is one of the most common neglected tropical diseases (NTDs) transmitted by the bite of the tsetse fly (*Glossina* genus) and widespread in the sub-Saharan Africa region (Figure 1), with about 70 million people at risk of infection.<sup>1</sup> HAT is caused by two subspecies of protozoa of *Trypanosoma* genus: *Trypanosoma brucei gambiense* and *T. b. rhodesiense*,<sup>2</sup> which are responsible for two different forms of the disease. *T. b. gambiense*, widespread in central and western Africa, causes the chronic form of the disease (gambiense HAT), which represents more than 95% of all reported HAT cases, characterized by a slow development. On the other hand, in the southern and eastern Africa regions, *T. b. rhodesiense* is responsible for the acute form of HAT (rhodesiense HAT), characterized by rapid-onset, swift progression and higher mortality rate.<sup>3</sup> HAT is characterized by two main stages: in the early-stage, also known as stage 1 or hemolymphatic stage, the parasite invades the bloodstream and then transfers to lymph nodes, spleen and spinal fluid, causing non-specific symptoms like headache, malaise, weight loss and fatigue.

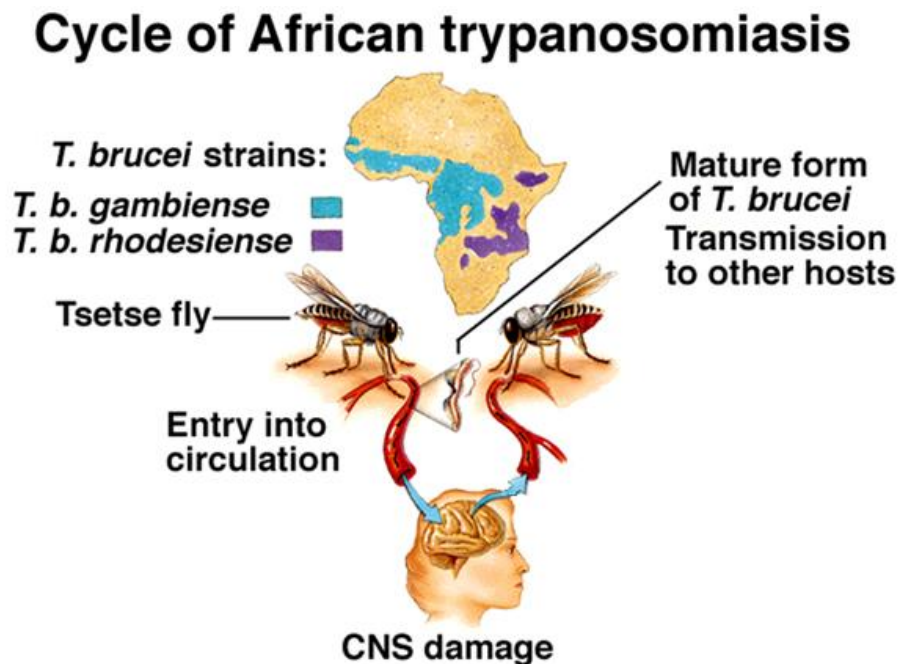


**Figure 1.** HAT distribution and cycle of *Trypanosoma brucei*.

If untreated, the stage 1 evolves to the neurological stage 2 (or late stage), during which the parasite crosses the blood-brain barrier (BBB) reaching the central nervous system (CNS), causing mental deterioration, sleep alterations, coma and lastly death.<sup>4</sup> Unfortunately, an effective vaccine has not been developed yet, because of the high degree of antigenic



variation by variant surface glycoproteins (VSGs)<sup>5</sup> and, consequently, chemotherapy is the sole strategy to control the infection. Only four drugs are currently available for the treatment of HAT,<sup>6</sup> showing several problems like toxicity, parasite resistance and route of administration. Suramin and pentamidine are used only in the hemolymphatic stage, while melarsoprol and eflornithine are effective on the neurological stage, since they are able to cross the BBB. At present, eflornithine is administered in combination with nifurtimox (Nifurtimox-Eflornithine Combination Therapy: NECT), to treat melarsoprol-refractory stage 2 rhodesiense HAT and as first-line treatment for stage 2 gambiense HAT.

Within this context, several studies<sup>7</sup> demonstrated that rhodesain, the major cysteine protease of *T. b. rhodesiense*, could be considered the primary target for the development of novel antitrypanosomal agents.<sup>8</sup> Rhodesain plays key functions in the survival of the parasite and in the disease progression. In fact, it is involved in the BBB alteration<sup>9</sup> (Figure 2A), necessary to switch from stage 1 to the neurological stage. In addition, it is also involved in the turnover of VSGs<sup>10</sup> (Figure 2B), which allows the parasites to evade the host immune response, and in the degradation of host immunoglobulins<sup>11</sup> (Figure 2C). Lastly, rhodesain shows an intensive lysosome proteolytic activity,<sup>12</sup> both of parasite proteins and intracellularly transported host proteins.

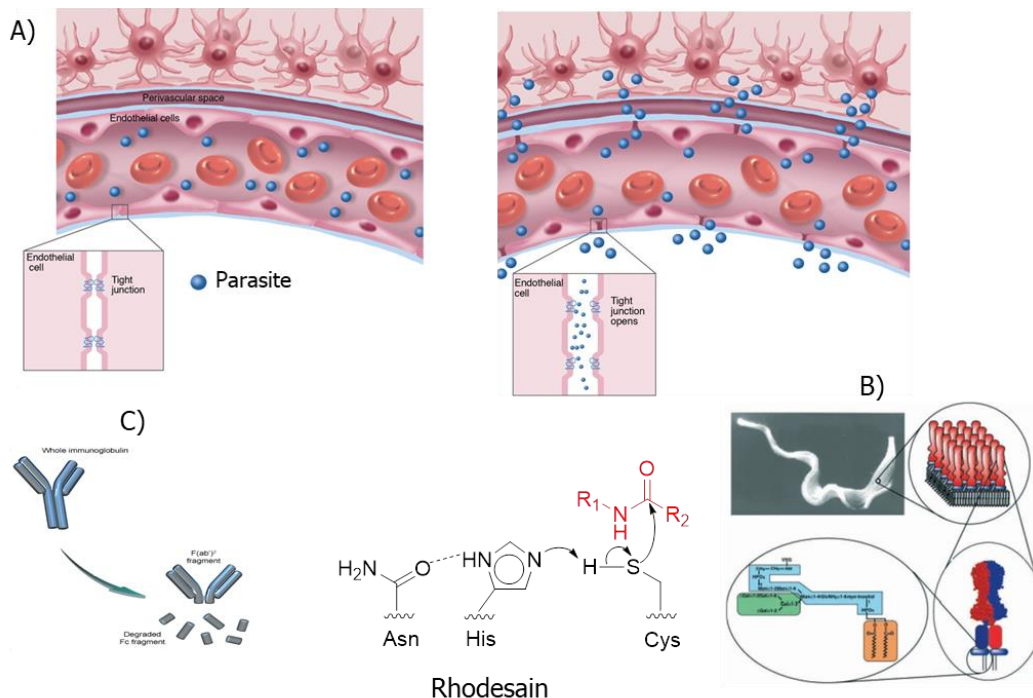


**Figure 2.** Rhodesain main functions.

Considering the key roles played by rhodesain, during my PhD period, together with my research group, I focused my efforts on the development of novel rhodesain inhibitors as potential agents to treat HAT. We developed six different series (A-F) of molecules with the aim to obtain potent and selective rhodesain inhibitors, coupled with a good antiparasitic activity.

In series A (Figure 3), we developed novel dipeptide-like rhodesain inhibitors bearing the 3-bromoisoxazoline warhead in a constrained conformation.<sup>13</sup> The idea to introduce 3-bromoisoxazoline nucleus takes place because 3-bromo acivicin is a potent trypanocidal agent,<sup>14</sup> targeting the cytidine triphosphate synthetase, a glutamine amidotransferase equipped with the catalytic triad Cys/His/Glu. Starting from the potent rhodesain inhibitor AZN-16,<sup>15</sup> we developed novel dipeptidyl analogues by replacing the azanitrile portion with a rigid bicyclic system containing the 3-bromoisoxazoline nucleus, as the warhead (Figure 3).

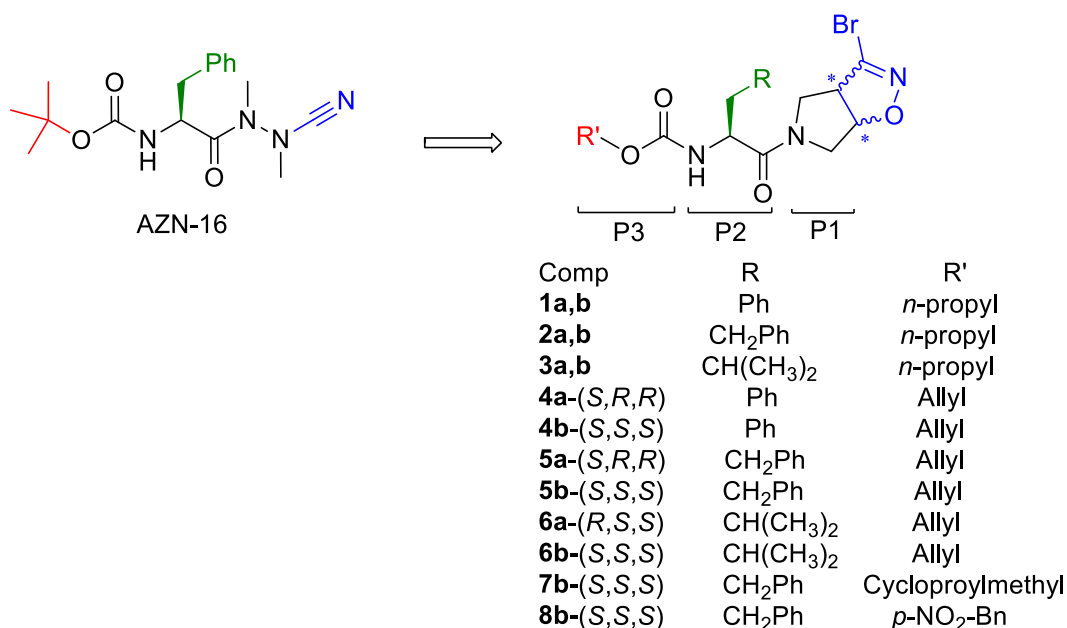


**Figure 3.** Design of series A compounds starting from AZN-16 as lead compound.

At the P2 position we inserted the amino acids towards which rhodesain showed a strong preference, like Phe, hPhe and Leu, while the *N*-terminal portion was functionalised to give different carbamates, to evaluate the impact of various aliphatic and aromatic substituents in this position. Previously, another member of my research group synthesized compounds with Cbz, Boc and Alloc as *N*-protecting group, and final products were obtained as racemic mixture of diastereomers. When evaluated against rhodesain, the mixture of

diastereomeric bearing the hPhe residue at the P2 site and Alloc as *N*-protecting group showed the best results. Starting from these findings, we continued our investigation by replacing the allyl chain with the saturated analogue propyl group (**1-3a,b**), to evaluate the effect of double bond on the activity. Subsequently, we evaluated the role played by the warhead stereochemistry on the biological activity, developing the single diastereoisomers **4a**-(*S,R,R*), **4b**-(*S,S,S*), **5a**-(*S,R,R*), **5b**-(*S,S,S*), **6a**-(*S,R,R*) and **6b**-(*S,S,S*). Lastly, considered that hPhe residue was well tolerated at the P2 site and *S,S* configured warhead showed the best inhibition results, we decided to further explore the S3 pocket by replacing *N*-allyl group with cyclopropylmethyl and *p*-NO<sub>2</sub>-Bn moieties, developing inhibitors **7b**-(*S,S,S*) and **8b**-(*S,S,S*), respectively.

In series B of inhibitors, we decided to combine the 3-bromoisoxazoline warhead with a 1,4-benzodiazepine (BDZ) scaffold as specific recognition moiety, typical of various cysteine protease inhibitors.<sup>16</sup> In particular, one of the most promising inhibitors was proven to be the Michael acceptor **9** (Figure 4), with  $k_{2nd}$  value of 4.620.000 M<sup>-1</sup> min<sup>-1</sup>, coupled with a good antitrypanosomal activity (EC<sub>50</sub> = 4.8 μM).<sup>17</sup>

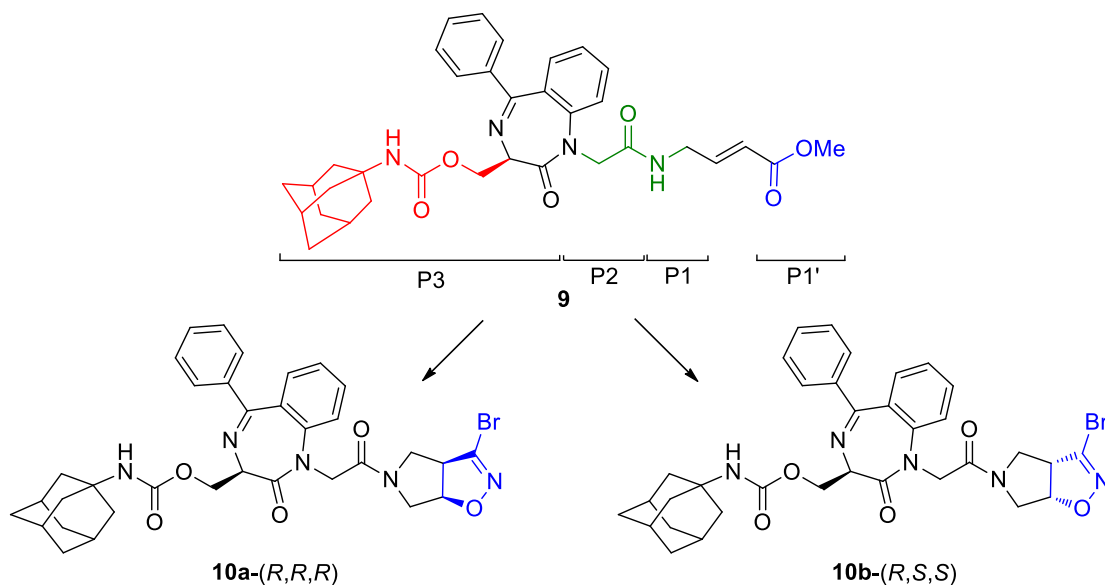


**Figure 4.** Lead compound **9** and novel 3-bromoisoxazoline derivatives.

In this molecule, the BDZ scaffold was inserted into a peptide backbone, in which the condensed aromatic ring could mimic the Phe residue at the P2 position, while the adamantyl nucleus linked to methyl carbamoyl side chain could occupy the S3 pocket of the enzyme. Starting from this lead compound, we decided to replace the vinyl ester portion with the 3-bromoisoxazoline nucleus incorporated into a bicyclic ring, to obtain the

diastereoisomers **10a**-(*R,R,R*) and **10b**-(*R,S,S*).<sup>18</sup> It is important to note that the lead compound **9** is an irreversible inhibitor, while the replacement of vinyl ester portion with the 3-bromoisoxazoline nucleus will lead to reversible inhibitors.

In series B, we discovered peptidomimetics as rhodesain inhibitors containing a 3-bromoisoxazoline nucleus, with antitrypanosomal activity similar to the lead compound **9**. Inhibitors **10a**-(*R,R,R*) and **10b**-(*R,S,S*), showed activity against the target enzyme, in the low micromolar range, considerably lower compared to the lead compound (3 order of magnitude). We supposed that this big difference is mainly due to the warhead: probably, compounds bearing a Michael acceptor portion, with a peptidomimetic recognition moiety, are able to inhibit rhodesain to a greater extent with respect to the 3-bromoisoxazoline nucleus. The same EC<sub>50</sub> values towards the parasite could be explained by better drug-like properties shown by inhibitor **10b**-(*R,S,S*). Although the latter inhibitor and the Michael acceptor **9** displayed good properties to be considered potential agents for the treatment of HAT, their high molecular weight (674.58 and 598.69, respectively), represents a great limit. Based on these considerations, we developed novel simplified BDZs **11-13a-c** (Series C) bearing a Michael acceptor portion (Figure 5), with the aim to maintain/increase activity against rhodesain and parasite, and optimize the drug-like properties.<sup>19</sup> We choose inhibitor **9** as lead compound given the deep difference between rhodesain inhibition mediated by 3-bromoisoxazoline and Michael acceptor derivatives.

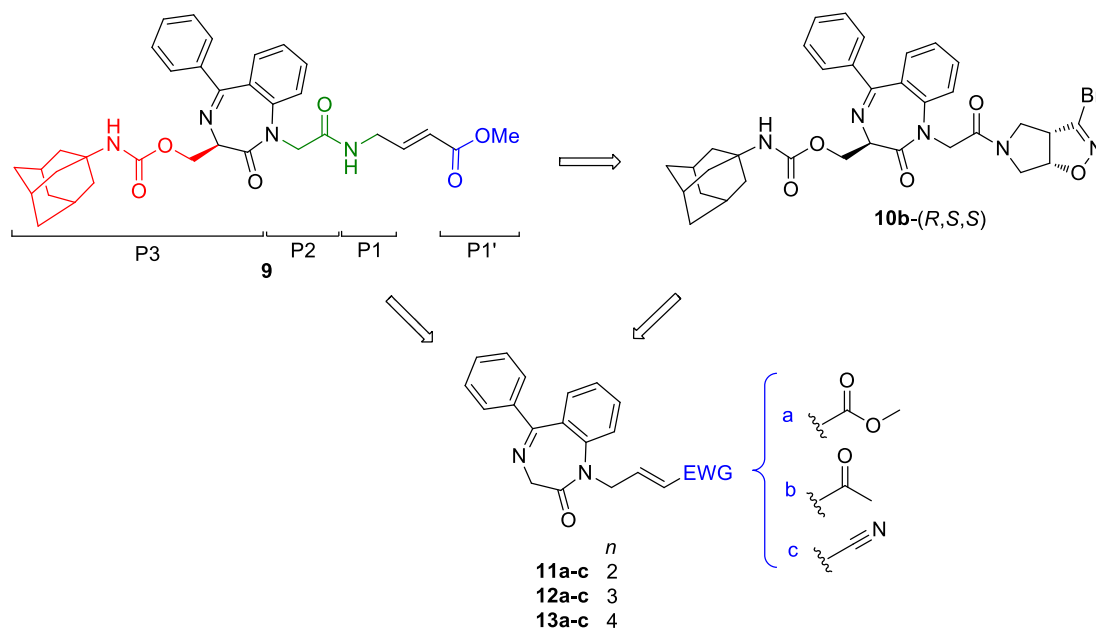


**Figure 5.** Novel BDZ simplified **11-13a-c**, designed starting from lead compound **9**.

In series D of my PhD work, we focused our efforts on the development of novel peptide-based Michael acceptors **14-17a-d**,<sup>20</sup> starting from vinyl sulfone K11777 (Figure 6), a potent rhodesain inhibitor with whom the cysteine protease was co-crystallized.<sup>21</sup>

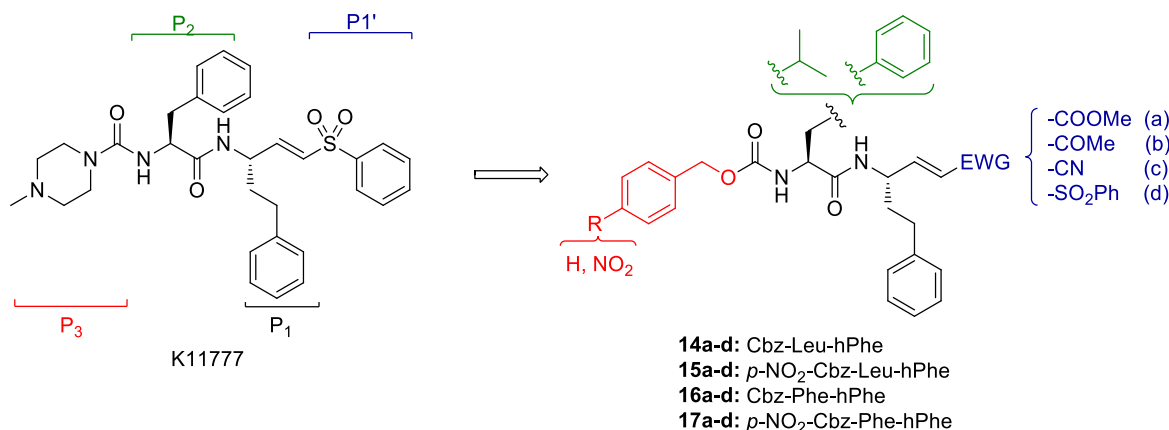


**Figure 6.** Vinyl sulfones K11777 and design of novel Michael acceptors.

Considering the high preference for bulky hydrophobic residues at the P2 position showed by rhodesain, we decided to maintain a Phe residue, as in K11777, or we inserted a Leu at the P2 site, while the hPhe residue was left unmodified. The *N*-terminal amino group was protected with Cbz or *p*-NO<sub>2</sub>-Cbz, the latter in agreement with the structure of inhibitor **8b**-(*S,S,S*): the hydrophobic features of these substituents and the electron withdrawing effect mediated by the nitro group could increase the  $\pi$ - $\pi$  interactions at the S3 pocket. Lastly, we introduced different  $\alpha,\beta$ -unsaturated portions at the P1' site, to evaluate their different reactivity.

In light of the results obtained in series D, inhibitors bearing the vinyl ketone warhead showed the best  $k_{2nd}$  values. Based on these data, we developed **16b** derivatives, i.e. **18a-b**, **19a-c**, **20** and **19a-d** (Figure 7), with the aim to increase selectivity and the activity against the parasite. We decided to carry out the structure-activity relationship (SAR) study introducing novel substituents only in one position (e. g. P1', P2 or P3), maintaining unchanged the other sites of **16b**. With regard to P3 position, we inserted several substituents, linked to the amino group of Phe *via* urea or amide portions. In urea derivatives **18a-b**, we replaced the Cbz group with *N*-methylpiperazine and morpholine rings, because these two portions are present in the potent rhodesain inhibitors K11777 and K11002,<sup>21,22</sup> respectively. On the other hand, in the amide derivatives we inserted 1,3-difluorophenyl (**19a**) and 2,3-dihydro-1,4-benzodioxin-6-yl (**19b**) moieties, which are

present in potent rhodesain inhibitors reported in literature.<sup>23,15</sup> Furthermore, we decided to introduce 5-methylbenzodioxolan-5-yl ring (**19c**), to evaluate the impact on the biological activity of the presence of five- or six-membered rings, both bearing two oxygen atoms.

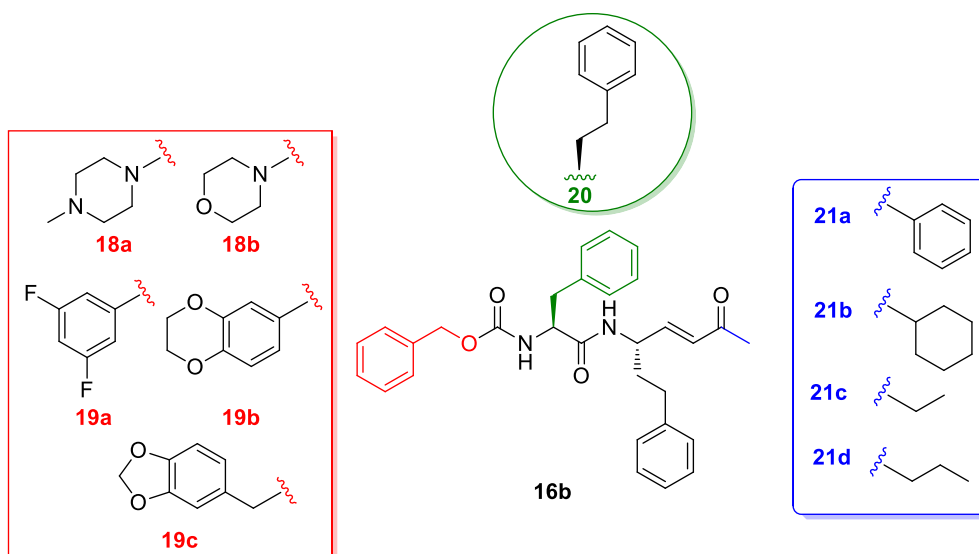


**Figure 7.** Optimization of the inhibitor **16b**.

At the P2 site, we replaced the Phe with the hPhe residue (**20**), to evaluate the impact of the chain stretch: this modification could be well tolerated, considering the size and the hydrophobic character of S2 pocket. Lastly, at the P1' site, we decided to replace the methyl group with bulkier substituents like phenyl, cyclohexyl, ethyl and propyl groups (**21a-d**), to evaluate possible additional interactions with S1' pocket.

At the same time, based on the data obtained in series D, we decided to develop another series of molecules (F, Figure 8), bearing vinyl ketone warhead. Docking studies carried out on inhibitor **16b** indicated the involvement of carbonyl oxygen in binding interaction by means of two H-bonds with Gln19 and Trp184 at the S1' enzyme pocket.

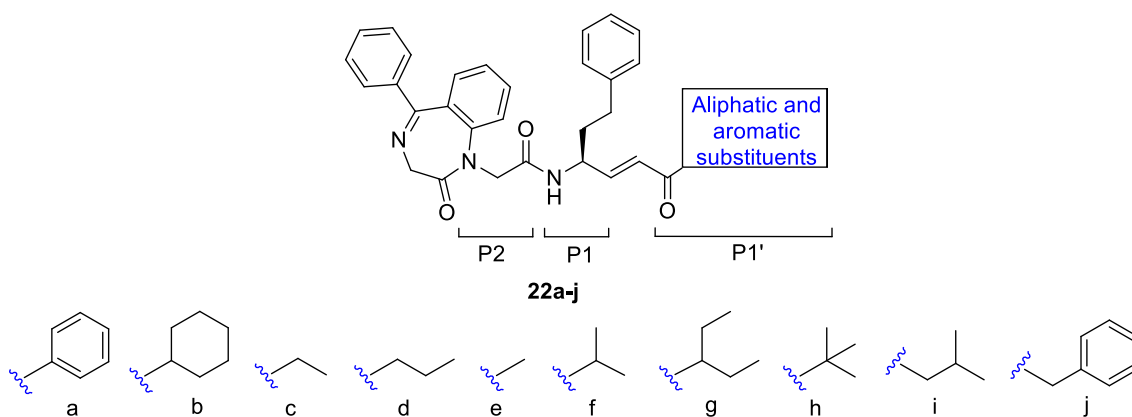


**Figure 8.** Design of BDZ derivatives bearing several substituents at the P1' site.

Based on these data, we developed novel peptidomimetics characterized by a BDZ scaffold as recognition moiety, able to mimic Phe residue at the P2 site, hPhe at P1 position, and vinyl ketone warhead. Furthermore, we introduced several aliphatic or aromatic substituents at the carbonyl group of the warhead, with the aim to explore S1' enzyme pocket and evaluate possible additional interactions.

The results of this wide investigation will be reported and discussed in the “Results and discussions” chapter of my PhD thesis.

## CHAPTER 2. HUMAN AFRICAN TRYPANOSOMIASIS

### 2.1 Introduction

Human African Trypanosomiasis (HAT), also known as sleeping sickness, is one of the most common neglected tropical diseases (NTDs), widespread in the sub-Saharan Africa and affecting 37 countries in 1.55 million km<sup>2</sup>, between latitudes 14° north and 20° south (Figure 9), with about 70 million people at risk of infection.<sup>1</sup> It is caused by two distinct subspecies of protozoa, both belonging to *Trypanosoma* genus: *T. brucei gambiense* and *T. b. rhodesiense*.<sup>2</sup> These parasites are transmitted to human by the bite of the blood-sucking tsetse fly of *Glossina* genus, with a high index of infectivity and an estimated number of actual cases of 10000 per year,<sup>24</sup> although this number is under estimated with respect to the number of real cases. As shown in figure 9, HAT is an endemic disease in the north and south of sub-Saharan region, while the highest number of HAT cases were recorded in the central area (Angola, Democratic Republic of the Congo and Tanzania).

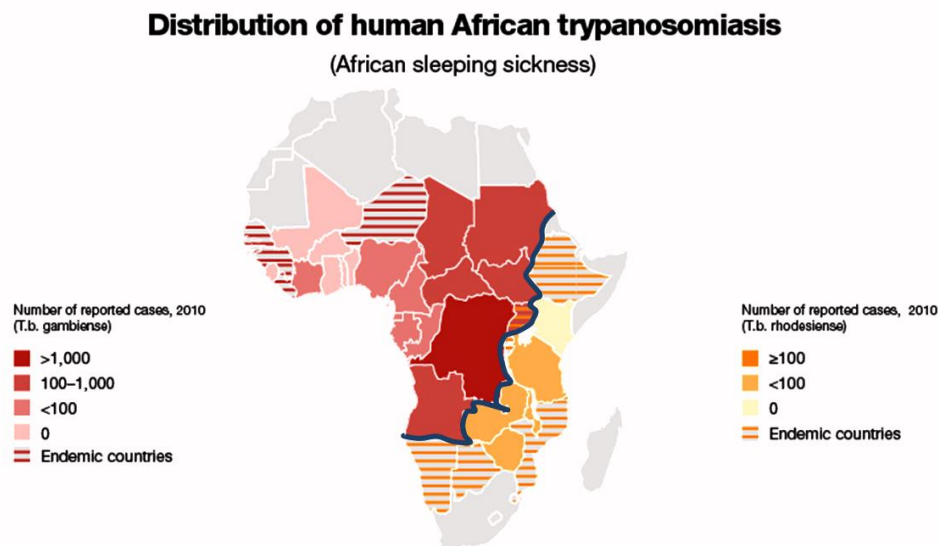


**Figure 9.** The annual country reports of HAT distribution, carried out by WHO.

### 2.2 The parasite

*T. brucei* is a typical unicellular eukaryotic cell, with a length between 8 and 50 µm; it has a lengthened body and a streamlined and tapered shape. Its cell membrane, named pellicle, encloses the cell organelles, as the nucleus, mitochondria, endoplasmic reticulum, Golgi apparatus, ribosomes and the kinetoplast, a network of circular DNA (called kDNA) inside a large mitochondrion that contains many copies of the mitochondrial genome.<sup>25</sup> Kinetoplast is near the basal body, but it is not distinguishable under the microscope. *T.*



*brucei* life cycle<sup>26</sup> (Figure 10) starts with the infection of a mammalian host, when a tsetse fly bite delivers growth-arrested metacyclic trypomastigotes to the mammalian bloodstream. Then, metacyclic trypomastigotes differentiate into proliferating long forms, which maintain a bloodstream infection. Parasites eventually penetrate the blood vessel endothelium and invade extravascular tissues, including the central nervous system (CNS).

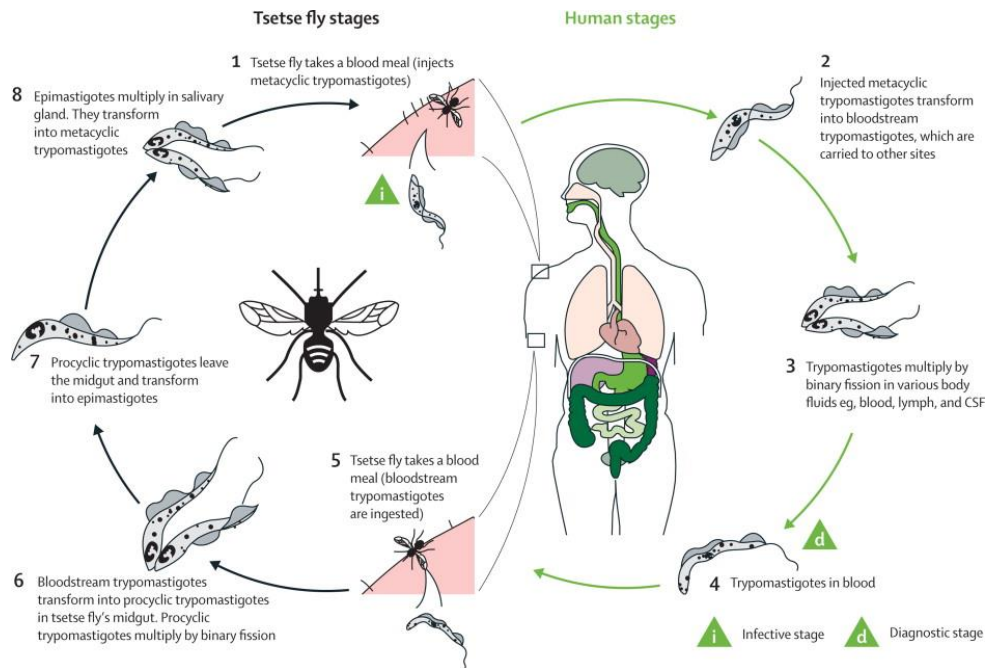


**Figure 10.** Life cycle of *Trypanosoma brucei*.

In the bloodstream, a quorum sensing-like mechanism, carries out to the differentiation of long slender forms into short stumpy forms, called also bloodstream form (BSF), which are pre-adapted for survival in the tsetse fly. When an infected host is bitten by a tsetse fly, parasites are taken up during the blood meal into the midgut, where short stumpy forms differentiate into procyclic trypomastigotes, or procyclic form (PCF), that resume cell division and establish a midgut infection. Midgut procyclic trypomastigotes initiate a migration, crossing the proventriculus, and from there onwards through the mouthparts, arrive to the salivary gland, where they attach to the salivary gland epithelium. During this migration, in the proventriculus, procyclic trypomastigotes undergo extensive restructuring, coupled to an asymmetric division, to generate one long epimastigote and one short epimastigote, which attaches to epithelial cells following arrival in the salivary gland. Attached epimastigotes replicate and ultimately complete the life cycle *via* an asymmetric division to generate metacyclic trypomastigotes that are free in the salivary gland lumen and are uniquely adapted to survive in the mammalian host. The *T. brucei*

possesses a single flagellum attached along the length of the cell (Figure 11), from which exits by a flagellar pocket, which is located at the posterior end.<sup>26</sup> The flagellum has several functions, because is involved in cell morphogenesis and cell division, locomotion *via* oscillations along the attached flagellum and cell body, establishment to the fly gut during the procyclic phase and in in host–parasite interactions. The cell surface of the BSFs is wrapped in a dense coat of variant surface glycoproteins (VSGs), and it is replaced by an equally dense coat of procyclins when the parasite differentiates into the PCF in the tsetse fly midgut.<sup>27</sup> The trypanosome basal bodies form the main organiser for the cytoskeleton, membranous structures and organelles.<sup>28</sup>

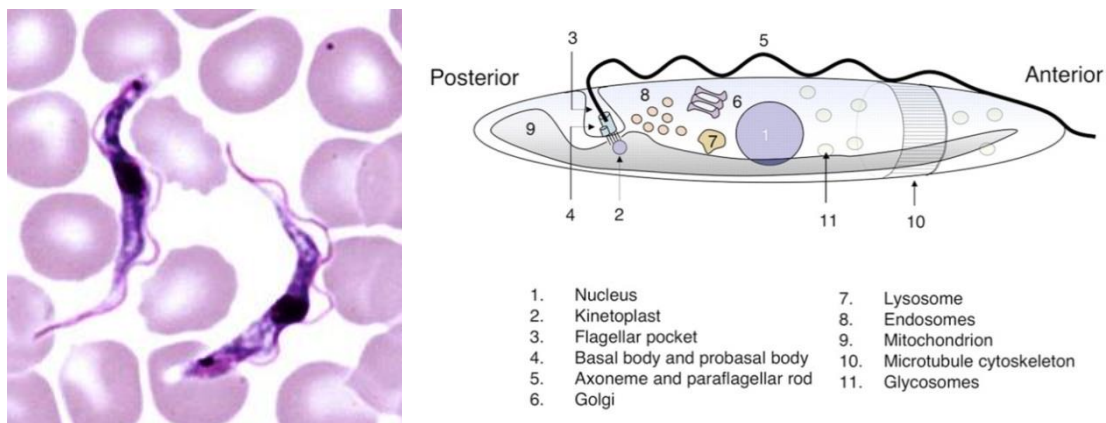


**Figure 11.** *Trypanosoma b. brucei* in thin blood film and simplified representation of *Trypanosoma* cell architecture.

Furthermore, they serve another function to ensure inheritance of the mitochondrial genome. The kinetoplast is connected to the proximal end of both the mature basal body and pro-basal body *via* the tripartite attachment complex (TAC).<sup>29</sup> The TAC represents an intricate network of filaments, connected from the proximal end of each basal body to a specialised region of the outer mitochondrial membrane, with a further set of filaments connecting the inner mitochondrial membrane and the mitochondrial DNA. This physical connection remains unchanged during cell division: the kinetoplast DNA is replicated in a periodic S phase, together with the basal body duplication. The basal body segregation ensures inheritance of the duplicated mitochondrial DNA to the two daughter cells.

### 2.3 HAT forms: symptoms and progression of the disease

There are two different forms of HAT (Table 1). *T. b. gambiense*, widespread in central and western Africa, causes the chronic gambiense form of the disease, which represents more than 95% of all reported HAT cases, characterised by a slow development

(gambiense HAT). On the other hand, in the southern and eastern Africa regions, *T. b. rhodesiense* is responsible for the acute form of the HAT (rhodesiense HAT), which is manifested with a rapid-onset, swift progression and a higher mortality rate.<sup>3</sup>

<b>Table 1. Main differences between gambiense and rhodesiense HAT forms</b>		
<b>HAT</b>	<b><i>T. b. gambiense</i></b>	<b><i>T. b. rhodesiense</i></b>
Progress	Slow	Rapid
Symptoms of stage I	Non-specific, commons, uncorrected diagnosis	
CNS invasion	Months (3-4)	Weeks (1-2)
Symptoms of stage II	Motor disturbances, mental alterations, delirium	
Time to death	A few week	A few days

HAT is characterized by two main stages. Early-stage, also known as stage 1 or hemolymphatic stage, is characterized by non-specific symptoms.<sup>30</sup> During this stage, the parasite invades the bloodstream causing headache, malaise, weight loss, fatigue and intermittent fever, with an onset 1–3 weeks after the tsetse fly bite. Over this time, patients might develop several problems including lymphadenopathy, enlargement of the spleen and the liver, myocarditis, pericarditis, heart attack, keratitis, conjunctivitis, endocrine dysfunction and fertility problems. Another finding that has begun to challenge the classical symptom complex is the occurrence of neurological features during early-stage disease. Some patients showed the neurological features during early-stage disease: tremors, somnolence, urinary incontinence and cranial neuropathies, symptoms that can hardly be explained by nonspecific effects at peripheral level. It is clear how the above mentioned non-specific symptoms lead to both an extension of the time to diagnose the disease and, sometimes, to an uncorrected diagnosis. This stage has a variable duration, depending on the specific subspecies: generally, 7-10 days for rhodesiense form, months for gambiense form. If untreated, the hemolymphatic stage evolves into the neurological stage (named stage 2 or late), during which the parasite invades the CNS,<sup>30</sup> and a wide series of symptoms can take place, with almost all regions of the nervous system involved. These features include motor disturbances, as motor weakness reported, gait disturbance, tremor, abnormal movements, speech disturbances and mental alterations as the typical sleep disturbances, thus justifying the disease name, sleep abnormalities, with an inversion of the normal sleep/wake cycle, uncontrollable episodes of sleep, and an alteration of the structure of sleep itself, with the early onset of rapid eye movement sleep rather than at the end of stage 4 sleep. The behavioural disturbances like hallucinations, delirium, headache are very common. Lastly, the patients fall into a coma and, eventually, die.

Obtaining an accurate and early diagnosis is fundamental, considered the final outcome of the disease. In the rhodesiense HAT form, trypanosomes should be identifiable on a thin layer of peripheral blood, since of the typically high level of parasitaemia.<sup>31</sup> On the other hand, for gambiense HAT form, the parasitaemia is rarer, but the diagnosis is also possible by identifying parasites in the peripheral blood or in the lymph node aspirate. Different methods of concentration techniques might be needed to identify parasites.<sup>32</sup>

## 2.4 Diagnostic methods

The CATT method (Card Agglutination Test for Trypanosomiasis, figure 12) is simple and quick to effectuate, and its use is very common, in particular for population screening. Nevertheless, CATT has limitations, first and foremost the high frequency of equivocal results and limited sensitivity.<sup>33</sup> PCR has been used to increase diagnostic accuracy,<sup>34</sup> but such advanced equipment are not generally available in remote rural areas of Africa.

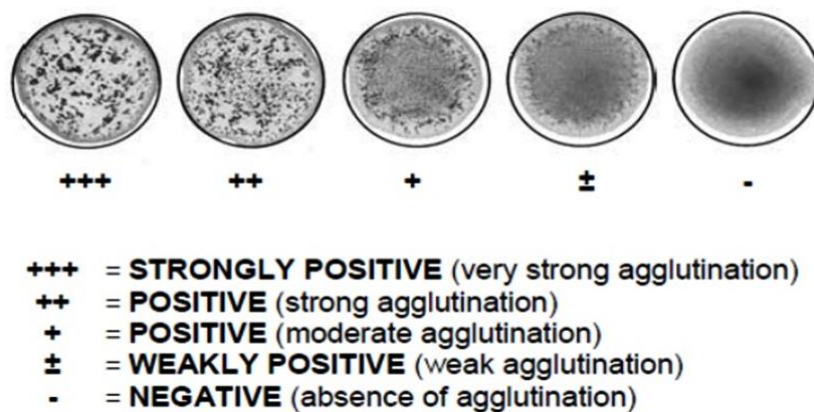


**Figure 12.** The example shows how interpret the CATT.

Considering the absence of reliable clinical criteria,<sup>35</sup> a positive diagnosis by lumbar puncture, to examine the cerebrospinal fluid (CSF), is essential.<sup>36</sup> The most widely used methods for late-stage diagnosis are the WHO criteria, meaning the presence of trypanosomes in the CSF or a white blood cell count of more than 5 cells per  $\mu\text{L}$ , or both. A valid method to late-stage diagnosis is measurement of CSF IgM concentrations, values that are increased when there is CNS involvement.<sup>37</sup> Over the past few years, a great deal of efforts has gone into devising better and more reliable CNS staging markers. However, all these approaches have an intrinsic drawback: there is no standard of CNS diagnosis with which to compare any new methodology, meaning the argument is therefore somewhat circular. The problem is compounded by the dual issues of disagreement as to what criteria define CNS involvement in HAT and controversy as to which CSF

parameters should be used as an indication to use late-stage drugs.<sup>31</sup> The sensitivity of the assay can be considerably improved by the inclusion of detergent in the reaction mix.<sup>38</sup> For any new diagnostic test for HAT to be applicable in the affected areas in Africa, it needs to be quick, easy to undertake, inexpensive and reliable.<sup>39</sup>

## 2.5 Pharmacological treatment

The development of an effective vaccine is not possible due to the high degree of antigenic variation expressed from VSGs.<sup>5</sup> The dense coat covering parasite, plays a key role against the innate immune mechanism, as it hampers the normal antibody functions of recognition of surface proteins. This shielding strategy is effective, but has one weakness: the VSG itself is recognized as an antigen and total antibody responses arise against a range of epitopes on the VSG. To permit the *Trypanosoma* to evade the immune response, random and background spontaneous point mutation is not enough. *Trypanosoma* possesses an enormous set of silent VSG genes, that differ from each other in the epitopes they encode: each silent gene has the possibility to be transcribed creating novel VSGs, which will not be recognised by immune system. In following chapter, the mechanism which allows the parasite to evade the immune system response will be examined in depth.

With this in mind, chemotherapy is the sole strategy to control the infection. Unfortunately, only four drugs are currently available<sup>6</sup>: suramin, pentamidine, melarsoprol and eflornithine.

The first-line treatment for rhodesiense HAT stage 1 is suramin<sup>32</sup> (Figure 13), a polyanionic sulphated naphthylamine unable to cross the BBB, bearing an urea functional moiety and six sulfonic acid groups. It is administered as the sodium sulfonate salt by injection into a vein, because it is water-soluble but air sensitive. The mechanism of action for suramin is not completely clear: it is thought that *Trypanosoma* is able to selectively uptake suramin by receptor-mediated endocytosis of drug that is bound to low-density lipoproteins.

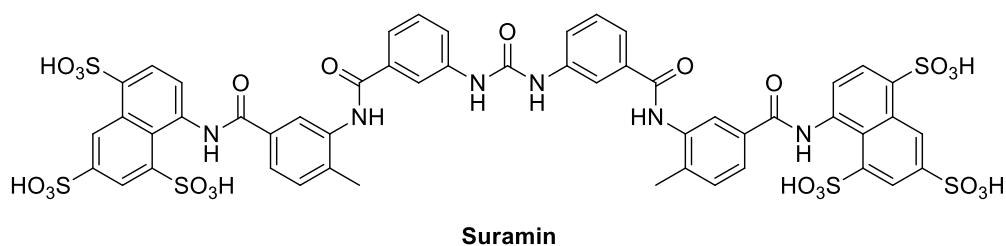


**Figure 13.** Chemical structure of suramin.

Inside parasite, suramin binds to proteins, particularly to the trypanosomal glycolytic enzymes, in order to inhibit energy metabolism. Suramin was used since 1920s and, although usually effective, can result in potential complications such as renal failure, skin lesions, anaphylactic shock, bone marrow toxicity, and neurological complications such as peripheral neuropathy.

On the other hand, pentamidine (Figure 14), an aromatic diamidine, is the first-choice drug for the early-stage gambiense HAT.<sup>32</sup> It was first used to treat HAT in 1937 and today is commercially available as white crystalline powder for reconstitution with sterile water and subsequent administration by injection or inhalation. The mechanism of action is not well understood: however, it was assumed that through cross-link between two adenines, four to five base pairs apart, pentamidine interferes with critical functions in DNA, RNA and protein synthesis. Similarly, pentamidine inhibits mitochondrial type II topoisomerase, resulting in breaks and unravelling circular mitochondrial DNA. Common side effects are burning, pain, sensation of lump in throat, chest pain, coughing, difficulty in breathing, skin rash, leukopenia, nephrotoxicity and hypotension.

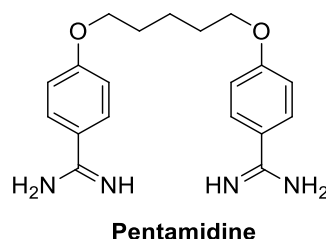


**Figure 14.**Chemical structure of pentamidine.

The treatment of neurological stage, when the parasite crossed the BBB and invaded the CNS, provides for the use two drugs, melarsoprol and eflornithine, with serious issues, first and foremost the toxicity.

Melarsoprol (Figure 15) is a trivalent organic arsenical derivative, classified as prodrug, which is metabolized to melarsen oxide (Mel Ox) as its active form. Mel Ox is able to reacts with trypanothione,<sup>40</sup> a spermidine-glutathione adduct that replaces glutathione in trypanosomes, forming a melarsen oxide-trypanothione adduct (Mel T, Figure 16) that competitively inhibits trypanothione reductase, killing the parasitic cell. Furthermore, it binds the vicinal sulfhydryl groups on pyruvate kinase, disrupting with energy production in the parasite. Melarsoprol was used for HAT in 1949, administered intravenously in

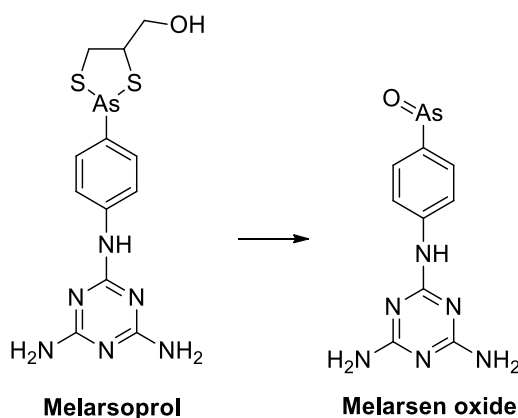


**Figure 15.** Melarsoprol and melarsen oxide after activation *in vivo*.

propylene glycol (extremely painful), and cannot be administered by the oral route. The inability to distinguish between host and parasites renders this drug highly toxic with many side effects. The main side effect is a post-treatment reactive encephalopathy in 10% of patients, half of whom die<sup>41</sup>: the cause of the post-treatment reactive encephalopathy is not yet known, but it is characterized by rapidly developing coma, seizures or status epilepticus and cerebral oedema. Its treatment may involve anticonvulsants, intravenous corticosteroids and acute medical supportive measures.

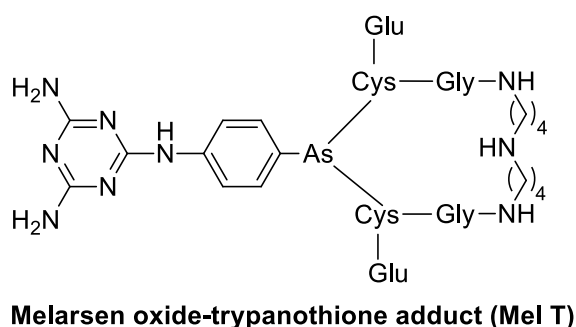


**Figure 16.** Inactivation of trypanothione by melarsen oxide.

Others common side effects are agranulocytosis, skin rashes, peripheral neuropathy, cardiac arrhythmias and a multifocal inflammatory disorder that is responsive to corticosteroids.

Eflornithine (Figure 17), also known as difluoromethylornithine (DFMO), is the first-choice drug to treat late-stage *gambiense* HAT and it was administered, by injection or applied to the skin, for first time in 1990.<sup>42</sup> However, eflornithine has a principal drawback: it is ineffective against *T. b. rhodesiense*. It is a "suicide inhibitor," because able to bind irreversibly to the ornithine decarboxylase (ODC) and impeding the access at the

active site of the natural substrate ornithine (Figure 18). Once attached, eflornithine initially undergoes transamination which occurs with cofactor pyridoxal 5'-phosphate (PLP), followed by decarboxylation. During the decarboxylation, the fluoride atoms attached to the additional methyl group drag towards themselves the resulting negative charge from the release of carbon dioxide, with consequent release a fluoride ion.

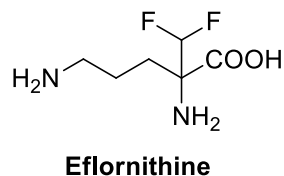


**Figure 17.** Chemical structure of eflornithine.

The remaining fluoride atom, generates an electrophilic carbon, which is attacked by the nearby thiol group of Cys360, allowing eflornithine to remain permanently attached to the enzyme following the release of the second fluoride atom and subsequent transamination. The eflornithine common side effects are acne, skin reactions, itching and rash when administered topically. Otherwise, hematologic abnormalities, thrombocytopenia and reversible hearing loss are common when eflornithine is used by injection. Unfortunately, this drug with reduced toxicity is not effective in the treatment of late-stage rhodesiense HAT, due to the parasite's low sensitivity to the molecule.

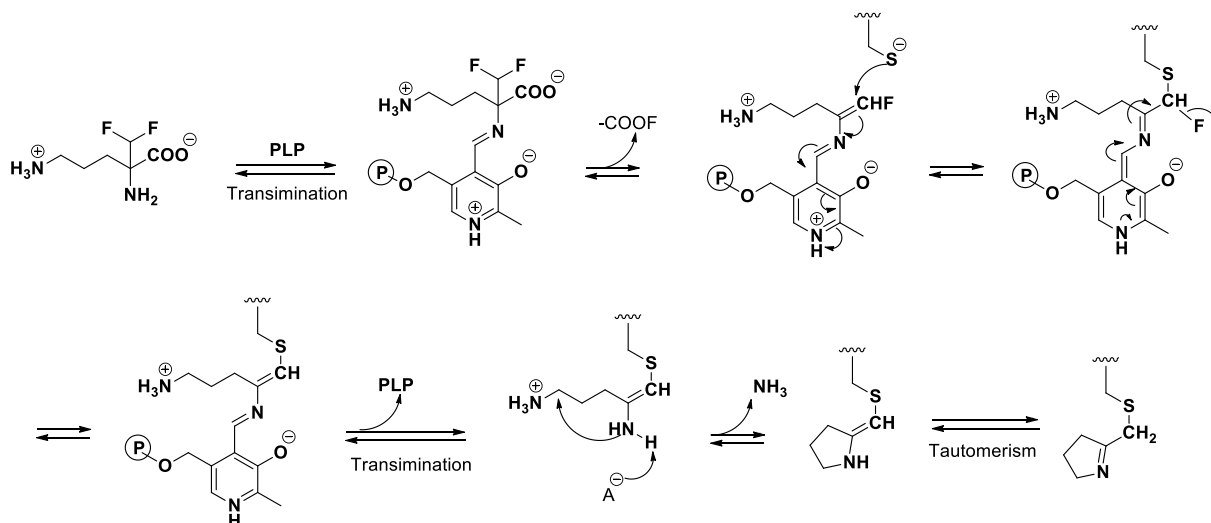


**Figure 18.** Mechanism of action of eflornithine.

Furthermore, several cases of drug resistance has been reported after a few years to marketing, through loss of the putative amino acid transporter TbAAT6, which has been shown *in vitro*.<sup>43</sup>



An important step forward was the development of the nifurtimox–eflornithine combination therapy (NECT)<sup>44</sup>: this combination is recommended for melarsoprol-refractory late stage rhodesiense HAT and as first-line treatment oh stage 2 gambiense HAT. Nifurtimox (Figure 19), an orally bioavailable 5-nitrofuran analogue,<sup>45</sup> used for the treatment of Chagas disease, caused by *T. cruzi*: it acts through the generation of nitroanion radical causing damages to the parasite, unable to defend himself. The enzyme involved in this process is the nitro reductase, which needs oxygen for its functions. The off-label use of nifurtimox associated to eflornithine improved the late stage HAT therapy,<sup>46</sup> above all safety and patient compliance: monotherapy with eflornithine includes infusion every 6 h for 14 days, while in combination with nifurtimox one infusion every 12 h for 7 days.

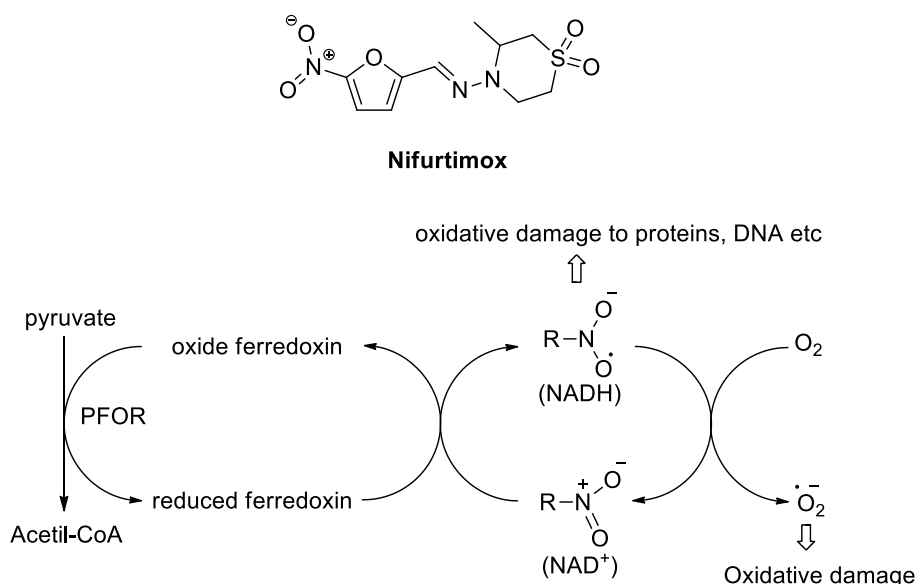


**Figure 19.** Chemical structure of nifurtimox and its mechanism of action.

In the last few years, the research developed two novel molecules as potential antitrypanosomal agents. The first-one is the diamine derivate pafuramidine (DB289, Figure 20),<sup>47</sup> orally bioavailable and active against the early-stage of HAT.

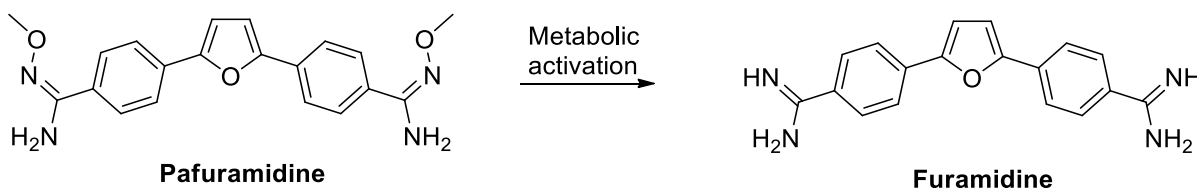
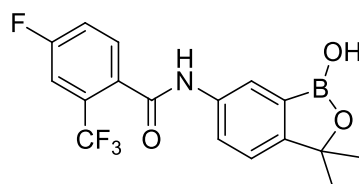


**Figure 20.** Pafuramidine and its active metabolite furamidine.

This is a prodrug, which is converted in its active form furamidine (DB75): the mechanism of action is the same suggested for pentamidine. Unfortunately, in 2008 the development of this prodrug was halted in phase III clinical trials, due to its hepatic toxicity.<sup>48</sup>

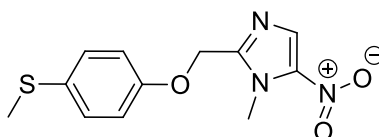
At present, high expectations were addressed in the benzoxaborole derivative SCYX-7158 (Figure 21), a boron-containing molecule able to cure mice infected with *T. brucei*, both in hemolymphatic and neurological stage.<sup>49</sup> Administered by oral route, in 2012, SCYX-7158 entered into phase I clinical trials,<sup>50</sup> to evaluate its pharmacokinetic properties and toxicity for the treatment of both HAT stages: these studies confirmed that the drug penetrates the BBB and kills the parasite, coupled with acceptable values of tolerability and safety. Based on the results, in 2016, SCYX-7158 entered phase IIb/III studies in the Democratic Republic of the Congo, where numerous cases of HAT are reported.



**Benzoxaborole**

**Figure 21.** Chemical structure of benzoxaborole.

Currently, the drug candidate for the treatment of advanced-stage sleeping sickness after nearly thirty years is fexinidazole (Figure 22), a 5-nitroimidazole derivative and orally bioavailable.<sup>51</sup> The mechanism of action of fexinidazole is not clear, but it could involve bioreductive activation mediated by parasite nitroreductases. Two complementary cohort studies with fexinidazole were completed in 2016, and the results of the phase II/III study support the submission of a regulatory dossier to the European Medicines Agency, probably by the end of 2017.<sup>52</sup>



**Fexinidazole**

**Figure 22.** Fexinidazole chemical structure.

In the present scenario, there is a clear need to find novel antitrypanosomal agents, endowed with an efficacy and safety profile, with the aim to introduce them for the

treatment of HAT. Even more interesting is the challenge to identify new trypanosomal targets on which acting for alternative therapies.

## CHAPTER 3. CYSTEINE PROTEASES: ALTERNATIVE AND VALID TARGETS

### 3.1 The ideal drug

Table 2. Features of ideal, acceptable and NECT approach in the HAT treatment		
Ideal	Acceptable improvement to current stage 2	NECT
Effective against stages 1 and 2	Effective against stages 1 and 2, but only used against stage 2.	stage 1+2 (used stage 2 only)
Effective against infection due to <i>T. b. gambiense</i> and <i>T. b. rhodesiense</i> .	Effective against infection due to <i>T. b. gambiense</i> only.	<i>T. b. gambiense</i>
Clinical efficacy >95% at 18 months follow-up		clinical efficacy: 96.5%
Effective in melarsoprol-refractory patients		Effective
<0.1% drug related mortality	<1% drug related mortality	1.2% possibly related mortality
Safe during pregnancy, for breastfeeding women and children.		no specific adverse event found in babies born or being breastfed after treatment
Adult and paediatric formulations		DFMO paediatric dosing available + Nifurtimox 5 mg tablets to be cut
No monitoring for adverse events required.	Weekly simple lab testing (field testing)	Hospitalization required
<7 days p.o.q.d.	10 days p.o.uptod.	7 days IV infusion (bid) + 10 days po (tid)
<7 days i.m. q.d.	10 days i.m. q.d.	
Stability in zone 4 for >3 years	Stability in zone 4 for >12 months	Stability in Zone 4 for > 24 months
Multitarget	Unique target (but not through uptake via P2-transporter only).	
<30€/ course (drug cost)	<100€/ course	222.5 € / course (in 4 treatments kits; WHO)

Concerning protozoal infections, the principle of magic bullet, created by Paul Ehrlich, is always the aim to be achieved: the ideal drug should be directed against a target exclusive

for the parasite, or otherwise significantly different in the human. Drug for Neglected Diseases initiative (DNDi) reported a list (Table 2) of requirements about ideal drug for HAT treatment.<sup>53</sup>

These include features such as the efficacy against both stages, acceptable range of toxicity, the duration of treatment, the appropriate physicochemical and pharmacokinetic properties for oral bioavailability. In the same way, an ideal target could be essential for viability of the parasite when it is inside the body both in stage 1 and stage 2, and the alteration of its functions must generate a trypanocidal effect.

### 3.2 Potential targets

Different proteins and metabolic pathways are identified as potential target to develop novel antitrypanosomal agents: table 3 summarises the candidate molecular targets with the respective cellular activity.<sup>54</sup> Among those, cysteine proteases play several key roles in the life cycle of parasitic organisms: their function is to catalyse the cleavage of amide linkages in macromolecular proteins and oligomeric peptides, essential function in the parasite survival into human body, tissue invasion and failure of the immune system response.<sup>55</sup>

<b>Table 3. Candidate immunotherapeutic targets</b>	
<b>Molecular target</b>	<b>Cellular activity</b>
Acyl carrier proteins	Fatty acid biosynthesis
Inhibitors of mitochondrial function	Glycolysis
Tubulin multigene family	Cytoskeleton
Cysteine proteases	Proteolytic enzymes
Plasma membrane proteins	Cellular physiology
Cytosolic fractions	Cellular biochemistry

The catalytic activity can initiate both within a polypeptide chain (endoprotease activity) and from carboxy- or amino- terminal regions, (exopeptidase activity). Proteases were divided into groups on the basis of the catalytic mechanism used during the hydrolytic function: the main catalytic types are serine-, threonine-, aspartic-, metallo- and cysteine proteases.

Cysteine proteases are ubiquitously expressed both in human and in protozoans, and were successfully targeted to treat human diseases: at the same way, they play a key role in parasitic diseases and for this reason were recognized as valuable targets for the parasitic infections. Furthermore, the relative lack of redundancy in mammalian system, highlights

the importance of these enzyme families for the development of novel antiparasitic agents. The validation of this target was carried out by Scory et co-workers,<sup>56</sup> which proved that the peptidyl inhibitor Cbz-Phe-Ala-CH<sub>2</sub>N<sub>2</sub> **23** (Figure 23) killed the bloodstream forms of *T. brucei*. In addition, another study<sup>57</sup> demonstrated that the treatment with biotinylated cysteine protease inhibitors induced *T. brucei* death.

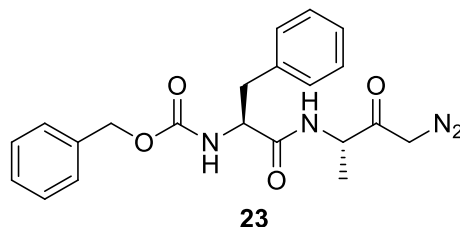


**Figure 23.** Chemical structure of peptidyl inhibitor **23**.

More in detail, cysteine proteases of parasitic organisms are divided into two main groups,<sup>55</sup> corresponding to clans CA and CD (Figure 24). Other minor groups are clans CB and CC, identified as viral proteases. In 1879, the first cysteine protease was characterised from the fruit of *Carica papaya*, and was therefore called papain, and the subsequent discovered cysteine proteases, with similar chemical structure to papain, were named “papain-like”. The assignment to a family rather than to another one is a function of a number of properties, as sequence homology, possession of inserted peptide loops, and biochemical specificity to small peptide substrates.

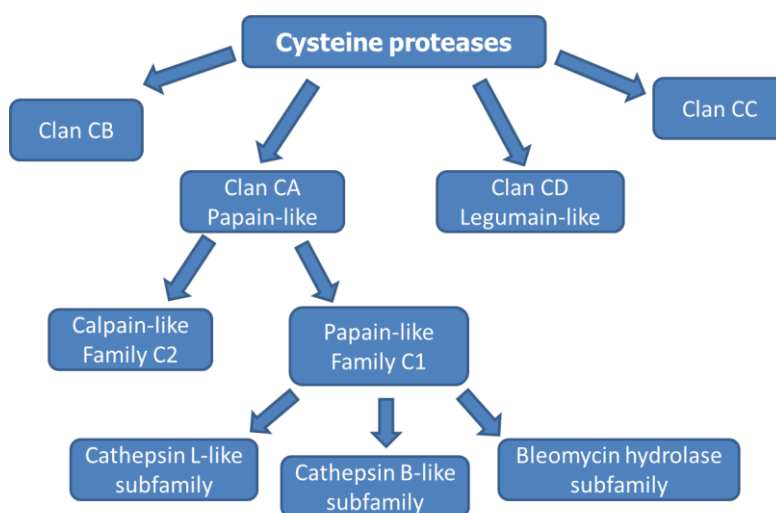


**Figure 24.** Schematic graphic of the cysteine proteases of parasitic organisms.

Like all the enzymes, cysteine proteases present a substrate specificity governed by the nature of the amino acid residues in the proximity at the cleavage site. The nomenclature

used to define the binding pockets<sup>58</sup> is relative to the cleavage site (Figure 25): S<sub>n</sub> represents the enzyme pockets which are numbered S<sub>1</sub>-S<sub>2</sub>-S<sub>n</sub> from cleavage site toward *N*-terminus (non-primed pockets), whereas are indicated as S<sub>1'</sub>-S<sub>2'</sub>-S<sub>n'</sub> toward *C*-terminus (primed pockets). At the same way, the number of substrate residues initiates from scissile bond and, in agreement with enzyme pocket numeration, they are numbered P<sub>1</sub>-P<sub>2</sub>-P<sub>n</sub>, and P<sub>1'</sub>-P<sub>2'</sub>-P<sub>n'</sub>, toward *N*-terminus and *C*-terminus, respectively.

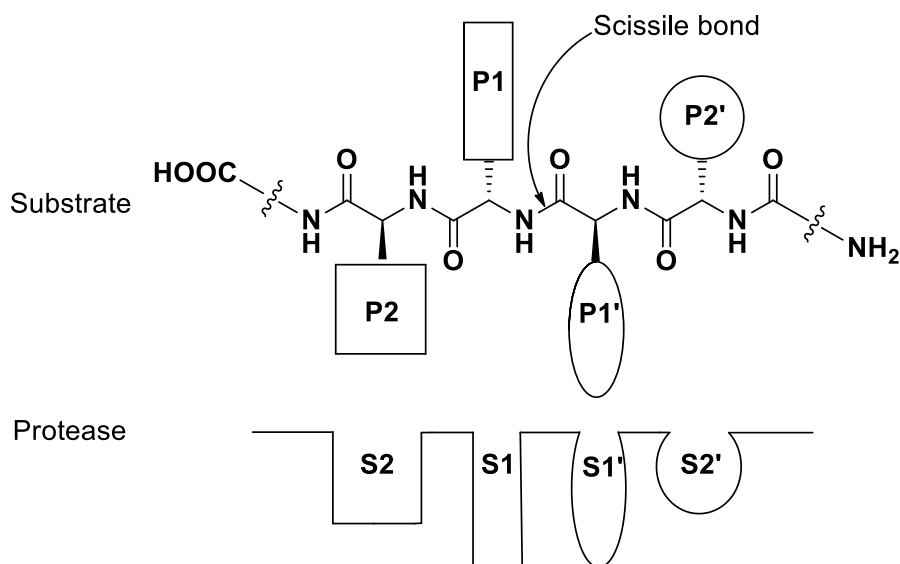


**Figure 25.** Nomenclature of the substrate specificity of protease.

The majority of parasitic cysteine proteases belong to the family C1, within clan CA. In turn, family C1 consists of three subfamily: cathepsin B-like, cathepsin-L-like and bleomycin-hydrolase. The two cathepsin subfamilies are distinct<sup>55</sup> for the presence in the cathepsin L-like subfamily of a highly conserved amino acid motif in the propeptide region of the protein, called ERFNIN motif, while cathepsin B-like proteases are characterized by the presence of an occluding loop.

The major cysteine proteases expressed by *T. brucei* are rhodesain, a cathepsin L-like protease also known as TbCatL, and the cathepsin B-like TbCatB: both represent promising targets for novel antitrypanosomal agents. Their importance was demonstrated in several studies<sup>7a,b</sup>: the silencing of TbCatB cured mice of trypanosomal infection, while rhodesain suppression only prevented the transition from stage 1 to stage 2 and prolonged the life span of the infected mice. Conversely, more recent studies carried out by Steverding<sup>7c</sup> and co-workers, suggested that TbCatL, rather than TbCatB, is the essential

cysteine protease of *T. brucei* and should be considered the primary target for HAT treatment.

### 3.3 Rhodesain: structure and functions

Rhodesain is the major cysteine protease of *T. b. rhodesiense*, consisting of a single polypeptide chain of 215 amino acids with typical papain-like folding, characterized by a (Figure 26) left (L) and a right (R) domain and with the catalytic triad (Cys25/His162/Asn182) located in a cleft between the two domains.<sup>22</sup>

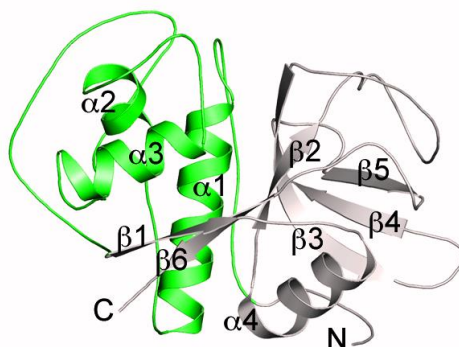


**Figure 26.** The figure shows the secondary structure of *T. brucei* rhodesain, with two domains left (green) and right (gray).

In *T. b. brucei*, the major cysteine protease is called brucipain, with a very high homology degree (98.4%) with rhodesain. Furthermore, rhodesain possesses a high structural similarity to cruzain, the main cysteine protease of *T. cruzi*, the aetiological agent of Chagas disease, and a slightly lower similarity with falcipain-2 (FP-2) and falcipain-3 (FP-3), the major cysteine proteases of the human malaria parasite *Plasmodium falciparum*.

Like all the cysteine proteases, the catalytic mechanism starts with the conversion of the weakly nucleophilic thiol group of the Cys25 to a highly nucleophilic thiolate anion (Figure 27), and this process involves the two remaining amino acids of the catalytic triad.

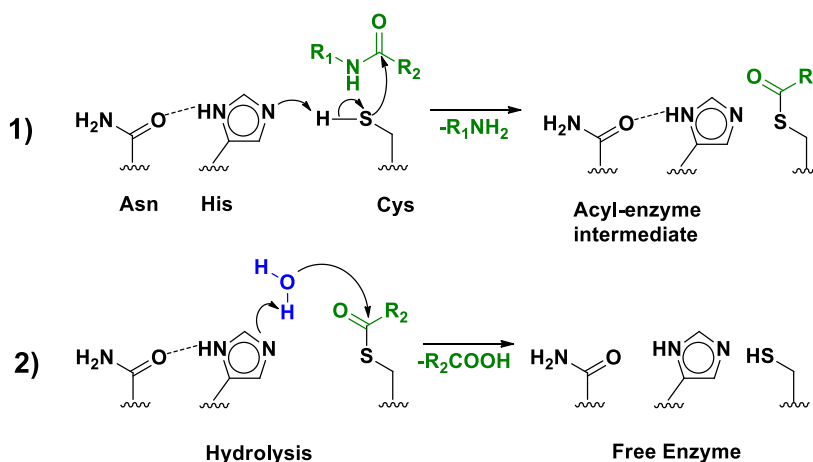


**Figure 27.** Mechanism of hydrolysis mediated by cysteine proteases.



The Asn182, acting as H-bond acceptor, is responsible for the stabilization of the correct tautomeric form of the His162 imidazole ring, which acts as base in the deprotonation process of thiol group. In this condition, the Cys25 thiolate anion is able, by nucleophilic attack, to cleave the amide bond. After that, other amino acid residues are concerned to permit amide bond hydrolysis and the regeneration of the free enzyme.

Two different crystal structures of rhodesain, in complex with vinyl sulfone inhibitors K11777 and K11002 (Figure 28), which will be described in the following chapter, were reported (PDB codes 2P7U<sup>21</sup> and 2P86,<sup>22</sup> respectively). Furthermore, northern blot analysis demonstrated that the amounts of rhodesain mRNA expressed, both the bloodstream and the procyclic forms of the parasite, are equal.<sup>7a</sup>

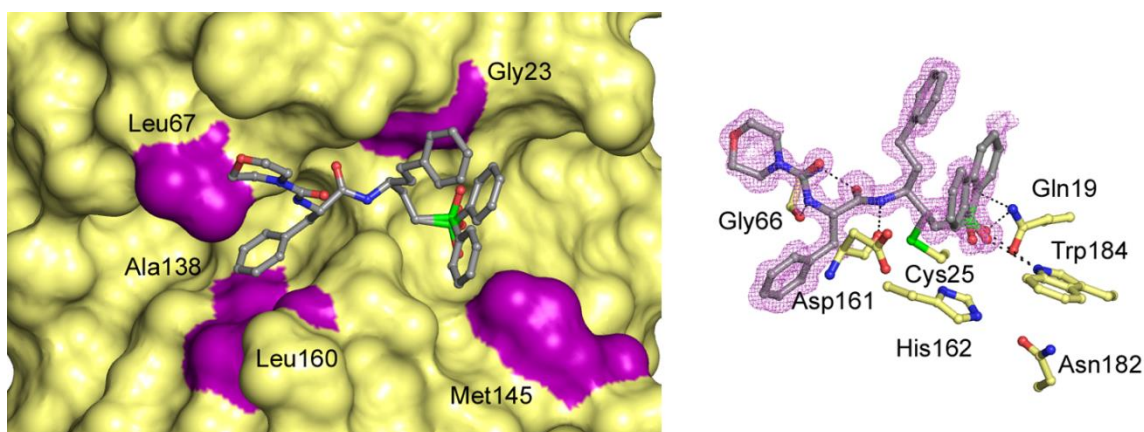


**Figure 28.** Crystal structure of rhodesain in complex with K11002.

Rhodesain plays key roles both in disease progression and in parasite survival, and it is considered a promising target towards which to develop novel potential antitrypanosomal agents.<sup>8</sup> Rhodesain is necessary to cross the BBB, promoting the disease evolution from stage 1 to stage 2.<sup>9</sup> It was hypothesized that BBB dysfunction are related to the interactions of rhodesain with G<sub>q</sub> Protein Coupled Receptors (GPCRs), also known as Protease Activated Receptors (PARs).<sup>59</sup> The activation of this protein enables to cross the BBB after cytoskeletal rearrangements, inducing cell retraction and loosening of junctional complexes. G<sub>q</sub> proteins activated by rhodesain, activate phospholipase C (PLC), in turn generating inositol-1,4,5-triphosphate (IP<sub>3</sub>) and diacylglycerol (DAG) from phosphatidylinositol-4,5-bisphosphate (PIP<sub>2</sub>). The binding of IP<sub>3</sub> to its receptor, placed on the endoplasmic reticulum, releases Ca<sup>2+</sup>: the resulting increase of intracellular calcium activates calmodulin of Myosin Light Chain Kinase (MLCK) and/or other effectors leading to cytoskeletal changes and barrier dysfunction. Beyond that pathway, Ca<sup>2+</sup>-independent

activation of the cytoskeleton generated by Ras-superfamily GTPases (i.e RhoA) traditionally activated by  $G_{\alpha 12/13}$ , could lead to alterations of the adherens junctions and tight junctions, by means the protein p63RhoGEF.<sup>60</sup>

As mentioned above, the surface of BSF of *T. brucei* is covered by a dense coat, consisting of VSGs, which is attached at the C-terminus to the cytoplasmic membrane *via* a glycosylphosphatidylinositol (GPI) anchor.<sup>61</sup> VSGs play a key role in elusion of the host immune response, through two main mechanisms. The first one is the duplicative transposition of a silent VSG gene into one of the telomeric VSG expression sites of the *Trypanosoma*, resulting in the replacement of the previously expressed VSG gene.<sup>62</sup> Only one of approximately one thousands of VSG genes is expressed from a VSG gene expression site: a combination of genetic recombination and VSG expression site switching is responsible for regular changes in VSG expression,<sup>63</sup> against which the host has not yet produced specific antibodies. On the other hand, VSGs are constantly removed from the parasite's surface by rapid internalization and recycling: it was suggested that rhodesain could act as congoxin, orthologous enzyme in *T. congolense*, which plays a key role in the degradation of VSGs within the lysosome.<sup>10,64</sup> This proteolytic process is fundamental to ensure the amino acids requested for synthesis of novel VSGs. The anti-VSG antibodies are internalized also, to be degraded: in particular, the peptidases destroyed the IgG, with decreasing of their amount. Pre-treatment of the *Trypanosoma* with cysteine protease inhibitors, K11777 and E-64<sup>65</sup> (Figure 29), prevented IgG degradation,<sup>11</sup> demonstrating as rhodesain contributes significantly to IgG degradation.

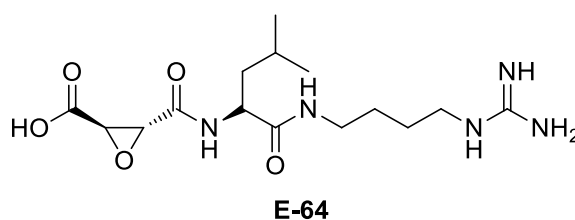


**Figure 29.** Chemical structure of potent cysteine proteases inhibitor E-64.

### 3.4 TbCatB: structure and functions

TbCatB is a Clan CA, family C1 (papain-like) cysteine protease belonging, differently to the rhodesain, to cathepsin B-like cysteine protease subfamily. It consists of 341 amino acids and it is composed by two domains (Figure 30), left (L) and right (R), with an

occluding loop of approximately 20 amino acids located on the surface of cathepsin B-like, and with the typical catalytic triad Cys42/His282/Asn302.<sup>22</sup>

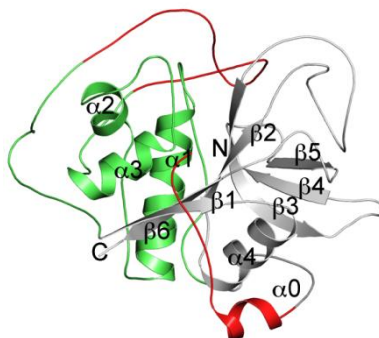


**Figure 30.** Secondary structure of TbCatB. It is noted the occluding loop (red).

Furthermore, TbCatB was co-crystallized in complex with CA074 (Figure 31), a peptidyl epoxide inhibitor (PDB code 3HHI).<sup>22</sup> By northern blot analysis it was demonstrated that TbCatB mRNA was less expressed with respect to rhodesain mRNA, both in the BSFs and PCFs.<sup>7a</sup> In addition, the mRNA for TbCatB was up-regulated in the BSF parasites: this expression difference suggests that TbCatB is regulated at the transcriptional level and carries out its activities mainly in this form. Because they lack cytochromes, the BSF of *T. brucei* acquires iron from the host transferrin,<sup>7a</sup> through its internalizing receptor-mediated endocytosis.

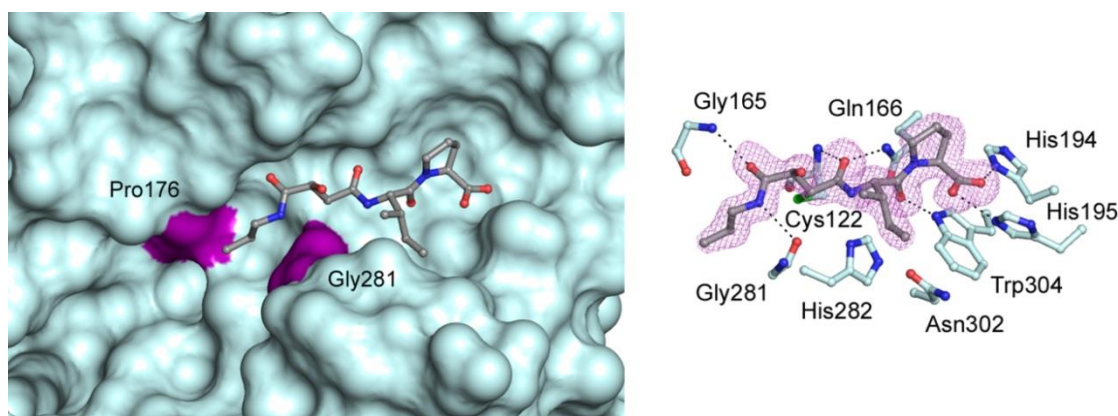


**Figure 31.** Co-crystal structure TbCatB-CA074.

Then, transferrin is rapidly degraded in the “endosome/lysosome” located between the nucleus and kinetoplast of the parasite: it was demonstrated that TbCatB is the major protease involved in this fundamental process. In addition, it was observed the parasite ability to complete multiple steps of genomic replication and mitosis, but were not able to

finish the cytokinesis. It is possible that TbCatB could also be involved in a microtubule-related event: lack of cytokinesis may be an indirect consequence of iron depletion because of the incapacity of the parasite to degrade transferrin.<sup>7a</sup>

A superimposition of the rhodesain-K11002 and TbCatB-CA074 complexes brings to highlight important structural differences between the two enzymes. The S2 site of rhodesain is restricted with respect to TbCatB, due to the presence of Ala208 at the bottom of S2 site, while at the S2 pocket bears Gly328, less bulky. Furthermore, the Leu67 residue presents around the S2 site of rhodesain creates a hydrophobic environment, where the Phe residue at P2 position of K11002 well fits. On the other hand, around S2 site of TbCatB is presents Asp166, with its relative acid function. Another relevant structural feature is due to the presence in TbCatB, of the occluding loop, which creates a large prime side pocket in the catalytic site cleft.

Considering the key roles of rhodesain and TbCatB during different phases of parasite life cycle, it is presumable that the co-inhibition of both enzymes could be certainly desirable in the development of novel antitrypanosomal agents.

## CHAPTER 4: RHODESAIN INHIBITORS

In this chapter, we describe the most active rhodesain inhibitors reported in the literature to date, with particular attention to their chemical composition, mechanism of action, binding mode and SAR.

### 4.1 Peptide-based inhibitors

Peptide molecules are recognized for their high selective, efficacy and tolerability. There is an important interest in peptides as potential therapeutic agents,<sup>66</sup> and a growing number of peptides, approximately 140, are currently evaluated in clinical trials. Sometimes, natural peptides are not suitable for use as convenient therapeutics because of their intrinsic weaknesses, as poor chemical and physical stability, and a short circulating plasma half-life. On the contrary, peptides designed for use as drugs show various advantages, summarised in table 4 (Source: Marx, V. 2005. "Watching Peptide Drugs Grow Up." Chemical & Engineering News).

<b>Table 4. Features of peptide drugs</b>	
<b>Advantages</b>	<b>Disadvantages</b>
High activity	Low orally bioavailability
High specificity	Injection required
Little unspecific binding to molecular structures other than desired target	Difficult delivery and challenge to transport across membranes
Minimization to drug-drug interactions	Less stable
Less accumulation in tissues	Challenging and costly synthesis
Lower toxicity	Solubility challenges
Often very potent	Risk of immunogenic effects
Biological and chemical diversity	Cleared of body quickly

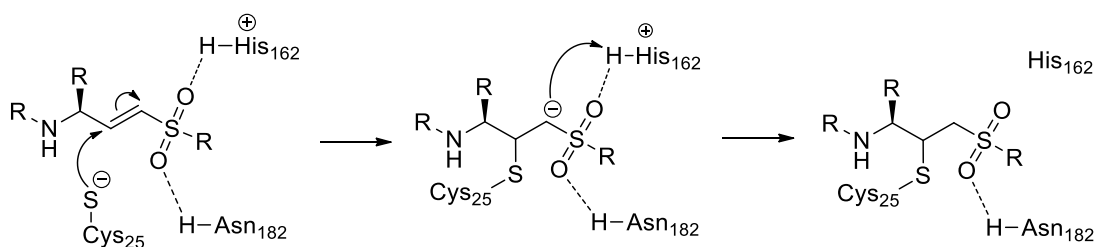
To date, peptide inhibitors targeting rhodesain show two common structural features: a peptide fragment necessary for recognition by the enzyme and an electrophilic portion, called warhead, which undergoes the nucleophilic attack of the cysteine residue of the catalytic site.

Diazomethylketone Cbz-Phe-Ala-CH<sub>2</sub>N<sub>2</sub> **23** and E-64 (see chapter 3) are potent cathepsin inhibitors, but they are not selective for the several type of cathepsin. To avoid indiscriminate reactivity with other thiol-containing enzymes, the intrinsic reactivity of the warhead must be sufficiently low, in order to reaction with Cys anion take places only after a specific noncovalent binding of recognition segment, in such a way that the warhead be at a distance and orientation favourable for the reaction. The important challenge is

represented on the development of cysteine protease selective inhibitors, endowed with a high selectivity degree between parasite and mammalian enzymes, by exploiting the few differences surrounding the catalytic site.

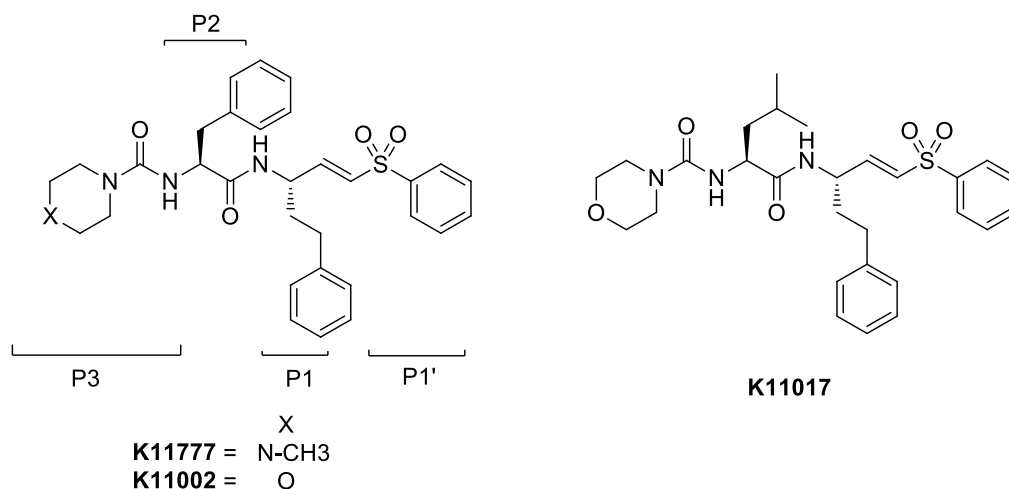
#### 4.1.1 Vinyl sulfones

One of the most relevant class of cysteine protease inhibitors are vinyl sulfones, who act as Michael acceptors, due to their ability to covalently trap the Cys residue at the catalytic site.<sup>67</sup> These inhibitors ensure an irreversible inhibition, because the novel covalent bond is stable and the enzyme cannot back to active form, even by increasing the concentration of natural substrate. Mechanism of action (Figure 32) was proposed: the sulfone oxygens interact by hydrogen bond with the catalytic triad residues His and Asn and these bonds would lead to polarization the vinyl group, with activating the  $\beta$ -carbon towards the nucleophilic attack. The negative charge resulting at the  $\alpha$ -carbon is immediately eliminated via protonation by the histidinium residue.



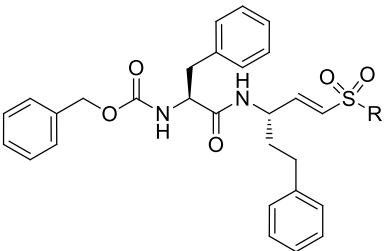
**Figure 32.** Mechanism of action of vinyl sulfones. Many vinyl sulfones were demonstrated to be potent rhodesain inhibitors.

As mentioned in chapter 3, given the high potency of peptide-based vinyl sulfones, two different crystal structures of rhodesain in complex with inhibitors K11777 (Figure 33) and K11002 were deposited to PDB, with codes 2P7U<sup>21</sup> and 2P86<sup>22</sup>, respectively.



**Figure 33.** Chemical structures of potent rhodesain inhibitor with vinyl sulfones warhead.

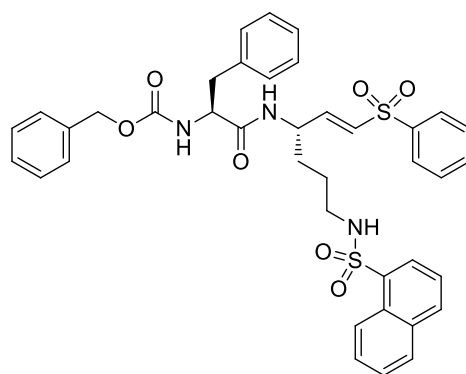
In 2001, Caffrey et al., carried out a study<sup>68</sup> to evaluate the different reactivity of several substituents at the P1' site, maintaining Cbz-Phe-hPhe as recognition moiety (Table 5). Data collected showed an emerging trend of reactivity: sulfonates were found to be the best inhibitors, with one order of magnitude above those displayed for aliphatic and aromatic sulfones. The introduction of bulky substituents at the P1' site, namely CH<sub>2</sub>CH<sub>2</sub>Ph (**24d**) and NPh (**24e**), respectively, led to a slight decrease of potency. On the contrary, the addition of a methylene group (**24b**) and an oxygen atom (**24a**), to afford benzyl and sulfonate analogues, respectively, increased the activity against the enzyme. At the P1 position, hPhe amino acid is strongly preferred by rhodesain: this residue possesses the essential features to well fit at the S1 pocket.

	Comp	R	$k_{2nd}$ (M <sup>-1</sup> min <sup>-1</sup> )
	<b>24a</b>	-OPh	3.48 x 10 <sup>8</sup>
	<b>24b</b>	-CH <sub>2</sub> Ph	5.35 x 10 <sup>7</sup>
	<b>24c</b>	-Ph	1.61 x 10 <sup>7</sup>
	<b>24d</b>	-CH <sub>2</sub> CH <sub>2</sub> Ph	1.09 x 10 <sup>7</sup>
	<b>24e</b>	-NPh	2.24 x 10 <sup>6</sup>

Additional studies have shown that the S2 site is responsible for the specificity of rhodesain against peptidyl substrates.<sup>69</sup> Rhodesain is able to tolerate various bulky hydrophobic residues within S2 pocket, due to the presence of the Leu67 residue which make S2 pocket mainly hydrophobic. More in detail, the highest preferences were shown towards leucine and phenylalanine, in equal measure. Moreover, Ala208 residue at the bottom of the S2 pocket makes the pocket deep, while Gln159 and Leu160 further narrow the pocket.<sup>21</sup> However, rhodesain is 50% less reactive towards a substrate with  $\beta$ -branched residue at the P2 site (i.e valine) and is completely inactive in the presence of arginine (Arg) at this site.<sup>68</sup> With regarding the S3 pocket, a comparison between the complexes rhodesain-K11777 and rhodesain-K11002, demonstrates that despite the cysteine protease is unable to establish specific polar interactions with morpholine urea portion of K11002, this group is preferred compared to *N*-methyl piperazine nucleus of K11777, of larger size. An comparative study<sup>21</sup> was carried out between inhibitor K11017 (Figure 33) and K11777, which differ for amino acid residue at the P2 site. Compound K11017 showed a  $k_{2nd}$  value slightly higher than K11777 ( $k_{2nd}$  = 15.84 x 10<sup>6</sup> M<sup>-1</sup> min<sup>-1</sup> vs 9.00 x 10<sup>6</sup> M<sup>-1</sup> min<sup>-1</sup>,

respectively): considering that both vinyl sulfones contain the amino acids preferred at the P2 site, the slight different  $k_{2nd}$  values can be explained by additional interactions. It was suggested that the morpholine ring at the P3 site of K11017 is able to create a network of water molecules that anchors the morpholine oxygen to the polar residues in the S3 pocket; on the contrary, K11777, containing the *N*-methyl-piperazine nucleus, is not able to create these polar interactions, and this might explain its reduced reactivity. When evaluated against BSFs of *T. brucei*, K11777 showed a good sub-micromolar activity ( $EC_{50}$  = 0.9  $\mu$ M), coupled with a poor oral bioavailability (19.9%), but better than K11002, with only 3%. In this case, the difference is primarily attributable to an increased solubility in intestinal fluids of K11777, due to *N*-methyl-piperazine ring.<sup>70</sup> In addition this nucleus might vehicular the drug to concentrate within the acidic compartments,<sup>71</sup> property known as lysosomotropism: this feature is highly desired, taking into consideration that rhodesain is mainly localized in the lysosomes. Currently, K11777 is into phase I clinical trials to evaluate tolerability, safety, and pharmacokinetics in healthy patient volunteers.

In 2013, vinyl sulfones bearing Phe or Leu at the P2 site and basic residues at the P1 site (Figure 34) were developed.<sup>72</sup> When tested against parasite, these molecules showed an optimal antitrypanosomal activity, with  $EC_{50}$  values ranging from 0.07 to 26.4  $\mu$ M. With a few exception, these inhibitors displayed a more than two fold selective inhibition of parasite with respect to mammalian cells: the most promising compound of the series was proven to be inhibitor **25**, with a selectivity index (SI) of 785.



**25**

*T. b. b.*:  $EC_{50}$  = 0.07  $\mu$ M  
Selectivity Index over HL-60 = 785.7

**Figure 34.** Chemical structure of best inhibitor developed and its biological evaluation.

In the same work, were carried out computational studies on rhodesain and TbCatB. Compound **25** interacts with both enzymes by key H-bonds, in the same way of K11777. An important difference was found relatively to binding mode of naphthylsulfonamido



moiety: in TbCatB, the Asn163 residue allows the formation of a hydrogen bond *via* water-mediated interaction, while in rhodesain Asn163 is replaced by Gly64, which is not able to create this interaction.

#### 4.1.2 Azadipeptide nitriles

Another important class of peptide-based cysteine protease inhibitors is represented by azadipeptide nitriles. The mechanism of action (Figure 35) of these molecules is based on the reaction between the nitrile carbon and Cys anion, with the formation of a reversible isothiosemicarbazide adduct,<sup>73</sup> with good stability, probably due to resonance of the nitrogen atom lone pair and the  $sp^2$ -hybridized carbon atom derived from the cyano group. Moreover, the modified amide bond by *N*-methylation presents an improved stability towards proteolytic degradation compared to typical peptide bond.

This class of compounds shows a reversible inhibition. This type of inhibition is characterized by weak interaction between enzyme and inhibitor, and when inhibitor is removed, enzymatic activity was fully restored.

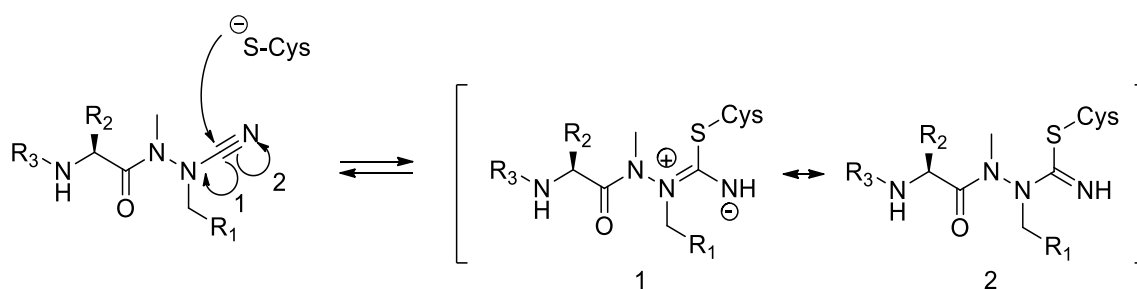


**Figure 35.** Mechanism of action of azadipeptide nitriles.

An equilibrium is established between the free enzyme and the non-covalent enzyme-inhibitor complex and is regulated by the dissociation constant  $K_i$  that measures the binding affinity towards the enzyme: lower is the  $K_i$  value higher is binding affinity. In 2012, Yang et al. developed novel azadipeptide nitriles<sup>15</sup> characterized by a common substituent at the P3 site, various hydrophobic amino acids at the P2 site (i.e Phe, Val and Leu), towards which rhodesain demonstrated a strong preference, and substituents of different sizes at the P1 site, both of aromatic and aliphatic chemical nature. As it was expected, derivatives bearing Phe (**26a-e**) and Leu (**26f-j**) residue at the P2 site showed  $IC_{50}$  values (Table 6) 1–2 orders of magnitude lower than the analogues bearing Val at the same position. With regard to the P1 site, the single methyl substituent was well tolerated by rhodesain, with respect to bulkier substituents, whose presence led to reduction of

Table 6. Biological evaluation of azadipeptide nitriles 26a-o				
<p style="text-align: center;"><b>26a-o</b></p>	<b>Comp</b>	<b>R<sub>1</sub></b>	<b>R<sub>2</sub></b>	<b>Rhodesain IC<sub>50</sub> (nM)</b>
	<b>26a</b>	H		0.14
	<b>26b</b>	Ph		0.51
	<b>26c</b>	Bn		1.86
	<b>26d</b>	CH <sub>2</sub> Bn		0.24
	<b>26e</b>	(CH <sub>2</sub> ) <sub>3</sub> Me		1.34
	<b>26f</b>	H		5.4
	<b>26g</b>	Ph		15.8
	<b>26h</b>	Bn		35.1
	<b>26i</b>	CH <sub>2</sub> Bn		54.0
	<b>26j</b>	(CH <sub>2</sub> ) <sub>3</sub> Me	54.6	
	<b>26k</b>	H	0.06	
	<b>26l</b>	Ph	0.33	
	<b>26m</b>	Bn	0.71	
	<b>26n</b>	CH <sub>2</sub> Bn	0.14	
	<b>26o</b>	(CH <sub>2</sub> ) <sub>3</sub> Me	0.33	

inhibitory activity towards the target enzyme. After that, an optimization study of the most active Phe analogue **26a** was carried out: replacement of the 2,3-dihydro-1,4-benzodioxin-6-yl portion with Boc group, led to more potent rhodesain inhibitor **27** (AZN-16), with an impressive IC<sub>50</sub> value of 0.06 nM (Table 7).

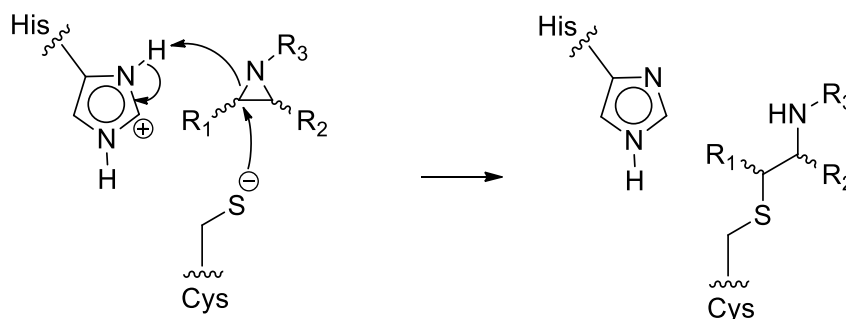
Further optimization of compound **27** was carried out, introducing Cbz protecting group at the P3 site and the substituents previously used for compounds **26a-o** at the P1 site: compounds with Cbz moiety were proven to be potent rhodesain inhibitor, with EC<sub>50</sub>

Table 7. Potent azadipeptide nitriles and their biological					
	<b>R<sub>1</sub></b>	<b>R<sub>2</sub></b>	<b>Rhodesain IC<sub>50</sub> nM</b>	<b>BSF</b>	<b>PCF</b>
				<b>EC<sub>50</sub> μM</b>	
<b>27 (AZN-16)</b>	H	Boc	0.06		
<b>28a</b>		Cbz		0.4	n.d.
<b>28b</b>	Ph		0.19	1.1	0.4
<b>28c</b>	Bn		0.81	n.d.	n.d.
<b>28d</b>	CH <sub>2</sub> Bn		2.0	1.2	0.7
<b>28e</b>	(CH <sub>2</sub> ) <sub>3</sub> Me		0.06	1.4	0.7
n.d. : not determined					

values in the low micromolar/submicromolar range against *T. b. brucei*, both towards BSF and PCF. All in all, azadipeptide nitriles displayed good correlation between the rhodesain inhibition and antitrypanosomal activity, probably due to both their ability to cross the parasite membrane and their high stability against proteolysis. To consider these compounds as novel agents for HAT treatment, should be carried out additional studies, like evaluation of target selectivity and of cytotoxicity.

#### 4.1.3 Aziridine-2,3-dicarboxylates

Another class of irreversible rhodesain inhibitors is represented by aziridine-2,3-dicarboxylates,<sup>74</sup> which undergo the Cys anion attack at one of the electrophilic ring carbon atoms followed by opening of the aziridine ring (Figure 36).



**Figure 36.** Mechanism of action of aziridines.

The most active inhibitors towards rhodesain, with  $K_i$  values in submicromolar range, are displayed in Table 8: each of them bears a Cbz group at both membered ring carbons with trans stereochemistry,<sup>75</sup> while the *N*-substituents are characterised by another ring of different size and Boc protected leucine.

Selectivity assays were carried out: the results indicated a modest activity against human cathepsin L (hCatL) in the range 0.013-6.4  $\mu\text{M}$ , while, with the only exception of compound **29b** and **29f**, no inhibition of human cathepsin B (hCatB) was recorded. Antitrypanosomal activity of these inhibitors is relatively low, with  $\text{EC}_{50}$  values ranging from 10.9 to 34.0  $\mu\text{M}$ , while generally no cytotoxicity was exhibited, except for inhibitors **29a** and **29f**.

**Table 8. Chemical structures and biological activity of the most potent aziridines.**

Comp	Rhodesain	hCatL	hCatB	<i>T. b. b.</i>	Macrophages
	$K_i$ $\mu\text{M}$			$\text{EC}_{50}$ ( $\mu\text{M}$ )	$\text{TC}_{50}$ ( $\mu\text{M}$ )
<b>29a</b>	0.8	3.8	n.i.	30.8	37.2
<b>29b</b>	0.5	0.4	115	10.9	> 125
<b>29c</b>	0.7	6.4	n.i.	27.6	n.d.
<b>29d</b>	0.6	4.4	n.i.	25.6	> 100
<b>29e</b>	0.7	4.2	n.i.	34.0	> 100
<b>29f</b>	0.3	0.013	9.4	25.7	50.0
n.d.: not determined; n.i.: no inhibitor					

#### 4.1.4 Peptidyl aldehydes and ketones

Peptidyl aldehydes and ketones represent an interesting class of rhodesain inhibitors. Peptidyl aldehydes, despite covalently interacting to the Cys25, are time-independent inhibitors (Figure 37), because the nucleophilic attack on the carbonyl creates a reversible tetrahedral hemithioacetal.

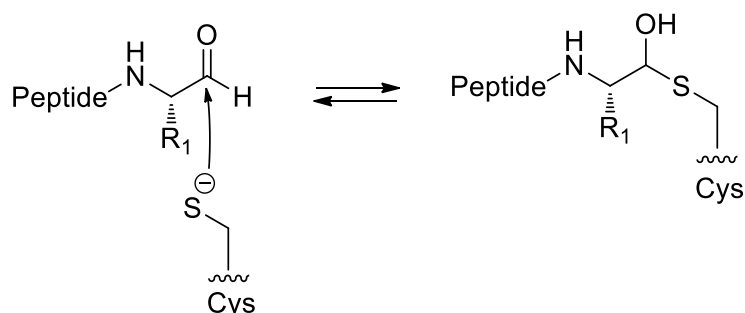
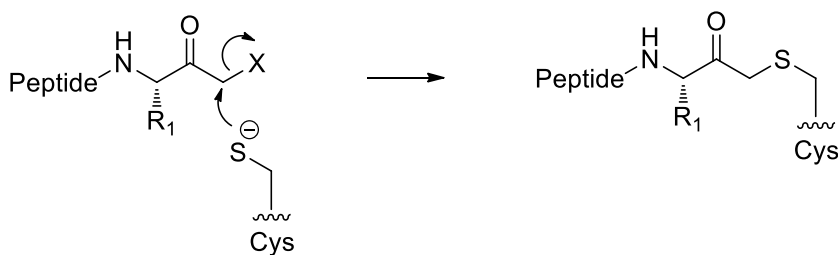


**Figure 37.** Mechanism of action on peptidyl aldehydes.

In 2003,<sup>76</sup> compounds **30** and **31** (Table 9), previously reported as hCatL inhibitors, were evaluated towards rhodesain with better results. Compound **30**, bearing a Tyr at the P1 site, showed a great potency towards rhodesain, as well as inhibitor **31**, with  $k_{2nd}$  value 1 order of magnitude lower than those reported towards cathepsins. Both compounds exhibited  $EC_{50}$  values in the nanomolar range against *T. b. brucei*, with a very high SI. In particular, compound **31** showed the best profile, probably due to naphthyl substituent at the P3 position, able to increase the lipophilicity and promote the membrane's crossing.<sup>77</sup>

Table 9. Chemical structures of potent aldehydes				
Comp	Rhodesain $k_{2nd}$ ( $M^{-1}\cdot min^{-1}$ )	<i>T. b. brucei</i> $EC_{50}$ (nM)	HL-60 $TC_{50}$ (nM)	SI $TC_{50}/EC_{50}$
<b>30</b>	$1.38 \times 10^8$	45	21500	482
<b>31</b>	$3.54 \times 10^7$	18	21000	1150

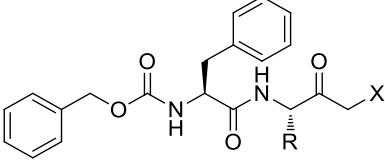
On the contrary, chloro-, fluoro- or diazo-methylketones create an irreversible covalent bond, with leaving non-metal atom (Figure 38). Several methylketone analogues inhibit rhodesain with very high  $k_{2nd}$  values, coupled with low micromolar activity against *T. b. brucei*.<sup>56,57</sup>



**Figure 38.** Mechanism of action of peptidyl ketones.

The best antiparasitic activity (Table 10) was recorded for inhibitors **33a** and **33b**, both bearing Phe residue at the P2 site: probably, the presence of three phenyl ring with respect

to methyl analogues **32a-c**, confers to the molecules higher capacity to cross the biological membranes. To date, no selectivity assays were reported.

	Comp	R	X	Rhodesain $k_{2nd}$ ( $M^{-1} min^{-1}$ )	<i>T. b. b.</i> EC <sub>50</sub> ( $\mu M$ )
	<b>32a</b>	CH <sub>3</sub>		N <sub>2</sub>	$3.8 \times 10^7$
<b>32b</b>	Cl			$6.7 \times 10^7$	21
<b>32c</b>	F			$9.2 \times 10^7$	31
<b>33a</b>	CH <sub>2</sub> Ph		N <sub>2</sub>	$1.4 \times 10^7$	4.8
<b>33b</b>			Cl	$12.9 \times 10^7$	3.6

## 4.2 Peptidomimetics

In this section, features of peptidomimetics will be described and, in particular, the potential use for the treatment of HAT. A peptidomimetic is a molecule designed to mimic the peptide structure.<sup>78</sup> Usually, arise both from modification of a known peptide or by rational design of fragments that mimic peptides, with the aim to improve the stability, the drug-like properties and the biological effect. Among the many possible modifications,<sup>79</sup> the most well-known are the modifications of the peptide backbone, the replacement with non-natural amino acid and the introduction of a rigid scaffold able to create a locked conformation.

The 1,4-benzodiazepine (BDZ) scaffold is a  $\beta$ -turn mimetic<sup>16</sup> on which various cysteine protease inhibitors were developed. This structural motif was widely used, as demonstrated in literature: anxiolytics, hypnotics and anticonvulsants are just a few examples of drug commercially available bearing a BDZ scaffold. Furthermore, this scaffold is characterized by a good oral bioavailability and tolerability. Observing the chemical structure, it is noted that the condensed aromatic ring could be able to mimic the Phe residue at the P2 site (Figure 39).

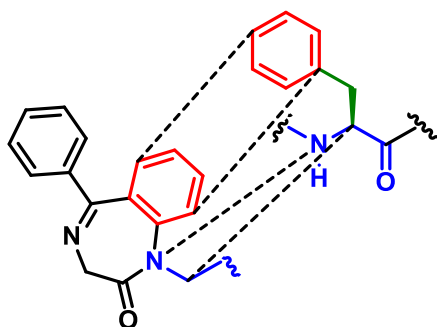


**Figure 39.** Superimposition between BDZ scaffold and Phe residue.

#### 4.2.1 BDZ derivatives with aldehyde warhead

Starting from these considerations, Micale et al.<sup>80a</sup> developed a first series of cysteine protease inhibitor containing the BDZ scaffold functionalized at C3 (Figure 40), by introduction of a hydroxymethyl group in *R* configuration, which was used to insert different substituents, so that it can create additional interactions with the S3 pocket of cysteine protease. To be noticed that, the hydroxymethyl portion mimics the serine amino acid side chain. On the other hand, at the *C*-terminal moiety an aspartic aldehyde warhead was introduced, while at C2 of lactone ring, *S*-*t*Butyl and *O*-Bn groups were inserted, to accommodate into S1 pocket.

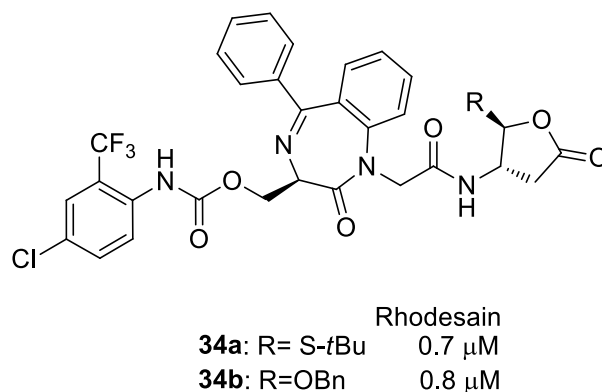


**Figure 40.** Chemical structures and biological evaluation of inhibitor **34a-b**

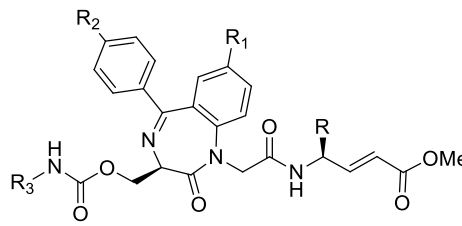
Compounds **34a-b** were tested against rhodesain and  $K_i$  values in submicromolar range were recorded.<sup>80b</sup> These results highlighted the strong preference of rhodesain for bulky substituents at the P1 site, as we also discussed for vinyl sulfone inhibitors. Compound **34b** was evaluated for its antiparasitic activity towards *T. b. brucei*, showing an  $EC_{50}$  value of 14.2  $\mu$ M, comparable to rhodesain inhibition.

#### 4.2.2 BDZ derivatives bearing vinyl ester portion as warhead

To further explore the rhodesain pockets, analogues of compounds **34a-b** were developed,<sup>17</sup> where the lactone ring was replaced with a vinyl ester portion (Table 11). At the P1 site, a leucine was inserted (**35**), to evaluate the impact of a bulkier substituent with respect than glycine. Chlorine and bromine, in compound **36** and **37**, respectively, were introduced in *para* position of the phenyl on the BDZ scaffold and at C-4' on the fused benzene ring. At P3 position, the 4-chloro-2-trifluoromethylphenyl group was replaced with 1-naphthyl (**40**) and 1-adamantyl portions (**9**) and *p*-MeOPh ring (**39**). With the exception of compound **39-40**, the inhibitors inhibited rhodesain in an irreversible manner:

the best results were obtained by compound **9**, bearing an adamantyl nucleus able to create hydrophobic interactions with the P3 pocket. Compound **39-40** showed time-independent activity, probably due to P3 substituent, which can induce an incorrect fit of the warhead, preventing the formation of the irreversible Michael adduct.

**Table 11. Biological result of inhibitors 9 and-35-40**

					
Comp	R	R <sub>1</sub>	R <sub>2</sub>	R <sub>3</sub>	Rhodesain <i>k</i> <sub>2nd</sub> (M <sup>-1</sup> x min <sup>-1</sup> )
<b>35</b>	H	H	H	4-Cl-2-CF <sub>3</sub> C <sub>6</sub> H <sub>4</sub>	3.46 x 10 <sup>4</sup>
<b>36</b>	<i>i</i> -C <sub>4</sub> H <sub>9</sub>	H	H		3.60 x 10 <sup>4</sup>
<b>37</b>	H	Cl	H		2.20 x 10 <sup>5</sup>
<b>38</b>	H	H	Br		4.60 x 10 <sup>4</sup>
<b>39</b>	H	H	H	<i>p</i> -MeOC <sub>6</sub> H <sub>4</sub>	Time-independent inhibition
<b>40</b>	H	H	H	1-naphthyl	
<b>9</b>	H	H	H	1-adamantyl	4.62 x 10 <sup>6</sup>

With a few exceptions, all compounds showed an excellent target selectivity: the obtained *K<sub>i</sub>* values against hCatB and hCatL were 1–2 orders of magnitude higher than those reported for rhodesain inhibition. The best selectivity was shown by compound **9** which showed a poor inhibition of hCatL (*k*<sub>2nd</sub> = 4.62 x 10<sup>6</sup> M<sup>-1</sup> min<sup>-1</sup> and 0.55 x 10<sup>3</sup> M<sup>-1</sup> min<sup>-1</sup> for rhodesain and hCatL, respectively). Considering these good features, compound **9** was evaluated for its antitrypanosomal activity: the obtained EC<sub>50</sub> value of 4.8 μM, indicates the ability of this compound to cross the parasitic membranes, probably due to its lipophilic properties.

#### 4.2.3 3-Bromo isoxazoline inhibitors

Recently, another important class of peptidomimetics was developed to inhibit rhodesain.<sup>81</sup> Starting from the BDZ scaffold, the 3-bromoisoxazoline nucleus, free or incorporated into a bicyclic system, was used as innovative warhead (Table 12). This idea takes place because 3-bromo acivicin is a potent trypanocidal agent,<sup>14</sup> targeting the cytidine triphosphate synthetase, an ubiquitous cysteine protease.



The natural product acivicin, with a chlorine atom at C3, acts by the attack of the thiol function directly on C-3 of the isoxazoline ring, with leaving of the halogen atom and formation of a covalent bond.<sup>82</sup>

Table 12. Biological evaluation of isoxazolines 41-42a-b			
Comp	Warhead	Rhodesain $K_i$ ( $\mu\text{M}$ )	<i>T. b. b.</i> $\text{EC}_{50}$ ( $\mu\text{M}$ )
41a		3.52	16.91
41b		4.63	17.64
42a		0.96	14.04
42b		2.22	17.86

However, peptidomimetics bearing a 3-bromo isoxazoline as warhead were proven to be reversible inhibitors, with time-independent activity. When tested against rhodesain, compounds **41-42a-b** showed  $K_i$  values in the low micromolar/submicromolar range, coupled with an excellent selectivity towards both hCatL and hCatB, and antitrypanosomal activity in the range 14.04-17.86  $\mu\text{M}$ .

In 2014, Ettari et al. designed structurally simplified inhibitors<sup>83</sup> bearing the 3-bromoisoxazoline nucleus (Table 13), with the aim to stabilize the molecules to proteolysis, by replacing the amide bond with aliphatic chains of different lengths (2-4 carbon atoms) connecting the BDZ scaffold and the warhead. At the C3 position, the methylcarbamoyl chain was modified or removed, to evaluate the impact of different interactions at the S3 pocket, or the absence of substituents in this site. With the exception of compound **43c**, inhibitors showed low micromolar activity against rhodesain and an excellent selectivity, because no inhibition of hCatB and hCatL was recorded.

**Table 13. Biological result of inhibitors 43-45a-c**

Comp	Rhodesain $K_i$ ( $\mu\text{M}$ )	<i>T. b. b.</i> $\text{EC}_{50}$ $\mu\text{M}$	J774.1 $\text{TC}_{50}$ $\mu\text{M}$
<b>43a</b>	4.38	10.83	>100
<b>43b</b>	2.48	3.78	>100
<b>43c</b>	>10	3.27	>100
<b>44a</b>	2.85	>40	22.3
<b>44b</b>	3.33	>40	22.5
<b>44c</b>	2.44	12.22	12.2
<b>45a</b>	1.70	5.29	>100
<b>45b</b>	2.84	3.54	43.4
<b>45c</b>	1.52	24.58	9.4

Furthermore, derivatives **43b**, **43c**, **45a** and **45b** displayed a single-digit micromolar activity, probably due to an improvement of drug-like properties, necessary to allow them to penetrate into the parasite. In addition, inhibitors with the highest antitrypanosomal activity were tested on macrophages J774.1, revealing lack of cytotoxicity ( $\text{TC}_{50} > 100 \mu\text{M}$ ).

### 4.3 Non peptide inhibitors

In addition to peptide and peptidomimetic inhibitors, various classes of nonpeptidyl molecules were identified as rhodesain and TbCatB inhibitors. The chemical structure of these molecules is extremely variable, including thiosemicarbazones, triazine, purine nitriles, ureas and thioureas, generally identified by virtual screening or high throughput screening approaches.

#### 4.3.1 Triazine nitriles

Triazine nitriles are well-known competitive time-independent cysteine protease inhibitors,<sup>84</sup> bearing and electrophilic portion able to form a reversible covalent thioimidate adduct with Cys anion (Figure 41).

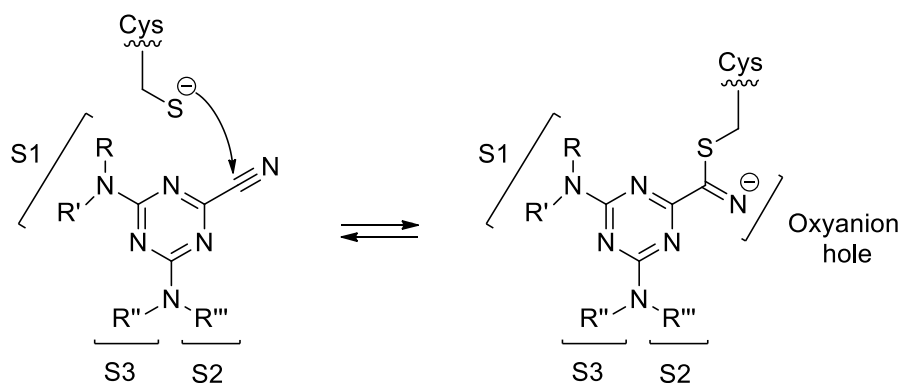


**Figure 41.** Mechanism of action of triazine nitriles.

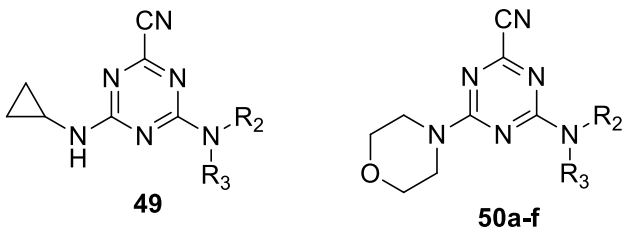
The diamino-triazine nucleus is considered a suitable scaffold to fit substituents present at the two amine groups in the corresponding enzyme pockets. Starting from triazine nitrile **46** (Table 14), Mott et al.<sup>23</sup> synthesized a series of analogues to evaluate the impact of removing one phenyl ring and inserting an electron-donating group (EDG) or an electron-withdrawing (EWG) group on the additional phenyl, while at the other amino group a cyclopentyl ring (**47a-k**) or a 2,2-F<sub>2</sub>-ethyl chain (**48**) were inserted. These molecules were

Table 14. Biological results of triazine nitrile inhibitors <b>46</b> , <b>47a-k</b> and <b>48</b>						
<p style="text-align: center;"><b>46</b></p>		<p style="text-align: center;"><b>47a-k, 48</b></p>				
Comp	R	R <sub>1</sub>	Rhodesain IC <sub>50</sub> μM	TbCatB IC <sub>50</sub> μM	<i>T. b. b.</i> EC <sub>50</sub> μM	
<b>46</b>	-	-	> 10	> 1	> 100	
<b>47a</b>	3-CF <sub>3</sub>	Cyclopentyl	0.07	> 10	25	
<b>47b</b>	3-F		0.02	> 1	100	
<b>47c</b>	3-Cl		0.006	> 100	6	
<b>47d</b>	3-Br		0.006	> 100	6	
<b>47e</b>	3-NO <sub>2</sub>		0.008	> 1	100	
<b>47f</b>	3-CH <sub>3</sub>		0.05	6	25	
<b>47g</b>	3-Ph		0.03	> 10	25	
<b>47h</b>	4-F		0.04	> 1	> 100	
<b>47i</b>	4-Br		0.1	> 10	> 100	
<b>47j</b>	3,5-F <sub>2</sub>		0.005	4	6	
<b>47k</b>	3,5-Cl <sub>2</sub>		0.03	> 10	25	
<b>48</b>	3,5-F <sub>2</sub>		2,2-F <sub>2</sub> -ethyl	0.006	1	6

evaluated on both rhodesain and TbCatB, showing a strong preference for rhodesain. More in detail, compounds with a double substitution in meta position with fluorine atoms (**47j**) showed the best activity, and a comparable potency was shown by compounds bearing an EWG at position 3 of the aromatic ring (**47c-e**). The analogues with an EDG at position 3 (**47f-g**) displayed a slight reduction of activity, as well as the introduction of an EWG at position 4 (**47h-i**) decreased the inhibitory potency. With regard to TbCatB, compounds inhibited the protease in the micromolar range with at least 2 order of magnitude higher compared to rhodesain. Selectivity assays were performed for the most active compounds **47c** and **47j**: activity <1  $\mu\text{M}$  was recorded towards hCatL, while no inhibition (i.e. **47c**) or  $\text{IC}_{50} > 1 \mu\text{M}$  (i.e. **47j**) were registered against hCatB. The best antitrypanosomal activity was shown by 3,5-difluoro substituted compounds **47j** and **48** and by compounds **47c-d**, substituted in the *meta*-position by a halogen atom.

Another SAR study was carried out by Ehmke et. al.,<sup>85</sup> to determine the nature of substituents for the accommodation into the S1, S2 and S3 pockets of rhodesain. The first amino group was enclosed into a morpholine ring (**50a-f**): this substitution gave the best results with respect to *N*-substitution with a cyclopropyl ring (**49**), as shown in table 15.

**Table 15. Biological result recorded for inhibitors 49 and 50a-f**

						
Comp	R2	R3	Rhodesain	hCatL	hCatB	<i>T. b. rhodesiense</i>
			$K_i$ (nM) or % of inh. at 20 $\mu\text{M}$			$\text{EC}_{50}$ ( $\mu\text{M}$ )
<b>49</b>	CyHexyl	CyHexyl	970	30%	10%	25.8
<b>50a</b>			490	2650	10%	31.9
<b>50b</b>	4-propyl-CyHexyl	1,3-benzodioxol-5-ylmethyl	8	33	15%	30.1
<b>50c</b>		Ph	2	690	n.i.	31.2
<b>50d</b>	Ph	Ph	36	124	50%	18.9
<b>50e</b>		CyHexyl	34	230	20%	16.7
<b>50f</b>	<i>o</i> -F-Ph	CyHexyl	11	66	35%	15.0

CyHexyl: cyclohexyl; n.i. : no inhibition.

On the other hand, the double substitution with bulky residues on the other amino group was essential to bind both S2 and S3 pockets of rhodesain. More in detail, the mono-substitution with a cyclohexyl group, coupled with 1,3-benzodioxol-5-ylmethyl (**50c**) or *o*-F-phenyl moieties (**50f**) was well tolerated. Interestingly, a double substitution with a cyclohexyl group showed a strong decreasing of activity (**50a**). Interestingly, a double substitution with phenyl rings (**50d**) displayed excellent  $K_i$  against enzyme. However, the best result was obtained with inhibitor **50c**, bearing 4-(*n*-propyl)cyclohexyl and 1,3-benzodioxol-5-ylmethyl moieties, with a  $K_i$  value of 2 nM. Selectivity assays exhibited a poor activity towards hCatL; on the contrary, compound **50c** showed no inhibition against hCatB, while the other compounds displayed almost absence of activity. In addition, compounds **50d-f** showed the best antitrypanosomal activity, with  $EC_{50}$  values ranging from 15.0 to 18.9  $\mu$ M. It is to note the lack of correlation between rhodesain inhibition and the antitrypanosomal activity, which suggests off-target interactions or general cytotoxicity, as also indicated by the toxicity recorded towards rat myoblast cells, with  $TC_{50}$  in the range 11.4-22.0  $\mu$ M.

In an effort to improve the antitrypanosomal activity of the lead compound **50c**, another series of molecules was developed.<sup>86</sup> At the P1 site, morpholine ring was replaced with the chloroquine-derived 5-diethylaminopent-2-yl side chain, and slight improvement of binding affinity was recorded. With regard P2 position, 4-propyl-cyclohexyl substituent was maintained, while at P3 site, in addition to the 1,3-benzodioxol-5-ylmethyl moiety, was also introduced *p*-chloro-benzyl moiety (Figure 42).

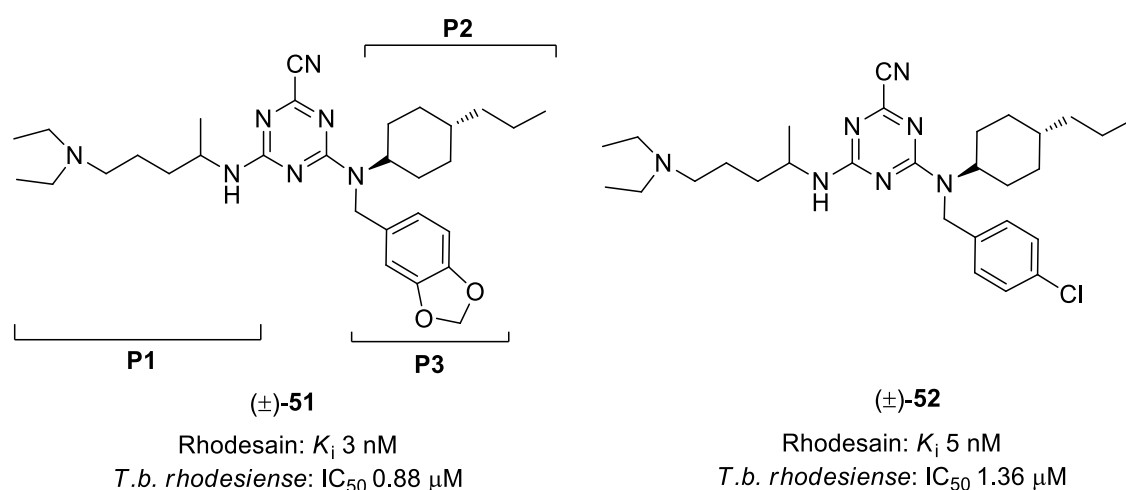


**Figure 42.** Chemical structures and biological result of inhibitor ( $\pm$ )-**51** and ( $\pm$ )-**52**.

Significant and relevant results were obtained combining all the moieties: compounds (±)-**51** and (±)-**52** showed  $K_i$  values of 3 nM and 5 nM, and a selectivity ratio hCatL/rhodesain of 150 and 15 respectively. Furthermore, these inhibitors exhibited  $EC_{50}$  values in the low micromolar/submicromolar range against *T. b. rhodesiense*, suggesting an increased ability to cross the parasitic cell membranes with respect to lead compound **50c**.

#### 4.3.2 Purine nitriles

This series of inhibitors is based on the idea to incorporate one of the distal nitrogen atoms, linked to the triazine nucleus, into a heterocyclic ring, forming two different models of the purine core (Figure 43).

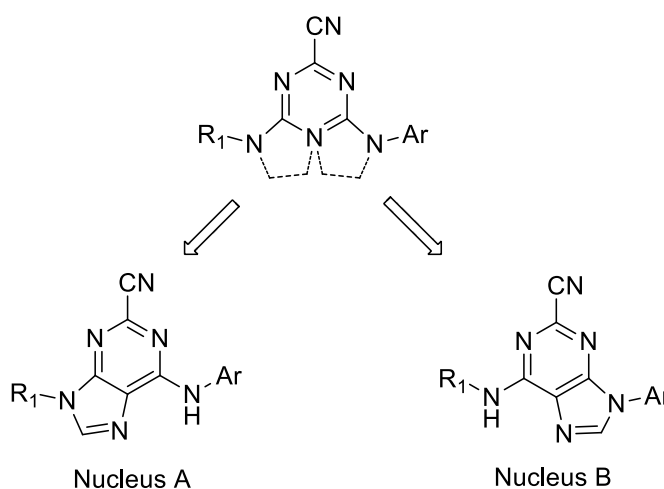
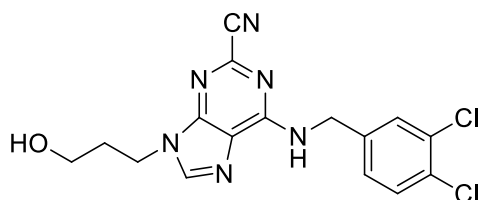


**Figure 43.** Possible structural rigidification of the triazine core.

Nucleus A derivatives showed the best results against cysteine proteases,<sup>23</sup> and for this reason it was used by medicinal chemists in the effort to develop rhodesain and TbCatB inhibitors. Purine nitrile class inhibits cysteine proteases with the same mechanism of action reported for triazine nitriles.

A series of purine nitriles, designed to be TbCatB inhibitors, was developed by Mallari et al.<sup>87</sup> They focused their efforts on the amino substituents at position 6, which fit into the P2 pocket, developing compounds bearing a cyclohexyl or Bn ring in the corresponding S2 site. More in detail, the 3,4-dichloro substitution showed the best results. On the other hand, to better fit into the S1 site, the evaluation of the key structural requirements at N-9 position was carried out, by introduction of various oxygen-bearing chains (alcohols, ethers, diols). Compound **53** (Figure 44) containing a 3-hydroxypropyl group and with 3,4-Cl<sub>2</sub>-Bn at the 6-amino position, was proven to be the best inhibitor of the series, with IC<sub>50</sub>

value of 0.27  $\mu\text{M}$ . However, this compound showed absence of selectivity over hCatL, while a weaker inhibition of hCatB was recorded ( $\text{IC}_{50} < 13.5 \mu\text{M}$ ). When tested against the parasite, compound **53** displayed an  $\text{EC}_{50}$  value of 0.11  $\mu\text{M}$ , coupled with a high degree of selectivity towards *T. b. brucei* over mammalian cell lines, with a SI value  $> 100$ .



**53**

TbCatB,  $\text{IC}_{50}$ : 0.27  $\mu\text{M}$   
*T. b. brucei*,  $\text{EC}_{50}$ : 0.11  $\mu\text{M}$

**Figure 44.** Biological results of purine nitrile inhibitor **53**.

In 2009, another SAR study was carried out by Mallari and co-workers,<sup>88</sup> with the aim to optimize the profile of compound **53**, with particular attention towards selectivity over rhodesain, hCatL and hCatB. The S2 pocket of TbCatB is larger and more negatively charged compared to the S2 pocket of rhodesain: therefore, the introduction of bulky substituents on the 6-amino group would improve exponentially the activity and selectivity for TbCatB. Various substituted aromatic rings were introduced at position 3' of compound **53**, and both the chlorine atoms were removed (Table 16). *Orto*-substitution produced the most active compounds some of which with activity, comparable to compound **53**, towards TbCatB. Furthermore, a high specificity degree for TbCatB over

**Table 16. Biological activity of inhibitors 54a-f**

Comp	R	TbCatB	Rhodesain	hCatL	hCatB	<i>T. b. b.</i>
		$\text{IC}_{50}$ , $\mu\text{M}$				$\text{EC}_{50}$ , $\mu\text{M}$
<b>54a</b>	2-CF <sub>3</sub>	0.28	8	1.5	> 15	0.46
<b>54b</b>	2-Cl	1.3	20	16	> 15	4.6
<b>54c</b>	2-Me	0.39	> 50	1.1	> 15	1.05
<b>54d</b>	2,6-dimethyl	0.27	> 15	1.0	> 15	0.63
<b>54e</b>	2-isopropyl	0.31	> 15	0.9	> 15	0.63
<b>54f</b>	2-methoxy-carbonyl	1.0	> 10	1.4	> 15	0.7

both rhodesain and hCatL was recorded, demonstrating how the nature of S2 site is essential for selectivity. When tested on cultures of *T. b. brucei*, inhibitors **54a-f** showed an excellent antitrypanosomal activity, with a perfect correlation between enzyme inhibition and antiparasitic activity. Overall, purine nitriles derivatives exhibited good drug-like properties, probably due to their lipophilicity.

### 4.3.3 Thiosemicarbazones

Thiosemicarbazones are known in literature for their antiparasitic properties, especially for *P. falciparum*<sup>89</sup> and *Trypanosoma cruzi*.<sup>90</sup> These molecules act as time independent inhibitors<sup>91</sup>: the thiolate anion attacks the electrophilic carbon C=S, and the novel tetrahedral adduct formed is stabilized by a His residue as shown in figure 45.

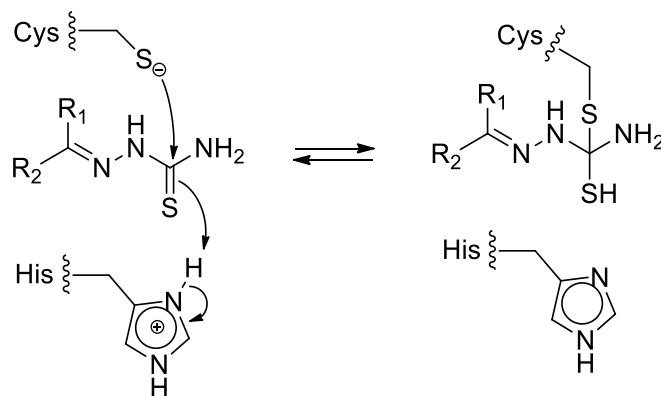


**Figure 45.** Mechanism of action of thiosemicarbazones.

In 2004, a series of thiosemicarbazone derivatives was developed<sup>92</sup> (Table 17), to evaluate the importance of various substituents at position 3' and 4' on the aromatic ring, which fit into the S2 pocket of cysteine proteases. At the same time, possible substitutions at the N1 of the thiosemicarbazone were evaluated: this moiety is important, as suggested by the binding mode, for the interactions with S1'-S2' pockets. Introduction of several substituents at position 3' and 4' of the phenyl ring was well tolerated (**55-58**), while *N*-disubstitution (**59-61**) showed decreasing of activity towards rhodesain, but enhanced the antitrypanosomal activity, probably due to better crossing of the parasite membranes. In addition, was evaluated the removal of amino group and the addition of a thiomethyl substituent, to obtain compound **62**, which was inactive against rhodesain and showed a modest antiparasitic activity. The replacement of the phenyl ring with the 3'-bromo substituted pyridine nucleus (**63**), maintained inactivity towards rhodesain, but exhibited submicromolar EC<sub>50</sub> value against *T. b. brucei*, putting in evidence its ability to cross the

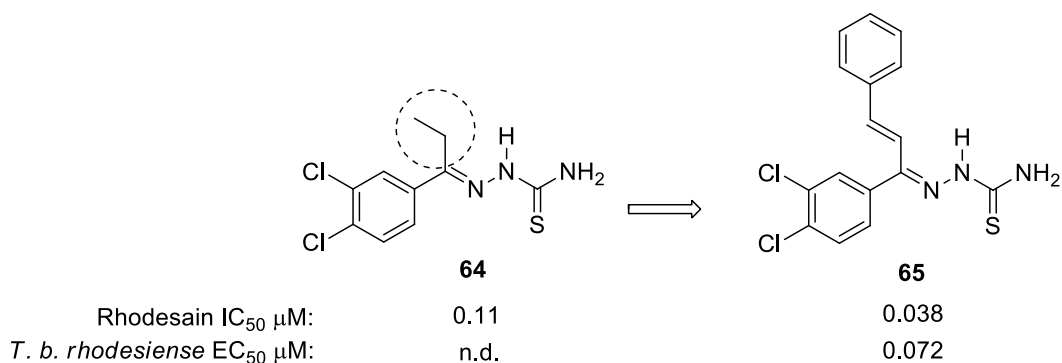


selectivity over hCatL and hCatB was not determined. parasite membranes and kill the parasite via a protease-independent mechanism.

Table 17. Biological activity of thiosemicarbazones 55-63					
Comp	R1	R2	X	Rhodesain IC <sub>50</sub> (μM)	<i>T. b. b.</i> EC <sub>50</sub> (μM)
55	4'-Ph	NH <sub>2</sub>	CH	0.09	10
56	3'-O-Ph			0.55	6
57	3'-NH-Ph			0.8	8
58	3'-Br	Pip		0.05	> 20
59				4	3
60		N(Et) <sub>2</sub>		1.8	3
61		<i>N</i> -Me-Pip		4	2
62		S-CH <sub>3</sub>		> 20	10
63	S-CH <sub>3</sub>	N	> 20	0.3	

Piperidyl= Pip; N-methylpiperazinyl = N-Mpip

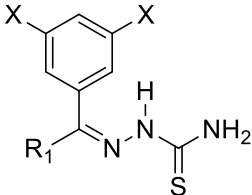
Another study was carried out starting from compound **63** (Figure 46), to evaluate the impact of ethyl chain linked to electrophilic carbon.<sup>93</sup> Bulkier alkyl substituents (e.g. *t*-butyl, cyclohexyl etc..) were not tolerated, while the introduction of a *n*-butyl, or a phenylethyl or a phenylethenyl chain improved the inhibitory activity towards rhodesain. Compound **65** showed the best result, with IC<sub>50</sub> value of 0.11 μM against the enzyme, coupled with an excellent activity towards *T. b. rhodesiense*. Cytotoxicity assays over human macrophages exhibited toxic values at doses higher than 10 μM.



**Figure 46.** Lead compound **64** and best inhibitor developed.

Starting from these findings, another series of thiosemicarbazones was developed, introducing several aryl substituents at the electrophilic carbon, and maintaining the terminal nitrogen atom free.<sup>94</sup> Inhibitors bearing the phenylethyl (**66-67**) or 4-methylphenyl (**68-69**) residues showed absence of inhibition and weak activity (Table 18), respectively, towards TbCatB, while excellent activity was recorded against rhodesain, ranging from 44 to 57 nM.

**Table 18. Biological evaluation of thiosemicarbazones 66-71**

							
Comp	R <sub>1</sub>	X	Rhodesain	TbCatB	hCatL	hCatB	<i>T. b. b.</i>
			IC <sub>50</sub> (μM)				EC <sub>50</sub> (μM)
<b>66</b>	Ph-ethyl	CF <sub>3</sub>	0.053	> 25	0.017	3.0	2
<b>67</b>		Cl <sub>2</sub>	0.057	> 25	0.039	4.9	1.3
<b>68</b>	4-methyl-Ph	CF <sub>3</sub>	0.044	15	0.007	3.3	1.3
<b>69</b>		Cl <sub>2</sub>	0.046	6	0.011	1.8	1.1
<b>70</b>	2-thiophene	CF <sub>3</sub>	0.007	0.15	0.010	0.30	7
<b>71</b>		Cl <sub>2</sub>	0.011	0.45	0.004	0.30	7

On the contrary, the introduction of 2-thiophene ring (**70-71**) slightly enhanced the activity towards rhodesain, as well as against TbCatB, with IC<sub>50</sub> value in sub-micromolar range. It is worth noting that the presence of CF<sub>3</sub> or Cl at positions 3 and 5 of phenyl ring did not show any significant difference. With regard to the selectivity over human cathepsins, inhibitors displayed the same trend of inhibition shown for parasitic proteases, and no specificity was recorded. All inhibitors exhibited activity on *T. b. brucei* in the low micromolar range, putting in evidence that the inhibition of rhodesain was correlated with the best results against parasite.

#### 4.3.4 Other non-peptide inhibitors

Isoquinoline derivatives with general structure **72** (Figure 47), are known wide-spectrum antimicrobials.<sup>95</sup> In 2009, Grasso et al. developed a series of variously substituted isoquinolinones,<sup>96</sup> in order to evaluate the impact of several substitutions at N2, C3, C6 and C7. All compounds inhibited rhodesain in the micromolar range, with the most active derivative **73** showing a *K<sub>i</sub>* value of 4.0 μM: likely, the presence of two benzyl substituents

create multiple interactions with catalytic triad. Unfortunately a lack of selectivity was recorded, due to the contemporary inhibition of hCatL and hCatB, and assays against parasite were not performed.

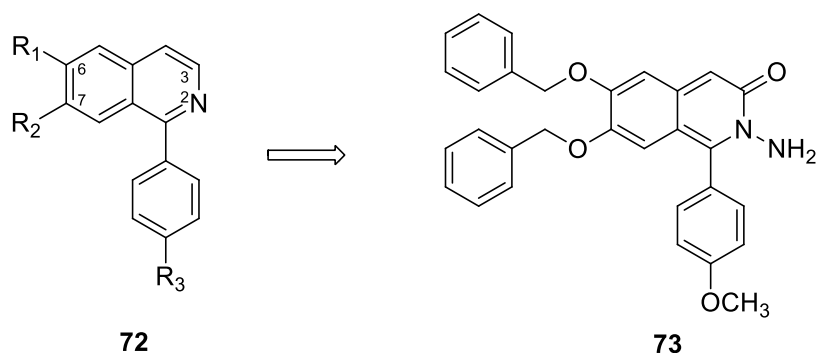


**Figure 47.** Base-structure and the most active rhodesain inhibitor developed.

Other class of non-peptide molecules able to inhibit rhodesain are the guanidino-furan and pyrrole derivatives.<sup>97</sup> Molecular modelling studies point out multiple interactions between ligands and enzyme: Cbz-protected guanidine portion fits well into the hydrophobic S2 pocket, while H-bonds were established by the amide portion. Generally, no difference between pyrrole- or furan-based inhibitors was recorded, as well as the introduction on the amide moiety of a phenyl or benzyl substituent. The most active compound **74** (Figure 48) exhibited a good correlation between the enzymatic ( $K_i = 0.11 \mu\text{M}$ ) and antiparasitic activity ( $\text{EC}_{50} = 0.22 \mu\text{M}$ ). When tested on J774.1 mammalian macrophages, compound **74** showed moderate cytotoxicity ( $\text{TC}_{50} = 18.69 \mu\text{M}$ ), with SI of 85.

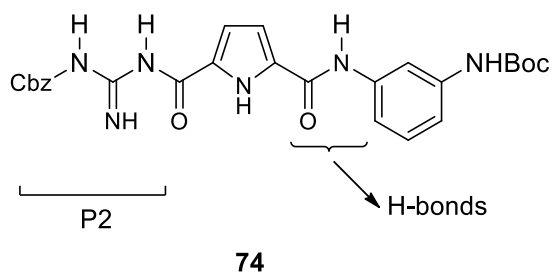
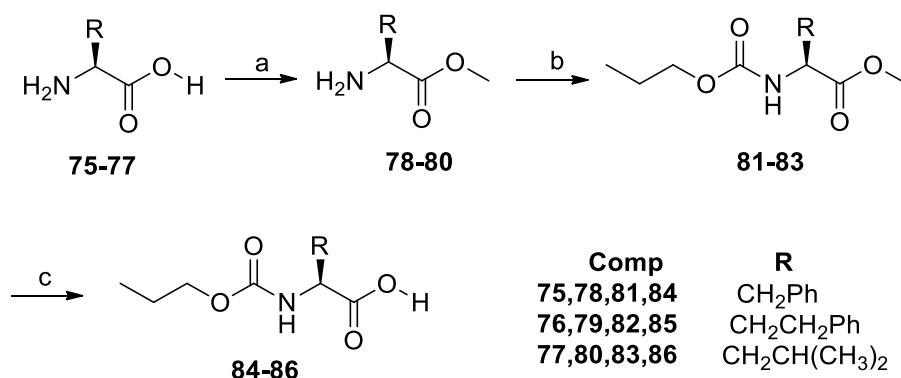


**Figure 48.** The most active pyrrole derivative rhodesain inhibitor.

## CHAPTER 5. RESULTS AND DISCUSSIONS

### 5.1 Series A

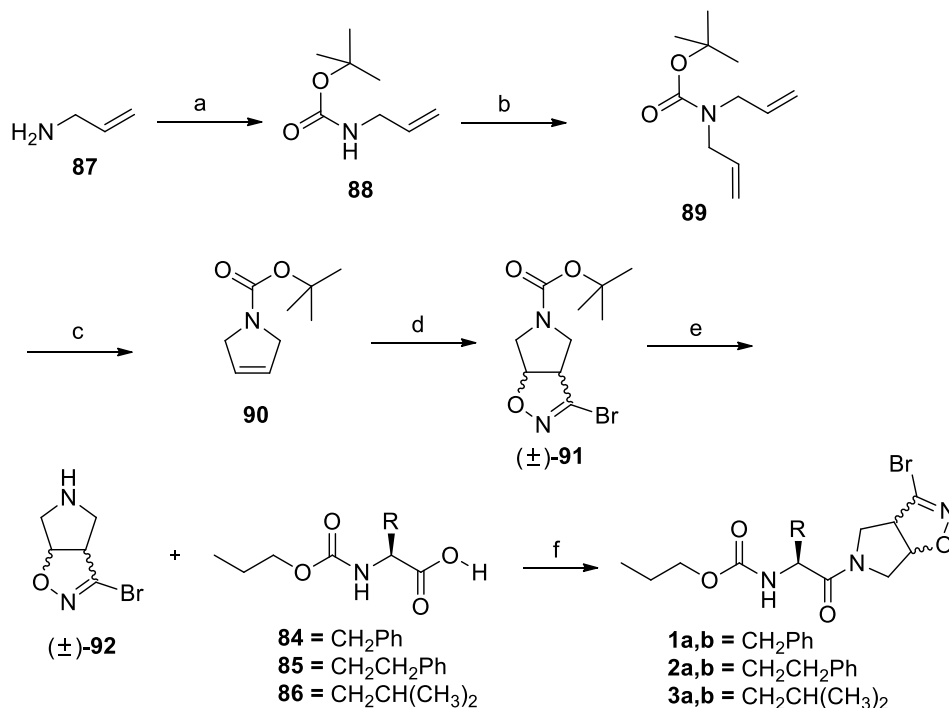
The synthesis of propyl analogues **1-3a,b** (Scheme 1) was carried out starting from natural L-amino acids Phe, hPhe and Leu **75-77**, whose carboxylic function was converted into the corresponding methyl ester (**78-80**) by treatment with methanol in acidic conditions. The amino group was functionalized as a carbamate (**81-83**) using *n*-propyl chloroformate and then, the ester function was hydrolysed with LiOH, to give the corresponding carboxylic acids **84-86**.



**Scheme 1.** Reagents and conditions: a) MeOH, HCl conc., rt, 12h; b) *n*-propylchloroformate, NaHCO<sub>3</sub>/dioxane (7:3), rt, 12h; c) LiOH, MeOH/H<sub>2</sub>O/dioxane (1:1:1), 0° C, 10 min, then 12h.

The bicyclic ring containing 3-bromoisoxazoline nucleus was synthesized (Scheme 2) starting from allylamine **87**, commercially available, on which the amino group was protected using (Boc)<sub>2</sub>O. The intermediate **88**, by reaction with allyl bromide, provided Boc-diallylamine **89**, which *via* Ring-Cross Metathesis (RCM) reaction, using the Hoveyda-Grubbs catalyst 2nd generation under microwave irradiation, allowed to obtain Boc-pyrroline **90**. Subsequently, 1,3-dipolar cycloaddition between the dipolarophile **90** and bromonitrileoxide, generated *in situ* by dehydrohalogenation of the stable precursor dibromoformaldoxime (DBF), gave bicyclic amine (±)-**91**, which by treatment with 30% TFA in CH<sub>2</sub>Cl<sub>2</sub> provided the free amine (±)-**92** as diastereomeric mixture. Coupling reactions between acids **84-86** and amine (±)-**92** allowed to obtain compounds **1-3a,b**. The diastereomeric mixtures (±)-**80**-(±)-**82** were tested against rhodesain (Table 19) to evaluate their inhibitory properties, using Cbz-Phe-Arg-7-amino-4-methylcoumarin (Z-Phe-Arg-AMC) as fluorogenic substrate. In a preliminary screening carried out at 100 μM, the

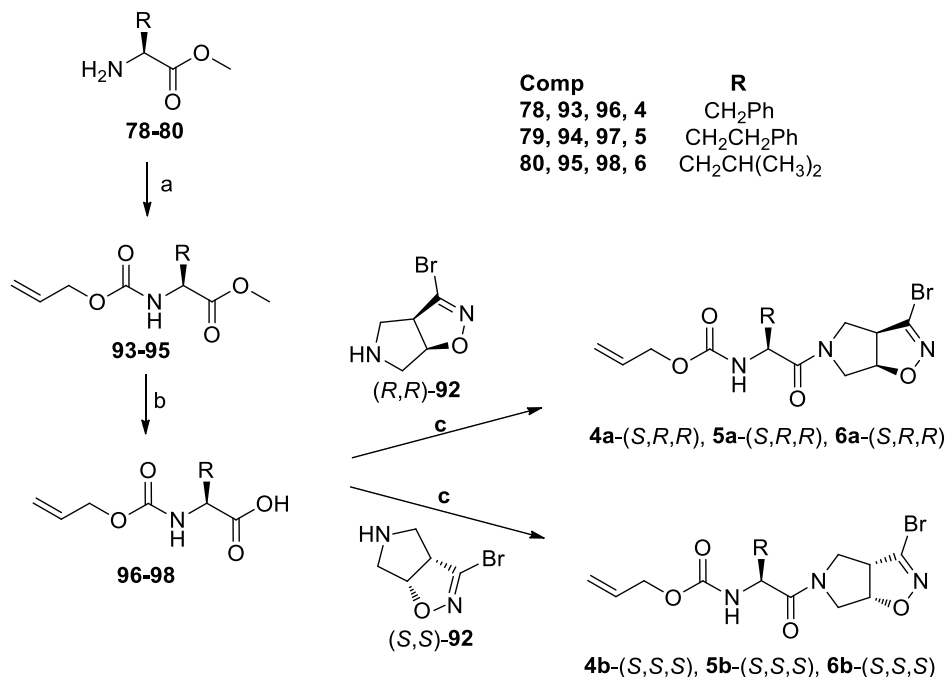
molecules showed very low percentages of inhibition, probably for the lack of interactions between the S3 pocket and the propyl chain.



**Scheme 2.** Reagents and conditions: a) (Boc)<sub>2</sub>O, Et<sub>3</sub>N, CH<sub>2</sub>Cl<sub>2</sub>, 0° C, 2h, then rt, 12h; b) allyl bromide, DMF, NaH, 0° C, 30 min, then rt, 16h; c) Hoveyda-Grubbs catalyst 2nd generation, CH<sub>2</sub>Cl<sub>2</sub>, MW, 100° C, 2h; d) DBF, NaHCO<sub>3</sub>, EtOAc, rt, 72h, e) TFA, CH<sub>2</sub>Cl<sub>2</sub>, rt, 4h; f) HOBT, EDCI, DIPEA, CH<sub>2</sub>Cl<sub>2</sub>/DMF, 0° C, 10 min, then 12h.

Once clarified the key role played by allyl group, we focused on the stereochemistry of the warhead, in order to evaluate its effect on the biological activity: for this reason we synthesized the single diastereoisomers **4a**-(*S,R,R*), **4b**-(*S,S,S*), **5a**-(*S,R,R*), **5b**-(*S,S,S*), **6a**-(*S,R,R*) and **6b**-(*S,S,S*). The synthesis of the single diastereomers (Scheme 3) was possible by chiral resolution of intermediate (±)-**91**, carried out in collaboration with University of Milan. It was obtained an excellent enantiomeric separation (both in 99% enantiomeric excess) by preparative chiral HPLC, using tris-(3,5-dimethylphenyl)carbamoyl amylose as stationary phase and *n*-hexane/*i*PrOH (9:1) as eluent mixture. To establish their absolute configuration, X-ray diffractometric study was previously carried out on the (+)-**91** enantiomer: due to an anomalous scattering by bromine atom, the absolute configuration was unequivocally determined as (+)-(*S,S*)-**91**.<sup>81</sup> The synthesis of the single diastereomers was accomplished by coupling reactions between acids **96-98** and the enantiopure amines (*R,R*)-**92** and (*S,S*)-**92**. Biological evaluation highlighted a marginal role of the warhead

stereocenters on the rhodesain inhibition: diastereomers with *S,S* configuration displayed  $K_i$  values comparable to corresponding *R,R* analogues (Table 19).



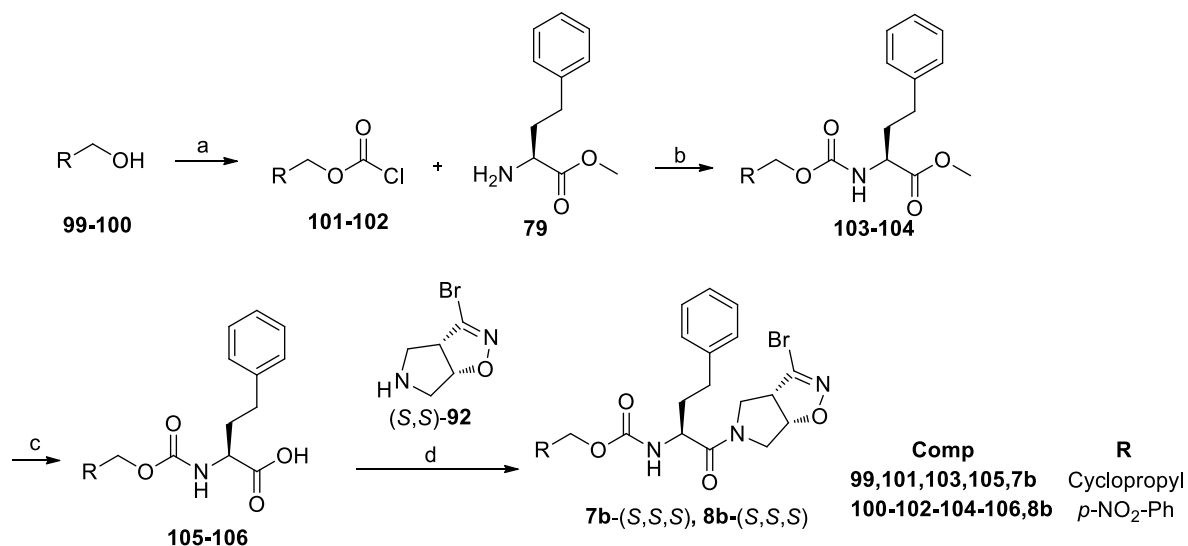
**Scheme 3.** Reagents and conditions: b) allylchloroformate,  $\text{NaHCO}_3/\text{dioxane}$  (7/3), rt, 12h; c)  $\text{LiOH}$ ,  $\text{MeOH}/\text{H}_2\text{O}/\text{dioxane}$  (1:1:1),  $0^\circ\text{C}$ , 10 min, then 12h; d) HOBt, EDCI, DIPEA,  $\text{CH}_2\text{Cl}_2/\text{DMF}$ ,  $0^\circ\text{C}$ , 10 min, then 12h.

Considered that most active inhibitor **5b**-(*S,S,S*) bears a hPhe residue at the P2 site and *S,S* configured warhead (Table 19), we decided to further explore the S3 pocket by replacing *N*-allyl group with cyclopropylmethyl and *p*- $\text{NO}_2$ -Bn moieties.

Table 19. Biological evaluation of 3-bromoisoaxaline inhibitors		
Comp	Rhodesain	<i>T. b. brucei</i>
	$K_i$ ( $\mu\text{M}$ ) or % of inhibition at 100 $\mu\text{M}$	$\text{EC}_{50}$ , $\mu\text{M}$
<b>1a,b</b>	13.1%	n.d.
<b>2a,b</b>	15.3%	n.d.
<b>3a,b</b>	11.3%	n.d.
<b>4a</b> -( <i>S,R,R</i> )	$16.58 \pm 0.59$	n.d.
<b>4b</b> -( <i>S,S,S</i> )	$15.14 \pm 0.16$	n.d.
<b>5a</b> -( <i>S,R,R</i> )	$3.35 \pm 0.12$	n.d.
<b>5b</b> -( <i>S,S,S</i> )	$2.73 \pm 0.29$	$32.04 \pm 2.78$
<b>6a</b> -( <i>S,R,R</i> )	$9.05 \pm 0.08$	n.d.
<b>6b</b> -( <i>S,S,S</i> )	$8.52 \pm 0.57$	n.d.
<b>7b</b> -( <i>S,S,S</i> )	15.7%	n.d.
<b>8b</b> -( <i>S,S,S</i> )	$6.81 \pm 0.23$	$14.68 \pm 1.98$

n.d. no determined; values are the mean  $\pm$  SD of two experiments performed in duplicate

Starting from the alcohols **99-100** (Scheme 4), the treatment with triphosgene provided the corresponding chloroformates **101-102**, which by reaction with hPhe methyl ester **79** and subsequent alkaline hydrolysis, provided carboxylic acids **105-106**. Lastly, coupling reaction with enantiopure amine (*S,S*)-**92** gave final products **7b-(S,S,S)** and **8b-(S,S,S)**. Cyclopropylmethyl derivative was proven to be inactive (Table 19), while the corresponding *p*-NO<sub>2</sub>-Bn analogue showed a *K<sub>i</sub>* value of 6.81 μM, somewhat higher compared to reference compound **5b-(S,S,S)**. It is important to note how the introduction of NO<sub>2</sub> group allows the compound to inhibit the target enzyme, while the corresponding analogue with Cbz moiety without substituent, previously synthesized by another member of research group, was found to be completely inactive.



**Scheme 4.** Results and conditions: a) triphosgene, DIPEA, dry THF, 0° C, N<sub>2</sub>, 30 min, then rt, 2h; b) NaHCO<sub>3</sub>/dioxane (7/3), rt, 12h; c) LiOH, MeOH/H<sub>2</sub>O/dioxane (1/1/1), 0°C, 10 min, then 12h; d) HOBt, EDCl, DIPEA, CH<sub>2</sub>Cl<sub>2</sub>/DMF, 0°C, 10 min, then 12h.

Selectivity assays were performed by testing the inhibitors towards hCatL and hCatB: none of compounds showed inhibitory properties > 40% at 100 μM, thus demonstrating an excellent selectivity against parasitic proteases. Rhodesain inhibitors were also tested on *T. b. brucei* (in collaboration with the University of Mainz): the best results were shown by compound **8b-(S,S,S)**, while a modest activity was exhibited by compound **5b-(S,S,S)**, which displayed the best inhibitory potency towards rhodesain. Cytotoxicity assays were performed by testing the inhibitors towards murine macrophages and TC<sub>50</sub> values > 100 μM were recorded. It seems clear a triple correlation between rhodesain inhibition, antiparasitic activity and aromatic ring at the P3 position, since the latter could be

responsible for the appropriate lipophilic character necessary to cross the parasite cell membranes.

With the aim to clarify the SAR of the inhibitors, covalent docking studies were carried out, in collaboration with University of Naples. Inhibitor **5b**-(*S,S,S*) fully occupies the S2 pocket, because hPhe residue interacts with many hydrophobic amino acids as Ala138, Leu160 and Ala208 (Figure 49). At the P3 site, the Alloc group fits well into the S3 pocket, establishing hydrophobic interactions with Phe61 and Leu67. Furthermore, docking experiments indicate that when hPhe residue gets into S2 pocket, the Alloc group is the best tolerated portion at the S3 binding site: these findings suggest a strong interdependency between substituents at P2 and P3 positions. The inactivity of propyl derivatives **1-3a,b** and **7b**-(*S,S,S*) can be explained considering the simultaneous presence of bulky substituents at P2 and P3 position, which hinder the simultaneous proper occupation of the two corresponding pockets. Compounds bearing the Phe residue at the P2 site prefer aromatic substituent at the P3 position with respect to Alloc group, while opposite properties occur when hPhe fits the S2 pocket. With regard to Leu analogues at the P2 position, it was suggested that molecules might fit the side chain in S2 or in S3 pocket, on the basis the P3 substituent type.

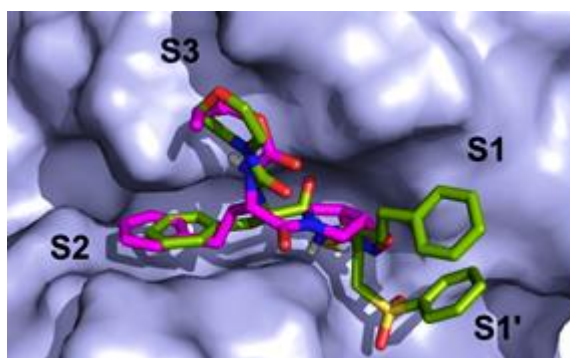


**Figure 49.** Superposition of the binding mode of **5b**-(*S,S,S*) (magenta) with the co-crystallized inhibitor K11002 (green).

In addition, the electron withdrawing properties of nitro group in compound **8b**-(*S,S,S*), would increase the  $\pi$ - $\pi$  interaction between aromatic ring and Phe61 at P3 pocket, as well as might establish one or more water-bridged interactions with the protein surface.

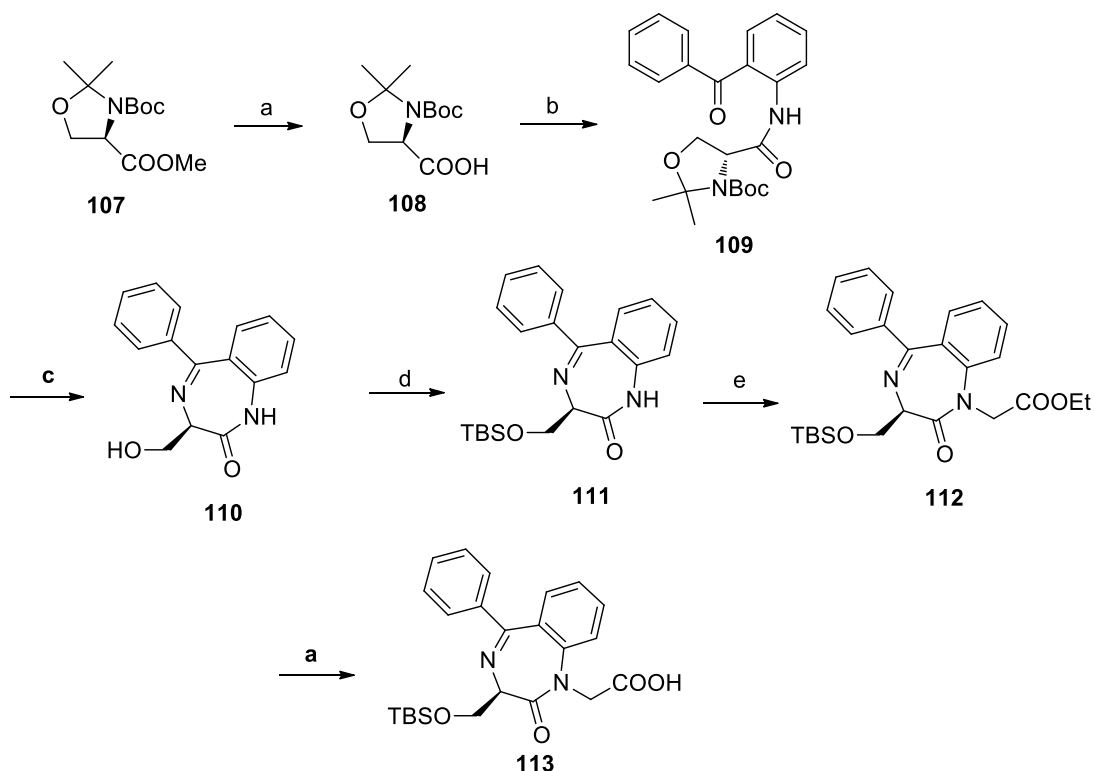
In conclusion, in the series A we developed dipeptide-like rhodesain inhibitors containing a 3-bromoisoxazoline nucleus as the warhead. We investigated various substituents at P2



and P3 position, which are strictly interdependent. The allyl group was proven to be the best moiety at the P3 site, and the introduction of nitro group in para position of Cbz increases the activity. On the contrary, saturated portions at the P3 site are not tolerated. Molecules bearing *S,S* configuration on the warhead showed a slight better activity with respect to *R,R* counterparty. Only a few compounds showed a modest activity towards parasite, while an excellent selectivity was recorded over hCatL, hCatB and human macrophages.

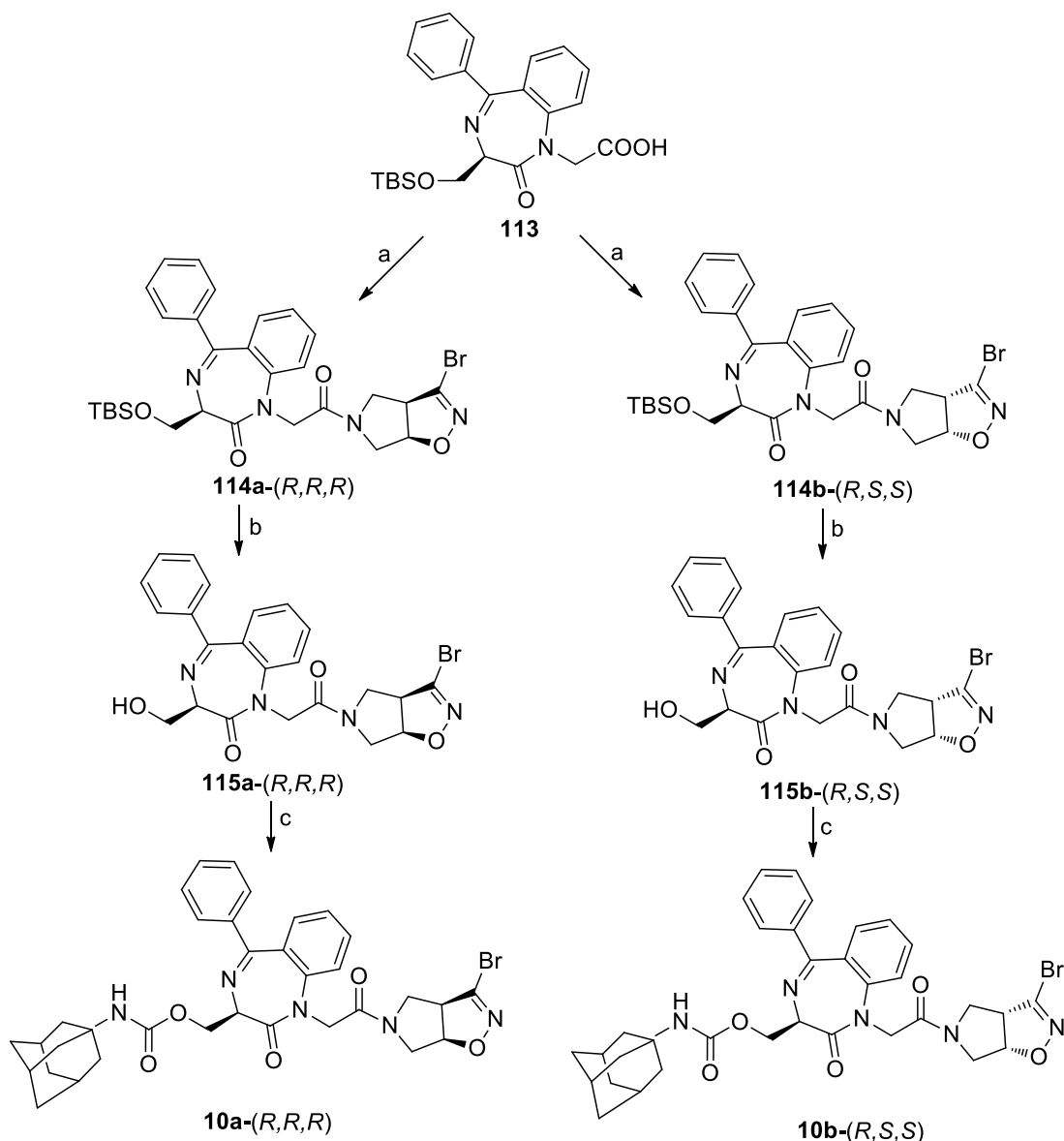
## 5.2 Series B

To synthesize novel peptidomimetics (Scheme 5), we followed a procedure reported in literature<sup>80a</sup> to obtain acid **113**. Starting from the Garner ester **107**, the ester moiety was first converted into the carboxylic function by alkaline hydrolysis to obtain the corresponding acid **108**, which by reaction with *i*-BuOCOCl and 2-aminobenzophenone, in presence of *N*-methyl morpholine, provided the intermediate **109**. The treatment with HCl at reflux led to Boc deprotection, cleavage of the oxazolidine ring and subsequent cyclization, with formation of the BDZ scaffold **110**.



**Scheme 5.** Reagents and conditions: a) LiOH, MeOH/H<sub>2</sub>O/dioxane (1:1:1), 0° C, 10 min, then 12h; b) *i*-BuOCOCl, *N*-methylmorpholine, CH<sub>2</sub>Cl<sub>2</sub>, 0 °C to rt, 1h, then 2-aminobenzophenone, 12h; c) 5% HCl/MeOH (1:5), reflux, 7 h; d) TBS-Cl, imidazole, CH<sub>2</sub>Cl<sub>2</sub>, 0 °C, 10 min, then rt, 12h; e) NaH, DMF, 0 °C to rt, 1h, then BrCH<sub>2</sub>COOEt, 12h.

The hydroxyl group was protected using *tert*-butyldimethylsilyl chloride to obtain compound **111**, which by reaction with ethyl bromoacetate in presence of NaH, allowed to obtain the *N*-alkylation product **112**. The hydrolysis of methyl ester using LiOH gave the desired carboxylic acid **113**. Coupling reactions (Scheme 6) with enantiopure amines (*R,R*)-**92** or (*S,S*)-**92** provided intermediates **114a-(R,R,R)** and **114b-(R,S,S)**, on which the hydroxyl group was deprotected by treatment with TBAF. Lastly, reaction between intermediate **115a-(R,R,R)** or **115b-(R,S,S)** with 1-adamantyl isocyanate in presence of Et<sub>3</sub>N, gave the desired diastereomers **10a-(R,R,R)** and **10b-(R,S,S)**.



**Scheme 6.** Reagents and conditions: a) HOBt, EDCI, CH<sub>2</sub>Cl<sub>2</sub>, 0° C, 10 min, then amine (*R,R*)-**92** or (*S,S*)-**92**, rt, 12h; b) TBAF, THF, rt, 6h; c) 1-adamantyl isocyanate, Et<sub>3</sub>N, CH<sub>2</sub>Cl<sub>2</sub>, rt, 3 days.

The novel compounds were tested against rhodesain, in the same condition described in series A. Initially, a preliminary screening with the inhibitor concentration of 100  $\mu\text{M}$  was performed, using an equivalent volume of DMSO as negative control. Both compounds showed an enzymatic activity more than 70% and they were evaluated in detail to determine  $K_i$  values. Continuous assays were performed with progress curve method, at seven different concentration from top to bottom, as for inhibitors series A (Figure 50).

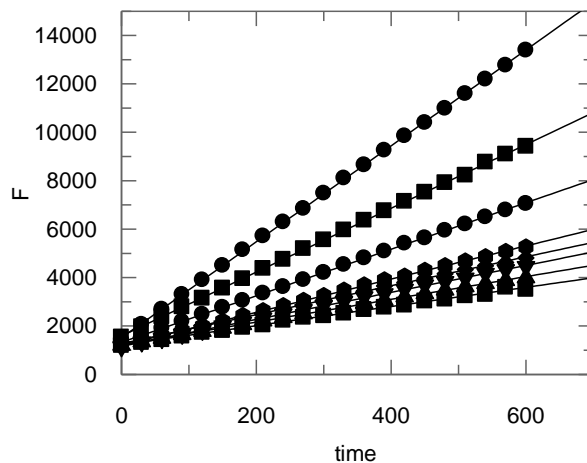


**Figure 50.** Progress curves of substrate hydrolysis in the presence of the inhibitor **10b**-(*R,S,S*). F = fluorescence units.

The two molecules showed an enzymatic activity towards rhodesain in the low micromolar range (Table 20) and **10b**-(*R,S,S*) displayed an activity slightly better with respect to counterpart with *R,R* configuration on the warhead, in agreement with results obtained in series A. Selectivity assays were performed testing compounds over hCatL: at 100  $\mu\text{M}$ , a poor % of inhibition was recorded, demonstrating a good selectivity against the parasitic cysteine protease. Antitrypanosomal activity was evaluated towards *T. b. brucei*. Inhibitor **10a**-(*R,R,R*) showed  $\text{EC}_{50}$  value of 12.27  $\mu\text{M}$ , while compound **10b**-(*R,S,S*) exhibited a better antiparasitic activity ( $\text{EC}_{50} = 4.71 \mu\text{M}$ ), similar to that of the lead compound **9** ( $\text{EC}_{50} = 4.8 \mu\text{M}$ ). It is clear the correlation between rhodesain inhibition and antitrypanosomal activity.

<b>Table 20. Biological evaluation of 10a-(<i>R,R,R</i>) and 10b-(<i>R,S,S</i>)</b>			
<b>Comp</b>	<b>Rhodesain</b>	<b>hCatL</b>	<b><i>T. b. brucei</i></b>
	<b><math>K_i</math> (<math>\mu\text{M}</math>) or % of inhibition at 100 <math>\mu\text{M}</math></b>		<b><math>\text{EC}_{50}</math> (<math>\mu\text{M}</math>)</b>
<b>10a-(<i>R,R,R</i>)</b>	2.49±0.43		12.27±0.14
<b>10b-(<i>R,S,S</i>)</b>	1.26±0.04		4.71±1.23
Values are the mean $\pm$ SD of two experiments performed in duplicate			

Considering the good antitrypanosomal activity of **10b**-(*R,S,S*), we decided to predict its physicochemical and pharmacokinetic properties, by using Qikprop program, in collaboration with University of Campania Luigi Vanvitelli (Caserta). It was predicted that **10b**-(*R,S,S*) has acceptable QPPCaco value, which indicates the gut/blood barrier permeability, high potential of crossing BBB (QPlogBB and QPPMDCK values) and 83.5% human oral absorption. Thus, novel inhibitor showed predicted parameters falling within the range calculated for the 95% drugs on the market. Crossing the BBB is an essential feature for novel potential antitrypanosomal agents, because without this property, inhibitors are inactive in the neurological stage.

In conclusion, in series B we identified novel rhodesain inhibitors containing 3-bromoisoxazoline nucleus. Compared with inhibitors of series A, peptidomimetics **10a**-(*R,R,R*) and **10b**-(*R,S,S*) showed an improved activity towards the target enzyme, in addition a good target selectivity was recorded by testing inhibitors against hCatL, and inhibitor **10b**-(*R,S,S*) showed EC<sub>50</sub> value of 4.71 μM towards *T. b. brucei*, similar to lead compound **9**. In addition, pharmacokinetic features predicted for **10b**-(*R,S,S*) support its drug-like properties as potential antitrypanosomal agent.

### 5.3 Series C

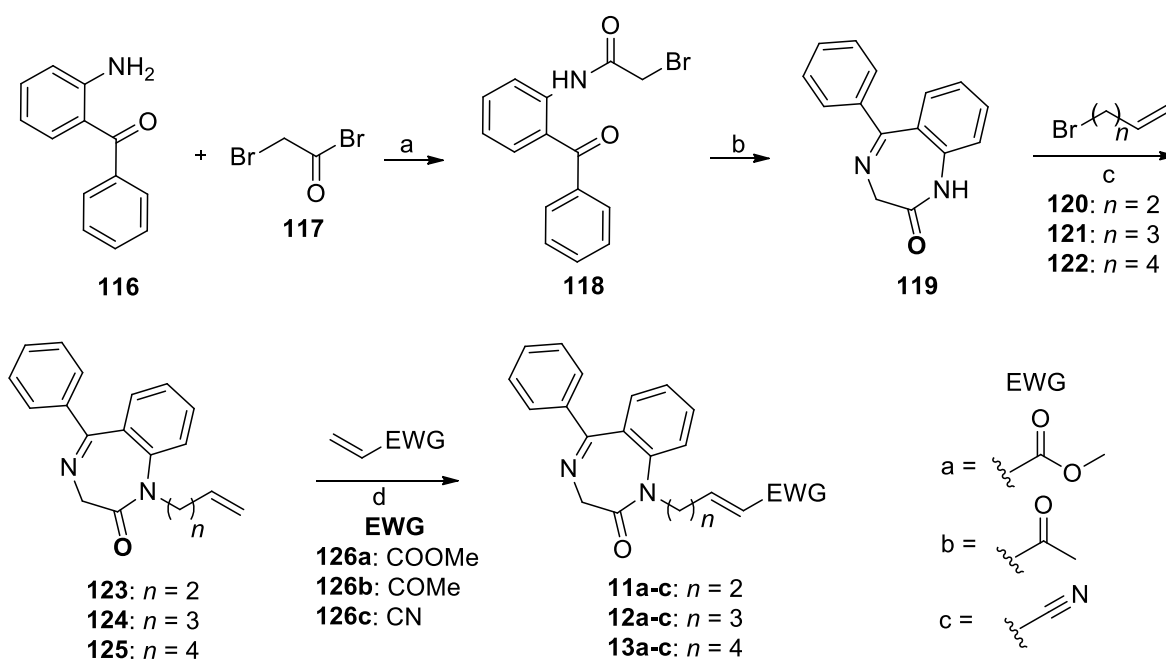
To design new analogues of compound **9**, we decided to take advantage of the computational predictions of pharmacokinetics parameters (Table 21), by using Qikprop software. This analysis showed that Michael acceptor **9** has an almost null solubility in water, with consequently no absorption in vivo, the LogP<sub>o/w</sub> higher five and weak CNS activity. To optimize pharmacokinetic parameters of compound **9**, we decided to remove the methyl carbamoyl side chain, appended to C3 position of the BDZ scaffold, in order to increase the water solubility. Moreover, we replaced the amide bond with aliphatic chains of different lengths, to evaluate the best distance between the BDZ scaffold and α,β-unsaturated portion. Furthermore, being the methylene group an isostere both of the carbonyl and of the amino group, it could confer proteolytic resistance. In addition, we decided to explore P1' enzyme pocket by introduction of various EWGs at the P1' position. Qikprop calculations for novel simplified BDZs, showed that, with a few exception, all the molecules should be active in CNS, with high human oral absorption and more water solubility. In addition, the molecular weight of these compounds is ranging

from 315.14 to 376.18, in agreement with Lipinsky's Rule of Five, as well as  $\text{LogP}_{o/w}$  value.

Table 21. Structure of novel BDZ derivatives and calculated parameters										
Comp	n	EWG	CNS <sup>a</sup>	$\text{LogPo/w}^b$	$\text{LogS}^c$	$\text{LogHERG}^d$	$\text{PCaco}^e$	$\text{LogBB}^f$	$\text{pMDCK}^g$	$\text{HOA}^h$
<b>9</b>			-2	5.9	-9.2	-7.3	427.8	-1.6	197.6	1
<b>11a</b>	2		-1	3.6	-5.1	-6.3	763.3	-0.9	369.5	3
<b>11a</b>	3	COOMe	-1	4.0	-5.6	-6.5	762.9	-1.0	369.3	3
<b>11a</b>	4		-2	4.4	-6.0	-6.6	762.9	-1.1	369.2	3
<b>12b</b>	2		-1	3.5	-4.7	-6.1	1013.5	-0.7	501.9	3
<b>12b</b>	3	COMe	-1	3.9	-5.1	-6.3	1012.3	-0.8	501.3	3
<b>12b</b>	4		-1	4.3	-5.6	-6.5	1012.6	-0.9	501.4	3
<b>13c</b>	2		-1	3.2	-5.3	-6.0	665.0	-0.9	318.3	3
<b>13c</b>	3	CN	-1	3.6	-5.7	-6.2	664.7	-1.0	318.2	3
<b>13c</b>	4		-2	4.0	-6.2	-6.4	664.6	-1.1	318.1	1

<sup>a</sup> Predicted central nervous system activity on a -2 (inactive) to +2 (active) scale.  
<sup>b</sup> Predicted octanol/water partition coefficient.  
<sup>c</sup> Predicted aqueous solubility,  $\log S$ .  $S$  in  $\text{mol dm}^{-3}$  is the concentration of the solute in a saturated solution that is in equilibrium with the crystalline solid.  
<sup>d</sup> Predicted  $\text{IC}_{50}$  value for blockage of HERG  $\text{K}^+$  channels.  
<sup>e</sup> Predicted apparent Caco-2 cell permeability in  $\text{nm}^2/\text{sec}$ . Caco2 cells are a model for the gut-blood barrier.  
<sup>f</sup> Predicted brain/blood partition coefficient.  
<sup>g</sup> Predicted brain/blood partition coefficient. MDCK cells are considered to be a good mimic for the BBB.  
<sup>h</sup> Predicted qualitative human oral absorption: 1, 2, or 3 for low, medium or high.

BDZ scaffold was synthesized (Scheme 7) following a procedure known in literature,<sup>98</sup> starting from 2-aminobenzophenone **116**, which was treated with 2-bromoacetyl bromide **117**, followed by gaseous ammonia. Subsequently, intermediate **119**, by *N*-alkylation reaction with bromoalkenes **120-122**, in presence of NaH, gave terminal olefins **123-125**. To introduce the Michael acceptor portion, we carried out Cross-Metathesis (CM) reaction in a microwave reactor, by treatment with the required CM partners **126a-c** in the presence of the Hoveyda-Grubbs catalyst 2nd generation, obtaining the CM products **11-13a-c** in high yields (76-92%).



**Scheme 7.** Reagents and conditions: a)  $\text{CH}_2\text{Cl}_2$ ,  $\text{H}_2\text{O}$ ,  $-10^\circ\text{C}$ , 4h; b)  $\text{NH}_3(\text{g})$ , MeOH,  $-15^\circ\text{C}$ , 2h then  $65^\circ\text{C}$ , 2h; c) NaH, DMF,  $0^\circ\text{C}$ ,  $\text{N}_2$ , 1 h, then **120-122**, r.t., 12h; d) Hoveyda-Grubbs catalyst 2nd generation, dry  $\text{CH}_2\text{Cl}_2$ ,  $100^\circ\text{C}$ , MW, 2h.

Michael acceptors **11-13a-c** were tested towards *T. b. brucei* (Table 22) showing, with the exception of compound **11a**, **11c** and **12c**, an antitrypanosomal activity ranging from 4.62 to 23.53  $\mu\text{M}$ . The most active compounds bearing vinyl ketone warhead **11b-13b**, and inhibitors containing three methylene units **12b** was proven to be the best, with  $\text{EC}_{50}$  value similar to that of lead compound **9**. Compound **11b** with a spacer of two methylene units showed a comparable antitrypanosomal activity ( $\text{EC}_{50} = 5.29 \mu\text{M}$ ), while a slight decrease was recorded in compound **13b** ( $\text{EC}_{50} = 13.14 \mu\text{M}$ ) with four methylene units. A different trend was displayed with Michael acceptors bearing ester (**11a-13a**) or nitrile (**11c-13c**)  $\alpha,\beta$ -unsaturated portions: in both cases, the most active compounds were those with four methylene units as spacer (**13a** and **13c**), but with an antitrypanosomal activity 3 fold

lower with respect the most potent inhibitor **12b**. Molecules were tested against rhodesain, to identify cellular target. A preliminary screening carried out at 100  $\mu\text{M}$ : compounds **11-13a-c** showed only a weak inhibition of rhodesain ranging from 27 to 60%, which do not justify the good observed antitrypanosomal activity, thus suggesting a different target, probably TbCatB. Finally, the most active inhibitors **11b** and **12b** were tested against murine macrophages, to evaluate their cytotoxicity: compound **12b** showed a  $\text{TC}_{50}$  value of 31.81  $\mu\text{M}$  ( $\text{SI} = 7$ ), while the analogue **11b** was proven to be lack of cytotoxicity ( $\text{TC}_{50} > 100 \mu\text{M}$ ), thus highlighting its preference for parasite rather than for human cells.

Comp	<i>T. b. brucei</i> $\text{EC}_{50}$ ( $\mu\text{M}$ )	Rhodesain % of inhibition at 100 $\mu\text{M}$	$\text{TC}_{50}$ ( $\mu\text{M}$ )
<b>11a</b>	> 40	27	n.d.
<b>12a</b>	23.5 $\pm$ 1.4	32	n.d.
<b>13a</b>	15.9 $\pm$ 0.3	40	n.d.
<b>11b</b>	5.29 $\pm$ 0.5	49	> 100
<b>12b</b>	4.6 $\pm$ 0.2	55	31.81
<b>13b</b>	13.1 $\pm$ 1.9	60	n.d.
<b>11c</b>	> 40	36	n.d.
<b>12c</b>	> 40	48	n.d.
<b>13c</b>	14.5 $\pm$ 0.3	34	n.d.

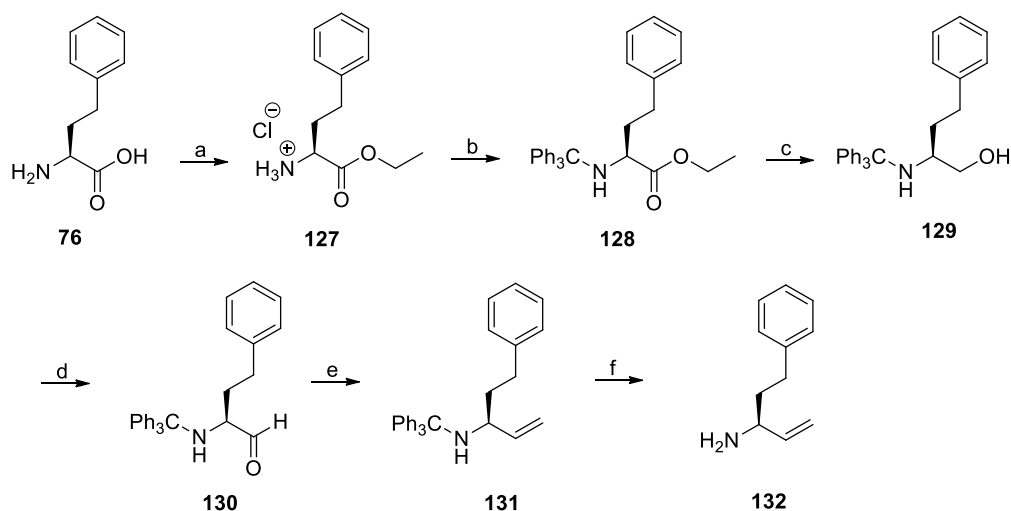
n.d = not determined; Values are the mean  $\pm$  SD of two experiments performed in duplicate

In conclusion, in series C we developed novel BDZ Michael acceptors, which possess optimal drug-like properties. Compounds **11b** and **12b** showed antitrypanosomal activity in the low micromolar range, coupled with weak or absence of cytotoxicity against mammalian cells. Peptidomimetic derivatives lacking of substituents at the P3 position exhibited a weak activity inhibitory towards rhodesain, suggesting an important role played by interactions in the corresponding S3 pocket.

#### 5.4 Series D

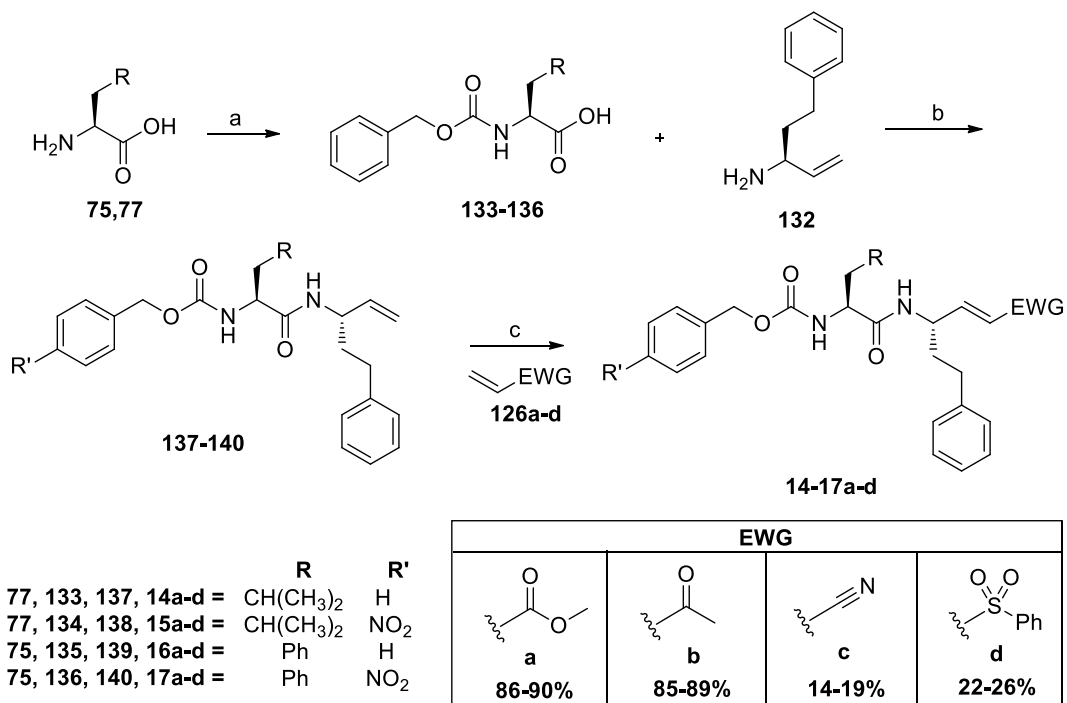
To synthesize novel Michael acceptors we started from the P1 hPhe synthon (Scheme 8), namely terminal olefin hPhe with the free amino group, in agreement with the procedure reported in literature.<sup>99</sup> L-hPhe **76** in ethanol was treated with  $\text{SOCl}_2$  for 48h, to obtain the corresponding ester as chloride salt **127**, which by reaction with trityl chloride, in presence of  $\text{Et}_3\text{N}$ , provided intermediate **128**. The reduction with  $\text{LiAlH}_4$  gave the alcohol **129**, and

Swern oxidation allowed to obtain the corresponding aldehyde **130**. The subsequent Wittig reaction gave terminal olefin **131**, which by treatment with TFA provided amine **132**.



**Scheme 8.** Reagents and conditions: a) ethanol,  $\text{SOCl}_2$ ,  $0^\circ\text{C}$ , then rt, 48 h; b)  $\text{Ph}_3\text{CCl}$ ,  $\text{Et}_3\text{N}$ ,  $\text{CH}_2\text{Cl}_2$ , t.a., 12 h; c)  $\text{LiAlH}_4$ , dry THF,  $\text{N}_2$ ,  $0^\circ\text{C}$ , then rt, 6h; d) oxalyl chloride/DMSO,  $-78^\circ\text{C}$ , 30 min, then  $\text{Et}_3\text{N}$ ,  $-23^\circ\text{C}$ , 40 min; e)  $\text{PhPCH}_3^+\text{I}^-$ ,  $n\text{-BuLi}$ , dry THF,  $0^\circ\text{C}$  then rt, 5 h; f) 2% TFA in  $\text{CH}_2\text{Cl}_2$ , rt, 4 h.

On the other hand, synthesis of the P2-P3 fragment (Scheme 9) was carried through in one step, starting from L-Phe or L-Leu by treatment with Cbz or *p*- $\text{NO}_2$ -Cbz chloroformate, in



**Scheme 9.** Results and conditions: a)  $\text{Na}_2\text{CO}_3$ , Cbz-Cl or **102**,  $0^\circ\text{C}$ , 10 min, then rt, 12h; b) HOBt, EDCl, dry DMF/ $\text{CH}_2\text{Cl}_2$  (1:1),  $0^\circ\text{C}$ ,  $\text{N}_2$ , then 10 min DIPEA, rt, 12h; Hoveyda-Grubbs catalyst 2nd generation, dry  $\text{CH}_2\text{Cl}_2$ ,  $100\text{-}150^\circ\text{C}$ , MW, 2-4 h.



alkaline conditions. The carboxylic acids **133-136** were coupled with the amine **132** in presence of HOBt and EDCI as coupling reagents, to obtain dipeptides **137-140**, which by CM reactions with different CM partners **126a-d**, in presence of Hoveyda-Grubbs catalyst 2nd generation, provided Michael acceptors **14-17a-d**.

All molecules were tested against rhodesain. Initially, a preliminary screening was performed at 50  $\mu\text{M}$ , using an equivalent volume of DMSO as negative control and E-64, the irreversible standard inhibitor of clan CA family C1 cysteine proteases (see chapter 3), used as positive control. With exception of compound **15c**, all Michael acceptors showed inhibitory activity ranging from 85% to 100%. Continuous assays were then performed at seven different concentrations ranging from minimally inhibitory to fully inhibitory concentrations, in order to determine the first-order rate constants of inhibition  $k_{\text{inac}}$  ( $\text{min}^{-1}$ ), the dissociation constants  $K_i$  (nM), and the second-order rate constants of inhibition  $k_{2\text{nd}}$  ( $\text{M}^{-1} \text{min}^{-1}$ ), as  $k_{2\text{nd}} = k_{\text{inac}}/K_i$ . As was predictable, Michael acceptors showed time-dependent inhibition, as can be deduced from an analysis of the progress curves (Figure 51) at seven different concentrations.

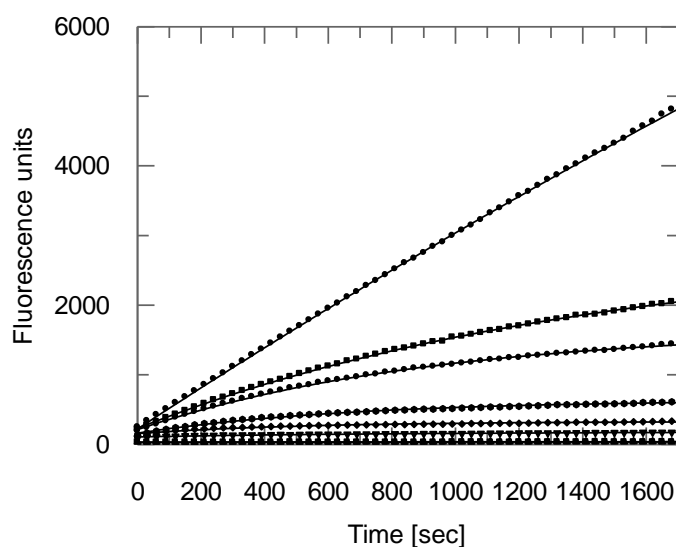


**Figure 51.** Progress curves of substrate hydrolysis in the presence of the inhibitor **14b**. Inhibitor concentrations (from top to bottom): 0, 0.005, 0.01, 0.025, 0.05, 0.1, 0.5, 1  $\mu\text{M}$ .

With exception of nitriles **14c**, **16c** and **17c**, which showed  $k_{2\text{nd}}$  values  $< 19 \cdot 10^3 \text{ M}^{-1} \text{min}^{-1}$ , all Michael acceptors were proven to be potent rhodesain inhibitors, with  $k_{2\text{nd}}$  value ranging from  $152 \cdot 10^3$  to  $67000 \cdot 10^3 \text{ M}^{-1} \text{min}^{-1}$  (Table 23), with a trend of inhibition : ketones  $\gg$  esters  $>$  sulfones  $>$  nitriles.

<b>Table 23. Activity of the Michael acceptors 14-17a-d against rhodesain</b>			
<b>Comp</b>	<b>Rhodesain</b>		
	$k_{\text{inac}}$ ( $\text{min}^{-1}$ )	$K_i$ (nM)	$k_{2\text{nd}}$ ( $\times 10^3 \text{ M}^{-1} \text{ min}^{-1}$ )
<b>14a</b>	0.0038±0.0002	7.5±0.4	509 ±2
<b>15a</b>	0.0023±0.00004	17±6	152±20
<b>16a</b>	0.0018±0.0001	2.0±0.2	919±51
<b>17a</b>	0.0012±0.0001	3.6±0.02	347±44
<b>14b</b>	0.0016±0.0004	0.5±0.2	3795±834
<b>15b</b>	0.0027±0.0009	0.9±0.1	2969±1152
<b>16b</b>	0.00255±0.00075	0.038±0.011	67000±432
<b>17b</b>	0.0017±0.0006	0.074±0.032	24354±1873
<b>14c</b>	0.001±0.0001	53±1	19±2
<b>15c</b>	n.d. <sup>a</sup>	n.d. <sup>a</sup>	n.d. <sup>a</sup>
<b>16c</b>	0.0005±0.0002	46±3	12±6
<b>17c</b>	0.0004±0.0005	1743±3	0.26±0.03
<b>14d</b>	0.0028±0.0003	9.1±2.6	342±129
<b>15d</b>	0.0043±0.0005	14±3	304±20
<b>16d</b>	0.0033±0.0004	5.0±0.6	663±15
<b>17d</b>	0.0024±0.0005	7.2±0.03	334±71
<b>E-64</b>	0.009±0.0004	35±5	261± 27

<sup>a</sup> n.d. = not determined (compound **15c** did not pass the initial screening)

With regard to P2 position, generally, compound bearing a Phe residue were more active compared to the corresponding Leu analogues (**17b** vs **15b**, **16b** vs **14b**, **16a** vs **14a**), while the Cbz-derivatives were more potent than inhibitors with a *p*-NO<sub>2</sub>-Cbz group at the P3 position (**16b** vs **17b**, **16d** vs **17d**, **16a** vs **17a**). All in all, the most potent rhodesain inhibitor was the vinyl ketone **16b**, which showed a  $k_{2\text{nd}}$  value of  $67000 \cdot x 10^3 \text{ M}^{-1} \text{ min}^{-1}$  coupled with the highest binding affinity expressed by  $K_i$  values of 38 pM.

Selectivity assays were also performed (Table 24), by testing the active inhibitors towards cathepsin L, using an equivalent volume of DMSO as negative control, and E-64 as positive control. The obtained results displayed that all tested compounds inhibited cathepsin L to a lower extent compared to rhodesain, with  $k_{2\text{nd}}$  values 1–2 orders of magnitude lower than those recorded for rhodesain inhibition. The best selectivity was shown by vinyl ketones **14b**, **16b** and **17b** and by vinyl sulfones **15d** and **16d**.

The most potent rhodesain inhibitors were tested against cultured *T. b. brucei*, to evaluate their antitrypanosomal activity, using chlorhexidine as positive control. With the exception of compounds **17a** and **16d**, all Michael acceptors showed single-digit micromolar activity (Table 25). Vinyl ketones **16b** and **17b** were proven to be the most active compounds, in correlation with rhodesain inhibition.

<b>Table 24. Biological evaluation against hCatL.</b>			
<b>Comp</b>	<b>Human Cathepsin L</b>		
	$k_{inac}$ (min <sup>-1</sup> )	$K_i$ (nM)	$k_{2nd}$ (x 10 <sup>3</sup> M <sup>-1</sup> min <sup>-1</sup> )
<b>14a</b>	0.0032±0.0002	40±7	81±10
<b>15a</b>	0.0014±0.00005	41±3	35±2
<b>16a</b>	0.0040±0.0004	27±7	153±23
<b>17a</b>	0.0016±0.00005	25±0.2	64±1
<b>14b</b>	0.0013±0.0001	110±40	13±4
<b>15b</b>	0.0026±0.00005	3.5±0.1	739±2
<b>16b</b>	0.002±0.0004	0.4±0.1	5754±523
<b>17b</b>	0.0016±0.0002	2.2±0.2	737±14
<b>14c</b>	0.0012±0.00005	330±67	3.8±0.6
<b>15c</b>	n.d.	n.d.	n.d.
<b>16c</b>	0.0022±0.00005	240±11	9.3±0.2
<b>17c</b>	n.d.	n.d.	n.d.
<b>14d</b>	0.0009±0.00005	0.61±0.05	1571±213
<b>15d</b>	0.005±0.00005	250±20	22±1
<b>16d</b>	0.0014±0.0009	290±87	4.4±1.9
<b>17d</b>	0.003±0.0002	45±5	65±2
<b>E-64</b>	0.0032±0.0001	30±3	110±6
n.d. = not determined			

It is to note that the improvement of the activity from 24h to 48h, which confirms a time-dependent inhibition. Finally, cytotoxicity of the most active compounds was evaluated in HeLa cell lines: inhibitors showed a selectivity index in the range 2.6-4.6.

<b>Table 25. Biological evaluation against <i>T. b. brucei</i> and HeLa cell lines</b>				
<b>Comp</b>	<b><i>T. b. brucei</i>, EC<sub>50</sub> (µM)</b>		<b>HeLa cell</b>	<b>SI</b>
	<b>24 h</b>	<b>48 h</b>	<b>TC<sub>50</sub> (µM)</b>	<b>TC<sub>50</sub>/EC<sub>50</sub></b>
<b>14a</b>	6.08±1.72	5.02±2.67	n.d.	
<b>16a</b>	12.9±7.24	8.28±6.41	n.d.	
<b>17a</b>	97.2±60.32	#	n.d.	
<b>14b</b>	3.85±2.61	3.20±1.77	9.58 ± 1.16	3
<b>15b</b>	3.23±1.98	2.48±1.33	8.20 ± 0.08	3.3
<b>16b</b>	3.18±2.16	2.97±1.19	7.90 ± 0.26	2.6
<b>17b</b>	6.05±1.36	4.98±1.45	n.d.	
<b>14d</b>	2.50±0.46	2.62±0.76	12.17 ± 0.90	4.6
<b>16d</b>	23.7±9.45	18.5±9.81	n.d.	
<b>17d</b>	5.48±0.49	4.07±0.85	n.d.	
<b>Chlorhexidine</b>	0.67±0.13	0.53±0.16	n.d.	
n.d. = not determine; # the compound was unstable after 24 h.				

As reported in chapter 3, rhodesain possesses a high structural homology with FP-2, and for this reason we also tested the molecules against this cysteine protease, in collaboration with Prof. Rhosental of California University. The obtained IC<sub>50</sub> values (Table 26) indicated a weaker inhibition with respect rhodesain, but with similar trend of activity: ketones > sulfones > esters > nitriles. Also towards FP-2, vinyl ketones showed the best activity: in particular, inhibitors **14b** and **15b** exhibited IC<sub>50</sub> values of 0.25 μM and 0.11 μM, respectively. Generally, all active compounds towards FP-2 confirmed their inhibitory properties against cultured *P. falciparum*, with EC<sub>50</sub> values in the low micromolar range, indicating a clear correlation between FP-2 inhibition and antiplasmodium activity (Table 26). Furthermore, inhibition of FP-2 and cultured parasites was consistently better with a leucine rather than Phe amino acid at P2 position, in agreement with the known inhibitory specificity of the plasmodial protease.<sup>100</sup>

<b>Table 26. Biological evaluation against FP-2 and <i>P. falciparum</i></b>		
Comp	FP-2 IC <sub>50</sub> μM	<i>P. falciparum</i> EC <sub>50</sub> μM
<b>14a</b>	9.53±0.095	4.40±1.62
<b>15a</b>	9.63±7.15	3.97±0.72
<b>16a</b>	>50	>10
<b>17a</b>	>50	>10
<b>14b</b>	0.25±0.03	3.16±1.14
<b>15b</b>	0.11±0.04	2.74±1.02
<b>16b</b>	3.01±0.22	7.03±1.65
<b>17b</b>	0.78±0.17	7.18±0.81
<b>14c</b>	>50	>10
<b>15c</b>	>50	>10
<b>16c</b>	>50	>10
<b>17c</b>	>50	>10
<b>14d</b>	0.78±0.069	1.53±0.091
<b>15d</b>	1.32±0.22	2.31±0.01
<b>16d</b>	7.33±1.02	>10
<b>17d</b>	>50	>10
<b>E-64</b>	0.25±0.06	
<b>Artemisinin</b>		0.023±0.002
<b>Chloroquine</b>		0.057±0.009

To complete SAR study of Michael acceptors **14-17a-d**, we carried out docking calculations and molecular dynamics (MD) simulations, in collaboration with Dr. Cosconati (University of Campania Luigi Vanvitelli, Caserta). The crystal structure of rhodesain bound to the inhibitor K11002 (PDB code 2P86)<sup>22</sup> was used, by employing

AutoDock4.2 software. We observed that binding mode of novel inhibitors closely resemble that of K11002, interacting with the same set of key residues, as shown in figure 52. In particular, novel Michael acceptors bind rhodesain by several H-bonds interactions with residues near the catalytic site.

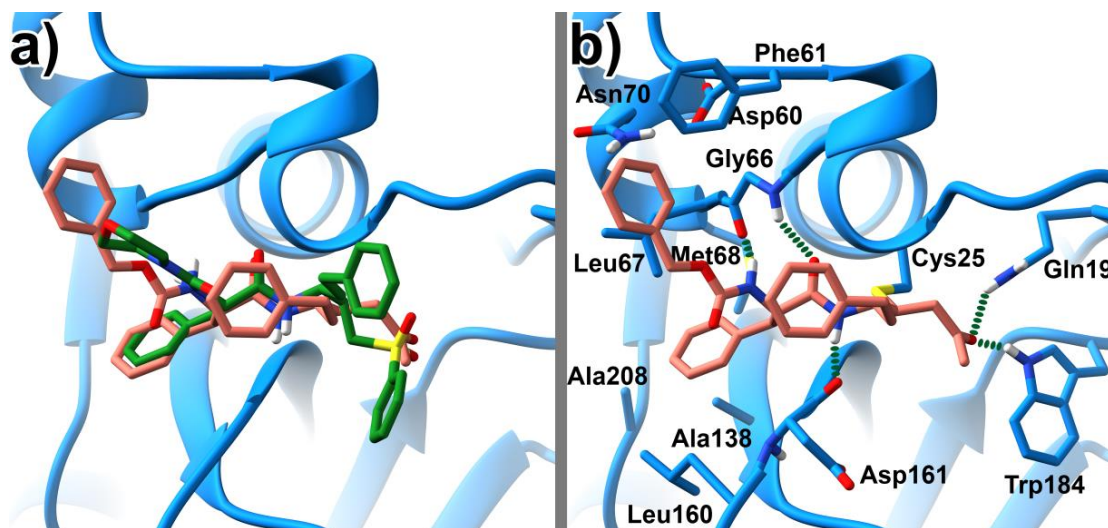


**Figure 52.** a) Superimposition of co-crystal ligand K11002 (green) and **16b** docked conformation (pink) in rhodesain. b) Rhodesain/**16b** (pink) complex. H-bonds are shown in green dashed lines.

The peptide backbone of the Phe and hPhe amino acids of compound **16b** is involved in H-bonds with the backbone atoms of rhodesain Gly66 and Asp161, respectively. In addition, ester, ketone and sulfone warheads are favourably positioned to accept two H-bonds from the Trp184 and Gln19 side chains. On the other hand, nitrile group would not adopt a pose which is conducive to the formation of these two H-bonds: this could explain the considerably lower activity of the compounds bearing this EWG. With regarding P2 position, our docking studies confirmed that the bulky Phe residue provides a better fit into the hydrophobic S2 binding site, which comprises Ala208, Leu160, Ala138, Met68 and Leu67 residues. This likely explains the better activity of the Phe-containing derivatives against rhodesain and cultured trypanosomes, with respect those bearing a Leu residue at the P2 site (see **14b** vs **16b**). The Cbz group accommodates in the S3 pocket, establishing a T-shaped charge-transfer interaction with the phenyl ring of Phe61. Furthermore, the *p*-NO<sub>2</sub> substituent of the Cbz group seems to have two opposite effects on the stability of the binding: while enhancing the above-described charge-transfer contacts, the same partially negative group is unfavourably pointing towards a negatively charged region of the S3 pocket (Asp60), which probably justifies why the nitro group decreases the activity.

Unexpectedly, the hPhe residue at the P1 site does not play a key role in stabilizing inhibitor/rhodesain interactions, since it points towards the outer part of the enzyme active site. When analysing  $K_i$  values (Table 23), it is clear that the different potencies cannot be entirely attributed to the different reactivity of the employed warheads: we suggest that the contacts established by the warheads (e.g. H-bonds) are instrumental in stabilizing the inhibitor in a pose which is conducive for the formation of the covalent bond with the reactive Cys25. The rigid nitrile-containing derivatives were the least active ones, since they cannot adopt the proper orientation within the enzyme cleft, while the ketone moiety seems to be well positioned to fulfil steric and electrostatic demands, which probably explains the higher potencies of these compounds **14b-17b**. Furthermore, the covalent **16b**/rhodesain complex was subjected to an 80 ns long MD simulation. In table 27, we reported the data regarding the stability of key H-bonds that **16b** forms with the enzyme residues.

<b>Table 27. H-bonds statistics from the MD simulation.</b>				
<b>Enzyme Residue Atom</b>	<b>Ligand Atoms</b>	<b>Focc<sup>a</sup></b>	<b>AvgDist<sup>b</sup>(Å)</b>	<b>AvgAng<sup>c</sup>(°)</b>
Asp161 – Backbone C=O	hPhe - NH	0.8554	2.82	163.64
Gly66 – Backbone C=O	Phe - NH	0.7246	2.84	156.88
Gln19 – Sidechain NH <sub>2</sub>	Warhead - C=O	0.6410	2.84	160.35
Trp184 – Sidechain NH	Warhead - C=O	0.5489	2.86	158.56
Gly66 – Backbone NH	Phe - C=O	0.4391	2.88	154.55
<sup>a</sup> Frequency of occurrence of the H-Bond in the frames of the simulation. <sup>b</sup> Mean distance (in Ångstroms) of the H-bond along the simulation. <sup>c</sup> Mean angle (in degrees) H-bond recorded along the simulation.				

In addition, we covalently docked **16b** into FP-2 (Figure 53), by employing the crystal structure of the enzyme with an inhibitor (PDB code 2OUL).<sup>100</sup> Interestingly, the binding mode of **16b** with FP-2 is virtually superimposable to that of rhodesain, although a number of changes were found in the S2 pocket of FP-2, which, as described in chapter 3, plays a key role in determining selectivity in this class of proteases. More in detail Ala208, Ala138 and Gly163 of rhodesain are replaced in FP-2 by aspartate, serine, and alanine residues, respectively. These modifications make the cleft narrower and more polar, thereby inducing the Phe residue in the P2 position to establish less favourable contacts with the corresponding pocket. Varied interactions with residues above mentioned may explain the observed loss of potency against FP-2 compared to that towards rhodesain.

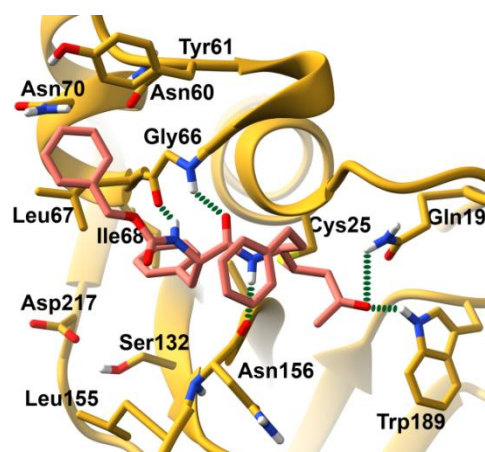


**Figure 53.** Predicted FP-2/**16b** complex. The enzyme is depicted as yellow ribbons and sticks and the ligand is depicted as pink sticks. H-bonds are shown as green dashed lines.

Lastly, we predicted physicochemical and pharmacokinetic features (Table 28) of inhibitor **16b**, by using Qikprop software.

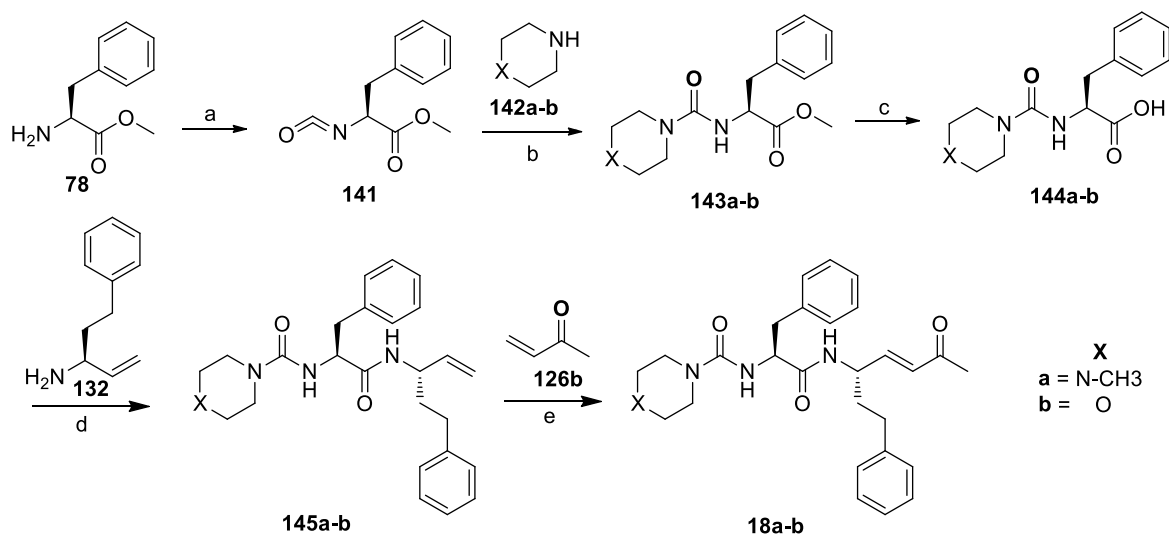
<b>Table 28. Predicted physicochemical and pharmacokinetic properties of inhibitor 16b</b>		
<b>Parameter</b>	<b>16b</b>	<b>Range covered by the 95% of Drugs</b>
mol_MW	484.594	130.0 – 725.0 Molecular weight of the molecule.
donorHB	1.250	0.0 – 6.0 Estimated number of hydrogen bonds that would be donated by the solute to water molecules in an aqueous solution.
accptHB	6.250	2.0 – 20.0 Estimated number of hydrogen bonds that would be accepted by the solute from water molecules in an aqueous solution.
QPlogPo/w	6.005	-2.0 – 6.5 Predicted octanol/water partition coefficient.
QPPCaco	659.806	<25 poor, >500 great Predicted apparent Caco-2 cell permeability in nm/sec. Caco-2 cells are a model for the gut blood barrier.
QPlogBB	-1.387	-3.0 – 1.2 Predicted brain/blood partition coefficient for orally delivered drugs.
QPPMDC K	473.226	<25 poor, >500 great Predicted apparent MDCK cell permeability in nm/sec. MDCK cells are considered to be a good mimic for the BBB
% Human Oral Absorption	100	>80% is high, <25% is poor Predicted human oral absorption on 0 to 100% scale.
Rule Of Five	1	maximum is 4 Number of violations of Lipinski's rule of five. The rules are: mol_MW < 500, QPlogPo/w < 5, donorHB ≤ 5, acctpHB ≤ 10. Compounds that satisfy these rules are considered drug-like.

The obtained results showed that **16b** would feature a substantial gut/blood barrier permeability (see QPPCaco values), and an acceptable probability of crossing the BBB, in agreement with QPlogBB and QPPMDCK values. Furthermore, **16b** is predicted to have a 100% human oral absorption.

In conclusion, in series D we developed novel peptide-based Michael acceptors, which showed impressive  $k_{2nd}$  values and picomolar binding affinity against rhodesain, coupled with single-digit micromolar activity against *T. b. brucei*, good target selectivity and promising drug-like properties. Inhibitory activity against FP-2 was lower, but several compounds demonstrated low micromolar activity against cultured *P. falciparum*. The vinyl ketone **16b**, represents a new hit compound for the development of novel antitrypanosomal agents. Further structural variations may be necessary to improve the cell permeability and target selectivity.

### 5.5 Series E

To synthesize urea derivatives **18a-b** (Scheme 10), Phe methyl ester **78** was treated with triphosgene, to obtain isocyanates **141**, which by reaction with *N*-methyl-piperazine (**142a**) and morpholine (**142b**) gave P3-P2 fragments **143a-b**. The hydrolysis in alkaline conditions provided the corresponding acids **144a-b** and subsequent coupling reactions with the amine **132** allowed to obtain terminal olefins **145a-b**.

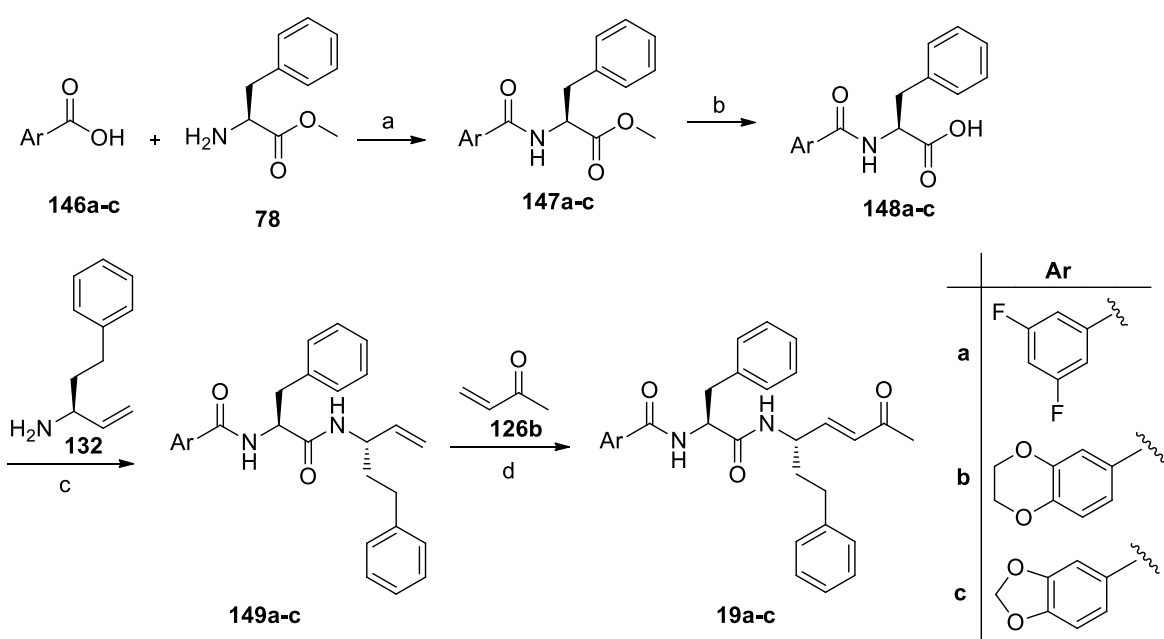


**Scheme 10.** Result and conditions: a) triphosgene,  $\text{CH}_2\text{Cl}_2$ ,  $\text{NaHCO}_3$ ,  $0^\circ\text{C}$  15 min; b) dry THF,  $0^\circ\text{C}$ , 10 min, then rt, 4h; c)  $\text{LiOH}$ ,  $\text{MeOH}/\text{H}_2\text{O}/\text{dioxane}$  (1:1:1),  $0^\circ\text{C}$ , 10 min, then 12h; d)  $\text{HOBt}$ ,  $\text{EDCI}$ , dry  $\text{DMF}/\text{CH}_2\text{Cl}_2$  (1:1),  $0^\circ\text{C}$ , 10 min, then  $\text{DIPEA}$ , rt, 12h; e) Hoveyda-Grubbs catalyst 2nd generation, dry  $\text{CH}_2\text{Cl}_2$ ,  $100^\circ\text{C}$ , MW, 4 h.



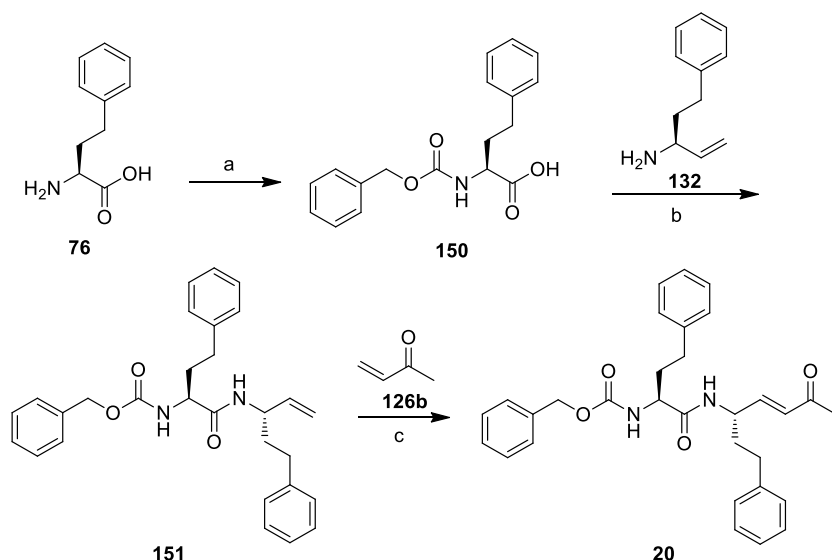
Final products **18a-b** were obtained by CM reactions, using the Hoveyda-Grubbs catalyst 2nd generation and methyl vinyl ketone **126b**.

To synthesize derivatives **19a-c** (Scheme 11), coupling reactions between Phe methyl ester **78** and different acids **146a-c** were carried out, to obtain the esters **147a-c**, which were converted in the corresponding carboxylic acids **148a-c** *via* hydrolysis in alkaline conditions. Subsequently, coupling reactions with amine **132** provided intermediates **149a-c**, which by treatment with methyl vinyl ketone **126b**, in presence of Hoveyda-Grubbs catalyst 2nd generation and under microwave irradiation, allowed us to obtain the CM products **19a-c**.



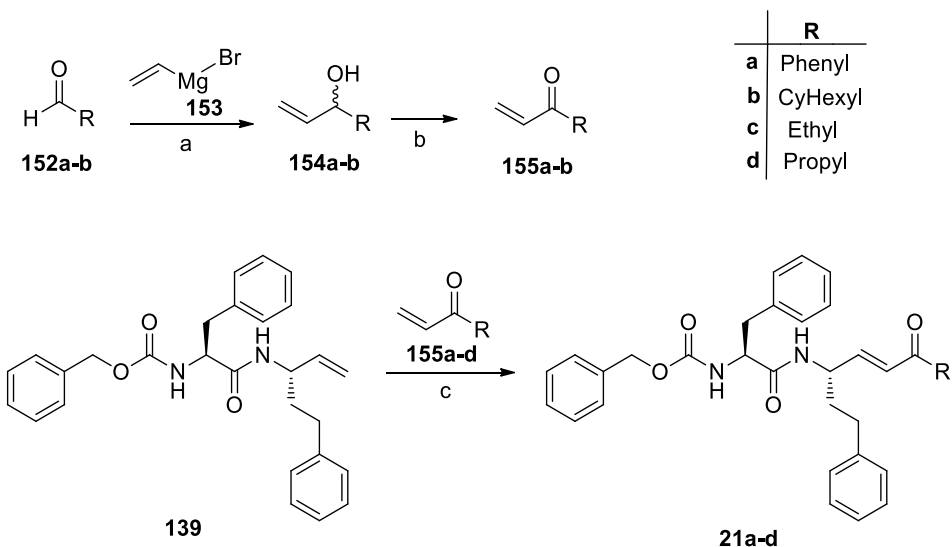
**Scheme 11.** Result and conditions: a) HOBt, EDCI, dry DMF/CH<sub>2</sub>Cl<sub>2</sub>, 0°C, 10 min, then DIPEA, rt, 12h; b) LiOH, MeOH/H<sub>2</sub>O/dioxane (1:1:1), 0° C, 10 min, then 12h; c) HOBt, EDCI, dry DMF/CH<sub>2</sub>Cl<sub>2</sub>, 0°C, 10 min, then DIPEA, rt, 12h; e) Hoveyda-Grubbs catalyst 2nd generation, dry CH<sub>2</sub>Cl<sub>2</sub>, 100 °C, MW, 2 h.

Synthesis of compound **20** (Scheme 12) was performed starting from L-hPhe **76**, which by treatment with Cbz chloroformate provided acid **150**. Coupling reaction between acid **150** and amine **132** gave the terminal olefin **151**, and subsequent CM reaction with methyl vinyl ketone **126b** using the Hoveyda-Grubbs catalyst 2nd generation allowed to obtain the desired product **20**.



**Scheme 12.** Result and conditions: a)  $\text{Na}_2\text{CO}_3$ , Cbz-Cl,  $0^\circ\text{C}$ , 10 min, then rt, 12h; b) HOBt, EDCl, dry  $\text{DMF}/\text{CH}_2\text{Cl}_2$  (1:1),  $0^\circ\text{C}$ ,  $\text{N}_2$ , then 10 min DIPEA, rt, 12h; c) Hoveyda-Grubbs catalyst 2nd generation, dry  $\text{CH}_2\text{Cl}_2$ ,  $100^\circ\text{C}$ , MW, 2 h.

Compounds **21a-d** with modifications at the P1' site were synthesized starting from terminal olefin **139** (Scheme 13), which by CM reaction with several vinyl ketone **155a-d**, allowed to obtain final products.



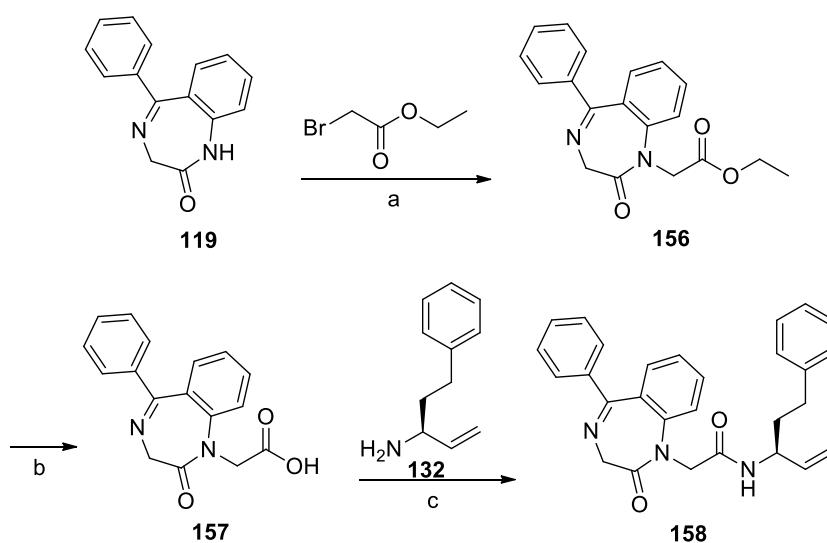
**Scheme 13.** Result and conditions: a) dry THF,  $\text{N}_2$ ,  $0^\circ\text{C}$ , then 153, rt, 12h; b)  $\text{MnO}_2$ ,  $\text{CH}_2\text{Cl}_2$ ,  $\text{N}_2$ , reflux, 24h; c) Hoveyda-Grubbs catalyst 2nd generation, dry  $\text{CH}_2\text{Cl}_2$ ,  $100^\circ\text{C}$ , MW, 2h.

While ethyl (**155c**) and propyl (**155d**) vinyl ketones are commercially available, phenyl and cyclohexyl analogues (**155a** and **155b**, respectively) were synthesized starting from aldehydes **152a-b**, which by treatment with vinyl magnesium bromide **153** gave alcohols **154a-b** and subsequent oxidation with  $\text{MnO}_2$  provide vinyl ketones desired **155a-b**.

These compounds are currently under biological investigation, in order to evaluate their activity against rhodesain.

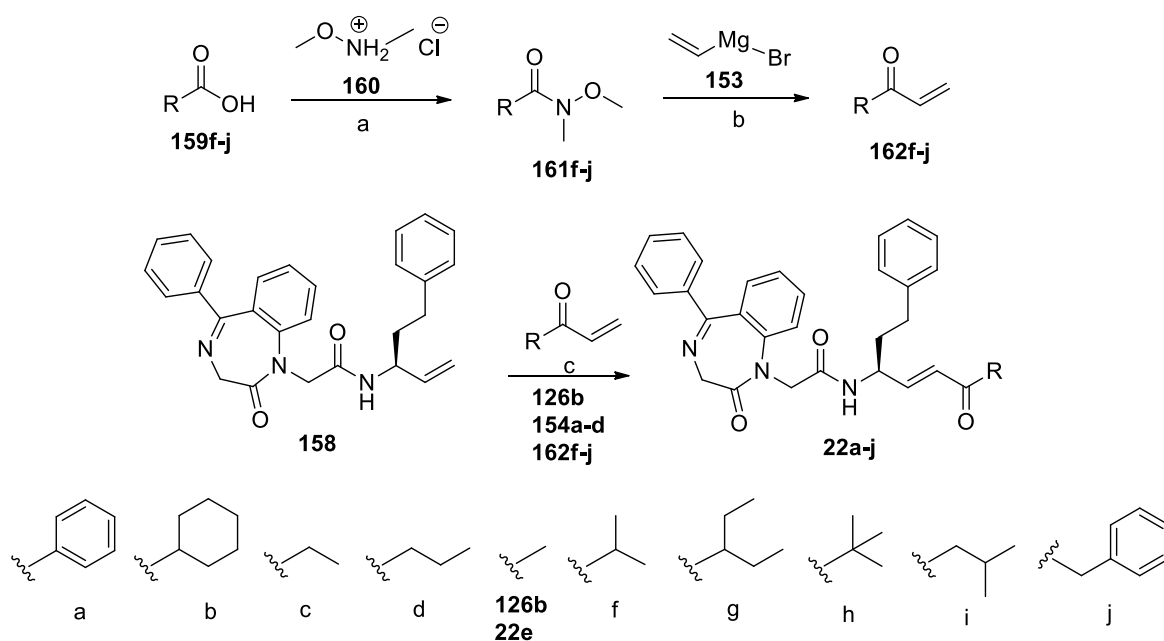
### 5.6 Series F

To obtain novel compounds, we started from BDZ scaffold **119** (Scheme 14), synthesized in agreement to procedure described in series C, by reaction with ethyl bromoacetate, we obtained the intermediate **156**, which by alkaline hydrolysis allowed us to obtain the corresponding acid **157**. Coupling reaction with amine **132** gave the terminal olefin **158**.



**Scheme 14.** Reagents and conditions: a) NaH, DMF, 0 °C to rt, 1h, then BrCH<sub>2</sub>COOEt, rt, 12h; b) LiOH, MeOH/H<sub>2</sub>O/dioxane (1:1:1), 0°C, 10 min, then 12h; c) HOBt, EDCl, DIPEA, CH<sub>2</sub>Cl<sub>2</sub>/DMF, 0°C, 10 min, then 12h;

Then, we synthesized several warheads (Scheme 15), following a different synthetic pathway with respect to that used in series E. With exception of methyl, ethyl and propyl vinyl ketones (**126b**, **154c** and **154d**, respectively), which are commercially available, and phenyl (**154a**) and cyclohexyl (**154b**) vinyl ketones, synthesized as described in series E, the others  $\alpha,\beta$ -unsaturated portions (**162f-j**) were synthesized starting from carboxylic acids (**159f-j**), by treatment with *N,O*-dimethylhydroxylamine hydrochloride **160**: we obtained the corresponding Weinreb amides **161f-j**, which were converted to vinyl derivatives **162f-j** by reaction with vinyl magnesium bromide **153**. Subsequently, CM reactions with several vinyl ketones **126b**, **154a-d** or **162f-j**, using Hoveyda-Grubbs catalyst 2nd generation under microwave irradiation, provided final products **22a-j**.



**Scheme 15.** Reagents and conditions: a) CDI,  $\text{CH}_2\text{Cl}_2$   $0^\circ\text{C}$  for 30 min, then **160**,  $\text{Et}_3\text{N}$ , rt, 12h; b) dry THF,  $\text{N}_2$ ,  $0^\circ\text{C}$  for 10 min, then rt, 6h; c) Hoveyda-Grubbs catalyst 2nd generation, dry  $\text{CH}_2\text{Cl}_2$ ,  $100^\circ\text{C}$ , MW, 2h.

These compounds are currently under biological investigation, in order to evaluate their activity against rhodesain.

## CHAPTER 6. EXPERIMENTAL SECTION

### 6.1 Chemistry.

In this section, we have listed all synthesized molecules grouped according to series A-F: the description was carried out without following the numerical order of molecules, but rather the steps and the temporal sequence of the synthetic pathways, starting from commercially available products and describing the various intermediates until final compounds.

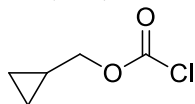
All reagents and solvents were obtained from commercial suppliers and were used without further purification. Reactions under microwave irradiation were performed on a CEM Discover apparatus. Elemental analyses were carried out on a C. Erba Model 1106 (Elemental Analyser for C, H and N) instrument, and the obtained results are within  $\pm 0.4\%$  of the theoretical values. Merck silica gel 60 F254 plates were used for analytical TLC; flash column chromatography was performed on Merck silica gel (200–400 mesh). Polarimetric analyses were carried out on a Perkin–Elmer Polarimeter 341.  $^1\text{H}$  and  $^{13}\text{C}$  and NMR spectra were recorded on Bruker Avance 300 MHz NMR spectrometer equipped with a BBI probe and operating at frequencies of 300.13 and 75.47 MHz. Other experiments were performed on a Varian 500 MHz spectrometer equipped with a ONE\_NMR probe and operating at 499.74 and 125.73 MHz for  $^1\text{H}$  and  $^{13}\text{C}$  and NMR spectra, respectively. We used the residual signal of the deuterated solvent as an internal standard. Splitting patterns are described as singlet (s), doublet (d), doublet of doublet (dd), triplet (t), quartet (q), multiplet (m), or broad singlet (bs).  $^1\text{H}$  and  $^{13}\text{C}$  NMR chemical shifts ( $\delta$ ) are expressed in ppm and coupling constants ( $J$ ) are given in Hz.

### Series A

#### General procedure for the synthesis of chloroformates 101-102

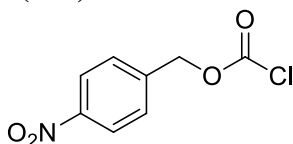
To a solution di alcohol **99** or **100** (0.7 equiv.) in dry THF, at  $0^\circ\text{C}$  and under nitrogen atmosphere, DIPEA (1 equiv.) and triphosgene (1 equiv.) in dry THF were added dropwise. The reaction mixture was stirred for 10 min at  $0^\circ\text{C}$ , and then at rt for 2 h. After this time, the reaction was quenched with saturated solution  $\text{NH}_4\text{Cl}$  and THF was evaporated. The organic layer was extracted with EtOAc (x 3) and then washed with brine (x 3), dried over  $\text{Na}_2\text{SO}_4$ , filtered and concentrated in *vacuo*, to obtain chloroformate to use for next step, without further purification.

### Cyclopropylmethyl carbonochloridate (101)



Yield: 63%; Consistency: yellow oil;  $R_f = 0.28$  (light petroleum/EtOAc, 1:1);  $^1\text{H NMR}$  (300 MHz,  $\text{CDCl}_3$ ) =  $\delta$ : 0.31-0.44 (m, 2H), 0.58-0.73 (m, 2H), 1.02-1.21 (m, 1H), 3.84 (d,  $J = 7.6$  Hz, 1H).

### 4-Nitrobenzyl carbonochloridate (102)

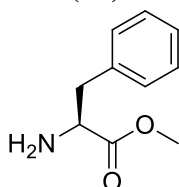


Yield: 84%; Consistency: yellow oil;  $R_f = 0.54$  (light petroleum/EtOAc, 1:1);  $^1\text{H NMR}$  (300 MHz,  $\text{CDCl}_3$ ) =  $\delta$ : 5.37 (s, 2H), 7.56 (d,  $J = 7.5$  Hz, 2H), 8.16 (d,  $J = 7.5$  Hz, 2H).

### General procedure for esters 78-80 synthesis

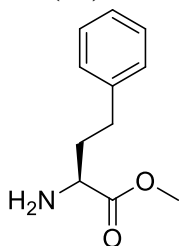
To a suspension of the natural amino acids **75-77** in methanol, 6 N HCl in catalytic quantities was added dropwise. The reaction mixture was stirred at room temperature for 12h. After this time, reaction was quenched at  $0^\circ\text{C}$  with saturated solution of  $\text{K}_2\text{CO}_3$ , until pH 7, and methanol was evaporated. The organic layer was extracted with EtOAc (x 3), dried over anhydrous  $\text{Na}_2\text{SO}_4$ , filtered and the solvent was removed under reduced pressure, to afford the esters desired **78-80**, without further purification.

### (S)-Methyl 2-amino-3-phenylpropanoate (78)



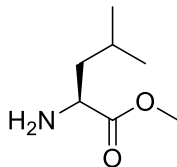
Yield: 79%; Consistency: colourless oil;  $R_f = 0.61$  ( $\text{CH}_2\text{Cl}_2/\text{CH}_3\text{OH}$ , 9:1);  $^1\text{H NMR}$  (300 MHz,  $\text{CDCl}_3$ ) =  $\delta$ : 2.97-3.20 (m, 2H), 3.23-3.37 (m, 1H), 3.70 (s, 3H), 7.09-7.34 (m, 5H).

### (S)-Methyl 2-amino-4-phenylbutanoate (79)



Yield: 81%; Consistency: colourless oil;  $R_f = 0.66$  ( $\text{CH}_2\text{Cl}_2/\text{CH}_3\text{OH}$ , 9:1);  $^1\text{H NMR}$  (300 MHz,  $\text{CDCl}_3$ ) =  $\delta$ : 1.65-1.84 (m, 1H), 1.85-2.04 (m, 1H), 2.49-2.70 (m, 2H), 3.24-3.39 (m, 1H), 3.56 (s, 3H), 6.94-7.20 (m, 5H).

**(S)-Methyl 2-amino-4-methylpentanoate (80)**

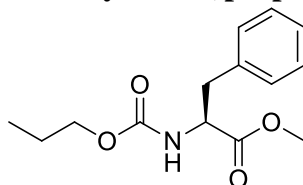


Yield: 84%; Consistency: colourless oil;  $R_f = 0.54$  ( $\text{CH}_2\text{Cl}_2/\text{CH}_3\text{OH}$ , 9:1);  $^1\text{H NMR}$  (300 MHz,  $\text{CDCl}_3$ ) =  $\delta$ : 0.72 (d,  $J = 6.1$  Hz, 3H), 0.74 (d,  $J = 6.1$  Hz, 3H), 1.16-1.29 (m, 1H), 1.31-1.48 (m, 1H), 1.54-1.67 (m, 1H), 3.25-3.32 (m, 1H), 3.52 (s, 3H).

**General procedure for the synthesis of carbamates 81-83, 96-98 and 103-104.**

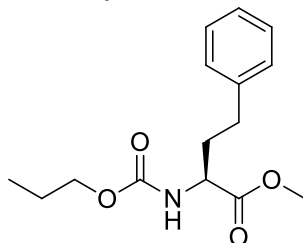
To a solution of ester **78**, **79** or **80** (1 equiv.) in a mixture of saturated solution of  $\text{NaHCO}_3$  and dioxane (7:3) at  $0^\circ\text{C}$ , *n*-propyl chloroformate, allyl chloroformate, **101** or **102** (1.5 equiv.) was added dropwise in a period of 10 min. The mixture was stirred for 12 h at rt. After this time, dioxane was evaporated and the reaction mixture was diluted with EtOAc, washed with a 3 N HCl, dried over anhydrous  $\text{Na}_2\text{SO}_4$ , filtered and concentrated under reduced pressure. The residue was purified by flash chromatography, using as eluent mixture light petroleum/EtOAc in several ratios, to obtain the desired carbamates.

**(S)-Methyl 3-phenyl-2-(propoxycarbonylamino)propanoate (81)**



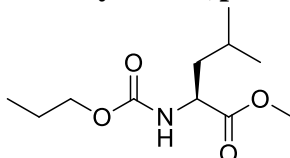
Yield: 57%; Consistency: colourless oil;  $R_f = 0.42$  (light petroleum /EtOAc, 3:2);  $^1\text{H NMR}$  (300 MHz,  $\text{CDCl}_3$ ) =  $\delta$ : 0.94 (t,  $J = 7.8$  Hz, 3H), 1.54-1.70 (m, 2H), 3.06-3.17 (m, 1H), 3.21-3.33 (m, 1H), 3.73 (s, 3H), 4.11 (t,  $J = 6.9$  Hz, 2H), 4.68-4.81 (m, 1H), 5.43 (d,  $J = 7.6$  Hz, 1H), 7.16-7.33 (m, 5H).

**(S)-Methyl 4-phenyl-2-(propoxycarbonylamino)butanoate (82)**



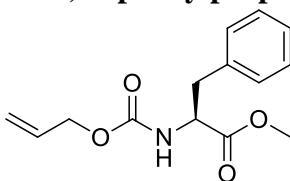
Yield: 61%; Consistency: colourless oil;  $R_f = 0.47$  (light petroleum/EtOAc, 3:2);  $^1\text{H NMR}$  (300 MHz,  $\text{CDCl}_3$ ) =  $\delta$ : 0.99 (t,  $J = 6.7$  Hz, 3H), 1.58-1.72 (m, 2H), 2.17-2.33 (m, 2H), 2.61 (t,  $J = 8.0$  Hz, 2H), 3.78 (s, 3H), 4.15 (t,  $J = 7.6$  Hz, 2H), 4.65 (t,  $J = 7.5$  Hz, 1H), 5.52 (d,  $J = 7.4$  Hz, 1H), 7.12-7.28 (m, 5H).

**(S)-Methyl 4-methyl-2-(propoxycarbonylamino)pentanoate (83)**



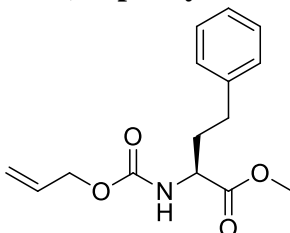
Yield: 60%; Consistency: colourless oil;  $R_f = 0.62$  (light petroleum/EtOAc, 3:2);  $^1\text{H NMR}$  (300 MHz,  $\text{CDCl}_3$ ) =  $\delta$ : 0.93-1.04 (m, 9H), 1.60-1.71 (m, 4H), 1.72-1.81 (m, 1H), 3.72 (s, 3H), 4.14 (t,  $J = 7.6$  Hz, 2H), 4.57 (t,  $J = 6.1$  Hz, 1H), 5.61 (d,  $J = 7.5$  Hz, 1H).

**(S)-Methyl 2-(allyloxycarbonylamino)-3-phenylpropanoate (93)**



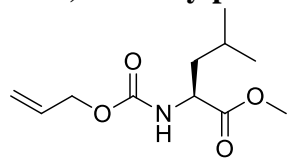
Yield: 88%; Consistency: brown oil;  $R_f = 0.65$  (light petroleum/EtOAc, 1:1);  $^1\text{H NMR}$  (300 MHz,  $\text{CDCl}_3$ ) =  $\delta$ : 3.00-3.18 (m, 2H), 3.72 (s, 3H), 4.56 (d,  $J = 5.5$  Hz, 2H), 4.65 (dd,  $J = 6.1, 14.0$  Hz, 1H), 5.14-5.34 (m, 3H), 5.80-5.96 (m, 1H), 7.12 (d,  $J = 7.3$  Hz, 2H), 7.20-7.36 (m, 3H).

**(S)-Methyl 2-(allyloxycarbonylamino)-4-phenylbutanoate (94)**



Yield: 86%; Consistency: brown oil;  $R_f = 0.69$  (light petroleum/EtOAc, 1:1);  $^1\text{H NMR}$  (300 MHz,  $\text{CDCl}_3$ ) =  $\delta$ : 1.92-2.04 (m, 1H), 2.12-2.24 (m, 1H), 2.62-2.74 (m, 2H), 3.72 (s, 3H), 4.36-4.46 (m, 1H), 4.59 (d,  $J = 5.5$  Hz, 2H), 5.18-5.38 (m, 3H), 5.85-6.00 (m, 1H), 7.15-7.23 (m, 3H), 7.25-7.32 (m, 2H).

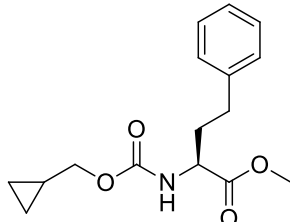
**(S)-Methyl 2-(allyloxycarbonylamino)-4-methylpentanoate (95)**





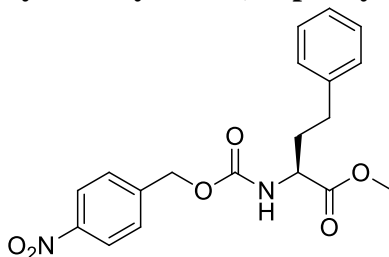
Yield: 85%; Consistency: brown oil;  $R_f = 0.85$  (light petroleum/EtOAc, 1:1);  $^1\text{H NMR}$  (300 MHz,  $\text{CDCl}_3$ ) =  $\delta$ : 0.92 (d,  $J = 6.59$ , 6H), 1.46-1.81 (m, 3H), 3.42 (s, 3H), 4.27-4.39 (m, 1H), 4.54 (d,  $J = 5.7$ , 2H), 5.13-5.46 (m, 2H), 5.80-5.93 (m, 1H), 8.52 (bs, 1H).

**(S)-Methyl 2-(cyclopropylmethoxycarbonylamino)-4-phenylbutanoate (103)**



Yield: 71%; Consistency: brown oil;  $R_f = 0.41$  (light petroleum/EtOAc, 3:2);  $^1\text{H NMR}$  (300 MHz,  $\text{CDCl}_3$ ) =  $\delta$ : 0.29-0.44 (m, 2H), 0.68-0.82 (m, 2H), 1.02-1.18 (m, 1H), 2.18-2.31 (m, 2H), 2.60 (t,  $J = 7.6$  Hz, 2H), 3.77 (s, 3H), 4.11 (d,  $J = 6.3$  Hz, 2H), 4.52 (t,  $J = 7.5$  Hz, 1H), 5.61 (d,  $J = 6.6$  Hz, 1H), 7.13-7.29 (m, 5H).

**(S)-Methyl 2-(4-nitrobenzyloxycarbonylamino)-4-phenylbutanoate (104)**

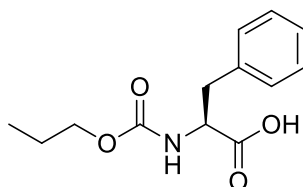


Yield: 71%; Consistency: brown oil;  $R_f = 0.82$  (light petroleum/EtOAc, 1:1);  $^1\text{H NMR}$  (300 MHz,  $\text{CDCl}_3$ ) =  $\delta$ : 2.21-2.34 (m, 2H), 2.57 (t,  $J = 7.6$  Hz, 2H), 3.74 (s, 3H), 4.60-4.72 (m, 1H), 5.21 (s, 2H), 5.29 (d,  $J = 7.5$  Hz, 1H), 7.06-7.33 (m, 5H), 7.46 (d,  $J = 7.3$  Hz, 2H), 8.20 (d,  $J = 7.3$  Hz, 2H).

**General procedure for the synthesis of acids 84-86, 96-98 and 105-106**

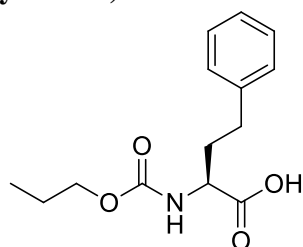
To a solution of carbamate **81-83**, **96-98**, **103** or **104** (1 equiv.) in a mixture methanol/water/dioxane (1:1:1), LiOH as powder (3 equiv.) was added at 0° C. The reaction mixture was then stirred at rt, until disappearance of the starting material, by monitoring in TLC. The solvents was then evaporated in *vacuo* and the reaction mixture was treated with 10% citric acid (x 2), extracted with EtOAc (x 3), dried over  $\text{Na}_2\text{SO}_4$  and concentrated to afford the pure carboxylic acids.

**(S)-3-Phenyl-2-(propoxycarbonylamino)propanoic acid (84)**



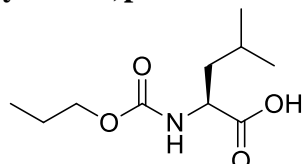
Yield: 98%; Consistency: colourless oil;  $R_f = 0.12$  ( $\text{CH}_2\text{Cl}_2/\text{CH}_3\text{OH}$ , 99:1);  $^1\text{H NMR}$  (300 MHz,  $\text{CDCl}_3$ ) =  $\delta$ : 0.90 (t,  $J = 8.0$  Hz, 3H), 1.51–1.63 (m, 2H), 3.05–3.12 (m, 1H), 3.15–3.24 (m, 1H), 4.00 (t,  $J = 7.0$  Hz, 2H), 4.64–4.71 (m, 1H), 5.38 (d,  $J = 7.5$  Hz, 1H), 7.16–7.31 (m, 5H), 10.32 (bs, 1H); Anal. calcd for  $\text{C}_{13}\text{H}_{17}\text{NO}_4$ : C 62.14; H 6.82; N 5.57; found: C 62.37, H 6.73; N 5.66.

**(S)-4-Phenyl-2-(propoxycarbonylamino)butanoic acid (85)**



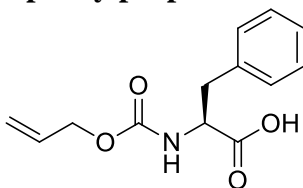
Yield: 97%; Consistency: colourless oil;  $R_f = 0.16$  ( $\text{CH}_2\text{Cl}_2/\text{CH}_3\text{OH}$ , 99:1);  $^1\text{H NMR}$  (300 MHz,  $\text{CDCl}_3$ ) =  $\delta$ : 0.94 (t,  $J = 6.8$  Hz, 3H), 1.57–1.71 (m, 2H), 1.94–2.11 (m, 1H), 2.15–2.30 (m, 1H), 2.72 (t,  $J = 7.9$  Hz, 2H), 4.04 (t,  $J = 7.2$  Hz, 2H), 4.36–4.48 (m, 1H), 5.25 (d,  $J = 8.3$  Hz, 1H), 7.15–7.32 (m, 5H), 10.30 (bs, 1H); Anal. calcd for  $\text{C}_{14}\text{H}_{19}\text{NO}_4$ : C 63.38; H 7.22; N 5.28; found: C 63.18; H 7.49; N 5.36.

**(S)-4-Methyl-2-(propoxycarbonylamino)pentanoic acid (86)**



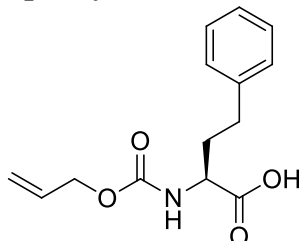
Yield: 95%; Consistency: colourless oil;  $R_f = 0.11$  ( $\text{CH}_2\text{Cl}_2/\text{CH}_3\text{OH}$ , 99:1);  $^1\text{H NMR}$  (300 MHz,  $\text{CDCl}_3$ ) =  $\delta$ : 0.88 (t,  $J = 7.4$  Hz, 3H), 0.92 (d,  $J = 7.4$  Hz, 3H), 0.95 (d,  $J = 7.3$  Hz, 3H), 1.41–1.76 (m, 5H), 4.01 (t,  $J = 7.4$  Hz, 2H), 4.31–4.42 (m, 1H), 5.05 (d,  $J = 6.8$  Hz, 1H), 10.31 (bs, 1H); Anal. calcd for  $\text{C}_{10}\text{H}_{19}\text{NO}_4$ : C 55.28; H 8.81; N 6.45; found: C 54.97; H 8.69; N 6.59.

**(S)-2-(Allyloxycarbonylamino)-3-phenylpropanoic acid (96)**



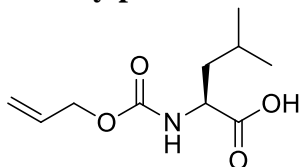
Yield: 90%; Consistency: brown oil;  $R_f = 0.19$  ( $\text{CH}_2\text{Cl}_2/\text{CH}_3\text{OH}$ , 99:1);  $^1\text{H NMR}$  (300 MHz,  $\text{CDCl}_3$ ) =  $\delta$ : 3.06-3.28 (m, 2H), 4.48-4.64 (m, 2H), 4.64-4.76 (m, 1H), 5.10-5.36 (m, 3H), 5.83-5.96 (m, 1H), 7.18 (d,  $J = 7.3$  Hz, 2H), 7.22-7.40 (m, 3H), 7.60-7.80 (bs, 1H). Spectroscopic data are in agreement to those reported in literature.<sup>101</sup>

**(S)-2-(Allyloxycarbonylamino)-4-phenylbutanoic acid (97)**



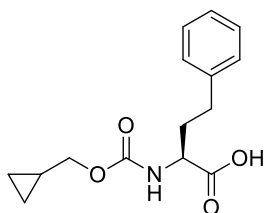
Yield: 92%; Consistency: brown oil;  $R_f = 0.23$  ( $\text{CH}_2\text{Cl}_2/\text{CH}_3\text{OH}$ , 99:1);  $^1\text{H NMR}$  (300 MHz,  $\text{CDCl}_3$ ) =  $\delta$ : 1.96-2.10 (m, 1H), 2.16-2.30 (m, 1H), 2.64-2.80 (m, 2H), 4.38-4.48 (m, 1H), 4.59 (d,  $J = 5.5$  Hz, 2H), 5.18-5.28 (m, 1H), 5.28-5.40 (m, 2H), 5.82-5.98 (m, 1H), 7.12-7.24 (m, 3H), 7.24-7.34 (m, 2H), 7.60-8.60 (bs, 1H). Spectroscopic data are in agreement to those reported in literature.<sup>102</sup>

**(S)-2-(Allyloxycarbonylamino)-4-methylpentanoic acid (98)**



Yield: 93%; Consistency: brown oil;  $R_f = 0.13$  ( $\text{CH}_2\text{Cl}_2/\text{CH}_3\text{OH}$ , 99:1);  $^1\text{H NMR}$  (300 MHz,  $\text{CDCl}_3$ ) =  $\delta$ : 0.92 (d,  $J = 6.6$  Hz, 3H), 0.97 (d,  $J = 6.6$  Hz, 3H), 1.52-1.63 (m, 1H), 1.64-1.83 (m, 2H), 3.66 (bs, 1H), 4.34-4.46 (m, 1H), 4.59 (d,  $J = 5.4$  Hz, 2H), 5.08 (d,  $J = 7.5$  Hz, 1H), 5.23 (dd,  $J = 10.4, 1.3$  Hz, 1H), 5.32 (d,  $J = 14.2$  Hz, 1H), 5.92 (ddt,  $J = 16.3, 10.9, 5.6$  Hz, 1H). Spectroscopic data are in agreement to those reported in literature.<sup>103</sup>

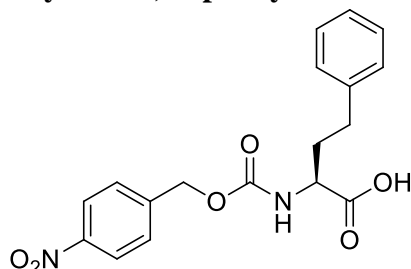
**(S)-2-(Cyclopropylmethoxycarbonylamino)-4-phenylbutanoic acid (105)**



Yield: 97%; Consistency: brown oil;  $R_f = 0.28$  ( $\text{CH}_2\text{Cl}_2/\text{CH}_3\text{OH}$ , 99:1);  $^1\text{H NMR}$  (300 MHz,  $\text{CDCl}_3$ ) =  $\delta$ : 0.22-0.35 (m, 2H), 0.50-0.65 (m, 2H), 0.80-0.91 (m, 1H), 1.97-2.13 (m, 1H), 2.18-2.33 (m, 1H), 2.75 (t,  $J = 7.9$  Hz, 2H), 3.94 (d,  $J = 7.1$  Hz, 2H), 4.38-4.48

(m, 1H), 5.27 (d,  $J = 7.7$  Hz, 1H), 7.13–7.37 (m, 5H). 10.32 (bs, 1H). Anal. calcd for  $C_{15}H_{19}NO_4$ : C 64.97; H 6.91; N 5.05; found: C 65.19; H 7.09; N 4.89.

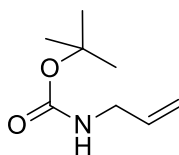
**(S)-2-(4-Nitrobenzyloxycarbonylamino)-4-phenylbutanoic acid (106)**



Yield: 98%; Consistency: brown oil;  $R_f = 0.32$  ( $CH_2Cl_2/CH_3OH$ , 99:1);  $^1H$  NMR (300 MHz,  $CDCl_3$ ) =  $\delta$ : 1.95–2.15 (m, 1H), 2.15–2.35 (m, 1H), 2.74 (t,  $J = 8.0$ , 2H), 4.39–4.51 (m, 1H), 5.22 (s, 2H), 5.56 (d,  $J = 8.5$  Hz, 1H), 7.14–7.35 (m, 5H), 7.51 (d,  $J = 8.4$  Hz, 2H), 8.21 (d,  $J = 8.4$  Hz, 2H) 10.31 (bs, 1H). Anal. calcd for  $C_{18}H_{18}N_2O_6$ : C, 60.33; H, 5.06; N, 7.82; found: C 60.04; H 4.83; N 8.02.

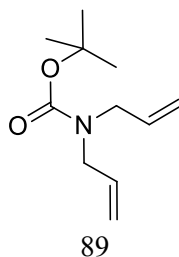
**Synthesis of racemic mixture ( $\pm$ )-92 and enantiomerically pure amines (*R,R*)-92 and (*S,S*)-92**

***tert*-Butyl allylcarbamate (88)**



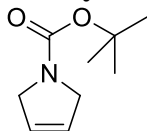
To a solution of allylamine **87** (1 equiv.) in dry  $CH_2Cl_2$  at rt,  $Et_3N$  (1.5 equiv.) and  $(Boc)_2O$  (1.2 equiv.) were added. The reaction mixture was stirred for 12h. After this time,  $CH_2Cl_2$  was added and the organic layer was washed with 10% citric acid solution (x 2),  $NaHCO_3$  saturated solution (x 2) and brine (x 2), dried over  $Na_2SO_4$ , filtered and concentrated in *vacuo*. The crude residue was purified by flash column chromatography using EtOAc/cyclohexane (3:2) as eluent. Yield: 90%; Consistency: yellow oil;  $R_f = 0.54$  (EtOAc/cyclohexane, 3:2);  $^1H$  NMR: ( $CDCl_3$ , 300 MHz) =  $\delta$ : 1.40 (s, 9H); 3.69 (bs, 2H); 4.70 (bs, 1H); 5.05 (d,  $J = 10.2$  Hz, 1H); 5.22 (d,  $J = 17.2$  Hz, 1H); 5.79 (ddt, 1H,  $J = 17.2, 10.2, 5.2$  Hz, 1H).

***tert*-Butyl diallylcarbamate (89)**



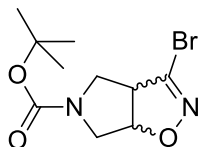
In a double neck round flask containing NaH 60% dispersion in mineral oil (1.7 equiv.), compound **88** (1 equiv.) in dry DMF was added dropwise at 0° C under nitrogen atmosphere. The reaction mixture was stirred for 1h and then allyl bromide (1.2 equiv.) was added and the reaction was maintain in stirred for 12h at rt. After this time, NH<sub>4</sub>Cl saturated solution was added, and the organic layer was extracted with EtOAc (x 5), dried over Na<sub>2</sub>SO<sub>4</sub>, filtered and concentrated in *vacuo*. The resulting residue was purified by flash column chromatography using light petroleum/EtOAc (95:5) as eluent mixture, to give compound **89**. Yield: 85%; Consistency: yellow oil;  $R_f = 0.72$  (light petroleum/EtOAc, 95:5); <sup>1</sup>H NMR: (CDCl<sub>3</sub>, 300 MHz) =  $\delta$ : 1.38 (s, 9H), 3.66-3.80 (m, 4H), 5.0-5.08 (m, 4H), 5.64-5.74 (m, 2H).

***tert*-Butyl 2,5-dihydro-1*H*-pyrrole-1-carboxylate (**90**)**



In a 10 mL microwave tube, equipped with a magnetic stirrer, containing compound **89** (1 equiv.) in dry CH<sub>2</sub>Cl<sub>2</sub>, Hoveyda-Grubbs catalyst 2nd generation [(1,3-bis-(2,4,6-trimethylphenyl)-2-imidazolidinylidene)-dichloro-(*o*-isopropoxyphenyl)methylene] ruthenium] was added (0.03 equiv.). The reaction mixture was stirred for 2h and irradiated at 100°C in a sealed glass tube. After, solvent was evaporated and the resulting residue was purified by flash column chromatography using light petroleum/EtOAc (95:5) as eluent mixture, to obtain intermediate **90**. Yield: 92%; Consistency: yellow oil;  $R_f = 0.52$  (light petroleum/EtOAc, 95:5); <sup>1</sup>H NMR (CDCl<sub>3</sub>, 300 MHz) =  $\delta$ : 1.46 (s, 9 H), 4.10 (m, 4 H), 5.75 (m, 2 H).

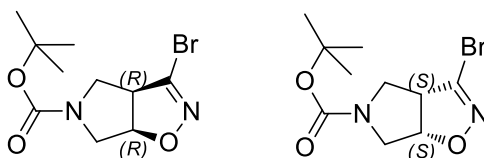
***tert*-Butyl 3-bromo-6,6a-dihydro-3*aH*-pyrrolo[3,4-*d*]isoxazole-5(4*H*)-carboxylate [(±)-**91**]**



To a solution of **90** (1 equiv.) in EtOAc at rt, dibromofomadoxime (2 equiv.) and NaHCO<sub>3</sub> (3.5 equiv.) were added. The reaction was stirred for 72h. After this time, EtOAc was added and the organic layer was washed with water (x 3), dried over Na<sub>2</sub>SO<sub>4</sub>, filtered and concentrated in *vacuo*. The crude product was purified by flash column chromatography using cyclohexane/EtOAc 7:3 as eluent, to give the racemic mixture (±)-**91**. Yield: 74%; Consistency: white solid;  $R_f = 0.35$  (cyclohexane/EtOAc, 7:3); <sup>1</sup>H NMR (300 MHz,

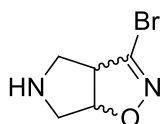
CDCl<sub>3</sub>) =  $\delta$ : 1.46 (s, 9 H), 3.39 (dd,  $J$  = 13.6, 6.2, Hz, 1 H), 3.48 (dd,  $J$  = 13.6, 4.6 Hz, 1 H), 3.78–4.13 (m, 3H), 5.16 (dd,  $J$  = 8.0, 5.2 Hz, 1 H). Spectroscopic data are in agreement to those reported in literature.<sup>104</sup>

**(3aR,6aR)-tert-Butyl 3-bromo-6,6a-dihydro-3aH-pyrrolo[3,4-d]isoxazole-5(4H)-carboxylate [(R,R)-91]** and **(3aS,6aS)-tert-butyl 3-bromo-6,6a-dihydro-3aH-pyrrolo[3,4-d]isoxazole-5(4H)-carboxylate [(S,S)-91]**



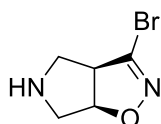
Enantiopure (R,R)-**91** and (S,S)-**91** were obtained from racemic mixture ( $\pm$ )-**91** by preparative chiral HPLC, using *n*-hexane/*i*PrOH (9:1) as eluent mixture, as reported in literature.<sup>81</sup> (S,S)-**91** =  $[\alpha]_{20}^D = + 86.2$  ( $c = 0.47$ , CHCl<sub>3</sub>); Consistency: white solid;  $R_f = 0.35$  (cyclohexane/EtOAc, 7:3); <sup>1</sup>H NMR (300 MHz, CDCl<sub>3</sub>) =  $\delta$ : 1.44 (s, 9H), 3.40 (dd,  $J = 12.2, 8.0$  Hz, 1H), 3.51 (dd,  $J = 13.0, 5.9$  Hz, 1H), 3.86–4.08 (m, 3H), 5.24 (dd,  $J = 8.4, 5.3$  Hz, 1H). Spectroscopic data are in agreement to those reported in literature.<sup>81</sup> (R,R)-**91** =  $[\alpha]_{20}^D = - 76.4$  ( $c = 0.41$ , CHCl<sub>3</sub>). Consistency,  $R_f$  and spectroscopic data are identical to those of the corresponding (S,S) enantiomer.

**(3aR,6aR)-3-Bromo-4,5,6,6a-tetrahydro-3aH-pyrrolo[3,4-d]isoxazole and (3aS,6aS)-3-bromo-4,5,6,6a-tetrahydro-3aH-pyrrolo[3,4-d]isoxazole [( $\pm$ )-92]**



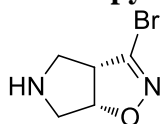
Compound ( $\pm$ )-**91** was treated with a 30% solution of TFA in CH<sub>2</sub>Cl<sub>2</sub> at 0° C, and then the reaction mixture was stirred for 4h at rt. After this time, water was added and CH<sub>2</sub>Cl<sub>2</sub> was evaporated. The aqueous phase was washed with diethyl ether (x 3) and subsequently, K<sub>2</sub>CO<sub>3</sub> saturated solution was added until pH 10. The resulting organic phase was extracted with EtOAc (x 3), dried over Na<sub>2</sub>SO<sub>4</sub>, filtered and concentrated in *vacuo*, to give amine ( $\pm$ )-**92**. Yield: 96%; Consistency: white-yellow powder;  $R_f = 0.21$  (EtOAc/MeOH, 9:1); <sup>1</sup>H NMR (300 MHz, CDCl<sub>3</sub>) =  $\delta$ : 2.04 (bs, 1H), 2.80-2.96 (m, 2H), 3.30-3.52 (m, 2H), 3.77-3.85 (m, 1H), 5.19-5.31 (m, 1H).

**(3aR,6aR)-3-Bromo-4,5,6,6a-tetrahydro-3aH-pyrrolo[3,4-d]isoxazole [(R,R)-92]**



Enantiopure amine (*R,R*)-**92** was synthesized following the same procedure for racemic mixture ( $\pm$ )-**92**.  $[\alpha]_{20}^D = -164.0$  ( $c=0.46$ ,  $\text{CHCl}_3$ ). Yield, consistency and  $R_f$  are identical to those of the racemic mixture ( $\pm$ )-**92**.  $^1\text{H NMR}$  (300 MHz,  $\text{CDCl}_3$ ) =  $\delta$ : 1.83 (bs, 1H), 2.84 (dd,  $J=3.6, 13.4$  Hz, 1H), 2.87 (dd,  $J=7.3, 12.4$  Hz, 1H), 3.38 (d,  $J=12.4$  Hz, 1H), 3.54 (d,  $J=13.4$  Hz, 1H), 3.83 (dd,  $J=7.3, 8.6$  Hz, 1H), 5.25 (dd,  $J=3.6, 8.6$  Hz, 1H);  $^{13}\text{C NMR}$  (75 MHz,  $\text{CDCl}_3$ ) =  $\delta$ : 52.3, 57.2, 59.9, 88.1, 139.5. Spectroscopic data are in agreement to those reported in literature.<sup>81</sup>

**(3*aS*,6*aS*)-3-Bromo-4,5,6,6*a*-tetrahydro-3*aH*-pyrrolo[3,4-*d*]isoxazole [(*S,S*)-**92**]**

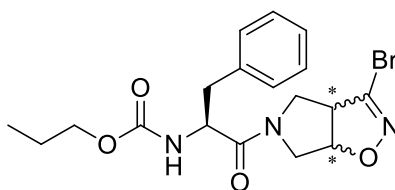


Enantiopure amine (*S,S*)-**92** was synthesized following the same procedure for racemic mixture ( $\pm$ )-**92**.  $[\alpha]_{20}^D = +167.0$  ( $c = 0.54$ ,  $\text{CHCl}_3$ ); Yield, consistency,  $R_f$  and spectroscopic data are identical to those of the corresponding (*R,R*) enantiomer.

**General procedure for the synthesis of coupling products**

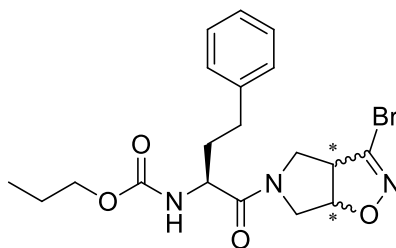
To a solution of carboxylic acid **84-86**, **96-98** or **105-106** (1 equiv.) in DMF/ $\text{CH}_2\text{Cl}_2$  (1:1), HOBt (1.2 equiv.) and EDCI (1.2 equiv.) were added at 0° C. After this time, DIPEA (1.5 equiv.) and racemic mixture ( $\pm$ )-**92**, or enantiopure amine (*R,R*)-**92** or (*S,S*)-**92** (1 equiv.) were added and the reaction mixture was stirred for 12 h at rt. Then, solvents were evaporated and the resulting residue was diluted with EtOAc, washed with a saturated solution of  $\text{NaHCO}_3$  (x 3), dried over  $\text{Na}_2\text{SO}_4$ , filtered and concentrated in *vacuo*. The crude product was purified by flash column chromatography using as eluent a mixture of light petroleum/EtOAc in different ratio, to give the final products.

***n*-Propyl (*S*)-1-((3*aR*,6*aR*)-3-bromo-3*a*,4,6,6*a*-tetrahydropyrrolo[3,4-*d*]isoxazol-5-yl)-1-oxo-3-phenylpropan-2-ylcarbamate and *n*-propyl (*S*)-1-((3*aS*,6*aS*)-3-bromo-3*a*,4,6,6*a*-tetrahydropyrrolo[3,4-*d*]isoxazol-5-yl)-1-oxo-3-phenylpropan-2-ylcarbamate (**1a,b**)**



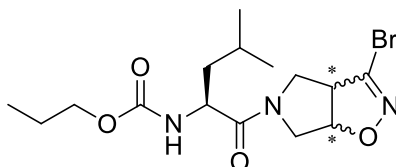
Yield: 84%; Consistency: brown oil;  $R_f = 0.39$  (EtOAc/light petroleum, 3:2);  $^1\text{H NMR}$  (300 MHz,  $\text{CDCl}_3$ ) =  $\delta$ : 0.93 (t,  $J = 8.0$  Hz, 3H), 1.55–1.68 (m, 2H), 2.88–3.02 (m, 1H), 3.02–3.15 (m, 1H), 3.37–3.46 (m, 0.5H), 3.46–3.56 (m, 0.5H), 3.61–3.84 (m, 2H), 3.97 (t,  $J = 7.0$ , 2H), 3.99–4.09 (m, 1H), 4.10 (d,  $J = 13.8$  Hz, 0.5H), 4.17 (d,  $J = 13.8$  Hz, 0.5H), 4.52–4.68 (m, 1H), 5.17–5.26 (m, 1H), 5.42 (d,  $J = 7.4$  Hz, 1H), 7.11–7.33 (m, 5H); MS:  $m/z$  424.1  $[\text{M}+\text{H}]^+$ ; Anal. calcd for  $\text{C}_{18}\text{H}_{22}\text{BrN}_3\text{O}_4$ : C 50.95; H 5.23; N 9.90; found: C 51.10; H 5.46; N 9.63.

***n*-Propyl (S)-1-((3*aR*,6*aR*)-3-bromo-3*a*,4,6,6*a*-tetrahydropyrrolo[3,4-*d*]isoxazol-5-yl)-1-oxo-4-phenylbutan-2-ylcarbamate and *n*-propyl (S)-1-((3*aS*,6*aS*)-3-bromo-3*a*,4,6,6*a*-tetrahydropyrrolo[3,4-*d*]isoxazol-5-yl)-1-oxo-4-phenylbutan-2-ylcarbamate (2*a*,*b*)**



Yield: 88%; Consistency: brown oil;  $R_f = 0.45$  (EtOAc/light petroleum, 3:2);  $^1\text{H NMR}$  (300 MHz,  $\text{CDCl}_3$ ) =  $\delta$ : 0.96 (t,  $J = 8.0$  Hz, 3H), 1.59–1.71 (m, 2H), 1.89–2.07 (m, 2H), 2.65–2.77 (m, 2H), 3.31–3.42 (m, 0.5H), 3.42–3.52 (m, 0.5H), 3.59–3.76 (m, 2H), 3.90–3.99 (m, 1H), 4.03 (t,  $J = 7.5$  Hz, 2H), 4.16–4.30 (m, 1H), 4.33–4.49 (m, 1H), 5.22–5.34 (m, 1H), 5.41 (bs, 1H), 7.17–7.39 (m, 5H); MS:  $m/z$  438.1  $[\text{M}+\text{H}]^+$ ; Anal. calcd for  $\text{C}_{19}\text{H}_{24}\text{BrN}_3\text{O}_4$ : C 52.06, H 5.52, N 9.59; found: C 52.15, H 5.19, N 9.85.

***n*-Propyl (S)-1-((3*aR*,6*aR*)-3-bromo-3*a*,4,6,6*a*-tetrahydropyrrolo[3,4-*d*]isoxazol-5-yl)-4-methyl-1-oxopentan-2-ylcarbamate and *n*-propyl (S)-1-((3*aS*,6*aS*)-3-bromo-3*a*,4,6,6*a*-tetrahydropyrrolo[3,4-*d*]isoxazol-5-yl)-4-methyl-1-oxopentan-2-ylcarbamate (3*a*,*b*)**

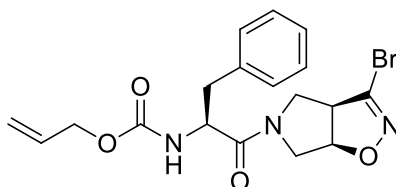


Yield: 86%; Consistency: brown oil;  $R_f = 0.50$  (EtOAc/light petroleum, 3:2);  $^1\text{H NMR}$  (300 MHz,  $\text{CDCl}_3$ ) =  $\delta$ : 0.91 (d,  $J = 7.5$  Hz, 3H), 0.96 (d,  $J = 7.3$  Hz, 3H), 1.02 (t,  $J = 7.4$  Hz, 3H), 1.48–1.80 (m, 5H), 3.47–3.84 (m, 2H), 3.87–4.15 (m, 4H), 4.21 (d,  $J = 13.4$  Hz,



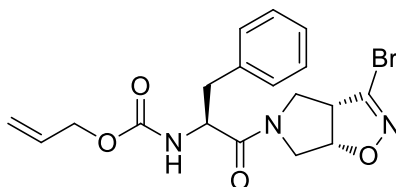
1H), 4.39–4.61 (m, 1H), 5.19–5.44 (m, 2H); MS:  $m/z$  390.1  $[M+H]^+$ ; Anal. calcd for  $C_{15}H_{24}BrN_3O_4$ : C 46.16, H 6.20, N 10.77; found: C 46.02, H 6.43, N 10.62.

**Allyl (S)-1-((3aR,6aR)-3-bromo-3a,4,6,6a-tetrahydropyrrolo[3,4-d]isoxazol-5-yl)-1-oxo-3-phenylpropan-2-ylcarbamate [4a-(S,R,R)]**



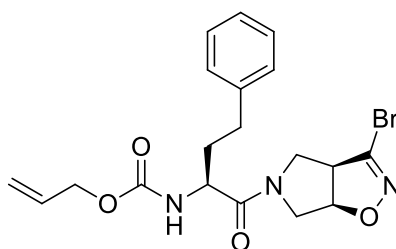
Yield: 89%; Consistency: brown oil;  $R_f = 0.40$  (EtOAc/light petroleum, 3:2);  $[\alpha]_D^{20} = -51.2$  ( $c = 0.40$ ,  $CH_2Cl_2$ );  $^1H$  NMR (300 MHz,  $CDCl_3$ ) =  $\delta$ : 2.86–3.19 (m, 2H), 3.27 (m, 1H), 3.38 (d,  $J = 11.8$  Hz, 1H), 3.67–3.85 (m, 1H), 3.88–4.03 (m, 1H), 4.19 (d,  $J = 11.8$  Hz, 1H), 4.51–4.69 (m, 3H), 5.22 (m, 2H), 5.30 (m, 1H), 5.58 (d,  $J = 8.8$  Hz, 1H), 5.81–6.00 (m, 1H), 7.13–7.38 (m, 5H);  $^{13}C$  NMR (75 MHz,  $CDCl_3$ ) =  $\delta$ : 40.40, 48.73, 53.38, 55.87, 57.54, 66.82, 85.43, 118.42, 128.80, 129.05, 129.47, 134.02, 136.05, 137.24, 155.80, 171.82; MS:  $m/z$  422.2  $[M+H]^+$ ; Anal. calcd for  $C_{18}H_{20}BrN_3O_4$ : C 51.20, H 4.77, N 9.95, found: C 51.39, H 4.62, N 10.24.

**Allyl (S)-1-((3aS,6aS)-3-bromo-3a,4,6,6a-tetrahydropyrrolo[3,4-d]isoxazol-5-yl)-1-oxo-3-phenylpropan-2-ylcarbamate [4b-(S,S,S)]**



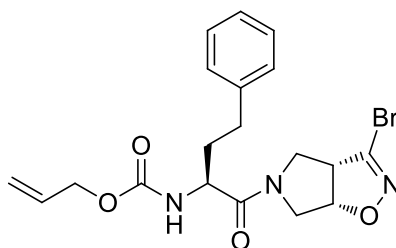
Yield: 92%; Consistency: brown oil;  $R_f = 0.40$  (EtOAc/light petroleum, 3:2);  $[\alpha]_D^{20} = +42.7$  ( $c = 0.18$ ,  $CH_2Cl_2$ );  $^1H$  NMR (300 MHz,  $CDCl_3$ ) =  $\delta$ : 2.83–3.16 (m, 2H), 3.34 (d,  $J = 12.30$  Hz, 1H), 3.54 (m, 1H), 3.73–3.96 (m, 2H), 4.07 (d,  $J = 12.30$  Hz, 1H), 4.51–4.72 (m, 3H), 5.19–5.37 (m, 3H), 5.51 (d,  $J = 7.6$  Hz, 1H), 5.82–6.00 (m, 1H), 7.13–7.36 (m, 5H);  $^{13}C$  NMR (75 MHz,  $CDCl_3$ ) =  $\delta$ : 40.42, 48.71, 53.41, 55.82, 57.50, 66.79, 85.38, 118.40, 128.78, 129.10, 129.51, 134.08, 136.08, 137.20, 155.78, 171.77; MS:  $m/z$  422.2  $[M+H]^+$ ; Anal. calcd for  $C_{18}H_{20}BrN_3O_4$ : C 51.20, H, 4.77, N 9.95; found: C 51.33, H 4.59, N 10.07.

**Allyl (S)-1-((3aR,6aR)-3-bromo-3a,4,6,6a-tetrahydropyrrolo[3,4-d]isoxazol-5-yl)-1-oxo-4-phenylbutan-2-ylcarbamate [5a-(S,R,R)]**



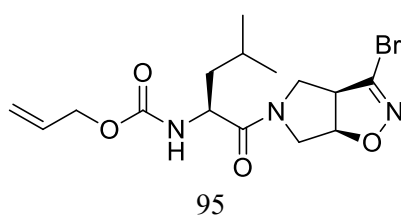
Yield: 81%; Consistency: brown oil;  $R_f = 0.46$  (EtOAc/light petroleum, 3:2);  $[\alpha]_D^{20} = -70.5$  ( $c = 0.39$ ,  $\text{CH}_2\text{Cl}_2$ );  $^1\text{H NMR}$  (300 MHz,  $\text{CDCl}_3$ ) =  $\delta$ : 1.87–2.06 (m, 2H), 2.60–2.82 (m, 2H), 3.42 (m, 1H), 3.57–3.77 (m, 1H), 3.68 (d,  $J = 13.4$  Hz, 1H), 3.88–4.05 (m, 1H), 4.13 (d,  $J = 13.4$  Hz, 1H), 4.39–4.55 (m, 1H), 4.54–4.66 (m, 2H), 5.20–5.32 (m, 1H), 5.28 (m, 2H), 5.62 (d,  $J = 8.1$  Hz, 1H), 5.85–6.01 (m, 1H), 7.17–7.38 (m, 5H);  $^{13}\text{C NMR}$  (75 MHz,  $\text{CDCl}_3$ ) =  $\delta$ : 29.50, 31.74, 47.91, 51.40, 53.09, 55.63, 66.11, 84.43, 117.22, 125.89, 128.68, 129.35, 133.11, 139.21, 141.28, 156.58, 171.78; MS:  $m/z$  436.1  $[\text{M}+\text{H}]^+$ ; Anal. calcd for  $\text{C}_{19}\text{H}_{22}\text{BrN}_3\text{O}_4$ : C 52.30, H 5.08, N 9.63; found: C 52.56, H 5.42, N 9.55.

**Allyl (S)-1-((3aS,6aS)-3-bromo-3a,4,6,6a-tetrahydropyrrolo[3,4-d]isoxazol-5-yl)-1-oxo-4-phenylbutan-2-ylcarbamate [5b-(S,S,S)]**



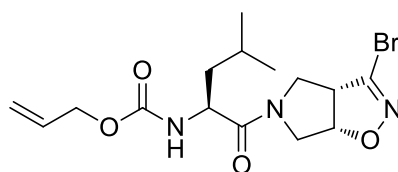
Yield: 85%; Consistency: brown oil;  $R_f = 0.46$  (EtOAc/light petroleum, 3:2);  $[\alpha]_D^{20} = +60.4$  ( $c = 0.22$ ,  $\text{CH}_2\text{Cl}_2$ );  $^1\text{H NMR}$  (300 MHz,  $\text{CDCl}_3$ ) =  $\delta$ : 1.88–2.13 (m, 2H), 2.63–2.78 (m, 2H), 3.46 (m, 1H), 3.60–3.72 (m, 2H), 3.94 (m, 1H), 4.21 (d,  $J = 13.0$  Hz, 1H), 4.33–4.45 (m, 1H), 4.55–4.63 (m, 2H), 5.20–5.39 (m, 3H), 5.60 (d,  $J = 7.7$  Hz, 1H), 5.85–6.01 (m, 1H), 7.15–7.38 (m, 5H);  $^{13}\text{C NMR}$  (75 MHz,  $\text{CDCl}_3$ ) =  $\delta$ : 29.57, 31.77, 47.93, 51.45, 53.15, 55.69, 66.08, 84.48, 117.28, 125.85, 128.62, 129.37, 133.09, 139.24, 141.26, 156.60, 171.80; MS:  $m/z$  436.1  $[\text{M}+\text{H}]^+$ ; Anal. calcd for  $\text{C}_{19}\text{H}_{22}\text{BrN}_3\text{O}_4$ : C 52.30, H 5.08, N 9.63; found: C 52.44, H 5.33, N 9.47.

**Allyl (S)-1-((3aR,6aR)-3-bromo-3a,4,6,6a-tetrahydropyrrolo[3,4-d]isoxazol-5-yl)-4-methyl-1-oxopentan-2-ylcarbamate [6a-(S,R,R)]**



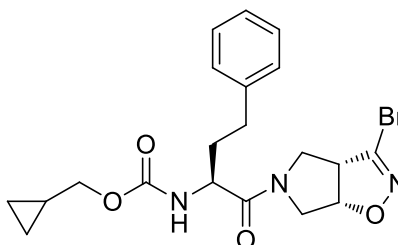
Yield: 93%; Consistency: brown oil;  $R_f = 0.48$  (EtOAc/light petroleum, 3:2);  $[\alpha]_D^{20} = -79.3$  ( $c = 0.75$ ,  $\text{CH}_2\text{Cl}_2$ );  $^1\text{H NMR}$  (300 MHz,  $\text{CDCl}_3$ ) =  $\delta$ : 0.94 (d,  $J = 6.5$  Hz, 3H), 1.01 (d,  $J = 6.7$  Hz, 3H), 1.31–1.45 (m, 1H), 1.44–1.62 (m, 1H), 1.64–1.81 (m, 1H), 3.58 (m, 1H), 3.67–3.82 (m, 1H), 3.96–4.11 (m, 1H), 4.00 (d,  $J = 14.1$  Hz, 1H), 4.17 (d,  $J = 14.1$  Hz, 1H), 4.41–4.50 (m, 1H), 4.50–4.62 (m, 2H), 5.24 (m, 2H), 5.24–5.42 (m, 1H), 5.49 (d,  $J = 8.1$  Hz, 1H), 5.82–5.98 (m, 1H);  $^{13}\text{C NMR}$  (75 MHz,  $\text{CDCl}_3$ ) =  $\delta$ : 21.75, 23.82, 26.50, 44.22, 47.91, 51.63, 53.73, 57.96, 65.93, 84.15, 119.09, 134.91, 139.68, 157.45, 172.23; MS:  $m/z$  388.3  $[\text{M}+\text{H}]^+$ ; Anal. calcd for  $\text{C}_{15}\text{H}_{22}\text{BrN}_3\text{O}_4$ : C 46.40, H 5.71, N 10.82; found: C 46.65, H 5.43, N 10.67.

**Allyl (S)-1-((3a*S*,6a*S*)-3-bromo-3a,4,6,6a-tetrahydropyrrolo[3,4-*d*]isoxazol-5-yl)-4-methyl-1-oxopentan-2-ylcarbamate [6b-(*S,S,S*)]**



Yield: 87%; Consistency: brown oil;  $R_f = 0.48$  (EtOAc/light petroleum, 3:2);  $[\alpha]_D^{20} = +62.2$  ( $c = 0.36$ ,  $\text{CH}_2\text{Cl}_2$ );  $^1\text{H NMR}$  (300 MHz,  $\text{CDCl}_3$ ) =  $\delta$ : 0.94 (d,  $J = 6.5$  Hz, 3H), 0.99 (d,  $J = 6.1$  Hz, 3H), 1.38–1.62 (m, 2H), 1.63–1.77 (m, 1H), 3.51 (m, 1H), 3.90–4.03 (m, 1H), 3.99 (d,  $J = 12.2$  Hz, 1H), 4.15–4.28 (m, 1H), 4.19 (d,  $J = 12.2$  Hz, 1H), 4.39–4.50 (m, 1H), 4.51–4.63 (m, 2H), 5.25 (m, 2H), 5.32–5.51 (m, 2H), 5.82–5.99 (m, 1H);  $^{13}\text{C NMR}$  (75 MHz,  $\text{CDCl}_3$ ) =  $\delta$ : 21.70, 23.79, 26.52, 44.19, 47.89, 51.61, 53.75, 57.93, 65.95, 84.09, 119.11, 134.92, 139.63, 157.40, 172.12; MS:  $m/z$  388.3  $[\text{M}+\text{H}]^+$ ; Anal. calcd for  $\text{C}_{15}\text{H}_{22}\text{BrN}_3\text{O}_4$ : C 46.40, H 5.71, N 10.82; found: C 46.23, H 5.88, N 10.59.

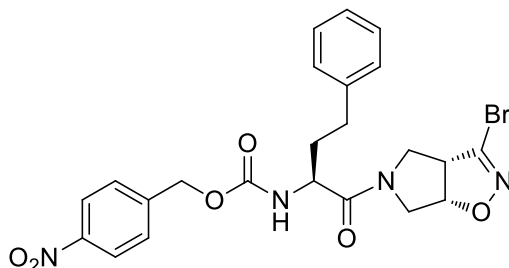
**Cyclopropylmethyl-(S)-1-((3a*S*,6a*S*)-3-bromo-3a,4,6,6a-tetrahydropyrrolo[3,4-*d*]isoxazol-5-yl)-1-oxo-4-phenylbutan-2-ylcarbamate [7b-(*S,S,S*)]**



Yield: 78%; Consistency: brown oil;  $R_f = 0.38$  (EtOAc/light petroleum, 3:2);  $[\alpha]_D^{20} = +65.0$  ( $c = 0.56$ ,  $\text{CH}_2\text{Cl}_2$ );  $^1\text{H NMR}$  (300 MHz,  $\text{CDCl}_3$ ) =  $\delta$ : 0.24–0.36 (m, 2H), 0.53–0.64 (m, 2H), 0.83–0.97 (m, 1H), 1.86–2.12 (m, 2H), 2.62–2.80 (m, 2H), 3.47 (m, 1H), 3.62–

3.71 (m, 2H), 3.86–4.00 (m, 3H), 4.22 (d,  $J = 12.7$  Hz, 1H), 4.33–4.44 (m, 1H), 5.24–5.31 (m, 1H), 5.45 (d,  $J = 8.4$  Hz, 1H), 7.18–7.38 (m, 5H);  $^{13}\text{C}$  NMR (75 MHz,  $\text{CDCl}_3$ ) =  $\delta$ : 4.10, 10.83, 32.70, 35.26, 48.73, 51.79, 54.33, 57.06, 71.51, 85.66, 127.05, 129.33, 129.83, 139.61, 141.87, 157.45, 173.95; MS:  $m/z$  450.1  $[\text{M}+\text{H}]^+$ ; Anal. calcd for  $\text{C}_{20}\text{H}_{24}\text{BrN}_3\text{O}_4$ : C 53.34, H 5.37, N 9.33; found: C 53.62, H 5.19, N 9.19.

**4-Nitrobenzyl-(S)-1-((3aS,6aS)-3-bromo-3a,4,6,6a-tetrahydropyrrolo[3,4-d]isoxazol-5-yl)-1-oxo-4-phenylbutan-2-ylcarbamate [8b-(S,S,S)]**

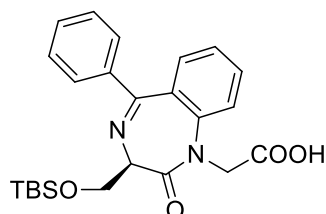


Yield: 92%; Consistency: brown oil;  $R_f = 0.23$  (EtOAc/light petroleum, 3:2);  $[\alpha]_{\text{D}}^{20} = +55.5$  ( $c = 1.32$ ,  $\text{CH}_2\text{Cl}_2$ );  $^1\text{H}$  NMR (300 MHz,  $\text{CDCl}_3$ ) =  $\delta$ : 1.89–2.12 (m, 2H), 2.61–2.80 (m, 2H), 3.45 (m, 1H), 3.60–3.69 (m, 2H), 3.96 (m, 1H), 4.23 (d,  $J = 12.8$  Hz, 1H), 4.35–4.45 (m, 1H), 5.22 (s, 2H), 5.25–5.31 (m, 1H), 5.65 (d,  $J = 7.6$  Hz, 1H), 7.19–7.37 (m, 5H), 7.53 (d,  $J = 8.3$  Hz, 2H), 8.25 (d,  $J = 8.3$  Hz, 2H);  $^{13}\text{C}$  (75 MHz,  $\text{CDCl}_3$ ) =  $\delta$ : 30.43, 33.61, 48.43, 51.91, 54.03, 56.38, 65.61, 87.86, 123.79, 126.97, 128.33, 129.61, 130.14, 139.45, 140.50, 142.85, 145.80, 157.68, 171.98; MS:  $m/z$  531.1  $[\text{M}+\text{H}]^+$ ; Anal. calcd for  $\text{C}_{23}\text{H}_{23}\text{BrN}_4\text{O}_6$ : C 51.99, H 4.36, N 10.54; found: C 52.24, H 4.47, N 10.29.

**Series B**

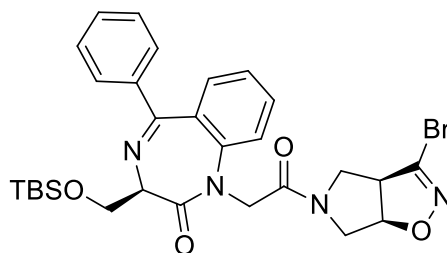
**Synthesis of diastereomers 10a-(R,R,R) and 10b-(R,S,S)**

Carboxylic acid **113** was synthesized following a previously procedure reported in literature.<sup>80a</sup>



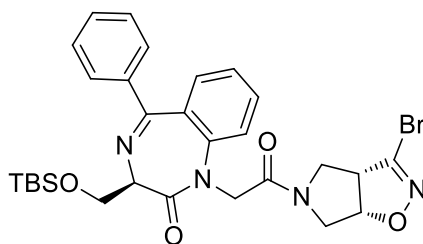
Overall yield: 68%; Consistency: white powder;  $R_f = 0.34$  ( $\text{CH}_2\text{Cl}_2/\text{MeOH}$ , 9:1);  $^1\text{H}$  NMR (300 MHz,  $\text{CDCl}_3$ ): 0.12 (s, 3H), 0.14 (s, 3H), 0.90 (s, 9H), 3.83 (t,  $J = 6.3$  Hz, 1H), 4.31 (dd,  $J = 10.0, 6.1$  Hz, 1H), 4.49–4.60 (m, 3H), 6.60 (bs, 1H), 7.18–7.60 (m, 9H).

**(R)-1-(2-((3aR,6aR)-3-bromo-6,6a-dihydro-3aH-pyrrolo[3,4-d]isoxazol-5(4H)-yl)-2-oxoethyl)-3-(((tert-butyldimethylsilyl)oxy)methyl)-5-phenyl-1H-benzo[e][1,4]diazepin-2(3H)-one [114a-(R,R,R)]**



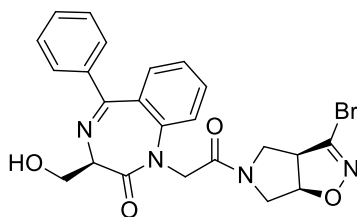
To a solution of carboxylic acid **113** (1 equiv.) in CH<sub>2</sub>Cl<sub>2</sub>, HOBt (1.2 equiv.) and EDCI (1.2 equiv.) were added at 0° C. After this time, DIPEA (1.2 equiv.) and enantiopure amine (*R,R*)-**92** (1 equiv.) were added and the reaction mixture was stirred for 12h at rt. Then, organic phase was washed with brine (x 5), filtered and concentrated in *vacuo*. The crude product was purified by flash column chromatography by light petroleum/EtOAc (3:2) as eluent mixture, to obtain coupling product **114a-(R,R,R)**. Yield: 93%; Consistency: brown oil; *R<sub>f</sub>* = 0.39 (light petroleum/EtOAc, 3:2); <sup>1</sup>H NMR (300 MHz, CDCl<sub>3</sub>) = δ: 0.15 (s, 3H), 0.19 (s, 3H), 1.02 (s, 9H), 3.53-3.61 (m, 1H), 3.79-4.09 (m, 5H), 4.19-4.35 (m, 2H), 4.41 (d, *J* = 16.1 Hz, 1H), 4.73 (d, *J* = 16.1 Hz, 1H), 5.36-5.44 (m, 1H), 7.11-7.56 (m, 9H).

**(R)-1-(2-((3aS,6aS)-3-bromo-6,6a-dihydro-3aH-pyrrolo[3,4-d]isoxazol-5(4H)-yl)-2-oxoethyl)-3-(tert-butyldimethylsilyloxymethyl)-5-phenyl-1H-benzo[e][1,4]diazepin-2(3H)-one [114b-(R,S,S)]**



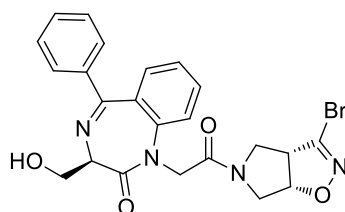
Intermediate **114b-(R,S,S)** was synthesized as described for compound **114a-(R,R,R)**, using (*S,S*)-**92** as amine. Yield, consistency, *R<sub>f</sub>* are identical to those of the corresponding (*R,R,R*) diastereomer. <sup>1</sup>H NMR (300 MHz, CDCl<sub>3</sub>) = δ: 0.16 (s, 3H), 0.20 (s, 3H), 1.04 (s, 9H), 3.54-3.61 (m, 1H), 3.20-4.11 (m, 5H), 4.22-4.36 (m, 2H), 4.47 (d, *J* = 16.0 Hz, 1H), 4.73 (d, *J* = 16.0 Hz, 1H), 5.37-5.46 (m, 1H), 7.13-7.57 (m, 9H).

**(R)-1-(2-((3aR,6aR)-3-bromo-6,6a-dihydro-3aH-pyrrolo[3,4-d]isoxazol-5(4H)-yl)-2-oxoethyl)-3-(hydroxymethyl)-5-phenyl-1H-benzo[e][1,4]diazepin-2(3H)-one [115a-(R,R,R)]**



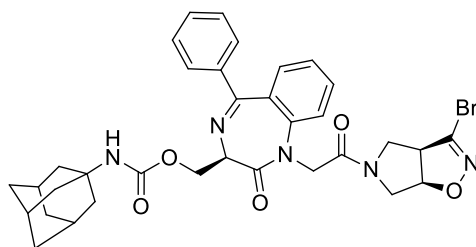
To a solution of **114a-(R,R,R)** (1 equiv.) in dry THF, TBAF 1M solution (1.5 equiv.) was added dropwise. The mixture was stirred at rt until disappearance of the starting material (TLC monitoring). Subsequently, the mixture was diluted with EtOAc and washed with water (x 2). The organic layer was separated, dried (Na<sub>2</sub>SO<sub>4</sub>), filtered, concentrated under reduced pressure and purified by flash column chromatography using EtOAc/light petroleum (4:1) as eluent mixture, to give **115a-(R,R,R)**. Yield = 98%; Consistency: brown oil;  $R_f$  = 0.11 (EtOAc/light petroleum, 4:1); <sup>1</sup>H NMR (300 MHz, CDCl<sub>3</sub>) =  $\delta$ : 3.55-3.63 (m, 1H), 3.82-4.05 (m, 5H), 4.12-4.19 (d,  $J$  = 16.1 Hz, 1H), 4.26-4.35 (m, 2H), 4.70-4.77 (d,  $J$  = 16.1, 1H), 5.34-5.41 (m, 1H), 7.17-7.65 (m, 9H).

**(R)-1-(2-((3a*S*,6a*S*)-3-bromo-6,6a-dihydro-3a*H*-pyrrolo[3,4-*d*]isoxazol-5(4*H*)-yl)-2-oxoethyl)-3-(hydroxymethyl)-5-phenyl-1*H*-benzo[*e*][1,4]diazepin-2(3*H*)-one** [**115b-(R,S,S)**]



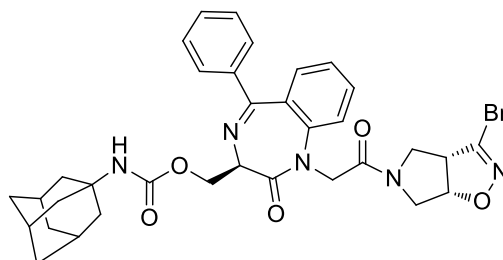
Compound **115b-(R,S,S)** was prepared in agreement to procedure described for compound **115a-(R,R,R)**. Yield, consistency,  $R_f$  are identical to those of the corresponding (*R,R,R*) diastereomer. <sup>1</sup>H NMR (300 MHz, CDCl<sub>3</sub>) =  $\delta$ : 3.38-3.48 (m, 1H), 3.69-3.83 (m, 2H), 3.84-3.98 (m, 3H), 4.11-4.18 (d,  $J$  = 15.2 Hz, 1H), 4.22-4.34 (m, 2H), 4.74-4.81 (d,  $J$  = 15.2 Hz, 1H), 5.28-5.36 (m, 1H), 7.20-7.66 (m, 9H).

**((R)-1-(2-((3a*R*,6a*R*)-3-bromo-6,6a-dihydro-3a*H*-pyrrolo[3,4-*d*]isoxazol-5(4*H*)-yl)-2-oxoethyl)-2-oxo-5-phenyl-2,3-dihydro-1*H*-benzo[*e*][1,4]diazepin-3-yl)methyl adamantan-1-ylcarbamate** [**10a-(R,R,R)**]



To a solution of compound **115a**-(*R,R,R*) (1 equiv.) in dry CH<sub>2</sub>Cl<sub>2</sub>, under nitrogen atmosphere, 1-adamantyl isocyanate (2 equiv.) and Et<sub>3</sub>N (2 equiv.) were added and the resulting mixture was stirred for 3 days at rt. After this time the mixture was washed with water (x 2), dried over Na<sub>2</sub>SO<sub>4</sub> and the solvent was removed under reduced pressure. The crude material was purified by flash column chromatography eluting with EtOAc/light petroleum 4:1 to obtained the title compound **10a**-(*R,R,R*). Yield: 32%; Consistency = brown powder; *R<sub>f</sub>* = 0.46 (EtOAc/light petroleum, 4:1); [α]<sub>D</sub><sup>20</sup> = -58.8 (c = 0.36, CHCl<sub>3</sub>); MS [M+1]<sup>+</sup>:674.1; <sup>1</sup>H NMR (300 MHz, CDCl<sub>3</sub>) = δ: 1.56-1.67 (m, 8H), 1.88-1.93 (m, 4H), 2.00-2.07 (m, 3H), 3.59-3.66 (m, 1H), 3.80-4.03 (m, 5H), 4.13 (d, *J* = 16.1 Hz, 1H), 4.28 (d, *J* = 16.1 Hz, 1H), 4.72-4.83 (m, 2H), 5.12 (bs, 1H), 5.31-5.40 (m, 1H), 7.12-7.66 (m, 9H); <sup>13</sup>C NMR (75 MHz, CDCl<sub>3</sub>) = δ: 29.55, 36.44, 42.54, 48.61, 50.81, 51.18, 53.97, 62.38, 63.29, 84.83, 122.20, 124.60, 128.31, 128.91, 129.52, 130.22, 130.67, 132.12, 138.34, 138.83, 139.66, 156.25, 166.77, 169.15, 169.42. Anal. calcd for C<sub>34</sub>H<sub>36</sub>BrN<sub>5</sub>O<sub>5</sub>: C 60.54, H 5.38, N 10.38; found C 60.71, H 5.67, N 10.22.

**((*R*)-1-(2-((3*aS*,6*aS*)-3-bromo-6,6*a*-dihydro-3*aH*-pyrrolo[3,4-*d*]isoxazol-5(4*H*)-yl)-2-oxoethyl)-2-oxo-5-phenyl-2,3-dihydro-1*H*-benzo[*e*][1,4]diazepin-3-yl)methyl adamantan-1-ylcarbamate [(10*b*-*R,S,S*)]**

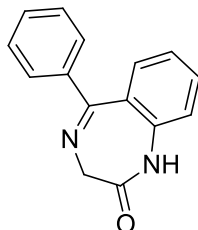


The title compound was prepared following the procedure reported for compound counterparty **10a**-(*R,R,R*), in the same conditions. Yield: 31%; Consistency = brown powder; *R<sub>f</sub>* = 0.46 (EtOAc/light petroleum, 4:1); [α]<sub>D</sub><sup>20</sup> = -15.5 (c = 0.18, CHCl<sub>3</sub>); MS [M+1]<sup>+</sup>:674.2; <sup>1</sup>H NMR (300 MHz, CDCl<sub>3</sub>) = δ: 1.59-1.68 (m, 8H), 1.93-1.97 (m, 4H), 2.04-2.10 (m, 3H), 3.61-3.69 (m, 1H), 3.85-4.08 (m, 5H), 4.15 (d, *J* = 15.8 Hz, 1H), 4.31 (d, *J* = 15.8 Hz, 1H), 4.75-4.88 (m, 2H), 5.18 (bs, 1H), 5.32-5.46 (m, 1H), 7.16-7.67 (m, 9H); <sup>13</sup>C NMR (75 MHz, CDCl<sub>3</sub>) = δ: 29.53, 36.42, 42.55, 48.60, 50.79, 51.20, 53.96, 62.35, 63.28, 84.80, 122.18, 124.58, 128.29, 128.92, 129.50, 130.20, 130.69, 132.10, 138.37, 138.80, 139.64, 156.27, 166.78, 169.16, 169.40. Anal. calcd for C<sub>34</sub>H<sub>36</sub>BrN<sub>5</sub>O<sub>5</sub>: C 60.54, H 5.38, N 10.38; found C 60.83, H 5.54, N 10.13.

## Series C

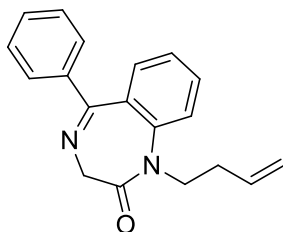
### Synthesis of compounds 11-13a-c

Scaffold **BDZ 119** was synthesized following a previously procedure reported in literature.<sup>98</sup>



Overall yield: 80%; Consistency: orange powder;  $R_f = 0.53$  (light petroleum/EtOAc 1:1);  $^1\text{H NMR}$  (300 MHz,  $\text{CDCl}_3$ ) =  $\delta$ : 4.10 (s, 2H), 7.08-7.28 (m, 3H), 7.34-7.60 (m, 6H), 10.54 (bs, 1H).

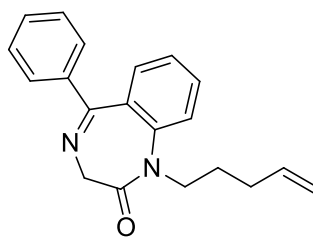
### 1-(But-3-en-1-yl)-5-phenyl-1H-benzo[e][1,4]diazepin-2(3H)-one (**123**)



In a double neck round flask containing NaH 60% dispersion in mineral oil (1.5 equiv.), BDZ scaffold **119** (2 equiv.) in dry DMF was added dropwise at 0° C under nitrogen atmosphere. The reaction mixture was stirred for 1h and then 4-bromo-but-1-ene **120** (1.5 equiv.) was added dropwise. The reaction was stirred for 12h at rt. After this time,  $\text{NH}_4\text{Cl}$  saturated solution was added, and the organic layer was extracted with EtOAc (x 5), dried over  $\text{Na}_2\text{SO}_4$ , filtered and concentrated in *vacuo*. The crude material was purified by flash column chromatography using EtOAc/light petroleum (3:2) as eluent mixture, to obtain terminal olefin **123**. Yield 86%; Consistency: brown oil;  $R_f = 0.72$  (EtOAc/light petroleum, 3:2);  $^1\text{H NMR}$  (300 MHz,  $\text{CDCl}_3$ ) =  $\delta$ : 2.11–2.46 (m, 2H), 3.65–3.74 (m, 1H), 3.79 (d,  $J = 11.2$  Hz, 1 H), 4.42–4.57 (m, 1 H), 4.79 (d,  $J = 11.2$  Hz, 1 H), 4.85–4.98 (m, 2H), 5.55–5.67 (m, 1 H), 7.14–7.69 (m, 9H). Spectroscopic data are in agreement to those reported in literature.<sup>83</sup>

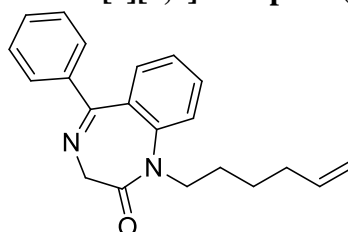
### 1-(Pent-4-en-1-yl)-5-phenyl-1H-benzo[e][1,4]diazepin-2(3H)-one (**124**)





Terminal olefin **124** was synthesized following the procedure described for compound **123**, using 5-bromopent-1-ene **121**. Yield: 81 %. Consistency: brown oil;  $R_f = 0.80$  (EtOAc/light petroleum, 3:2);  $^1\text{H NMR}$  (300 MHz,  $\text{CDCl}_3$ ) =  $\delta$ : 1.42–1.78 (m, 2H), 1.83–2.06 (m, 2H), 3.57–3.71 (m, 1 H), 3.79 (d,  $J = 10.3$  Hz, 1H), 4.33–4.47 (m, 1 H), 4.82 (d,  $J = 10.3$  Hz, 1H), 4.82–4.95 (m, 2H), 5.60–5.76 (m, 1H), 7.15–7.66 (m, 9H). Spectroscopic data are in agreement to those reported in literature.<sup>83</sup>

#### 1-(Hex-5-en-1-yl)-5-phenyl-1H-benzo[e][1,4]diazepin-2(3H)-one (**125**)

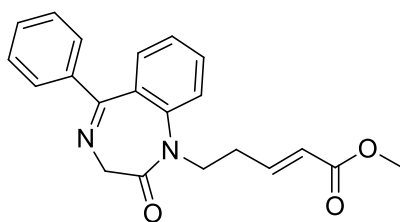


Terminal olefin **125** was synthesized following the procedure described for compound **123**, using 6-bromohex-1-ene **122**. Yield: 78 %; Consistency: brown oil;  $R_f = 0.86$  (EtOAc/light petroleum, 3:2);  $^1\text{H NMR}$  (300 MHz,  $\text{CDCl}_3$ ) =  $\delta$ : 1.36–1.73 (m, 4H), 1.84–1.97 (m, 2H), 3.55–3.70 (m, 1 H), 3.78 (d,  $J = 10.4$  Hz, 1H), 4.36–4.49 (m, 1 H), 4.78 (d,  $J = 10.4$  Hz, 1H), 4.85–4.93 (m, 2H), 5.54–5.69 (m, 1H), 7.14–7.65 (m, 9H). Spectroscopic data are in agreement to those reported in literature.<sup>83</sup>

#### General procedure for synthesis of compounds **11-13a-c**

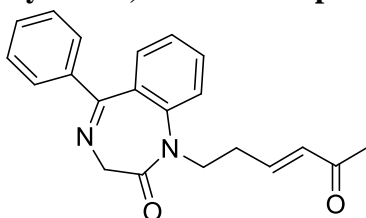
In a 10 mL microwave tube, equipped with a magnetic stirrer, a solution of terminal olefin **123**, **124** or **125** (1 equiv.) in dry  $\text{CH}_2\text{Cl}_2$  (3 mL) was treated with CM partners **126a**, **126b** or **126c** (10 equiv.) and Hoveyda–Grubbs catalyst 2nd generation [(1,3-bis-(2,4,6-trimethylphenyl)-2-imidazolidinylidene)-dichloro-(*o*-isopropoxyphenyl)methylene] ruthenium] (0.1 equiv.). The resulting mixture was heated under microwave irradiation at 100°C for 2 h, and then concentrated in *vacuo*. The residue was purified by flash chromatography using light petroleum/EtOAc in different ratio as eluent mixture, to give desired compounds **11-13a-c**.

#### Methyl (2E)-5-(2,3-dihydro-2-oxo-5-phenyl-1H-1,4-benzodiazepin-1-yl)pent-2-enoate (**11a**)



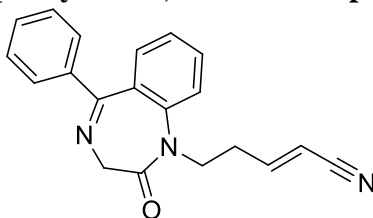
Yield: 85%; Consistency: brown oil;  $R_f = 0.24$  (light petroleum/EtOAc, 1:1);  $^1\text{H NMR}$  (300 MHz,  $\text{CDCl}_3$ ) =  $\delta$ : 2.36-2.61 (m, 2H), 3.58 (s, 3H), 3.71-3.83 (m, 1H), 3.78 (d,  $J = 10.6$  Hz, 1H), 4.47-4.60 (m, 1H), 4.81 (d,  $J = 10.6$  Hz, 1H), 5.72 (d,  $J = 15.4$  Hz, 1H), 6.67-6.81 (m, 1H), 7.19-7.66 (m, 9H);  $^{13}\text{C}$  (75 MHz,  $\text{CDCl}_3$ ) =  $\delta$ : 30.58, 45.36, 51.32, 57.02, 121.86, 123.04, 124.47, 128.25, 129.44, 129.54, 130.15, 130.35, 130.45, 130.57, 131.37, 138.48, 142.34, 144.39, 166.27, 169.65, 170.01; Anal. calcd for  $\text{C}_{21}\text{H}_{20}\text{N}_2\text{O}_3$ : C 72.40, H 5.79, N 8.04; found C 72.61, H 6.02, N 7.93.

**1-((E)-5-oxohex-3-enyl)-5-phenyl-1H-1,4-benzodiazepin-2(3H)-one (11b)**



Yield 76%; Consistency: brown oil;  $R_f = 0.16$  (light petroleum/EtOAc, 1:1);  $^1\text{H NMR}$  (300 MHz,  $\text{CDCl}_3$ ) =  $\delta$ : 1.86 (s, 3H), 2.31-2.45 (m, 1H), 2.47-2.56 (m, 1H), 3.73-3.80 (m, 1H), 3.77 (d,  $J = 10.8$  Hz, 1H), 4.54-4.64 (m, 1H), 4.80 (d,  $J = 10.8$  Hz, 1H), 5.87 (d,  $J = 15.7$  Hz, 1H), 6.43-6.54 (m, 1H), 7.20-7.61 (m, 9H);  $^{13}\text{C}$  (75 MHz,  $\text{CDCl}_3$ ) =  $\delta$ : 27.01, 30.39, 44.87, 56.92, 122.16, 124.91, 128.16, 128.66, 128.69, 130.02, 130.11, 131.21, 131.70, 131.74, 131.86, 138.28, 142.61, 143.13, 166.84, 169.88, 198.30; Anal. calcd for  $\text{C}_{21}\text{H}_{20}\text{N}_2\text{O}_2$ : C 75.88, H 6.06, N 8.43; found C 75.60, H 5.95, N 8.57.

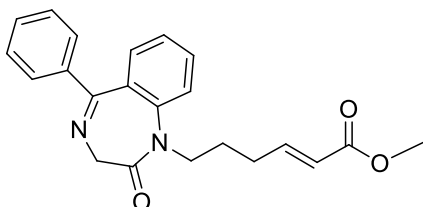
**(Z)-5-(2,3-dihydro-2-oxo-5-phenyl-1H-1,4-benzodiazepin-1-yl)pent-2-enenitrile (11c)**



Yield: 82%; Consistency: brown oil;  $R_f = 0.24$  (light petroleum/EtOAc, 1:1);  $^1\text{H NMR}$  (300 MHz,  $\text{CDCl}_3$ ) =  $\delta$ : 2.37-2.61 (m, 2H), 3.68-3.89 (m, 1H), 3.77 (d,  $J = 10.6$  Hz, 1H), 4.47-4.69 (m, 1H), 4.81 (d,  $J = 10.6$  Hz, 1H), 5.16 (d,  $J = 9.7$  Hz, 1H), 6.24-6.40 (m, 1H), 7.21-7.77 (m, 9H);  $^{13}\text{C}$  (75 MHz,  $\text{CDCl}_3$ ) =  $\delta$ : 30.26, 44.28, 56.78, 101.83, 115.42, 121.78, 124.82, 128.39, 128.52, 129.40, 129.52, 129.95, 130.75, 130.80, 131.82, 138.14, 141.67,

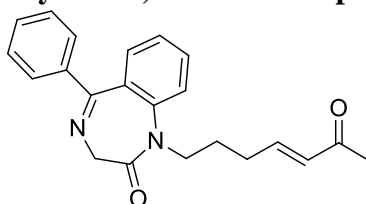
150.56, 169.75, 170.30; Anal. calcd for C<sub>20</sub>H<sub>17</sub>N<sub>3</sub>O: C 76.17, H 5.43, N 13.32; found C 76.01, H 5.65, N 13.08.

**Methyl (2E)-6-(2,3-dihydro-2-oxo-5-phenyl-1H-1,4-benzodiazepin-1-yl)hex-2-enoate (12a)**



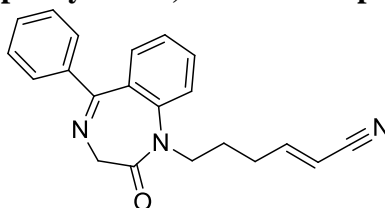
Yield: 87%; Consistency: brown oil;  $R_f$  = 0.28 (light petroleum/EtOAc, 1:1); <sup>1</sup>H NMR (300 MHz, CDCl<sub>3</sub>) =  $\delta$ : 1.63-1.87 (m, 2H), 1.95-2.18 (m, 2H), 3.70 (s, 3H), 3.75-3.86 (m, 1H), 3.79 (d,  $J$  = 10.6 Hz, 1H), 4.34-4.53 (m, 1H), 4.81 (d,  $J$  = 10.6 Hz, 1H), 5.63 (d,  $J$  = 15.4 Hz, 1H), 6.67-6.88 (m, 1H), 7.15-7.74 (m, 9H); <sup>13</sup>C (75 MHz, CDCl<sub>3</sub>) =  $\delta$ : 26.38, 29.03, 45.70, 51.40, 57.14, 121.57, 122.01, 124.45, 128.35, 128.38, 129.32, 129.46, 130.29, 130.44, 130.49, 131.37, 138.62, 142.33, 147.57, 166.79, 169.64, 170.06; Anal. calcd for C<sub>22</sub>H<sub>22</sub>N<sub>2</sub>O<sub>3</sub>: C 72.91, H 6.12, N 7.73; found C 72.80, H 6.33, N 7.59.

**1-((E)-6-oxohept-4-enyl)-5-phenyl-1H-1,4-benzodiazepin-2(3H)-one (12b)**



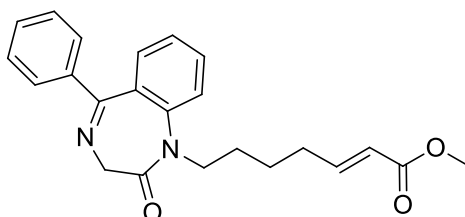
Yield: 79%; Consistency: brown oil;  $R_f$  = 0.19 (light petroleum/EtOAc, 1:1); <sup>1</sup>H NMR (300 MHz, CDCl<sub>3</sub>) =  $\delta$ : 1.53-1.68 (m, 1H), 1.69-1.80 (m, 1H), 1.97-2.11 (m, 2H), 2.15 (s, 3H), 3.62-3.71 (m, 1H), 3.80 (d,  $J$  = 11.2 Hz, 1H), 4.38-4.46 (m, 1H), 4.86 (d,  $J$  = 11.2 Hz, 1H), 5.86 (d,  $J$  = 16.1 Hz, 1H), 6.55-6.64 (m, 1H), 7.23-7.71 (m, 9H); <sup>13</sup>C (75 MHz, CDCl<sub>3</sub>) =  $\delta$ : 26.36, 27.04, 29.17, 46.02, 56.95, 122.34, 124.86, 128.17, 128.65, 128.71, 130.09, 130.13, 130.57, 131.28, 131.62, 131.65, 138.42, 142.64, 146.02, 166.83, 169.91, 198.34; Anal. calcd for C<sub>22</sub>H<sub>22</sub>N<sub>2</sub>O<sub>2</sub>: C 76.28, H 6.40, N 8.09; found C 76.38, H 6.64, N 7.86.

**(2Z)-6-(2,3-dihydro-2-oxo-5-phenyl-1H-1,4-benzodiazepin-1-yl)hex-2-enitrile (12c)**



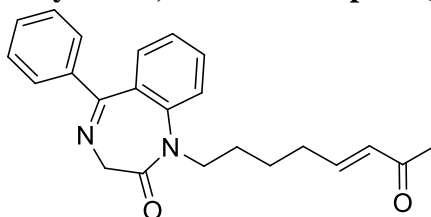
Yield: 86%; Consistency: brown oil;  $R_f = 0.26$  (light petroleum/EtOAc, 1:1);  $^1\text{H NMR}$  (300 MHz,  $\text{CDCl}_3$ ) =  $\delta$ : 1.60-1.80 (m, 2H), 2.20-2.37 (m, 2H), 3.55-3.68 (m, 1H), 3.76 (d,  $J = 10.6$  Hz, 1H), 4.32-4.40 (m, 1H), 4.77 (d,  $J = 10.6$  Hz, 1H), 5.23 (d,  $J = 10.8$  Hz, 1H), 6.33-6.41 (m, 1H), 7.18-7.64 (m, 9H);  $^{13}\text{C}$  (75 MHz,  $\text{CDCl}_3$ ) =  $\delta$ : 26.55, 28.85, 46.10, 56.98, 100.33, 115.69, 121.94, 124.58, 128.37, 128.41, 129.29, 129.40, 130.02, 130.54, 130.57, 131.61, 138.50, 142.45, 153.42, 169.46, 170.26; Anal. calcd for  $\text{C}_{21}\text{H}_{19}\text{N}_3\text{O}$ : C 76.57, H 5.81, N 12.76; found C 76.41, H 5.59, N 12.98.

**Methyl (2E)-7-(2,3-dihydro-2-oxo-5-phenyl-1H-1,4-benzodiazepin-1-yl)hept-2-enoate (13a)**



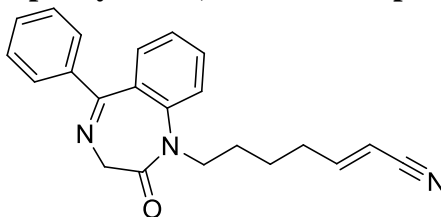
Yield: 92%; Consistency: brown oil;  $R_f = 0.33$  (light petroleum/EtOAc, 1:1);  $^1\text{H NMR}$  (300 MHz,  $\text{CDCl}_3$ ) =  $\delta$ : 1.39-1.76 (m, 4H), 2.01-2.12 (m, 2H), 3.58-3.69 (m, 1H), 3.71 (s, 3H), 3.79 (d,  $J = 10.6$  Hz, 1H), 4.35-4.49 (m, 1H), 4.80 (d,  $J = 10.6$  Hz, 1H), 5.66 (d,  $J = 15.4$  Hz, 1H), 6.69-6.83 (m, 1H), 7.19-7.65 (m, 9H);  $^{13}\text{C}$  (75 MHz,  $\text{CDCl}_3$ ) =  $\delta$ : 24.87, 27.38, 31.62, 46.10, 51.30, 57.16, 121.18, 122.05, 124.32, 128.30, 129.33, 129.89, 130.24, 130.39, 130.42, 131.15, 131.28, 138.63, 142.57, 148.48, 166.87, 169.57, 170.05; Anal. calcd for  $\text{C}_{23}\text{H}_{24}\text{N}_2\text{O}_3$ : C 73.38, H 6.43, N 7.44; found C 72.11, H 6.24, N 7.55.

**1-((E)-7-oxooct-5-enyl)-5-phenyl-1H-1,4-benzodiazepin-2(3H)-one (13b)**



Yield: 84%; Consistency: brown oil;  $R_f = 0.24$  (light petroleum/EtOAc, 1:1);  $^1\text{H NMR}$  (300 MHz,  $\text{CDCl}_3$ ) =  $\delta$ : 1.45-1.54 (m, 2H), 1.60-1.68 (m, 2H), 1.97-2.03 (m, 2H), 2.12 (s, 3H), 3.60-3.68 (m, 1H), 3.79 (d,  $J = 10.6$  Hz, 1H), 4.40-4.52 (m, 1H), 4.80 (d,  $J = 10.6$  Hz, 1H), 5.89 (d,  $J = 15.8$  Hz, 1H), 6.48-6.61 (m, 1H), 7.18-7.69 (m, 9H);  $^{13}\text{C}$  (75 MHz,  $\text{CDCl}_3$ ) =  $\delta$ : 25.42, 26.83, 27.07, 32.16, 46.58, 57.01, 122.53, 124.79, 128.19, 128.62, 128.74, 129.72, 130.10, 130.18, 131.25, 131.67, 131.72, 138.49, 142.69, 146.94, 166.77, 169.97, 198.37; Anal. calcd for  $\text{C}_{23}\text{H}_{24}\text{N}_2\text{O}_2$ : C 76.64, H 6.71, N 8.88; found C 76.45, H 6.86, N 8.61.

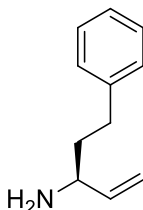
**(2Z)-7-(2,3-dihydro-2-oxo-5-phenyl-1H-1,4-benzodiazepin-1-yl)hept-2-enitrile (13c)**



Yield: 89%; Consistency: brown oil;  $R_f = 0.29$  (light petroleum/EtOAc, 1:1);  $^1\text{H NMR}$  (300 MHz,  $\text{CDCl}_3$ ) =  $\delta$ : 1.36-1.71 (m, 4H), 2.20-2.36 (m, 2H), 3.56-3.70 (m, 1H), 3.79 (d,  $J = 10.6$  Hz, 1H), 4.37-4.55 (m, 1H), 4.79 (d,  $J = 10.6$  Hz, 1H), 5.19 (d,  $J = 11.0$  Hz, 1H), 6.10-6.29 (m, 1H), 7.19-7.75 (m, 9H);  $^{13}\text{C}$  (75 MHz,  $\text{CDCl}_3$ ) =  $\delta$ : 25.01, 27.33, 31.35, 45.91, 57.04, 99.81, 115.85, 122.14, 124.51, 128.39, 128.41, 129.33, 129.40, 130.47, 130.62, 130.78, 131.56, 138.44, 142.38, 154.22, 169.52, 170.25; Anal. calcd for  $\text{C}_{22}\text{H}_{21}\text{N}_3\text{O}$ : C 76.94, H 6.16, N 12.24; found C 77.13, H 5.94, N 12.41.

**Series D**

Synthesis of (*S*)-5-phenylpent-1-en-3-amine (**132**) was carried out following a procedure previously reported in literature.<sup>99</sup>

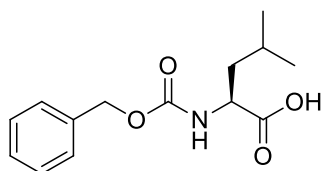


Overall yield: 61%; Consistency: yellow oil;  $R_f = 0.14$  ( $\text{CHCl}_3/\text{MeOH}$ , 99:1);  $^1\text{H NMR}$  (300 MHz,  $\text{CDCl}_3$ ):  $\delta = 1.92$ - $1.99$  (m, 2H),  $2.57$ - $2.70$  (m, 2H),  $3.94$  (q,  $J = 6.5$  Hz, 1H),  $5.01$ - $5.07$  (m, 2H),  $5.79$  (m, 1H),  $7.15$ - $7.21$  (m, 3H),  $7.25$ - $7.29$  (m, 2H).

**General procedure to synthesis acids 133-136**

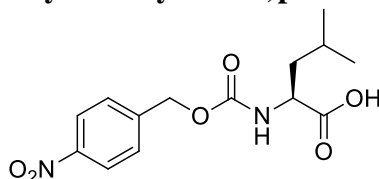
Amino acid Phe **75** (1 equiv.) or Leu (**77**) was solubilized in 2 M solution  $\text{Na}_2\text{CO}_3$ , and the reaction mixture was stirred until complete solubilisation, at  $0^\circ\text{C}$  and in nitrogen atmosphere. Subsequently, Cbz-Cl or **102** (1.1 equiv.) in dioxane was added dropwise in a period of 10 min. The reaction was stirred for 20h at rt. After this time, dioxane was evaporated and resulting mixture was washed with diethyl ether (x 2). The aqueous phase was acidified with diluted HCl until pH 1-2, and the organic phase was extracted with EtOAc (x 3), dried over  $\text{Na}_2\text{SO}_4$ , filtered and concentrated in *vacuo*, to give acids **133-136** desired.

**(S)-2-(benzyloxycarbonylamino)-4-methylpentanoic acid (133)**



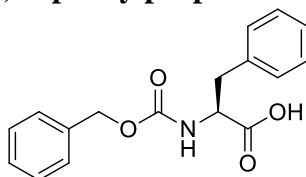
Yield: 93%; Consistency: colourless oil;  $R_f = 0.14$  ( $\text{CHCl}_3/\text{MeOH}$ , 9:1);  $^1\text{H NMR}$  (300 MHz,  $\text{CDCl}_3$ ) =  $\delta$ : 0.99 (s, 6H), 1.52-1.84 (m, 3H), 4.37-4.51 (m, 1H), 5.15 (s, 2H), 7.24-7.43 (m, 5H), 10.90 (bs, 1H). Spectroscopic data are in agreement to those reported in literature.<sup>105</sup>

**(S)-4-methyl-2-(4-nitrobenzyloxycarbonylamino)pentanoic acid (134)**



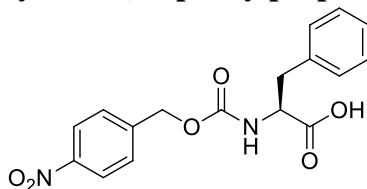
Yield: 90%; Consistency: colourless oil;  $R_f = 0.09$  ( $\text{CH}_2\text{Cl}_2/\text{MeOH}$ , 9:1);  $^1\text{H NMR}$  (300 MHz,  $\text{CDCl}_3$ ) =  $\delta$ : 0.85-1.01 (m, 6H), 1.54-1.82 (m, 3H), 4.32-4.45 (m, 1H), 5.21 (s, 2H), 5.77 (d,  $J = 8.5$  Hz, 1H), 7.49 (d,  $J = 8.6$  Hz, 2H), 8.15 (d,  $J = 8.6$  Hz, 2H), 10.56 (bs, 1H). Spectroscopic data are in agreement to those reported in literature.<sup>106</sup>

**(S)-2-(benzyloxycarbonylamino)-3-phenylpropanoic acid (135)**



Yield: 88%; Consistency: colourless oil;  $R_f = 0.11$  ( $\text{CHCl}_3/\text{MeOH}$ , 99:1);  $^1\text{H NMR}$  (300 MHz,  $\text{CDCl}_3$ ) =  $\delta$ : 2.96-3.21 (m, 2H), 4.59-4.72 (m, 1H), 5.03 (s, 2H), 5.48 (d,  $J = 7.3$  Hz, 1H), 7.02-7.45 (m, 10H), 11.09 (bs, 1H). Spectroscopic data are in agreement to those reported in literature.<sup>105</sup>

**(S)-2-(4-nitrobenzyloxycarbonylamino)-3-phenylpropanoic acid (136)**



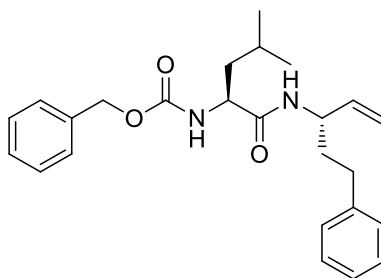
Yield: 91%; Consistency: colourless oil;  $R_f = 0.06$  ( $\text{CHCl}_3/\text{MeOH}$ , 99:1);  $^1\text{H NMR}$  (300 MHz,  $\text{CDCl}_3$ ) =  $\delta$ : 3.09 (dd,  $J = 14.0, 6.8$  Hz, 1H), 3.23 (dd,  $J = 14.0, 5.3$  Hz, 1H), 4.62-4.73 (m, 1H), 5.17 (s, 2H), 5.39 (d,  $J = 8.3$  Hz, 1H), 7.13-7.20 (m, 2H), 7.24-7.33 (m, 3H),

7.42 (d,  $J = 8.7$  Hz, 2H), 7.70 (bs, 1H), 8.17 (d,  $J = 8.7$  Hz, 2H). Spectroscopic data are in agreement to those reported in literature.<sup>106</sup>

#### General procedure for the synthesis of terminal olefines 137-140

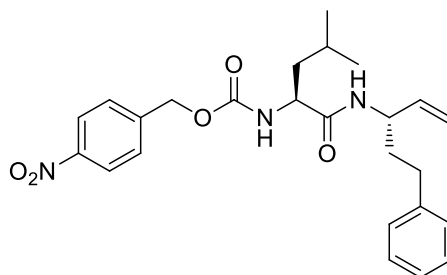
To a solution of acid **133**, **134**, **135** or **136** (1.2 equiv.) in dry DMF/CH<sub>2</sub>Cl<sub>2</sub> (1:1), HOBT (1.2 equiv.) and EDCI (1.2 equiv.) were added, in nitrogen atmosphere at 0° C. After 10 min, the amine **132** (1 equiv.) and DIPEA (1.2 equiv.) were added and the reaction mixture was stirred at rt for 12 h. After this time, the solvents were removed and the residue was diluted with EtOAc, washed with brine (x 5), dried over Na<sub>2</sub>SO<sub>4</sub>, filtered and concentrated in *vacuo*. The crude residue was purified by flash column chromatography using light petroleum/EtOAc in different ratio as eluent mixture, to obtain coupling products **137-140**, in high yields.

#### Benzyl ((S)-4-methyl-1-oxo-1-(((S)-5-phenylpent-1-en-3-yl)amino)pentan-2-yl)carbamate (**137**)



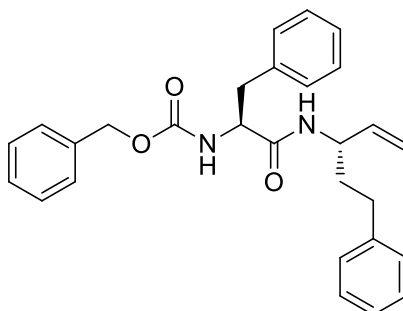
Yield: 83%; Consistency: white powder;  $R_f = 0.23$  (light petroleum/EtOAc, 4:1); <sup>1</sup>H NMR (500 MHz, CDCl<sub>3</sub>) =  $\delta$ : 0.91 (d,  $J = 6.5$  Hz, 3H), 0.94 (d,  $J = 6.5$  Hz, 3H), 1.48-1.54 (m, 1H), 1.61-1.70 (m, 2H), 1.75-1.93 (m, 2H), 2.61 (t,  $J = 7.7$  Hz, 2H), 4.13-4.21 (m, 1H), 4.44-4.52 (m, 1H), 5.02-5.20 (m, 2H), 5.08 (s, 2H), 5.29 (d,  $J = 8.2$  Hz, 1H), 5.70-5.81 (m, 1H), 6.20 (d,  $J = 7.0$  Hz, 1H), 7.10-7.20 (m, 4H), 7.22-7.32 (m, 6H); <sup>13</sup>C NMR (125 MHz, CDCl<sub>3</sub>) =  $\delta$ : 22.87, 23.88, 24.69, 32.04, 36.36, 41.16, 51.16, 53.71, 67.07, 115.19, 125.93, 128.01, 128.18, 128.39, 128.45, 128.50, 136.10, 137.82, 141.53, 156.33, 171.48; Elemental analysis: calcd for C<sub>25</sub>H<sub>32</sub>N<sub>2</sub>O<sub>3</sub>: C 73.50, H 7.90, N 6.86; found: C 73.88, H 7.68, N 6.99.

#### 4-Nitrobenzyl ((S)-4-methyl-1-oxo-1-(((S)-5-phenylpent-1-en-3-yl)amino)pentan-2-yl)carbamate (**138**)



Yield: 88%; Consistency: yellow powder;  $R_f = 0.12$  (light petroleum/EtOAc, 4:1);  $^1\text{H}$  NMR (300 MHz,  $\text{CDCl}_3$ ) =  $\delta$ : 0.91 (d,  $J = 6.6$  Hz, 3H), 0.94 (d,  $J = 6.6$  Hz, 3H), 1.48-1.73 (m, 3H), 1.76-1.91 (m, 2H), 2.60 (t,  $J = 7.9$  Hz, 2H), 4.08-4.21 (m, 1H), 4.42-4.55 (m, 1H), 5.05-5.22 (m, 2H), 5.16 (s, 2H), 5.44 (d,  $J = 8.3$  Hz, 1H), 5.68-5.85 (m, 1H), 6.02 (d,  $J = 8.3$  Hz, 1H), 7.07-7.30 (m, 5H), 7.44 (d,  $J = 8.5$  Hz, 2H), 8.14 (d,  $J = 8.5$  Hz, 2H);  $^{13}\text{C}$  NMR (75 MHz,  $\text{CDCl}_3$ ) =  $\delta$ : 22.11, 22.87, 24.71, 32.03, 36.42, 41.41, 51.23, 53.81, 65.41, 115.31, 123.73, 126.05, 127.94, 128.33, 128.50, 137.71, 141.37, 143.59, 147.53, 155.78, 171.27; Elemental analysis: calcd for  $\text{C}_{25}\text{H}_{31}\text{N}_3\text{O}_5$ : C 66.21, H 6.89, N 9.27; found: C 65.97, H 6.72, N 9.53.

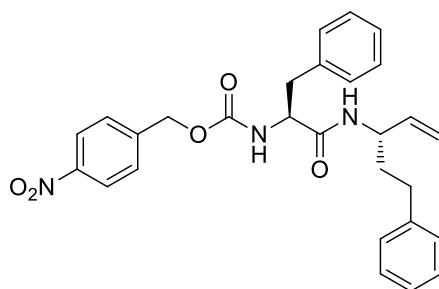
**Benzyl**                    **((S)-1-oxo-3-phenyl-1-((S)-5-phenylpent-1-en-3-ylamino)propan-2-yl)carbamate (139)**



Yield: 74%; Consistency: white powder;  $R_f = 0.38$  (light petroleum/EtOAc, 4:1);  $^1\text{H}$  NMR (300 MHz,  $\text{CDCl}_3$ ) =  $\delta$ : 1.62-1.85 (m, 2H), 2.54 (t,  $J = 7.9$  Hz, 2H), 2.97-3.13 (m, 2H), 4.28-4.49 (m, 2H), 4.86-5.04 (m, 2H), 5.07 (s, 2H), 5.32 (d,  $J = 6.6$  Hz, 1H), 5.51-5.64 (m, 1H), 5.71 (d,  $J = 8.3$  Hz, 1H), 7.03-7.39 (m, 15H);  $^{13}\text{C}$  NMR (75 MHz,  $\text{CDCl}_3$ ) =  $\delta$ : 31.94, 36.19, 38.50, 51.27, 56.54, 67.10, 115.36, 125.97, 127.05, 128.05, 128.24, 128.33, 128.45, 128.54, 128.75, 129.38, 136.03, 136.41, 137.40, 141.41, 156.02, 169.99; Elemental analysis: calcd for  $\text{C}_{28}\text{H}_{30}\text{N}_2\text{O}_3$ : C 75.99, H 6.83, N 6.33; found: C 76.19, 6.71, N 6.08.

**4-Nitrobenzyl**            **((S)-1-oxo-3-phenyl-1-((S)-5-phenylpent-1-en-3-ylamino)propan-2-yl)carbamate (140)**



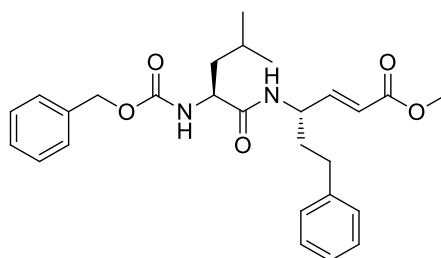


Yield: 74%; Consistency: yellow powder;  $R_f = 0.13$  (light petroleum/EtOAc, 4:1);  $^1\text{H}$  NMR (500 MHz,  $\text{CDCl}_3$ ) =  $\delta$ : 1.64-1.82 (m, 2H), 2.53 (bt, 2H), 2.99-3.12 (m, 2H), 4.36-4.48 (m, 2H), 4.84-5.04 (m, 2H), 5.11 (s, 2H), 5.51-5.63 (m, 1H), 5.83 (d,  $J = 6.5$  Hz, 1H), 5.98 (d,  $J = 7.2$  Hz, 1H), 7.03-7.30 (m, 10H), 7.36 (d,  $J = 7.3$  Hz, 2H), 8.10 (d,  $J = 7.3$  Hz, 2H);  $^{13}\text{C}$  NMR (125 MHz,  $\text{CDCl}_3$ ) =  $\delta$ : 31.75, 36.08, 38.58, 51.15, 56.47, 65.14, 115.16, 123.46, 125.78, 126.85, 127.65, 128.07, 128.22, 128.48, 129.15, 136.12, 137.15, 141.10, 143.41, 147.29, 155.37, 169.95; Elemental analysis: calcd for  $\text{C}_{28}\text{H}_{29}\text{N}_3\text{O}_5$ : C 68.98, H 6.00, N 8.62; found: C 68.77, H 5.83, N 8.81.

#### General procedure for the synthesis of Michael acceptors 14-17a-d

A solution of dipeptides **137**, **138**, **139** or **140** (1 equiv.) in dry  $\text{CH}_2\text{Cl}_2$  (3 mL), in a 10 mL microwave tube equipped with a magnetic stirrer, was treated with CM partner **126a**, **126b**, **126c** or **126d** (10 equiv.) and Hoveyda–Grubbs catalyst 2nd generation [(1,3-bis-(2,4,6-trimethylphenyl)-2-imidazolidinylidene)-dichloro-(*o*-isopropoxyphenyl)methylene] ruthenium] (0.1 equiv.) under microwave irradiation at 100 °C for 2 h for vinyl -esters, -ketones and -nitriles, at 150° C for vinyl sulfones. Subsequently, the solvent was removed under reduced pressure and the residue was purified by flash column chromatography eluting with light petroleum/EtOAc in different ratio, to obtain Michael acceptors **14-17a-d**.

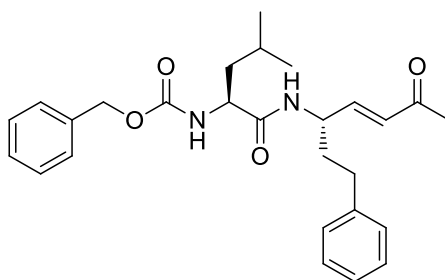
#### Benzyl (S)-1-((S,E)-5-(methylcarboxy)-1-phenylpent-4-en-3-ylcarbamoyl)-3-methylbutylcarbamate (14a)



Yield: 86%; Consistency: white powder;  $R_f = 0.15$  (light petroleum/EtOAc, 4:1);  $^1\text{H}$  NMR (300 MHz,  $\text{CDCl}_3$ ) =  $\delta$ : 0.90 (d,  $J = 6.5$  Hz, 3H), 0.93 (d,  $J = 6.5$  Hz, 3H), 1.46-1.69 (m,

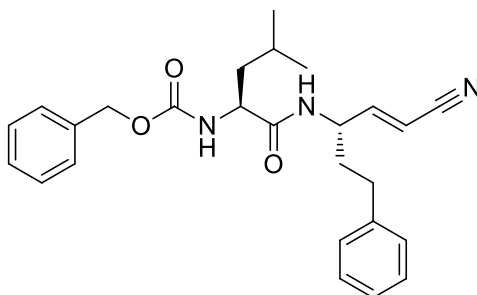
3H), 1.75-1.97 (m, 2H), 2.62 (t,  $J = 7.5$  Hz, 2H), 3.73 (s, 3H), 4.03-4.23 (m, 1H), 4.55-4.69 (m, 1H), 5.09 (s, 2H), 5.18 (d,  $J = 8.1$  Hz, 1H), 5.90 (d,  $J = 15.6$  Hz, 1H), 6.38 (d,  $J = 7.5$  Hz, 1H), 6.86 (dd,  $J = 15.6$  Hz, 5.3 Hz, 1H), 7.07-7.37 (m, 10H);  $^{13}\text{C}$  NMR (75 MHz,  $\text{CDCl}_3$ ) =  $\delta$ : 21.94, 22.92, 24.67, 31.92, 35.77, 40.79, 49.84, 51.71, 53.57, 67.23, 120.93, 126.19, 128.06, 128.28, 128.37, 128.55, 128.60, 135.95, 140.84, 147.44, 156.42, 166.61, 171.69; Elemental analysis: calcd for  $\text{C}_{27}\text{H}_{34}\text{N}_2\text{O}_5$ : C 69.50, H 7.35, N 6.00; found: C 69.73, H 7.54, N 5.81.

**Benzyl ((S)-4-methyl-1-oxo-1-(((S,E)-6-oxo-1-phenylhept-4-en-3-yl)amino)pentan-2-yl)carbamate (14b)**



Yield: 86%; Consistency: white powder;  $R_f = 0.26$  (light petroleum/EtOAc, 7:3);  $^1\text{H}$  NMR (300 MHz,  $\text{CDCl}_3$ ) =  $\delta$ : 0.90 (d,  $J = 6.6$  Hz, 3H), 0.93 (d,  $J = 6.6$  Hz, 3H), 1.45-1.68 (m, 3H), 1.75-2.00 (m, 2H), 2.22 (s, 3H), 2.63 (t,  $J = 9.7$  Hz, 2H), 4.07-4.22 (m, 1H), 4.55-4.67 (m, 1H), 5.09 (s, 2H), 5.23 (d,  $J = 8.3$  Hz, 1H), 6.13 (d,  $J = 15.8$  Hz, 1H), 6.50 (d,  $J = 8.0$  Hz, 1H), 6.65 (dd,  $J = 15.8$  Hz, 5.3 Hz, 1H), 7.09-7.38 (m, 10H);  $^{13}\text{C}$  NMR (75 MHz,  $\text{CDCl}_3$ ) =  $\delta$ : 21.92, 22.92, 24.67, 27.52, 32.00, 35.71, 40.72, 49.88, 53.55, 67.22, 126.23, 128.01, 128.28, 128.37, 128.54, 128.61, 129.84, 135.94, 140.77, 146.01, 156.45, 171.81, 198.20; Elemental analysis: calcd for  $\text{C}_{27}\text{H}_{34}\text{N}_2\text{O}_4$ : C 71.97, H 7.61, N 6.22; found: C 72.16, H 7.43, N 5.98.

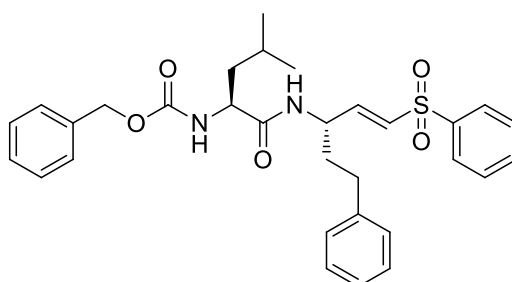
**Benzyl ((S)-1-(((S,E)-1-cyano-5-phenylpent-1-en-3-yl)carbamoyl)-3-methylbutyl)carbamate (14c)**



Yield: 16%; Consistency: brown powder;  $R_f = 0.32$  (light petroleum/EtOAc, 7:3);  $^1\text{H}$  NMR (500 MHz,  $\text{CDCl}_3$ ) =  $\delta$ : 0.90 (d,  $J = 6.5$  Hz, 3H), 0.93 (d,  $J = 6.5$  Hz, 3H), 1.60-1.71 (m,

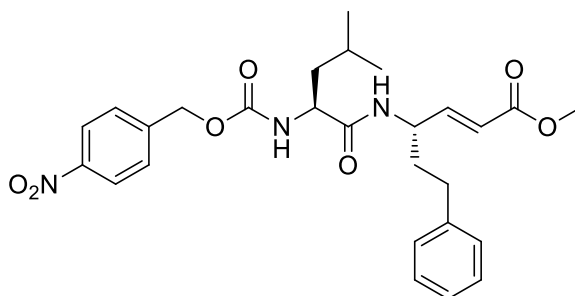
3H), 1.78-1.87 (m, 1H), 1.88-1.97 (m, 1H), 2.59-2.67 (m, 2H), 4.05-4.12 (m, 1H), 4.52-4.59 (m, 1H), 4.88 (bs, 1H), 5.13 (s, 2H), 5.42 (d,  $J = 15.2$  Hz, 1H), 6.13 (bs, 1H), 6.58 (dd,  $J = 15.2, 5.1$  Hz, 1H), 7.09-7.37 (m, 10H);  $^{13}\text{C}$  NMR (125 MHz,  $\text{CDCl}_3$ ) =  $\delta$ : 21.94, 22.88, 24.65, 31.90, 35.16, 40.24, 50.17, 53.49, 67.19, 100.46, 114.87, 126.32, 128.05, 128.27, 128.35, 128.59, 128.64, 135.96, 140.41, 152.84, 156.36, 171.64; Elemental analysis: calcd for  $\text{C}_{26}\text{H}_{31}\text{N}_3\text{O}_3$ : C 72.03, H 7.21, N 9.69; found: C 72.31, H 6.92, N 9.80.

**Benzyl** ((*S*)-4-methyl-1-oxo-1-(((*S,E*)-5-phenyl-1-(phenylsulfonyl)pent-1-en-3-yl)amino)pentan-2-yl)carbamate (**14d**)



Yield: 24%; Consistency: brown powder;  $R_f = 0.24$  (light petroleum/EtOAc, 7:3);  $^1\text{H}$  NMR (500 MHz,  $\text{CDCl}_3$ ) =  $\delta$ : 0.90 (d,  $J = 6.7$  Hz, 3H), 0.93 (d,  $J = 6.7$  Hz, 3H), 1.52-1.65 (m, 3H), 1.80-1.90 (m, 1H), 1.91-2.01 (m, 1H), 2.55-2.68 (m, 2H), 4.02-4.09 (m, 1H), 4.63-4.71 (m, 1H), 4.90 (bs, 1H), 5.08 (s, 2H), 6.18 (bs, 1H), 6.44 (d,  $J = 15.2$  Hz, 1H), 6.88 (dd,  $J = 15.2$  Hz, 4.9 Hz, 1H), 7.07-7.35 (m, 10H), 7.49-7.64 (m, 3H), 7.82-7.90 (m, 2H);  $^{13}\text{C}$  NMR (125 MHz,  $\text{CDCl}_3$ ) =  $\delta$ : 21.95, 22.94, 24.72, 32.03, 35.74, 40.77, 49.91, 53.54, 67.20, 126.22, 128.02, 128.28, 128.36, 128.56, 128.60, 128.72, 129.36, 131.15, 133.55, 135.92, 140.79, 141.64, 145.08, 156.44, 171.84; Elemental analysis: calcd for  $\text{C}_{31}\text{H}_{36}\text{N}_2\text{O}_5\text{S}$ : C 67.86, H 6.61, N 5.11; found: C 68.09, H 6.44, N 4.86.

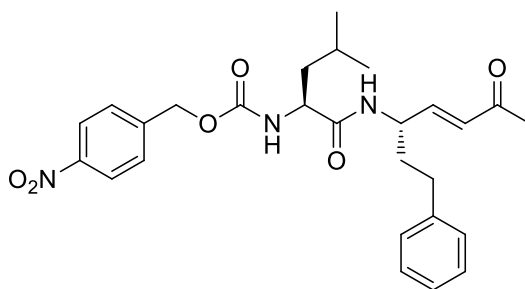
**4-Nitrobenzyl** (*S*)-1-(((*S,E*)-5-(methylcarboxy)-1-phenylpent-4-en-3-yl)carbamoyl)-3-methylbutylcarbamate (**15a**)



Yield: 90%; Consistency: yellow powder;  $R_f = 0.23$  (light petroleum/EtOAc, 7:3);  $^1\text{H}$  NMR (300 MHz,  $\text{CDCl}_3$ ) =  $\delta$ : 0.91 (d,  $J = 6.6$  Hz, 3H), 0.94 (d,  $J = 6.6$  Hz, 3H), 1.51-1.72

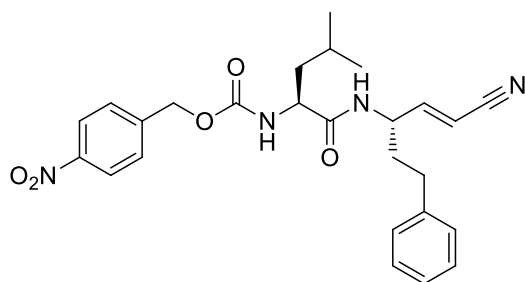
(m, 3H), 1.75-1.99 (m, 2H), 2.60 (t,  $J = 7.0$  Hz, 2H), 3.73 (s, 3H), 4.09-4.24 (m, 1H), 4.59-4.70 (m, 1H), 5.16 (s, 2H), 5.48 (d,  $J = 8.3$  Hz, 1H), 5.90 (d,  $J = 15.7$  Hz, 1H), 6.41 (d,  $J = 8.2$  Hz, 1H), 6.86 (dd,  $J = 15.7$  Hz, 5.3 Hz, 1H), 7.06-7.30 (m, 5H), 7.43 (d,  $J = 8.7$  Hz, 2H), 8.13 (d,  $J = 8.6$  Hz, 2H);  $^{13}\text{C}$  NMR (75 MHz,  $\text{CDCl}_3$ ) =  $\delta$ : 21.95, 22.86, 24.70, 31.88, 35.86, 41.10, 49.91, 51.74, 53.73, 65.50, 120.99, 123.72, 126.26, 127.94, 128.28, 128.58, 140.69, 143.46, 147.29, 147.55, 155.91, 166.54, 171.65; Elemental analysis: calcd for  $\text{C}_{27}\text{H}_{33}\text{N}_3\text{O}_7$ : C 63.39, H 6.50, N 8.21; found C 63.19, H 6.69, N 7.96.

**4-Nitrobenzyl**                      **((S)-4-methyl-1-oxo-1-((S,E)-6-oxo-1-phenylhept-4-en-3-ylamino)pentan-2-yl)carbamate (15b)**



Yield: 89%; Consistency: yellow powder;  $R_f = 0.13$  (light petroleum/EtOAc, 7:3);  $^1\text{H}$  NMR (500 MHz,  $\text{CDCl}_3$ ) =  $\delta$ : 0.89 (d,  $J = 6.7$  Hz, 3H), 0.92 (d,  $J = 6.7$  Hz, 3H), 1.50-1.72 (m, 3H), 1.81-1.99 (m, 2H), 2.23 (s, 3H), 2.46-2.54 (m, 2H), 4.13-4.24 (m, 1H), 4.60-4.70 (m, 1H), 5.18 (s, 2H), 5.52 (d,  $J = 6.9$  Hz, 1H), 6.13 (d,  $J = 16.0$  Hz, 1H), 6.48 (d,  $J = 6.1$  Hz, 1H), 6.66 (dd,  $J = 16.0$  Hz, 5.7 Hz, 1H), 7.07-7.30 (m, 5H), 7.45 (d,  $J = 7.8$  Hz, 2H), 8.13 (d,  $J = 7.8$  Hz, 2H);  $^{13}\text{C}$  NMR (125 MHz,  $\text{CDCl}_3$ ) =  $\delta$ : 22.06, 22.98, 24.84, 27.52, 32.09, 35.97, 41.13, 50.08, 53.86, 65.66, 123.83, 126.42, 128.07, 128.41, 128.72, 130.06, 140.75, 143.54, 145.97, 147.70, 156.07, 171.91, 198.25; Elemental analysis: calcd for  $\text{C}_{27}\text{H}_{33}\text{N}_3\text{O}_6$ : C 65.44, H 6.71, N 8.48; found: C 65.62, H 6.49, N 8.33.

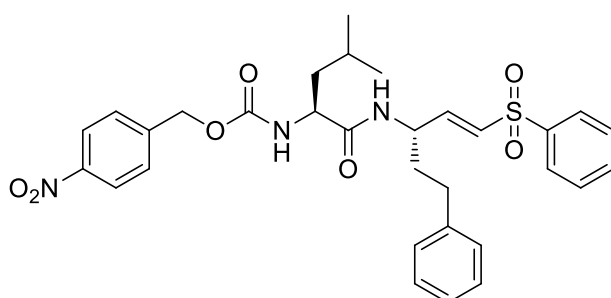
**4-Nitrobenzyl**                      **(S)-1-((S,E)-1-cyano-5-phenylpent-1-en-3-ylcarbamoyl)-3-methylbutylcarbamate (15c)**



Yield: 19%; Consistency: brown powder;  $R_f = 0.40$  (light petroleum/EtOAc, 3:2);  $^1\text{H}$  NMR (500 MHz,  $\text{CDCl}_3$ ) =  $\delta$ : 0.89 (d,  $J = 6.6$  Hz, 3H), 0.92 (d,  $J = 6.6$  Hz, 3H), 1.56-1.69 (m,

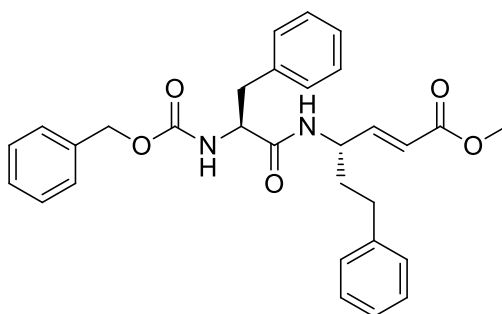
3H), 1.81-1.89 (m, 1H), 1.90-1.98 (1H), 2.56-2.68 (m, 2H), 4.05-4.13 (m, 1H), 4.54-4.61 (m, 1H), 5.12 (d,  $J = 7.3$  Hz, 1H), 5.19 (s, 2H), 5.43 (d,  $J = 16.6$  Hz, 1H), 6.06 (d,  $J = 6.4$  Hz, 1H), 6.59 (dd,  $J = 16.6, 5.2$  Hz, 1H), 7.08-7.31 (5H), 7.47 (d,  $J = 8.3$ , 2H), 8.16 (d,  $J = 8.3$  Hz, 2H);  $^{13}\text{C}$  NMR (125 MHz,  $\text{CDCl}_3$ ) =  $\delta$ : 21.92, 22.83, 24.76, 31.84, 35.19, 40.43, 50.54, 53.63, 65.64, 100.50, 114.84, 123.79, 126.54, 128.08, 128.27, 128.76, 140.12, 143.60, 146.60, 152.85, 155.95, 171.51; Elemental analysis: calcd for  $\text{C}_{26}\text{H}_{30}\text{N}_4\text{O}_5$ : C 65.26, H 6.32, N 11.71; found: C 65.56, H 6.51, N 11.53.

**4-Nitrobenzyl (S)-1-((S,E)-5-phenyl-1-(phenylsulfonyl)pent-1-en-3-ylcarbamoyl)-3-methylbutylcarbamate (15d)**



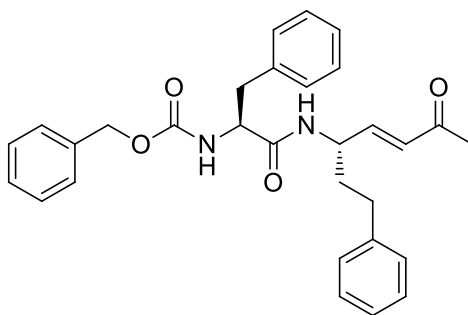
Yield: 26%; Consistency: brown powder;  $R_f = 0.16$  (light petroleum/EtOAc, 7:3);  $^1\text{H}$  NMR (500 MHz,  $\text{CDCl}_3$ ) =  $\delta$ : 0.91 (d,  $J = 6.6$  Hz, 3H), 0.94 (d,  $J = 6.6$  Hz, 3H), 1.53-1.71 (m, 3H), 1.82-1.91 (m, 1H), 1.93-2.02 (m, 1H), 2.54-2.66 (m, 2H), 4.01-4.08 (m, 1H), 4.65-4.72 (m, 1H), 5.07 (d,  $J = 7.2$  Hz, 1H), 5.17 (s, 2H), 6.03 (d,  $J = 7.4$  Hz, 1H), 6.41 (d,  $J = 15.1$  Hz, 1H), 6.88 (dd,  $J = 15.1$  Hz, 5.0 Hz, 1H), 7.04-7.28 (m, 5H), 7.46 (d,  $J = 8.5$  Hz, 2H), 7.50-7.64 (m, 3H), 7.82-7.89 (m, 2H), 8.16 (d,  $J = 8.5$  Hz, 2H);  $^{13}\text{C}$  NMR (125 MHz,  $\text{CDCl}_3$ ) =  $\delta$ : 22.32, 22.67, 24.73, 31.91, 34.72, 40.60, 49.23, 53.77, 65.70, 123.78, 126.44, 127.62, 128.14, 128.29, 128.71, 129.35, 131.13, 133.57, 140.24, 141.67, 143.45, 145.01, 147.67, 156.99, 171.15; Elemental analysis: calcd for  $\text{C}_{31}\text{H}_{35}\text{N}_3\text{O}_7\text{S}$ : C 62.71, H 5.94, N 7.08; found: C 62.55, H 6.18, N 7.31.

**(S,E)-Methyl 4-((S)-2-(((benzyloxy)carbonyl)amino)-3-phenylpropanamido)-6-phenylhex-2-enoate (16a)**



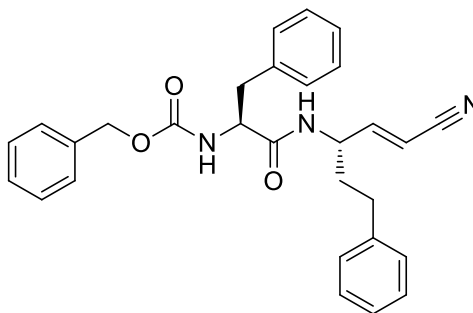
Yield: 88%, Consistency: white powder;  $R_f = 0.37$  (light petroleum/EtOAc, 7:3);  $^1\text{H NMR}$  (300 MHz,  $\text{CDCl}_3$ ) =  $\delta$ : 1.73-1.80 (m, 1H), 1.83-1.90 (m, 1H), 2.58 (t,  $J = 7.6$  Hz, 2H), 3.00-3.07 (m, 1H), 3.08-3.14 (m, 1H), 3.77 (s, 3H), 4.31-4.38 (m, 1H), 4.56-4.64 (m, 1H), 5.12 (s, 2H), 5.24 (bs, 1H), 5.70 (d,  $J = 15.7$  Hz, 1H), 5.72-5.78 (bs, 1H), 6.69 (dd,  $J = 15.7$  Hz, 5.9 Hz, 1H), 7.10-7.38 (m, 15H); The  $^1\text{H NMR}$  spectroscopic data are in agreement with that reported in literature;<sup>107</sup>  $^{13}\text{C NMR}$  (75 MHz,  $\text{CDCl}_3$ ) =  $\delta$ : 32.00, 35.79, 38.43, 50.08, 51.81, 56.71, 67.37, 121.29, 126.40, 127.43, 128.28, 128.47, 128.69, 128.74, 128.05, 129.45, 129.56, 136.20, 136.71, 140.87, 146.99, 155.27, 168.11, 170.38; Elemental analysis: calcd for  $\text{C}_{30}\text{H}_{32}\text{N}_2\text{O}_5$ : C 71.98, H 6.44, N 5.60; found: C 72.09, H 6.67, N 5.39.

**Benzyl ((S)-1-oxo-1-(((S,E)-6-oxo-1-phenylhept-4-en-3-yl)amino)-3-phenylpropan-2-yl)carbamate (16b)**



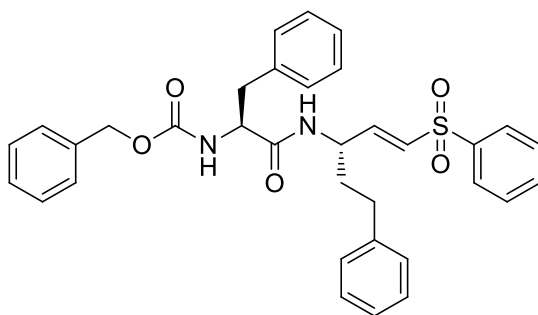
Yield: 85%; Consistency: white powder;  $R_f = 0.15$  (light petroleum/EtOAc, 7:3);  $^1\text{H NMR}$  (500 MHz,  $\text{CDCl}_3$ ) =  $\delta$ : 1.71-1.81 (m, 1H), 1.83-1.91 (m, 1H), 2.19 (s, 3H), 2.56 (t,  $J = 7.4$  Hz, 2H), 3.00-3.12 (m, 2H), 4.31-4.39 (m, 1H), 4.54-4.61 (m, 1H), 5.09 (s, 2H), 5.24 (bs, 1H), 5.84 (bs, 1H), 5.91 (d,  $J = 16.0$  Hz, 1H), 6.46 (dd,  $J = 16.0, 5.6$  Hz, 1H), 7.08-7.36 (m, 15H);  $^{13}\text{C NMR}$  (125 MHz,  $\text{CDCl}_3$ ) =  $\delta$ : 27.71, 31.91, 35.61, 38.16, 49.96, 56.56, 67.25, 126.27, 127.25, 128.08, 128.28, 128.32, 128.58, 128.60, 128.85, 129.30, 129.88, 135.95, 136.21, 140.65, 145.22, 156.05, 170.30, 197.81; Elemental analysis: calcd for  $\text{C}_{30}\text{H}_{32}\text{N}_2\text{O}_4$ : C 74.36, H 6.66, N 5.78; found: C 74.08, H 6.89, N 5.94.

**Benzyl ((S)-1-(((S,E)-1-cyano-5-phenylpent-1-en-3-yl)amino)-1-oxo-3-phenylpropan-2-yl)carbamate (16c)**



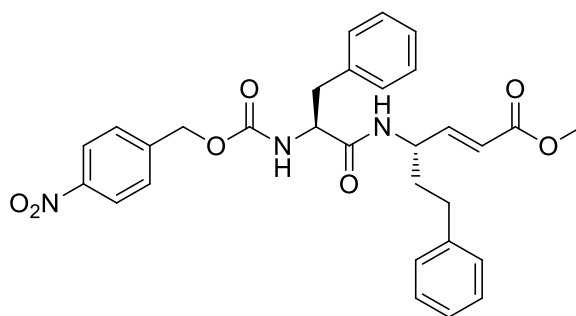
Yield: 14%; Consistency: brown powder;  $R_f = 0.36$  (light petroleum/EtOAc, 7:3);  $^1\text{H}$  NMR (500 MHz,  $\text{CDCl}_3$ ) =  $\delta$ : 1.64-1.74 (m, 1H), 1.77-1.86 (m, 1H), 2.48-2.62 (m, 2H), 2.96-3.04 (m, 1H), 3.06-3.13 (m, 1H), 4.26-4.34 (m, 1H), 4.46-4.54 (m, 1H), 4.78 (d,  $J = 16.1$  Hz, 1H), 5.11 (s, 2H), 5.19 (bs, 1H), 5.63 (bs, 1H), 6.34 (dd,  $J = 16.1, 4.8$  Hz, 1H), 7.03-7.38 (m, 15H);  $^{13}\text{C}$  NMR (125 MHz,  $\text{CDCl}_3$ ) =  $\delta$ : 31.96, 35.48, 38.41, 50.33, 56.62, 67.29, 100.24, 114.76, 126.29, 127.39, 128.18, 128.34, 128.49, 128.68, 128.76, 129.21, 129.41, 135.84, 136.52, 140.75, 152.78, 155.67, 170.26; Elemental analysis: calcd for  $\text{C}_{29}\text{H}_{29}\text{N}_3\text{O}_3$ : C 74.50, H 6.25, N 8.99; found C 74.82, H 6.03, H 9.23.

**Benzyl**      **((S)-1-oxo-3-phenyl-1-(((S,E)-5-phenyl-1-(phenylsulfonyl)pent-1-en-3-yl)amino)propan-2-yl)carbamate (16d)**



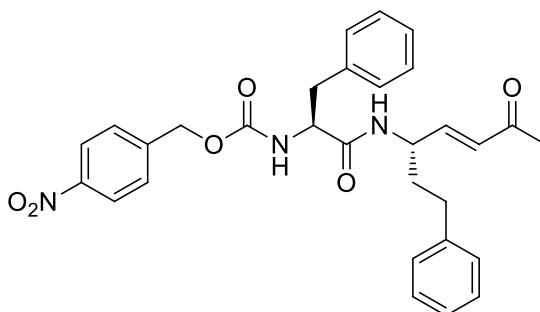
Yield: 26%; Consistency: brown powder;  $R_f = 0.16$  (light petroleum/EtOAc, 7:3);  $^1\text{H}$  NMR (300 MHz,  $\text{CDCl}_3$ ) =  $\delta$ : 1.71-1.78 (m, 1H), 1.84-1.91 (m, 1H), 2.47-2.61 (m, 2H), 2.92-3.09 (m, 2H), 4.21-4.37 (m, 1H), 4.56-4.71 (m, 1H), 5.07 (s, 2H), 5.20 (d,  $J = 8.1$  Hz, 1H), 5.80 (d,  $J = 7.1$  Hz, 1H), 6.04 (d,  $J = 15.2$  Hz, 1H), 6.76 (dd,  $J = 15.2, 4.6$  Hz, 1H), 6.98-7.41 (m, 15H), 7.47-7.69 (m, 3H), 7.78-7.97 (m, 2H);  $^{13}\text{C}$  NMR (75 MHz,  $\text{CDCl}_3$ ) =  $\delta$ : 31.72, 35.44, 38.16, 49.28, 56.54, 67.39, 127.32, 127.60, 128.14, 128.36, 128.56, 128.59, 128.64, 128.84, 129.22, 129.35, 130.67, 133.52, 135.91, 136.05, 140.08, 140.27, 145.23, 155.98, 170.43; Spectroscopic data are in agreement with those reported in literature.<sup>108</sup> Elemental analysis: calcd for  $\text{C}_{34}\text{H}_{34}\text{N}_2\text{O}_5\text{S}$ : C 70.08, H 5.88, N 4.81; found: C 70.21, H 5.52, N 4.93.

**(S,E)-Methyl**      **4-((S)-2-(4-nitrobenzyloxycarbonylamino)-3-phenylpropanamido)-6-phenylhex-2-enoate (17a)**



Yield: 90%; Consistency: yellow powder;  $R_f = 0.18$  (light petroleum/EtOAc, 7:3);  $^1\text{H}$  NMR (500 MHz,  $\text{CDCl}_3$ ) =  $\delta$ : 1.70-1.78 (m, 1H), 1.80-1.89 (m, 1H), 2.54 (t,  $J = 7.3$  Hz, 2H), 2.98-3.12 (m, 2H), 3.74 (s, 3H), 4.28-4.35 (m, 1H), 4.53-4.62 (m, 1H), 5.16 (s, 2H), 5.47 (d,  $J = 6.8$  Hz, 1H), 5.66 (d,  $J = 15.6$  Hz, 1H), 5.68 (bs, 1H), 6.64 (dd,  $J = 15.6, 5.2$  Hz, 1H), 7.04-7.34 (m, 10H), 7.42 (d,  $J = 8.3$  Hz, 2H), 8.16 (d,  $J = 8.3$  Hz, 2H);  $^{13}\text{C}$  NMR (125 MHz,  $\text{CDCl}_3$ ) =  $\delta$ : 31.79, 35.68, 38.60, 49.96, 51.67, 56.69, 65.52, 121.21, 123.75, 126.28, 127.37, 128.02, 128.25, 128.59, 128.92, 129.22, 136.03, 140.59, 143.43, 146.61, 146.90, 158.72, 166.36, 170.01; Elemental analysis: calcd for  $\text{C}_{30}\text{H}_{31}\text{N}_3\text{O}_7$ : C 66.04, H 5.73, N 7.70; found: C 66.26, H 5.46, N 7.88.

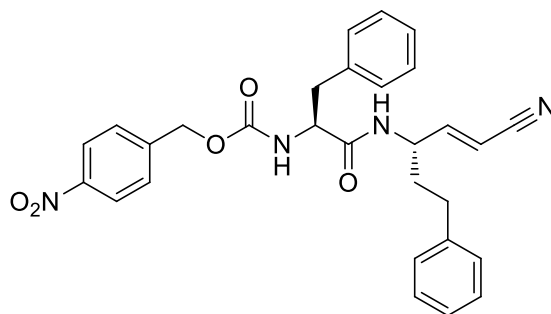
**4-Nitrobenzyl ((S)-1-oxo-1-(((S,E)-6-oxo-1-phenylhept-4-en-3-yl)amino)-3-phenylpropan-2-yl)carbamate (17b)**



Yield: 89%; Consistency: yellow powder;  $R_f = 0.16$  (light petroleum/EtOAc, 3:2);  $^1\text{H}$  NMR (500 MHz,  $\text{CDCl}_3$ ) =  $\delta$ : 1.71-1.80 (m, 1H), 1.82-1.93 (m, 1H), 2.19 (s, 3H), 2.48-2.60 (m, 2H), 2.98-3.12 (m, 2H), 4.29-4.42 (m, 1H), 4.51-4.66 (m, 1H), 5.16 (s, 2H), 5.57 (bs, 1H), 5.88 (d,  $J = 15.6$  Hz, 1H), 5.91 (bs, 1H), 6.45 (dd,  $J = 15.6, 4.2$  Hz, 1H), 7.04-7.33 (m, 10H), 7.41 (d,  $J = 8.3$  Hz, 2H), 8.14 (d,  $J = 8.3$  Hz, 2H);  $^{13}\text{C}$  NMR (125 MHz,  $\text{CDCl}_3$ ) =  $\delta$ : 27.62, 31.90, 35.73, 38.53, 50.01, 56.67, 65.54, 123.75, 126.32, 127.33, 128.00, 128.28, 128.61, 128.86, 129.27, 129.96, 136.09, 140.58, 143.42, 145.19, 147.61, 155.56, 170.27, 197.87; Elemental analysis: calcd for  $\text{C}_{30}\text{H}_{31}\text{N}_3\text{O}_6$ : C 68.04, H 5.90, N 7.93; found C 67.88, H 5.71, N 8.17.

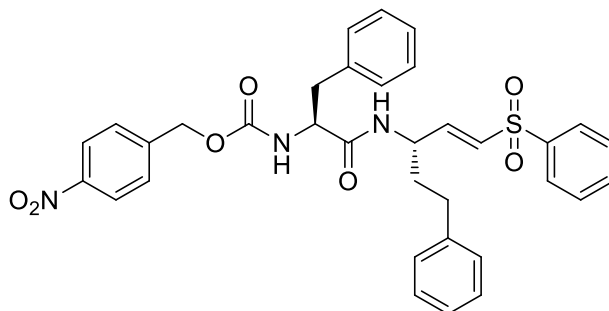


**4-Nitrobenzyl ((S)-1-((S,E)-1-cyano-5-phenylpent-1-en-3-ylamino)-1-oxo-3-phenylpropan-2-yl)carbamate (17c)**



Yield: 15%; Consistency: brown powder;  $R_f = 0.45$  (light petroleum/EtOAc, 3:2);  $^1\text{H}$  NMR (500 MHz,  $\text{CDCl}_3$ ) =  $\delta$ : 1.65-1.74 (m, 1H), 1.78-1.86 (m, 1H), 2.47-2.61 (m, 2H), 2.95-3.03 (m, 1H), 3.07-3.13 (m, 1H), 4.23-4.31 (m, 1H), 4.46-4.54 (m, 1H), 4.69 (d,  $J = 16.6$  Hz, 1H), 5.19 (s, 2H), 5.38 (bs, 1H), 5.44 (d,  $J = 7.8$  Hz, 1H), 6.31 (dd,  $J = 16.6, 5.1$  Hz, 1H), 7.02-7.40 (m, 10H), 7.46 (d,  $J = 8.5$  Hz, 2H), 8.17 (d,  $J = 8.5$  Hz, 2H);  $^{13}\text{C}$  NMR (125 MHz,  $\text{CDCl}_3$ ) =  $\delta$ : 31.76, 35.74, 38.58, 49.97, 56.63, 65.50, 101.44, 115.89, 123.73, 126.55, 127.41, 128.16, 128.24, 128.64, 128.94, 129.26, 136.08, 140.57, 143.46, 147.31, 152.86, 156.31, 170.21; Elemental analysis: calcd for  $\text{C}_{29}\text{H}_{28}\text{N}_4\text{O}_5$ : C 67.96, H 5.51, N 10.93; found: C 68.20, H 5.36, N 10.71.

**4-Nitrobenzyl ((S)-1-oxo-3-phenyl-1-((S,E)-5-phenyl-1-(phenylsulfonyl)pent-1-en-3-yl)amino)propan-2-yl)carbamate (17d)**



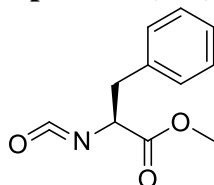
Yield: 22%; Consistency: brown powder;  $R_f = 0.11$  (light petroleum/EtOAc, 7:3);  $^1\text{H}$  NMR (500 MHz,  $\text{CDCl}_3$ ) =  $\delta$ : 1.71-1.80 (m, 1H), 1.83-1.92 (m, 1H), 2.47-2.60 (m, 2H), 2.94-3.07 (m, 2H), 4.21-4.28 (m, 1H), 4.60-4.68 (m, 1H), 5.17 (s, 2H), 5.33 (d,  $J = 6.8$  Hz, 1H), 5.59 (d,  $J = 8.4$  Hz, 1H), 5.99 (d,  $J = 15.1$  Hz, 1H), 6.73 (dd,  $J = 15.1, 4.8$  Hz, 1H), 7.01-7.30 (m, 10H), 7.43 (d,  $J = 8.6$  Hz, 2H), 7.51-7.67 (m, 3H), 7.80-7.87 (m, 2H), 8.15 (d,  $J = 8.6$  Hz, 2H);  $^{13}\text{C}$  NMR (125 MHz,  $\text{CDCl}_3$ ) =  $\delta$ : 31.43, 35.48, 38.30, 49.26, 56.77, 65.85, 123.78, 126.44, 127.52, 127.67, 128.10, 128.27, 128.68, 129.00, 129.13, 129.33,

130.82, 133.58, 135.85, 139.90, 140.17, 143.18, 144.82, 147.67, 156.73, 170.24; Elemental analysis: calcd for C<sub>34</sub>H<sub>33</sub>N<sub>3</sub>O<sub>7</sub>S: C 65.06, H 5.30, N 6.69; found: C 64.84, H 5.47, N 6.94.

## Serie E

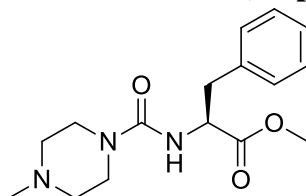
### Synthesis of urea-derivatives 18a-b

#### (S)-Methyl 2-isocyanato-3-phenylpropanoate (**141**)



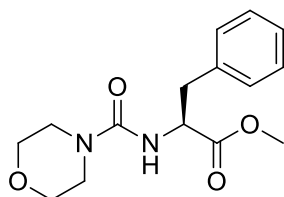
In a three-neck flask, CH<sub>2</sub>Cl<sub>2</sub>, saturated aqueous sodium bicarbonate (1:1) and L-Phe methyl ester **78** (3 equiv.) were added, at 0° C. Subsequently, triphosgene (1 equiv.) was added and the reaction mixture was stirred for 15 min. After this time, the organic phase was collected, while the aqueous phase was extracted with CH<sub>2</sub>Cl<sub>2</sub> (x 3). The combined layers are dried over anhydrous Na<sub>2</sub>SO<sub>4</sub>, filtered and concentrated under reduced pressure. Compound **141** was used for the next step without further purification. Yield: 96%; Consistency: colourless oil; *R*<sub>f</sub> = 0.78 (light petroleum/EtOAc, 7:3); <sup>1</sup>H NMR (300 MHz, CDCl<sub>3</sub>) = δ: 3.07 (dd, *J* = 13.8, 7.8 Hz, 1H), 3.28 (dd, *J* = 13.8, 7.8 Hz, 1H), 3.78 (s, 3 H), 4.23 (dd, 1 H, *J* = 7.8, 4.6), 7.18-7.44 (m, 5H). Spectroscopic data are in agreement to those reported in literature.<sup>109</sup>

#### (S)-Methyl 2-(4-methylpiperazine-1-carboxamido)-3-phenylpropanoate (**143a**)



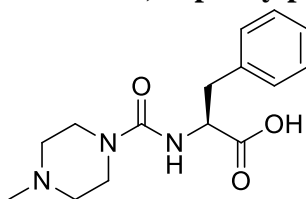
A solution of **141** (1 equiv.) in dry THF at 0° C, *N*-methylpiperazine **142a** (1.4 equiv.) in dry THF was added. The reaction mixture was stirred at rt for 2h, and after this time a second portion of *N*-methylpiperazine **142a** (0.3 equiv.) in dry THF was added. After 2h, the solvent was concentrated in *vacuo* and was used in the next step without further purification. Yield: 67%; Consistency: pale orange solid; *R*<sub>f</sub> = 0.19 (EtOAc/MeOH, 4:1); <sup>1</sup>H NMR (300 MHz, MeOD) = δ: 2.26 (s, 1H), 2.32-2.38 (m, 4H), 2.92-3.02 (m, 1H), 3.10-3.18 (m, 1H), 3.32-3.42 (m, 4H), 3.67 (s, 3H), 4.49 (dd, *J* = 9.4, 5.6 Hz, 1H), 7.17-7.32 (m, 5H). Spectroscopic data are in agreement to those reported in literature.<sup>110</sup>

#### (S)-Methyl 2-(morpholine-4-carboxamido)-3-phenylpropanoate (**143b**)



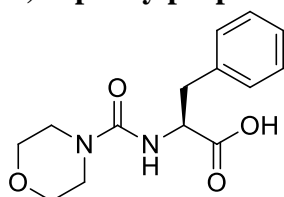
Synthesis of compound **143b** was carried following the procedure described for compound **143a**, using morpholine **142b**. Yield: 61%; Consistency: white solid;  $R_f = 0.55$  (EtOAc);  $^1\text{H NMR}$  (300 MHz, MeOD) =  $\delta$ : 2.90-3.02 (m, 1H), 3.09-3.18 (m, 1H), 3.25-3.36 (m, 4), 3.54-3.61 (m, 4H), 3.67 (s, 3H), 4.50 (dd,  $J = 9.3, 5.7$  Hz, 1H), 7.09-7.33 (m, 5H). Spectroscopic data are in agreement to those reported in literature.<sup>111</sup>

**(S)-2-(4-Methylpiperazine-1-carboxamido)-3-phenylpropanoic acid (144a)**



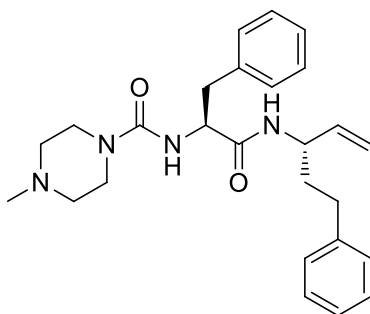
To a solution of the **143a** (1 equiv.) in a mixture methanol/water/dioxane (1:1:1), LiOH as powder (3 equiv.) was added at 0° C. The reaction mixture was then stirred at rt for 12h. After this time, the solvents were evaporated in *vacuo*. The residue was treated with 10% solution citric acid (x 2), and the organic phase was extracted with EtOAc (x 3), dried over  $\text{Na}_2\text{SO}_4$  and concentrated to afford the pure carboxylic acid **144a**. Yield: 94%; Consistency: white solid;  $R_f = 0.06$  (EtOAc/MeOH, 9:1);  $^1\text{H NMR}$  (300 MHz, MeOD) =  $\delta$ : 2.25 (s, 3H), 2.28-2.38 (m, 4H), 3.00 (dd,  $J = 13.5, 7.0$  Hz, 1H), 3.18 (dd,  $J = 13.5, 5.1$  Hz, 1H), 3.32-3.45 (m, 4H), 4.40 (dd,  $J = 7.0, 5.1$  Hz, 1H), 7.10-7.27 (m, 5H). Spectroscopic data are in agreement to those reported in literature.<sup>110</sup>

**(S)-2-(Morpholine-4-carboxamido)-3-phenylpropanoic acid (144b)**



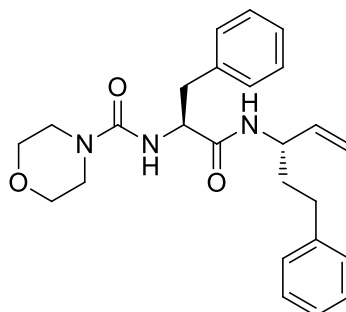
Synthesis of compound **144b** was carried following the procedure described for compound **144a**. Yield: 61%; Consistency: white solid;  $R_f = 0.05$  (EtOAc/MeOH, 9:1);  $^1\text{H NMR}$  (300 MHz, MeOD) =  $\delta$ : 2.96 (dd,  $J = 12.4, 7.2$  Hz, 1H), 3.21 (dd,  $J = 12.4, 7.2$  Hz, 1H), 3.25-3.39 (m, 4H), 3.52-3.61 (m, 4H), 4.48-4.56 (m, 1H), 7.12-7.31 (m, 5H). Spectroscopic data are in agreement to those reported in literature.<sup>112</sup>

**4-Methyl-N-((S)-1-oxo-3-phenyl-1-((S)-5-phenylpent-1-en-3-ylamino)propan-2-yl)piperazine-1-carboxamide (145a)**



To a solution of carboxylic acid **144a** (1.2 equiv.) in DMF/CH<sub>2</sub>Cl<sub>2</sub> (1:1), HOBT (1.2 equiv.) and EDCI (1.2 equiv.) were added at 0° C. After this time, DIPEA (1.5 equiv.) and amine **132** (1 equiv.) were added and the reaction mixture was stirred over night at rt. Then, solvents were evaporated and the resulting residue was diluted with EtOAc, washed with a saturated solution of NaHCO<sub>3</sub> (x 3), dried over Na<sub>2</sub>SO<sub>4</sub>, filtered and concentrated in *vacuo*. The crude product was purified by flash column chromatography using CH<sub>2</sub>Cl<sub>2</sub>/MeOH (9:1) as eluent mixture, to give the terminal olefin **145a**. Yield: 74%; Consistency: white solid; *R*<sub>f</sub> = 0.49 (CH<sub>2</sub>Cl<sub>2</sub>/MeOH, 9:1); <sup>1</sup>H NMR (300 MHz, CDCl<sub>3</sub>) = δ: 1.58-1.80 (m, 2H), 2.23 (s, 3H), 2.24-2.30 (m, 4H), 2.49 (t, *J* = 7.7 Hz, 2H), 3.02-3.10 (m, 2H), 3.28-3.36 (m, 4H), 4.28-4.42 (m, 1H), 4.70 (q, *J* = 7.3 Hz, 1H), 4.87-5.08 (m, 2H), 5.51-5.65 (m, 2H), 6.99-7.29 (m, 11H); <sup>13</sup>C NMR (300 MHz, CDCl<sub>3</sub>) = δ: 32.03, 36.43, 39.12, 43.62, 46.03, 51.15, 54.47, 55.92, 115.03, 125.82, 126.68, 128.32, 128.37, 128.39, 129.57, 137.13, 137.84, 141.48, 156.91, 171.70; Elemental analysis: calcd for C<sub>26</sub>H<sub>34</sub>N<sub>4</sub>O<sub>2</sub>: C 71.86; H 7.89; N 12.89; found: C 72.04, H 7.64, N 13.14.

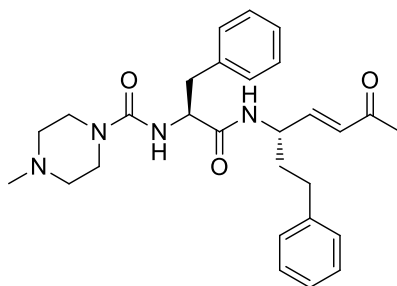
**N-((S)-1-oxo-3-phenyl-1-(((S)-5-phenylpent-1-en-3-yl)amino)propan-2-yl)morpholine-4-carboxamide (145b)**



Synthesis of terminal olefin **145b** was carried out following the procedure described for compound **145a**. Yield: 71%; Consistency: white solid; *R*<sub>f</sub> = 0.20 (light petroleum/EtOAc, 1:1); <sup>1</sup>H NMR (300 MHz, CDCl<sub>3</sub>) = δ: 1.58-1.71 (m, 2H), 2.46 (t, *J* = 7.8 Hz, 2H), 2.94-

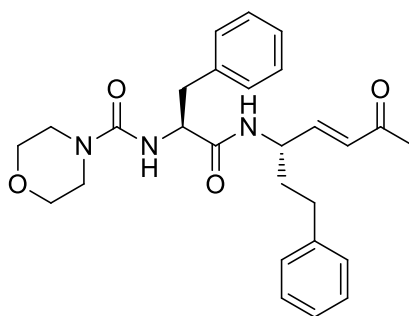
3.04 (m, 2H), 3.15-3.26 (m, 4H), 3.46-3.55 (m, 4H), 4.23-4.36 (m, 1H), 4.53 (q,  $J = 7.1$  Hz, 1H), 4.80-4.99 (m, 2H), 5.31 (d,  $J = 6.2$  Hz, 1H), 5.43-5.58 (m, 1H), 6.31 (d,  $J = 7.4$  Hz, 1H), 6.97-7.26 (m, 10H);  $^{13}\text{C}$  NMR (300 MHz,  $\text{CDCl}_3$ ) =  $\delta$ : 32.07, 36.53, 39.12, 44.08, 51.43, 56.11, 66.46, 115.40, 126.04, 126.99, 128.45, 128.50, 128.69, 129.59, 137.14, 137.77, 141.55, 157.23, 171.45; Elemental analysis: calcd for  $\text{C}_{25}\text{H}_{31}\text{N}_3\text{O}_3$ : C 71.23; H 7.41; N, 9.97; found: C 71.44, H 7.73, N 9.84.

**4-methyl-*N*-((*S*)-1-oxo-1-(((*S,E*)-6-oxo-1-phenylhept-4-en-3-yl)amino)-3-phenylpropan-2-yl)piperazine-1-carboxamide (18a)**



A solution of terminal olefin **145a** (1 equiv.) in dry  $\text{CH}_2\text{Cl}_2$  (3 mL), in a 10 mL microwave tube equipped with a magnetic stirrer, was treated with CM partner **126b** (10 equiv.) and Hoveyda–Grubbs catalyst 2nd generation [(1,3-bis-(2,4,6-trimethylphenyl)-2-imidazolidinylidene)-dichloro-(*o*-isopropoxyphenylmethylene) ruthenium] (0.1 equiv.) under microwave irradiation at 100 °C for 4 h. Subsequently, the solvent was removed under reduced pressure and the residue was purified by flash column chromatography using  $\text{CH}_2\text{Cl}_2/\text{MeOH}$  (9:1) as eluent mixture, to obtain CM product **18a**. Yield: 81%; Consistency: white solid;  $R_f = 0.34$  ( $\text{CH}_2\text{Cl}_2/\text{MeOH}$ , 9:1);  $^1\text{H}$  NMR (300 MHz,  $\text{CDCl}_3$ ) =  $\delta$ : 1.82-1.99 (m, 2H), 2.23 (s, 3H), 2.29 (s, 3H), 2.32-2.43 (m, 4H), 2.54 (t,  $J = 7.7$  Hz, 2H), 3.03-3.14 (m, 2H), 3.32-3.40 (m, 4H), 4.37-4.49 (m, 1H), 4.78-4.92 (m, 1H), 5.29 (d,  $J = 6.3$  Hz, 1H), 5.86 (d,  $J = 7.6$  Hz, 1H), 6.28 (d,  $J = 15.2$  Hz, 1H), 6.91 (dd,  $J = 15.2$  Hz, 5.2, 1H), 7.16-7.42 (m, 10H);  $^{13}\text{C}$  NMR (300 MHz,  $\text{CDCl}_3$ ) =  $\delta$ : 27.41, 31.87, 35.89, 39.04, 43.87, 46.10, 51.26, 54.60, 55.97, 125.93, 126.54, 128.34, 128.41, 128.44, 128.59, 130.87, 136.97, 141.24, 145.22, 157.02, 171.66, 197.64; Elemental analysis: calcd for  $\text{C}_{28}\text{H}_{36}\text{N}_4\text{O}_3$ : C 70.56; H 7.61; N 11.76; found: C 70.41, H 7.33, N 12.02.

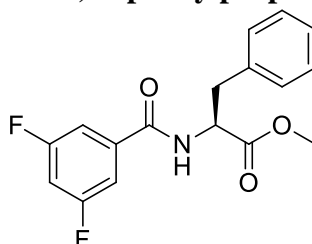
***N*-((*S*)-1-oxo-1-(((*S,E*)-6-oxo-1-phenylhept-4-en-3-yl)amino)-3-phenylpropan-2-yl)morpholine-4-carboxamide (18b)**



Synthesis of product **18b** was carried out following the procedure described for compound **18a**. Yield: 84%; Consistency: white solid;  $R_f = 0.27$  (EtOAc/light petroleum, 3:2);  $^1\text{H}$  NMR (300 MHz,  $\text{CDCl}_3$ ) =  $\delta$ : 1.62-1.75 (m, 2H), 2.28 (s, 3H), 2.51 (t,  $J = 7.6$  Hz, 2H), 2.98-3.11 (m, 2H), 3.21-3.34 (m, 4H), 3.49-3.64 (m, 4H), 4.34-4.47 (m, 1H), 4.72-4.83 (m, 1H), 5.37 (d,  $J = 6.6$  Hz, 1H), 5.88 (d,  $J = 7.5$  Hz, 1H), 6.31 (d,  $J = 15.2$  Hz, 1H), 6.88 (dd,  $J = 15.2$  Hz, 5.4, 1H), 7.11-7.38 (m, 10H);  $^{13}\text{C}$  NMR (300 MHz,  $\text{CDCl}_3$ ) =  $\delta$ : 27.62, 32.11, 36.64, 39.14, 44.20, 51.55, 56.17, 66.50, 126.14, 127.05, 128.46, 128.51, 128.72, 129.64, 129.97, 137.82, 141.48, 145.38, 157.38, 171.59, 197.77; Elemental analysis: calcd for  $\text{C}_{27}\text{H}_{33}\text{N}_3\text{O}_4$ : C 69.95; H 7.18; N 9.06; found: C 70.24, H 7.42, N 8.87.

#### Synthesis of compound 19a-c

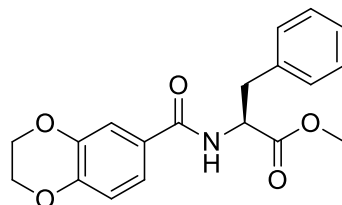
##### (S)-Methyl 2-(3,5-difluorobenzamido)-3-phenylpropanoate (**147a**)



To a solution of acid **146a** (1.2 equiv.) in dry DMF/ $\text{CH}_2\text{Cl}_2$  (1:1), HOBt (1.2 equiv.) and EDCI (1.2 equiv.) were added, in nitrogen atmosphere at  $0^\circ\text{C}$ . After 10 min, Phe methyl ester **78** (1 equiv.) and DIPEA (1.2 equiv.) were added and the reaction mixture was stirred at rt for 12 h. After this time, the solvents were removed and the residue was diluted with EtOAc, washed with brine (x 5), dried over  $\text{Na}_2\text{SO}_4$ , filtered and concentrated in *vacuo*. The crude residue was purified by flash column chromatography using light petroleum/EtOAc (9:1) as eluent mixture, to obtain compound **147a**. Yield: 77%; Consistency: white solid;  $R_f = 0.22$  (light petroleum/EtOAc, 9:1);  $^1\text{H}$  NMR (300 MHz,  $\text{CDCl}_3$ ) =  $\delta$ : 3.16 (qd,  $J = 13.9, 5.7$  Hz, 2H), 3.70 (s, 3H), 4.90-5.02 (m, 1H), 6.60 (d,  $J = 7.1$  Hz, 1H), 6.85 (t,  $J = 8.5$  Hz, 1H), 7.00-7.27 (m, 7H);  $^{13}\text{C}$  (75 MHz,  $\text{CDCl}_3$ ) =  $\delta$ : 37.71, 52.60, 53.71, 107.15 (t,  $J = 25.4$  Hz), 110.35 (q,  $J = 26.2$ , Hz), 127.37, 128.73, 129.25,

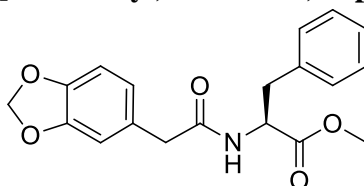
135.59, 137.16, 151.29, 162.92 (dd,  $J = 250.8, 12.0$  Hz), 171.88. Spectroscopic data are in agreement to those reported in literature.<sup>113</sup>

**(S)-Methyl 2-(2,3-dihydrobenzo[*b*][1,4]dioxine-6-carboxamido)-3-phenylpropanoate (147b)**



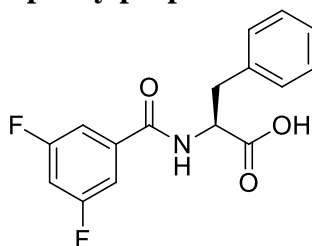
Synthesis of product **147b** was carried out following the procedure described for compound **147a**, using **146b** as acid. Yield: 81%; Consistency: white solid;  $R_f = 0.37$  (light petroleum/EtOAc, 7:3);  $^1\text{H NMR}$  (300 MHz,  $\text{CDCl}_3$ ) =  $\delta$ : 3.11 (dd,  $J = 12.4, 7.3$  Hz, 1H), 3.35 (dd,  $J = 12.4, 7.3$  Hz, 1H), 3.78 (s, 3H), 4.20-4.39 (m, 4H), 4.93-5.06 (m, 1H), 6.99 (d,  $J = 1.4$  Hz, 1H), 7.10-7.20 (m, 4H), 7.24-7.31 (m, 2H), 7.58 (d,  $J = 1.4$  Hz, 1H);  $^{13}\text{C}$  (75 MHz,  $\text{CDCl}_3$ ) =  $\delta$ : 37.90, 53.18, 53.98, 64.16, 64.53, 116.42, 116.83, 120.66, 127.37, 128.39, 129.13, 129.52, 135.96, 143.37, 146.73, 166.19, 172.17.

**(S)-Methyl 2-(2-(benzo[*d*][1,3]dioxol-5-yl)acetamido)-3-phenylpropanoate (147c)**



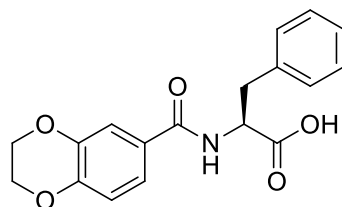
Synthesis of product **147c** was carried out following the procedure described for compound **147a**, using **146c** as acid. Yield: 77%; Consistency: white solid;  $R_f = 0.44$  (light petroleum/EtOAc, 1:1);  $^1\text{H NMR}$  (300 MHz,  $\text{CDCl}_3$ ) =  $\delta$ : 2.90-3.14 (m, 2H), 3.42 (s, 2H), 3.69 (s, 3H), 4.73-4.91 (m, 1H), 5.85-6.03 (bs, 1H), 5.93 (s, 2H) 6.57-6.77 (m, 3H), 6.88-6.98 (m, 2H), 7.13-7.29 (m, 3H);  $^{13}\text{C}$  (75 MHz,  $\text{CDCl}_3$ ) =  $\delta$ : 35.57, 43.12, 52.31, 52.93, 101.09, 108.56, 109.72, 122.57, 127.06, 127.97, 128.48, 129.15, 135.58, 146.86, 147.98, 170.56, 171.82.

**(S)-2-(3,5-Difluorobenzamido)-3-phenylpropanoic acid (148a)**



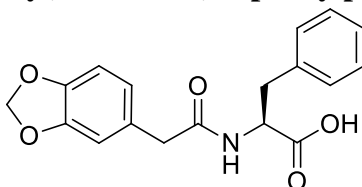
To a solution of the **147a** (1 equiv.) in a mixture methanol/water/dioxane (1:1:1), LiOH as powder (3 equiv.) was added at 0° C. The reaction mixture was then stirred at rt for 12h. After this time, the solvents were evaporated in *vacuo*. The residue was treated with 10% solution citric acid (x 2) and the organic phase was extracted with EtOAc (x 3), dried over Na<sub>2</sub>SO<sub>4</sub> and concentrated to afford the pure carboxylic acid **148a**. Yield: 96%; Consistency: white solid; *R<sub>f</sub>* = 0.02 (light petroleum/EtOAc, 9:1); <sup>1</sup>H NMR (300 MHz, MeOD) = δ: 3.07 (dd, *J* = 13.9, 10.1 Hz, 1H), 3.35 (dd, *J* = 13.9, 4.9 Hz, 1H), 4.84 (dd, *J* = 10.1, 4.9 Hz, 1H), 7.06-7.37 (m, 8H); <sup>13</sup>C (75 MHz, MeOD) = δ: 37.23, 53.61, 107.22 (t, *J* = 24.3 Hz), 107.22 (q, *J* = 24.3 Hz), 127.52, 128.84, 129.31, 135.32, 136.74, 151.04, 162.77 (dd, *J* = 251.0, 12.1 Hz), 170.36.

**(S)-2-(2,3-Dihydrobenzo[*b*][1,4]dioxine-6-carboxamido)-3-phenylpropanoic acid (148b)**



Synthesis of product **148b** was carried out following the procedure described for compound **148a**. Yield: 93%; Consistency: white solid; *R<sub>f</sub>* = 0.04 (light petroleum/EtOAc, 7:3); <sup>1</sup>H NMR (300 MHz, MeOD) = δ: 3.19 (dd, *J* = 12.4, 7.3 Hz, 1H), 3.39 (dd, *J* = 12.4, 7.3 Hz, 1H), 4.26-4.43 (m, 4H), 4.98-5.11 (m, 1H), 7.03 (d, *J* = 1.5 Hz, 1H), 7.12-7.22 (m, 4H), 7.25-7.34 (m, 2H), 7.63 (d, *J* = 1.5 Hz, 1H); <sup>13</sup>C (75 MHz, MeOD) = δ: 37.22, 53.68, 64.11, 64.47, 116.39, 116.77, 120.52, 127.48, 128.69, 129.52, 129.83, 136.03, 143.52, 146.87, 165.94, 171.87.

**(S)-2-(2-(Benzo[*d*][1,3]dioxol-5-yl)acetamido)-3-phenylpropanoic acid (148c)**

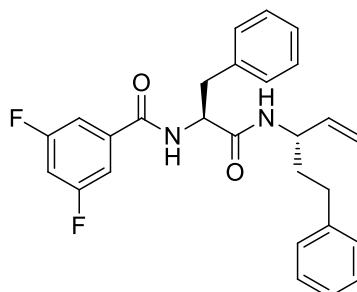


Synthesis of product **148c** was carried out following the procedure described for compound **148a**. Yield: 94%; Consistency: white solid; *R<sub>f</sub>* = 0.04 (light petroleum/EtOAc, 1:1); <sup>1</sup>H NMR (300 MHz, MeOD) = δ: 2.86 (dd, *J* = 13.8, 5.9 Hz, 1H), 3.17 (dd, *J* = 13.8, 5.9 Hz, 1H), 3.39 (s, 2H), 4.66 (dd, *J* = 13.8, 5.9 Hz, 1H), 5.91 (s, 2H), 6.58-6.74 (m, 3H), 7.08-



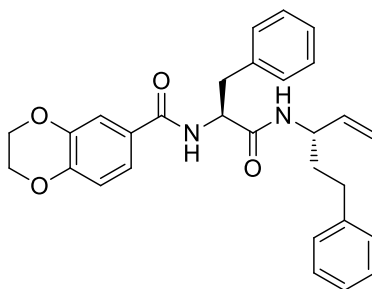
7.24 (m, 5H);  $^{13}\text{C}$  (75 MHz, MeOD) =  $\delta$ : 36.80, 41.72, 53.51, 100.85, 107.66, 109.05, 121.95, 126.38, 128.01, 128.69, 128.86, 136.77, 146.54, 147.68, 172.47, 173.22.

**3,5-Difluoro-*N*-((*S*)-1-oxo-3-phenyl-1-((*S*)-5-phenylpent-1-en-3-ylamino)propan-2-yl)benzamide (149a)**



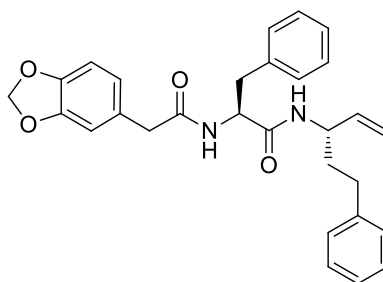
To a solution of acid **148a** (1.2 equiv.) in dry DMF/ $\text{CH}_2\text{Cl}_2$  (1:1), HOBt (1.2 equiv.) and EDCI (1.2 equiv.) were added, in nitrogen atmosphere at  $0^\circ\text{C}$ . After 10 min, the amine **132** (1 equiv.) and DIPEA (1.2 equiv.) were added and the reaction mixture was stirred at rt for 12 h. After this time, the solvents were removed and the residue was diluted with EtOAc, washed with brine (x 5), dried over  $\text{Na}_2\text{SO}_4$ , filtered and concentrated in *vacuo*. The crude residue was purified by flash column chromatography using light petroleum/EtOAc (4:1) as eluent mixture, to obtain terminal olefin **149a**. Yield: 74%; Consistency: white solid;  $R_f = 0.43$  (light petroleum/EtOAc, 4:1);  $^1\text{H}$  NMR (300 MHz,  $\text{CDCl}_3$ ) =  $\delta$ : 1.88-1.98 (m, 2H); 2.58 (t,  $J = 7.6$  Hz, 2H), 2.99-3.18 (m, 2H), 4.18-4.27 (m, 1H), 4.60-4.72 (m, 1H), 4.96-5.12 (m, 2H), 5.42 (d,  $J = 6.7$  Hz, 1H), 5.57-5.70 (m, 1H), 5.86 (d,  $J = 8.3$  Hz, 1H), 6.98-7.09 (m, 1H), 7.18-7.34 (m, 8H), 7.40-7.51 (m, 4H);  $^{13}\text{C}$  (75 MHz,  $\text{CDCl}_3$ ) =  $\delta$ : 31.93, 36.22, 38.64, 51.74, 55.84, 107.16 (q,  $J = 25.7$  Hz), 110.53 (t,  $J = 28.1$  Hz), 115.69, 125.80, 126.21, 128.23, 128.51, 129.20, 129.60, 136.38, 137.15, 137.40, 141.21, 162.88 (dd,  $J = 251.5, 10.0$  Hz), 164.81, 170.11; Elemental analysis: calcd for  $\text{C}_{27}\text{H}_{26}\text{F}_2\text{N}_2\text{O}_2$ : calcd C 72.30, H 5.84, N 6.25; found: C 71.98, H 5.66, N 6.04.

***N*-((*S*)-1-Oxo-3-phenyl-1-((*S*)-5-phenylpent-1-en-3-ylamino)propan-2-yl)-2,3-dihydrobenzo[*b*][1,4]dioxine-6-carboxamide (149b)**



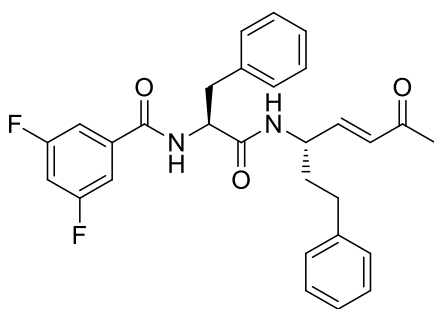
Synthesis of product **149b** was carried out following the procedure described for compound **149a**, using **148b** as acid. Yield: 80%; Consistency: white solid;  $R_f = 0.31$  (light petroleum/EtOAc, 1:1);  $^1\text{H NMR}$  (300 MHz,  $\text{CDCl}_3$ ) =  $\delta$ : 1.68-1.94 (m, 2H), 2.52 (t,  $J = 7.6$  Hz, 2H), 3.00-3.19 (m, 2H), 4.18-4.42 (m, 5H), 4.67-4.81 (m, 1H), 4.88-5.09 (m, 2H), 5.27 (d,  $J = 6.7$  Hz, 1H), 5.58-5.70 (m, 1H), 5.88 (d,  $J = 7.3$  Hz, 1H), 7.03 (d,  $J = 1.5$  Hz, 1H), 7.12-7.22 (m, 7H), 7.25-7.34 (m, 4H), 7.63 (d,  $J = 1.5$  Hz, 1H);  $^{13}\text{C}$  (75 MHz,  $\text{CDCl}_3$ ) =  $\delta$ : 31.84, 36.32, 38.59, 51.84, 56.02, 64.17, 64.51, 115.61, 116.44, 116.80, 120.74, 126.23, 126.78, 127.63, 128.01, 128.21, 128.63, 128.86, 136.74, 137.55, 141.20, 146.59, 147.73, 166.87, 170.38; Elemental analysis for  $\text{C}_{29}\text{H}_{30}\text{N}_2\text{O}_4$ : calcd for C 74.02; H 6.43; N 5.95; found: C 73.81, N 6.65, N 6.24.

**(S)-2-(2-(benzo[d][1,3]dioxol-5-yl)acetamido)-3-phenyl-N-((S)-5-phenylpent-1-en-3-yl)propanamide (149c)**



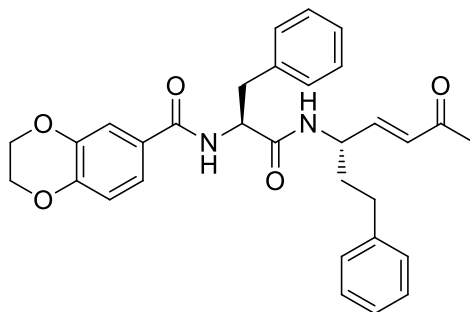
Synthesis of product **149c** was carried out following the procedure described for compound **149a**, using **148c** as acid. Yield: 83%; Consistency: white solid;  $R_f = 0.33$  (light petroleum/EtOAc, 1:1);  $^1\text{H NMR}$  (300 MHz,  $\text{CDCl}_3$ ) =  $\delta$ : 1.59-1.81 (m, 2H), 2.51 (t,  $J = 7.6$  Hz, 2H), 3.01-3.16 (m, 2H), 3.41 (s, 2H), 4.20-4.29 (m, 1H), 4.64-4.76 (m, 1H), 4.90-5.09 (m, 2H), 5.44 (d,  $J = 6.8$  Hz, 1H), 5.55-5.71 (m, 1H), 5.80 (d,  $J = 7.4$  Hz, 1H), 5.94 (s, 2H), 6.58-6.74 (m, 3H), 7.07-7.32 (m, 10H);  $^{13}\text{C}$  (75 MHz,  $\text{CDCl}_3$ ) =  $\delta$ : 31.97, 36.38, 38.15, 43.11, 51.42, 54.33, 101.09, 108.38, 109.43, 115.36, 122.67, 125.76, 126.16, 128.20, 128.38, 128.55, 128.79, 129.58, 136.42, 137.58, 141.40, 146.88, 148.13, 170.23, 171.31; Elemental analysis for  $\text{C}_{29}\text{H}_{30}\text{N}_2\text{O}_4$ : C 74.02; H 6.43; N 5.95; found: C 73.82, H 6.22, N 6.17.

**3,5-Difluoro-N-((S)-1-oxo-1-(((S,E)-6-oxo-1-phenylhept-4-en-3-yl)amino)-3-phenylpropan-2-yl)benzamide (19a)**



A solution of terminal olefin **149a** (1 equiv.) in dry  $\text{CH}_2\text{Cl}_2$  (3 mL), in a 10 mL microwave tube equipped with a magnetic stirrer, was treated with CM partners **126b** (10 equiv.) and Hoveyda–Grubbs catalyst 2nd generation [(1,3-bis-(2,4,6-trimethylphenyl)-2-imidazolidinylidene)-dichloro-(*o*-isopropoxyphenylmethylene) ruthenium] (0.1 equiv.) under microwave irradiation at 100 °C for 4 h. Subsequently, the solvent was removed under reduced pressure and the residue was purified by flash column chromatography using light petroleum/EtOAc (4:1) as eluent mixture, to obtain CM product **19a**. Yield: 83%; Consistency: white solid;  $R_f = 0.27$  (light petroleum/EtOAc, 4:1);  $^1\text{H}$  NMR (300 MHz,  $\text{CDCl}_3$ ) =  $\delta$ : 1.86-1.97 (m, 2H), 2.23 (s, 3H) 2.55 (t,  $J = 7.8$  Hz, 2H), 3.01-3.22 (m, 2H), 4.16-4.29 (m, 1H), 4.51-4.60 (m, 1H), 5.36 (bs, 1H), 5.94 (d,  $J = 8.3$  Hz, 1H), 6.01 (d,  $J = 15.2$  Hz, 1H), 6.54 (dd,  $J = 15.2, 6.1$  Hz, 1H), 7.02-7.11, (m, 1H), 7.16-7.32 (m, 8H), 7.44-7.57 (m, 4H);  $^{13}\text{C}$  (75 MHz,  $\text{CDCl}_3$ ) =  $\delta$ : 26.54, 32.14, 36.86, 38.41, 51.18, 56.67, 107.22 (q,  $J = 25.9$  Hz), 110.59 (t,  $J = 28.0$  Hz), 126.24, 126.97, 128.54, 128.79, 129.04, 129.51, 130.83, 136.78, 137.12, 141.29, 149.39, 163.51 (dd,  $J = 251.2, 9.8$  Hz), 164.94, 170.22, 197.58; Elemental analysis: calcd for  $\text{C}_{29}\text{H}_{28}\text{F}_2\text{N}_2\text{O}_3$ : C 71.01; H 5.75; N 5.71; found: C 70.86, H 5.97, N 5.93.

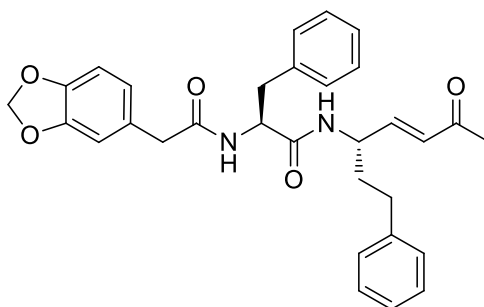
***N*-((*S*)-1-oxo-1-(((*S,E*)-6-oxo-1-phenylhept-4-en-3-yl)amino)-3-phenylpropan-2-yl)-2,3-dihydrobenzo[*b*][1,4]dioxine-6-carboxamide (**19b**)**



Synthesis of product **19b** was carried out following the procedure described for compound **19a**, using **149b** as terminal olefin. Yield: 87%; Consistency: white solid;  $R_f = 0.17$  (light petroleum/EtOAc, 1:1);  $^1\text{H}$  NMR (300 MHz,  $\text{CDCl}_3$ ) =  $\delta$ : 1.69-1.98 (m, 2H), 2.27 (s, 3H),

2.50 (t,  $J = 7.6$  Hz, 2H), 2.96-3.17 (m, 2H), 4.22-4.46 (m, 5H), 4.59-4.71 (m, 1H), 5.39 (d,  $J = 6.4$  Hz, 1H), 5.88 (d,  $J = 7.3$  Hz, 1H), 6.04 (d,  $J = 15.2$  Hz, 1H), 6.67 (dd,  $J = 15.2, 6.0$  Hz, 1H), 7.06 (d,  $J = 1.6$  Hz, 1H), 7.11-7.39 (m, 11H), 7.63 (d,  $J = 1.6$  Hz, 1H);  $^{13}\text{C}$  (75 MHz,  $\text{CDCl}_3$ ) =  $\delta$ : 26.83, 31.93, 36.41, 38.67, 51.94, 56.17, 64.20, 64.56, 116.52, 116.84, 120.89, 126.34, 126.74, 127.76, 128.07, 128.27, 128.69, 128.93, 130.77, 136.81, 141.35, 146.62, 147.86, 149.16, 166.90, 170.43, 197.65; Elemental analysis: calcd for  $\text{C}_{31}\text{H}_{32}\text{N}_2\text{O}_5$ : C 72.64; H 6.29; N 5.47; found: C 72.47, H 5.96, N 5.71.

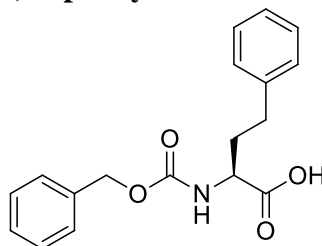
**(S)-2-(2-(Benzo[*d*][1,3]dioxol-5-yl)acetamido)-*N*-((S,E)-6-oxo-1-phenylhept-4-en-3-yl)-3-phenylpropanamide (119c)**



Synthesis of product **19c** was carried out following the procedure described for compound **19a**, using **149c** as terminal olefin. Yield: 81%; Consistency: white solid;  $R_f = 0.18$  (light petroleum/EtOAc, 1:1);  $^1\text{H}$  NMR (300 MHz,  $\text{CDCl}_3$ ) =  $\delta$ : 1.66-1.92 (m, 2H), 2.24 (s, 3H), 2.54 (t,  $J = 7.8$  Hz, 2H), 2.96-3.11 (m, 2H), 3.39 (s, 2H), 4.17-4.28 (m, 1H), 4.59-4.67 (m, 1H), 5.55 (d,  $J = 6.6$  Hz, 1H), 5.89 (d,  $J = 7.3$  Hz, 1H), 5.96 (s, 2H), 6.14 (d,  $J = 15.1$  Hz, 1H), 6.69 (dd,  $J = 15.1, 6.1$  Hz, 1H), 6.58-6.74 (m, 3H), 7.07-7.32 (m, 10H);  $^{13}\text{C}$  (75 MHz,  $\text{CDCl}_3$ ) =  $\delta$ : 27.51, 32.04, 38.21, 43.16, 51.54, 54.43, 101.17, 108.42, 109.49, 122.74, 125.80, 126.19, 128.29, 128.43, 128.62, 128.84, 129.66, 130.81, 136.42, 141.53, 146.95, 148.17, 149.24, 170.29, 171.33, 197.57; Elemental analysis: calcd for  $\text{C}_{31}\text{H}_{32}\text{N}_2\text{O}_5$ : C 72.64; H 6.29; N 5.47; found: C 72.40, H 6.55, N 5.19.

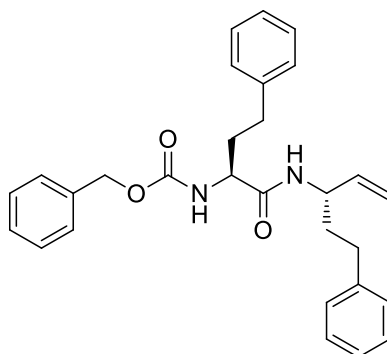
**Synthesis of compound 20**

**(S)-2-(Benzyloxycarbonylamino)-4-phenylbutanoic acid (150)**



The amino acid hPhe **76** (1 equiv.) was solubilized in 2 M Na<sub>2</sub>CO<sub>3</sub> solution, and then the reaction mixture was stirred until complete solubilisation, at 0° C and in nitrogen atmosphere. Subsequently, Cbz-Cl (1.1 equiv.) in dioxane was added dropwise in a period of 10 min. The reaction was stirred for 20h at rt. After this time, dioxane was evaporated and resulting mixture was washed with diethyl ether (x 2). The aqueous phase was acidified with diluted HCl until pH 1-2, and the organic phase was extracted with EtOAc (x 3), dried over Na<sub>2</sub>SO<sub>4</sub>, filtered and concentrated in *vacuo*, to give acid **150**. Yield: 87%; Consistency: pale yellow solid; *R<sub>f</sub>* = 0.10 (CH<sub>2</sub>Cl<sub>2</sub>/MeOH, 99:1); <sup>1</sup>H NMR (300 MHz, CDCl<sub>3</sub>) = δ: 1.90-2.09 (m, 1H), 2.11-2.30 (m, 1H), 2.67 (t, *J* = 7.9 Hz, 2H), 4.36-4.49 (m, 1H), 5.11 (s, 2H), 5.53 (d, *J* = 8.2 Hz, 1H), 7.07-7.38 (m, 10H), 10.01 (bs, 1H). Spectroscopic data are in agreement to those reported in literature.<sup>114</sup>

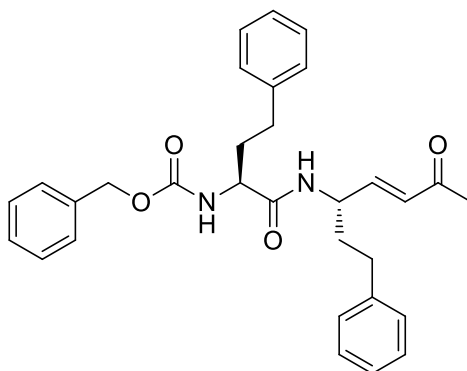
**Benzyl ((S)-1-oxo-4-phenyl-1-((S)-5-phenylpent-1-en-3-ylamino)butan-2-yl)carbamate (151)**



To a solution of carboxylic acid **150** (1.2 equiv.) in DMF/CH<sub>2</sub>Cl<sub>2</sub> (1:1), HOBt (1.2 equiv.) and EDCI (1.2 equiv.) were added at 0° C. After this time, DIPEA (1.5 equiv) and amine **132** (1 equiv.) were added and the reaction mixture was stirred over night at rt. Then, solvents were evaporated and the resulting residue was diluted with EtOAc, washed with a saturated solution of NaHCO<sub>3</sub> (x 3), dried over Na<sub>2</sub>SO<sub>4</sub>, filtered and concentrated in *vacuo*. The crude product was purified by flash column chromatography using light petroleum/EtOAc (9:1) as eluent mixture, to give the terminal olefin **151**. Yield: 79%; Consistency: white powder; *R<sub>f</sub>* = 0.41 (light petroleum/EtOAc, 9:1); <sup>1</sup>H NMR (300 MHz, CDCl<sub>3</sub>) = δ: 170-2.00 (m, 3H), 2.08-2.24 (m, 1H), 2.54-2.72 (m, 4H), 4.12 (dd, *J* = 14.3, 7.5 Hz, 1H), 4.42-4.56 (m, 1H), 5.03-5.22 (m, 2H), 5.09 (s, 2H), 5.32 (d, *J* = 7.6 Hz, 1H), 5.68-5.84 (m, 1H), 5.99 (d, *J* = 8.6 Hz, 1H), 7.09-7.37 (m, 15H); <sup>13</sup>C NMR (300 MHz, CDCl<sub>3</sub>) = δ: 31.70, 32.05, 34.03, 36.30, 51.27, 54.60, 67.12, 115.49, 126.00, 126.21, 128.09, 128.27, 128.38, 128.42, 128.43, 128.50, 128.55, 136.04, 137.69, 140.68, 141.42,

156.19, 170.61; Elemental analysis: calcd for C<sub>29</sub>H<sub>32</sub>N<sub>2</sub>O<sub>3</sub>: C 76.29; H 7.06; N 6.14; found: C 75.96, H 7.16, N 6.27.

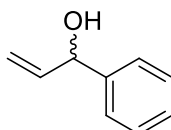
**Benzyl ((S)-1-oxo-1-((S,E)-6-oxo-1-phenylhept-4-en-3-ylamino)-4-phenylbutan-2-yl)carbamate (20)**



A solution of terminal olefin **151** (1 equiv.) in dry CH<sub>2</sub>Cl<sub>2</sub> (3 mL), in a 10 mL microwave tube equipped with a magnetic stirrer, was treated with CM partner **126b** (10 equiv.) and Hoveyda–Grubbs catalyst 2nd generation [(1,3-bis-(2,4,6-trimethylphenyl)-2-imidazolidinylidene)-dichloro-(*o*-isopropoxyphenylmethylene) ruthenium] (0.1 equiv.) under microwave irradiation at 100 °C for 2h. Subsequently, the solvent was removed under reduced pressure and the residue was purified by flash column chromatography using light petroleum/EtOAc (9:1) as eluent mixture, to obtain product **20**. Yield: 86%; Consistency: white powder; *R*<sub>f</sub> = 0.26 (light petroleum/EtOAc, 7:3); <sup>1</sup>H NMR (300 MHz, CDCl<sub>3</sub>) = δ: 1.71-2.01 (m, 4H), 2.21 (s, 3H), 2.53-2.72 (m, 4H), 4.02-4.20 (m, 1H), 4.53-4.70 (m, 1H), 5.10 (s, 2H), 5.26 (d, *J* = 7.4 Hz, 1H), 6.12 (d, *J* = 15.6 Hz, 1H), 6.30 (d, *J* = 6.9 Hz, 1H), 6.63 (dd, *J* = 15.6, 4.6 Hz, 1H), 7.02-7.42 (m, 15H); <sup>13</sup>C NMR (300 MHz, CDCl<sub>3</sub>) = δ: 27.61, 31.76, 32.01, 33.49, 35.70, 49.95, 54.51, 67.29, 126.28, 126.30, 128.08, 128.35, 128.37, 128.44, 128.48, 128.60, 128.63, 129.93, 135.91, 140.42, 140.68, 145.72, 156.39, 171.03, 198.05; Elemental analysis: calcd for C<sub>31</sub>H<sub>34</sub>N<sub>2</sub>O<sub>4</sub>: C 74.67; H 6.87; N 5.62; found: C 74.91, H 7.04, N 5.47.

**Synthesis of compounds 21a-d**

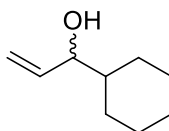
**1-phenylprop-2-en-1-ol (154a)**



In a double neck round-bottom flask, aldehyde **152a** (1 equiv.) in dry THF was stirred for 10 min in nitrogen atmosphere at 0 °C. Subsequently, 1 M vinyl magnesium bromide **153**

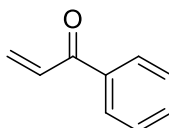
in dry THF (1.2 equiv.) was added in a period of 10 min. The reaction was stirred for 15 min, and then, for 2h at rt. After this time the reaction was quenched with saturated  $\text{NH}_4\text{Cl}$  solution and the organic phase was extracted with EtOAc (x 3), washed with brine, dried over  $\text{Na}_2\text{SO}_4$ , filtered and concentrated in *vacuo*. The crude residue was purified by flash column chromatography using light petroleum/EtOAc (4:1) as eluent mixture, to obtain alcohol **154a**. Yield: 76%; Consistency: yellow oil;  $R_f = 0.43$  (light petroleum/EtOAc, 4:1);  $^1\text{H}$  NMR (300 MHz,  $\text{CDCl}_3$ ) =  $\delta$ : 3.70 (bs, 1H), 5.15 (d,  $J = 6.0$  Hz, 1H), 5.19-5.40 (m, 2H), 6.00-6.1 (m, 1H), 7.31-7.45 (m, 5H). Spectroscopic data are in agreement to those reported in literature.<sup>115</sup>

#### 1-cyclohexylprop-2-en-1-ol (**154b**)



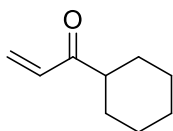
Synthesis of alcohol **154b** was carried out following the procedure described for compound **154a**, using aldehyde **152b**. Yield: 70%; Consistency: colourless oil;  $R_f = 0.46$  (light petroleum/EtOAc, 9:1, detected by  $\text{KMnO}_4$ );  $^1\text{H}$  NMR (300 MHz,  $\text{CDCl}_3$ ) =  $\delta$ : 1.09-1.29 (m, 4H), 1.31-1.46 (m, 1H), 1.58-1.90 (m, 6H), 2.09 (bs, 1H), 3.82 (t,  $J = 6.4$  Hz, 1H), 5.07-5.23 (m, 2H), 5.84 (ddd,  $J = 17.1, 10.3, 6.7$  Hz, 1H). Spectroscopic data are in agreement to those reported in literature.<sup>116</sup>

#### 1-phenylprop-2-en-1-one (**155a**)



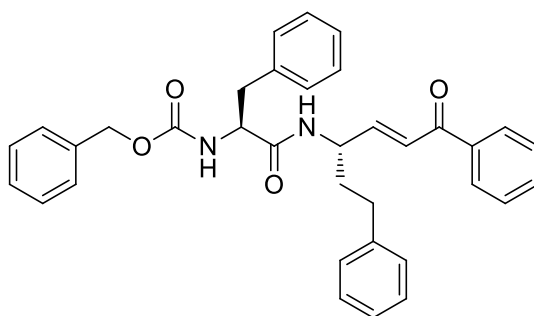
A mixture of **154a** (1 equiv.) and  $\text{MnO}_2$  (10 equiv.) in  $\text{CH}_2\text{Cl}_2$  was refluxed for 24h, in nitrogen atmosphere. After this time, cooling the precipitates were filtered off through Celite and the filtrate was evaporated in *vacuo*. The crude was purified by flash column chromatography using light petroleum/EtOAc (95:5) as eluent mixture, to obtain vinyl ketone **155a**. Yield: 93%; Consistency: pale yellow oil;  $R_f = 0.48$  (light petroleum/EtOAc, 95:5);  $^1\text{H}$  NMR (300 MHz,  $\text{CDCl}_3$ ) =  $\delta$ : 5.84 (d,  $J = 10.5$  Hz, 1H), 6.35 (d,  $J = 17.1$  Hz, 1H), 7.07 (dd,  $J = 17.1, 10.6$  Hz, 1H), 7.34-7.53 (m, 3H), 7.81-7.92 (m, 2H). Spectroscopic data are in agreement to those reported in literature.<sup>117</sup>

#### 1-cyclohexylprop-2-en-1-one (**155b**)



Synthesis of vinyl ketone **155b** was carried out following the procedure described for compound **155a**, using alcohol **154b**. Yield: 91%; Consistency: colourless oil;  $R_f = 0.51$  (light petroleum/EtOAc, 9:1, detected with  $\text{KMnO}_4$ );  $^1\text{H NMR}$  (300 MHz,  $\text{CDCl}_3$ ) =  $\delta$ : 1.16-1.33 (m, 4H), 1.49-1.76 (m, 6H), 2.42-2.59 (m, 1H), 5.69 (dd,  $J = 17.0, 10.4$  Hz, 1H), 6.20-6.58 (m, 2H). Spectroscopic data are in agreement to those reported in literature.<sup>117</sup>

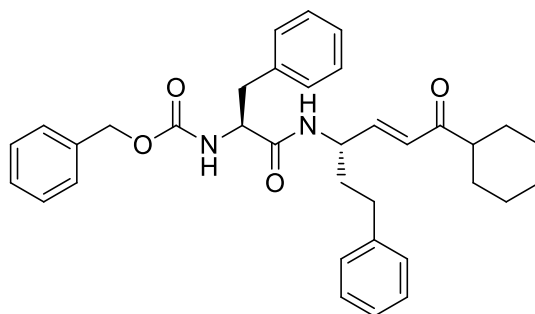
**Benzyl ((S)-1-oxo-1-((S,E)-6-oxo-1,6-diphenylhex-4-en-3-ylamino)-3-phenylpropan-2-yl)carbamate (21a)**



A solution of terminal olefin **139** (1 equiv.) in dry  $\text{CH}_2\text{Cl}_2$  (3 mL), in a 10 mL microwave tube equipped with a magnetic stirrer, was treated with CM partner **155a** (10 equiv.) and Hoveyda–Grubbs catalyst 2nd generation [(1,3-bis-(2,4,6-trimethylphenyl)-2-imidazolidinylidene)-dichloro-(*o*-isopropoxyphenylmethylene) ruthenium] (0.1 equiv.) under microwave irradiation at 100 °C for 2h. Subsequently, the solvent was removed under reduced pressure and the residue was purified by flash column chromatography using light petroleum/EtOAc (7:3) as eluent mixture, to obtain product **21a**. Yield: 75%; Consistency: pale yellow solid;  $R_f = 0.19$  (light petroleum/EtOAc, 7:3);  $^1\text{H NMR}$  (300 MHz,  $\text{CDCl}_3$ ):  $\delta = 1.69$ -1.91 (m, 2H), 2.54 (t,  $J = 7.5$  Hz, 2H), 2.91-3.10 (m, 2H), 4.23-4.38 (m, 1H), 4.59-4.73 (m, 1H), 5.09 (s, 2H), 5.24 (d,  $J = 8.1$  Hz, 1H), 5.87 (d,  $J = 7.1$  Hz, 1H), 6.14 (d,  $J = 15.0$  Hz, 1H), 6.86 (dd,  $J = 15.0, 4.6$  Hz, 1H), 7.02-7.40 (m, 15H), 7.48-7.67 (m, 3H), 7.80-7.92 (m, 2H);  $^{13}\text{C NMR}$  (300 MHz,  $\text{CDCl}_3$ ) =  $\delta$ : 32.04, 36.21, 38.47, 51.39, 56.65, 67.11, 126.03, 127.11, 128.13, 128.31, 128.36, 128.49, 128.57, 128.63, 128.77, 129.14, 129.41, 130.13, 133.78, 136.10, 136.47, 138.18, 141.44, 148.76, 156.08, 170.23, 191.91; Elemental analysis: calcd for  $\text{C}_{35}\text{H}_{34}\text{N}_2\text{O}_4$ : C 76.90, H 6.27, N 5.12; found: C 77.14, H 6.43, N 4.86.

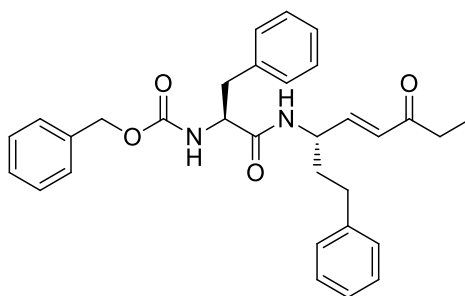


**Benzyl ((S)-1-(((S,E)-6-cyclohexyl-6-oxo-1-phenylhex-4-en-3-yl)amino)-1-oxo-3-phenylpropan-2-yl)carbamate (21b)**



Synthesis of product **21b** was carried out following the procedure described for compound **21a**, using **155b** as CM partner. Yield: 79%; Consistency: white powder;  $R_f = 0.29$  (light petroleum/EtOAc, 4:1);  $^1\text{H NMR}$  (300 MHz,  $\text{CDCl}_3$ ) =  $\delta$ : 1.26-1.47 (m, 4H), 1.67-2.04 (m, 8H), 2.47-2.63 (m, 3H), 2.96-3.11 (m, 2H), 4.21-4.37 (m, 1H), 4.57-4.75 (m, 1H), 5.07 (s, 2H), 5.44 (d,  $J = 8.1$  Hz, 1H), 5.88 (d,  $J = 7.1$  Hz, 1H), 6.22 (d,  $J = 15.2$  Hz, 1H), 6.82 (dd,  $J = 15.2, 4.6$  Hz, 1H), 7.09-7.49 (m, 15H);  $^{13}\text{C NMR}$  (300 MHz,  $\text{CDCl}_3$ ) =  $\delta$ : 25.09, 25.94, 29.68, 32.10, 36.24, 38.59, 47.17, 51.36, 56.66, 67.18, 126.09, 127.17, 128.12, 128.30, 128.37, 128.46, 128.58, 128.76, 129.40, 130.37, 136.02, 136.44, 141.45, 149.15, 156.09, 170.25, 203.84; Elemental analysis: calcd for  $\text{C}_{35}\text{H}_{40}\text{N}_2\text{O}_4$ : C 76.06, H 7.29, N 5.07; found: C 75.91, H 7.55, N 5.34.

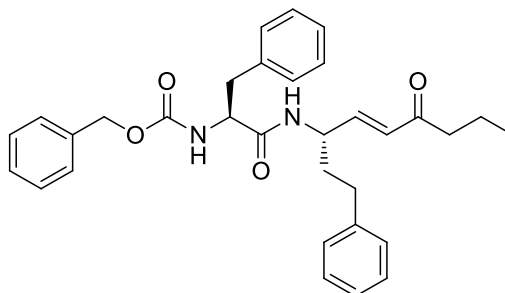
**Benzyl ((S)-1-oxo-1-(((S,E)-6-oxo-1-phenyloct-4-en-3-yl)amino)-3-phenylpropan-2-yl)carbamate (21c)**



Synthesis of product **21c** was carried out following the procedure described for compound **21a**, using **155c** as CM partner, commercially available. Yield: 86%; Consistency: white solid;  $R_f = 0.28$  (light petroleum/EtOAc, 7:3);  $^1\text{H NMR}$  (300 MHz,  $\text{CDCl}_3$ ) =  $\delta$ : 1.10 (t,  $J = 7.2$  Hz, 3H), 1.67-1.96 (m, 2H), 2.33-2.64 (m, 4H), 2.99-3.15 (m, 2H), 4.32-4.48 (m, 1H), 4.50-4.67 (m, 1H), 5.10 (s, 2H), 5.38 (d,  $J = 5.4$  Hz, 1H), 5.88-6.07 (m, 1H), 5.96 (d,  $J = 15.8$  Hz, 1H), 6.52 (dd,  $J = 15.8, 5.5$  Hz, 1H), 7.04-7.40 (m, 15H);  $^{13}\text{C NMR}$  (300 MHz,  $\text{CDCl}_3$ ) =  $\delta$ : 7.94, 32.04, 34.85, 35.87, 38.11, 51.04, 56.63, 67.21, 126.33, 127.22, 128.04,

128.38, 128.41, 128.63, 128.67, 128.86, 129.32, 130.04, 135.95, 136.21, 141.01, 146.13, 156.14, 170.47, 199.73; Elemental analysis: calcd for  $C_{31}H_{34}N_2O_4$ : C 74.67, H 6.87, N 5.62; found C 74.89, H 6.63, N 5.86.

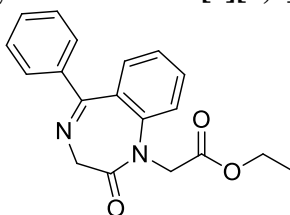
**Benzyl ((S)-1-oxo-1-(((S,E)-6-oxo-1-phenylnon-4-en-3-yl)amino)-3-phenylpropan-2-yl)carbamate (21d)**



Synthesis of product **21d** was carried out following the procedure described for compound **21a**, using **155d** as CM partner, commercially available. Yield: 90%; Consistency: white powder;  $R_f = 0.31$  (light petroleum/EtOAc, 7:3);  $^1H$  NMR (300 MHz,  $CDCl_3$ ) =  $\delta$ : 1.08 (t,  $J = 7.3$  Hz, 3H), 1.61-1.91 (m, 4H), 2.31-2.58 (m, 4H), 3.02-3.16 (m, 2H), 4.33-4.46 (m, 1H), 4.53-4.70 (m, 1H), 5.09 (s, 2H), 5.44 (d,  $J = 5.8$  Hz, 1H), 5.77 (d,  $J = 6.4$  Hz, 1H), 6.01 (d,  $J = 15.4$  Hz, 1H), 6.50 (dd,  $J = 15.4, 5.6$  Hz, 1H), 7.02-7.39 (m, 15H);  $^{13}C$  NMR (300 MHz,  $CDCl_3$ ) =  $\delta$ : 13.64, 18.42, 32.13, 35.84, 38.28, 42.57, 50.76, 56.47, 67.15, 126.30, 127.37, 128.12, 128.27, 128.33, 128.60, 128.64, 128.89, 129.34, 130.14, 136.08, 136.24, 141.13, 146.52, 156.17, 170.59, 201.28; Elemental analysis: calcd for  $C_{32}H_{36}N_2O_4$ : C 74.97, H 7.08, N 5.46; found: C 75.16, H 7.32, N 5.30.

**Series F**

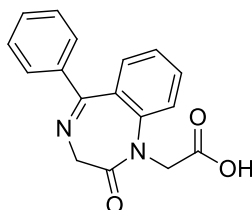
**Ethyl 2-(2-oxo-5-phenyl-2,3-dihydro-1H-benzo[e][1,4]diazepin-1-yl)acetate (156)**



In a double neck round flask containing NaH 60% dispersion in mineral oil (1.5 equiv.), BDZ scaffold **119** (2 equiv.) in dry DMF was added dropwise at  $0^\circ C$  under nitrogen atmosphere. The reaction mixture was stirred for 1h and then ethyl 2-bromoacetate (1.5 equiv.) was added dropwise. The reaction was stirred for 12h at rt. After this time,  $NH_4Cl$  saturated solution was added, and the organic layer was extracted with EtOAc (x 5), dried over  $Na_2SO_4$ , filtered and concentrated in *vacuo*. The crude material was purified by flash

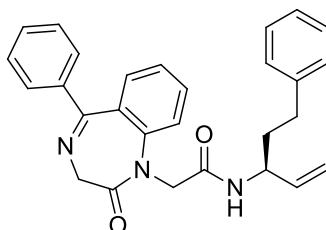
column chromatography using EtOAc/light petroleum (3:2) as eluent mixture, to obtain compound **156**. Yield: 61%; Consistency: brown oil;  $R_f = 0.24$  (EtOAc/light petroleum, 3:2);  $^1\text{H NMR}$  (300 MHz,  $\text{CDCl}_3$ ) =  $\delta$ : 1.20 (t,  $J = 7.1$  Hz, 3H), 3.08 (d,  $J = 15.3$  Hz, 1H), 3.57 (d,  $J = 15.3$  Hz, 1H), 3.71 (d,  $J = 10.5$  Hz, 1H), 4.17 (q,  $J = 7.0$  Hz, 1H), 4.24 (d,  $J = 10.5$  Hz, 1H), 7.18-7.41 (m, 3H), 7.49-7.64 (m, 5H), 7.94-8.05 (m, 1H). Spectroscopic data are in agreement to those reported in literature.<sup>83</sup>

**2-(2-Oxo-5-phenyl-2,3-dihydro-1H-benzo[e][1,4]diazepin-1-yl)acetic acid (157)**



A mixture of ester **156** (1 equiv.) in methanol/water/dioxane (1:1:1), LiOH as powder (3 equiv.) was added at 0° C. The reaction mixture was then stirred at rt, until disappearance of the starting material, by monitoring in TLC. The solvents were then evaporated in *vacuo* and the reaction mixture was treated with 10% citric acid (x 2), extracted with EtOAc (x 3), dried over  $\text{Na}_2\text{SO}_4$  and concentrated, to afford the pure carboxylic acid **156**. Yield: 97%; Consistency: orange solid;  $R_f = 0.29$  ( $\text{CH}_2\text{Cl}_2/\text{MeOH}$ , 9:1);  $^1\text{H NMR}$  (300 MHz,  $\text{CDCl}_3$ ) =  $\delta$ : 3.03 (d,  $J = 15.2$  Hz, 1H), 3.57 (d,  $J = 15.2$  Hz, 1H), 3.67 (d,  $J = 10.5$  Hz, 1H), 4.22 (d,  $J = 10.5$  Hz, 1H), 7.17-7.40 (m, 3H), 7.45-7.63 (m, 5H), 7.88-8.06 (m, 1H). Spectroscopic data are in agreement to those reported in literature.<sup>83</sup>

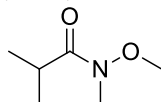
**(S)-2-(2-Oxo-5-phenyl-2,3-dihydro-1H-benzo[e][1,4]diazepin-1-yl)-N-(5-phenylpent-1-en-3-yl)acetamide (158)**



To a solution of acid **157** (1.2 equiv.) in dry  $\text{DMF}/\text{CH}_2\text{Cl}_2$  (1:1), HOBt (1.2 equiv.) and EDCI (1.2 equiv.) were added, in nitrogen atmosphere at 0° C. After 10 min, the amine **132** (1 equiv.) and DIPEA (1.2 equiv.) were added and the reaction mixture was stirred at rt for 12 h. After this time, the solvents were removed and the residue was diluted with EtOAc, washed with brine (x 5), dried over  $\text{Na}_2\text{SO}_4$ , filtered and concentrated in *vacuo*. The crude residue was purified by flash column chromatography using light

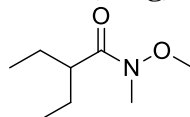
petroleum/EtOAc (1:1) as eluent mixture, to obtain coupling product **158**. Yield 78%; Consistency: pale yellow powder;  $R_f = 0.34$  (EtOAc/light petroleum, 1:1);  $^1\text{H NMR}$  (300 MHz,  $\text{CDCl}_3$ ) =  $\delta$ : 1.84-1.92 (m, 1H), 1.96-2.04 (m, 1H), 2.56 (t,  $J = 7.6$  Hz, 2H), 2.98 (d,  $J = 15.1$  Hz, 1H), 3.47 (d,  $J = 15.2$  Hz, 1H), 3.60 (d,  $J = 10.6$  Hz, 1H), 4.14 (d,  $J = 10.6$  Hz, 1H), 4.19-4.33 (m, 1H), 5.04-5.26 (m, 2H), 5.64-5.88 (m, 1H), 6.29 (d,  $J = 6.9$  Hz, 1H), 7.13-7.34 (m, 6H), 7.37-7.51 (m, 5H), 7.59-7.69 (m, 1H), 7.78-7.84 (m, 2H);  $^{13}\text{C NMR}$  (75 MHz,  $\text{CDCl}_3$ ) =  $\delta$ : 32.24, 36.27, 48.49, 51.67, 56.86, 114.98, 125.11, 126.40, 126.54, 128.26, 128.69, 128.74, 128.97, 129.38, 130.23, 130.41, 130.58, 138.66, 139.93, 141.71, 142.63, 168.45, 168.73, 170.03; Elemental analysis: calcd for  $\text{C}_{28}\text{H}_{27}\text{N}_3\text{O}_2$ : C 76.86, H 6.22, N 9.60; found: C 76.57, H 6.47, 9.27.

#### ***N*-Methoxy-*N*-methylisobutyramide (161f)**



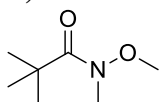
In a double neck round flask containing acid **159f** (1 equiv.) in  $\text{CH}_2\text{Cl}_2$ , carbonyldiimidazole (CDI, 1.3 equiv.) was added portion wise at rt. The reaction mixture was stirred for 1h and then *N,O*-dimethylhydroxylamine hydrochloride (2 equiv.) was added and stirred for 12h. After this time, the reaction mixture was treated with water and extracted with  $\text{CH}_2\text{Cl}_2$  (x 3). The organic phase was dried over  $\text{Na}_2\text{SO}_4$ , filtered and concentrated in *vacuo*. The crude residue was purified by flash column chromatography using light petroleum/EtOAc (1:1) as eluent mixture, to obtain compound **161f**. Yield: 59%; Consistency: colourless oil;  $R_f = 0.42$  (light petroleum/EtOAc, 1:1, detected with  $\text{KMnO}_4$ );  $^1\text{H NMR}$  (300 MHz,  $\text{CDCl}_3$ ) =  $\delta$ : 1.06 (d,  $J = 6.7$  Hz, 3H), 1.12 (d,  $J = 6.7$  Hz, 3H), 2.92 (bs, 1H), 3.13 (s, 3H), 3.64 (s, 3H). Spectroscopic data are in agreement to those reported in literature.<sup>118</sup>

#### **2-Ethyl-*N*-methoxy-*N*-methylbutanamide (161g)**



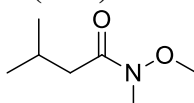
Synthesis of compound **161g** was carried out following the procedure described for compound **161f**, using **159g** as acid. Yield: 64%; Consistency: colourless oil;  $R_f = 0.52$  (light petroleum/EtOAc, 1:1, detected with  $\text{KMnO}_4$ );  $^1\text{H NMR}$  (300 MHz,  $\text{CDCl}_3$ ) =  $\delta$ : 0.84-0.97 (m, 6H), 1.33-1.51 (m, 4H), 2.40-2.61 (m, 1H), 2.70 (s, 3H), 3.64 (s, 3H). Spectroscopic data are in agreement to those reported in literature.<sup>119</sup>

#### ***N*-Methoxy-*N*-methylpivalamide (161h)**



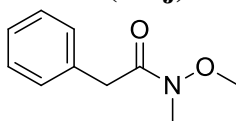
Synthesis of compound **161h** was carried out following the procedure described for compound **161f**, using **159h** as acid. Yield: 63%; Consistency: colourless oil;  $R_f = 0.44$  (light petroleum/EtOAc, 1:1, detected with  $\text{KMnO}_4$ );  $^1\text{H NMR}$  (300 MHz,  $\text{CDCl}_3$ ) =  $\delta$ : 1.21 (s, 9H), 3.06 (s, 3H), 3.62 (s, 3H). Spectroscopic data are in agreement to those reported in literature.<sup>120</sup>

#### ***N*-Methoxy-*N*,3-dimethylbutanamide (161i)**



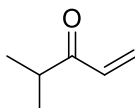
Synthesis of compound **161i** was carried out following the procedure described for compound **161f**, using **159i** as acid. Yield: 57%; Consistency: white solid;  $R_f = 0.47$  (light petroleum/EtOAc, 1:1, detected with  $\text{KMnO}_4$ );  $^1\text{H NMR}$  (300 MHz,  $\text{CDCl}_3$ ) =  $\delta$ : 1.01 (d,  $J = 6.5$  Hz, 3H), 1.06 (d,  $J = 6.5$  Hz, 3H), 1.91-2.16 (m, 3H), 3.06 (s, 3H), 3.69 (s, 3H). Spectroscopic data are in agreement to those reported in literature.<sup>121</sup>

#### ***N*-Methoxy-*N*-methyl-2-phenylacetamide (161j)**



Synthesis of compound **161j** was carried out following the procedure described for compound **161f**, using **159j** as acid. Yield: 82%; Consistency: colourless oil;  $R_f = 0.38$  (light petroleum/EtOAc, 1:1);  $^1\text{H NMR}$  (300 MHz,  $\text{CDCl}_3$ ) =  $\delta$ : 3.11 (s, 3H), 3.64 (s, 3H), 3.83 (s, 2H), 7.17-7.33 (m, 5H). Spectroscopic data are in agreement to those reported in literature.<sup>122</sup>

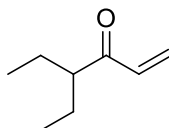
#### **4-Methylpent-1-en-3-one (162f)**



To the Weinreb amide **161f** (1 equiv.) in dry THF was added vinyl magnesium bromide **153** (1.2 equiv.) dropwise, at 0° C. The reaction was stirred for 15 min, and then, for 2h at rt. After this time the reaction was quenched with  $\text{NH}_4\text{Cl}$  saturated solution and the organic phase was extracted with EtOAc (x 3), washed with brine (x 5), dried over  $\text{Na}_2\text{SO}_4$ , filtered and concentrated in *vacuo*. The crude residue was purified by flash column chromatography using light petroleum/EtOAc (1:1), to obtain vinyl ketone **162f**. Yield:

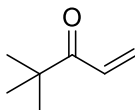
82%; Consistency: colourless oil;  $R_f = 0.58$  (light petroleum/EtOAc, 1:1, detected with  $\text{KMnO}_4$ );  $^1\text{H NMR}$  (300 MHz,  $\text{CDCl}_3$ ) =  $\delta$ : 1.04 (d,  $J = 6.3$  Hz, 3H), 1.09 (d,  $J = 6.3$  Hz, 3H), 1.55-1.85 (m, 2H) 3.72-3.90 (m, 1H) 5.13-5.27 (m, 2H), 5.93-6.06 (m, 1H). Spectroscopic data are in agreement to those reported in literature.<sup>123</sup>

#### 4-Ethylhex-1-en-3-one (162g)



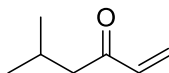
Synthesis of compound **162g** was carried out following the procedure described for compound **162f**, using **161g** as Weinreb amide. Yield: 87%; Consistency: colourless oil;  $R_f = 0.68$  (light petroleum/EtOAc, 1:1, detected with  $\text{KMnO}_4$ );  $^1\text{H NMR}$  (300 MHz,  $\text{CDCl}_3$ ) =  $^1\text{H NMR}$  ( $\text{CDCl}_3$ ) =  $\delta$ : 0.88 (t,  $J = 7.3$  Hz, 6H), 1.43-1.58 (m, 2H), 1.64-1.72 (m, 2H), 2.61-2.70 (m, 1H), 5.82 (dd,  $J = 10.2, 1.1$  Hz, 1H), 6.30 (dd,  $J = 16.0, 1.1$  Hz, 1H), 6.49 (dd,  $J = 16.0, 10.2$  Hz, 1H). Spectroscopic data are in agreement to those reported in literature.<sup>124</sup>

#### 4,4-Dimethylpent-1-en-3-one (162h)



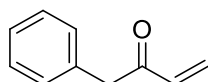
Synthesis of compound **162h** was carried out following the procedure described for compound **162f**, using **161h** as Weinreb amide. Yield: 83%; Consistency: colourless oil;  $R_f = 0.63$  (light petroleum/EtOAc, 1:1, detected with  $\text{KMnO}_4$ );  $^1\text{H NMR}$  (300 MHz,  $\text{CDCl}_3$ ) =  $^1\text{H NMR}$  ( $\text{CDCl}_3$ ) =  $\delta$ : 1.31 (s, 9H), 5.69 (dd,  $J = 9.8, 1.0$  Hz, 1H), 6.42 (dd,  $J = 15.8, 1.0$  Hz, 1H), 6.79 (dd,  $J = 15.8, 9.8$  Hz, 1H). Spectroscopic data are in agreement to those reported in literature.<sup>117</sup>

#### 5-Methylhex-1-en-3-one (162i)



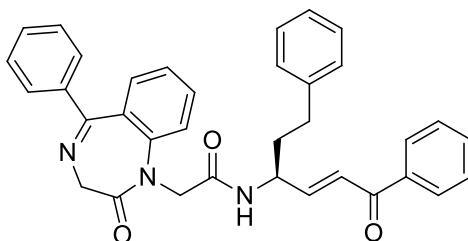
Synthesis of compound **162i** was carried out following the procedure described for compound **162f**, using **161i** as Weinreb amide. Yield: 91%; Consistency: yellow oil;  $R_f = 0.55$  (light petroleum/EtOAc, 1:1, detected with  $\text{KMnO}_4$ );  $^1\text{H NMR}$  (300 MHz,  $\text{CDCl}_3$ ) =  $\delta$ : 0.99 (d,  $J = 6.3$  Hz, 3H), 1.04 (d,  $J = 6.3$  Hz, 3H), 1.31-1.59 (m, 3H), 5.54 (dd,  $J = 10.4, 1.2$  Hz, 1H), 6.39 (dd,  $J = 16.0, 1.2$  Hz, 1H), 6.83 (dd,  $J = 16.0, 10.4$  Hz, 1H). Spectroscopic data are in agreement to those reported in literature.<sup>121</sup>

#### 1-Phenylbut-3-en-2-one (162j)



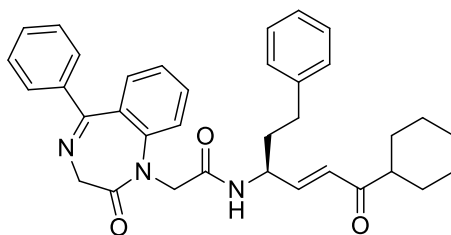
Synthesis of compound **162j** was carried out following the procedure described for compound **162f**, using **161j** as Weinreb amide. Yield: 94%; Consistency: yellow oil;  $R_f$  = 0.68 (light petroleum/EtOAc, 1:1);  $^1\text{H NMR}$  (300 MHz,  $\text{CDCl}_3$ ) =  $\delta$ : 3.94 (s, 2H), 5.80 (dd,  $J$  = 9.6, 1.4 Hz, 1H), 6.40 (dd,  $J$  = 15.8, 1.4 Hz, 1H), 6.53 (dd,  $J$  = 15.8, 9.6 Hz, 1H). Spectroscopic data are in agreement to those reported in literature.<sup>125</sup>

**(*S,E*)-*N*-(6-Oxo-1,6-diphenylhex-4-en-3-yl)-2-(2-oxo-5-phenyl-2,3-dihydro-1*H*-benzo[*e*][1,4]diazepin-1-yl)acetamide (22a)**



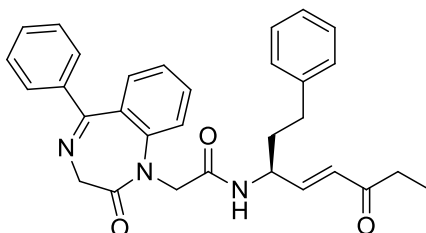
A solution of terminal olefin **158** (1 equiv.) in dry  $\text{CH}_2\text{Cl}_2$  (3 mL), in a 10 mL microwave tube equipped with a magnetic stirrer, was treated with CM partner **154a** (10 equiv.) and Hoveyda–Grubbs catalyst 2nd generation [(1,3-bis-(2,4,6-trimethylphenyl)-2-imidazolidinylidene)-dichloro-(*o*-isopropoxyphenylmethylene) ruthenium] (0.1 equiv.) under microwave irradiation at 100 °C for 2h. Subsequently, the solvent was removed under reduced pressure and the residue was purified by flash column chromatography using light petroleum/EtOAc (1:1), to obtain product **22a**. Yield: 76%; Consistency: white powder;  $R_f$  = 0.32 (light petroleum/EtOAc, 1:1);  $^1\text{H NMR}$  (300 MHz,  $\text{CDCl}_3$ ) =  $\delta$ : 1.78-1.89 (m, 1H), 1.98-2.11 (m, 1H), 2.52 (t,  $J$  = 7.8 Hz, 2H), 3.02 (d,  $J$  = 15.1 Hz, 1H), 3.41 (d,  $J$  = 15.1 Hz, 1H), 3.67 (d,  $J$  = 10.6 Hz, 1H), 4.20 (d,  $J$  = 10.6 Hz, 1H), 4.19-4.33 (m, 1H), 6.11 (d,  $J$  = 15.0 Hz, 1H), 6.29 (d,  $J$  = 6.9 Hz, 1H), 6.58 (dd,  $J$  = 15.0 Hz, 1H), 7.13-7.34 (m, 6H), 7.37-7.51 (m, 8H), 7.64-7.68 (m, 1H), 7.78-7.93 (m, 4H);  $^{13}\text{C NMR}$  (75 MHz,  $\text{CDCl}_3$ ) =  $\delta$ : 32.61, 36.43, 49.11, 51.74, 56.90, 125.14, 126.47, 126.62, 128.33, 128.51, 128.74, 128.85, 129.07, 129.43, 129.76, 130.16, 130.34, 130.50, 130.69, 133.94, 138.42, 140.05, 141.75, 142.83, 148.32, 168.71, 168.84, 170.53, 192.04; Elemental analysis: calcd for  $\text{C}_{35}\text{H}_{31}\text{N}_3\text{O}_3$ : C 77.61, H 5.77, N 7.76; found C 77.81, H 5.49, N 7.94.

**(*S,E*)-*N*-(6-Cyclohexyl-6-oxo-1-phenylhex-4-en-3-yl)-2-(2-oxo-5-phenyl-2,3-dihydro-1*H*-benzo[*e*][1,4]diazepin-1-yl)acetamide (22b)**



Synthesis of compound **22b** was carried out following the procedure described for compound **22a**, using **154b** as CM partner. Yield: 84%; Consistency: white powder;  $R_f = 0.23$  (light petroleum/EtOAc, 1:1);  $^1\text{H NMR}$  (300 MHz,  $\text{CDCl}_3$ ) =  $\delta$ : 1.32-1.54 (m, 4H), 1.82-2.08 (m, 8H), 2.42-2.59 (m, 3H), 3.03 (d,  $J = 15.0$  Hz, 1H), 3.44 (d,  $J = 15.0$  Hz, 1H), 3.58 (d,  $J = 10.8$  Hz, 1H), 4.11 (d,  $J = 10.8$  Hz, 1H), 4.23-4.38 (m, 1H), 6.18 (d,  $J = 15.5$  Hz, 1H), 6.46 (d,  $J = 7.3$  Hz, 1H), 6.90 (dd,  $J = 15.5, 5.1$  Hz, 1H), 7.16-7.36 (m, 6H), 7.40-7.56 (m, 5H), 7.69-7.85 (m, 3H);  $^{13}\text{C NMR}$  (75 MHz,  $\text{CDCl}_3$ ) =  $\delta$ : 25.13, 26.02, 29.57, 32.74, 36.56, 47.23, 49.18, 51.76, 56.95, 125.17, 126.51, 126.67, 128.30, 128.61, 128.77, 128.88, 129.03, 129.37, 130.39, 130.44, 130.62, 140.06, 141.74, 142.69, 148.46, 168.48, 168.79, 170.58, 203.86; Elemental analysis: calcd for  $\text{C}_{35}\text{H}_{37}\text{N}_3\text{O}_3$ : C 76.75, H 6.81, N 7.67; found C 76.84, H 6.40, N 7.92.

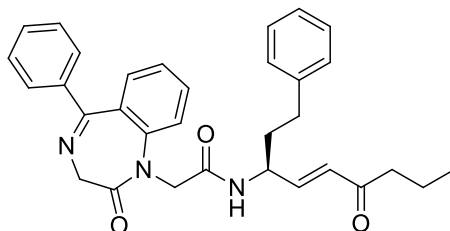
**(S,E)-N-(6-Oxo-1-phenyloct-4-en-3-yl)-2-(2-oxo-5-phenyl-2,3-dihydro-1H-benzo[e][1,4]diazepin-1-yl)acetamide (22c)**



Synthesis of compound **22c** was carried out following the procedure described for compound **22a**, using **154c** as CM partner. Yield: 87%; Consistency: white powder;  $R_f = 0.43$  (light petroleum/EtOAc, 3:2);  $^1\text{H NMR}$  (300 MHz,  $\text{CDCl}_3$ ) =  $\delta$ : 1.13 (t,  $J = 7.6$  Hz, 3H), 1.86-2.06 (m, 2H), 2.56 (t,  $J = 7.6$  Hz, 2H), 2.91-3.08 (m, 3H), 3.44 (d,  $J = 15.0$  Hz, 1H), 3.57 (d,  $J = 10.8$  Hz, 1H), 4.10 (d,  $J = 10.8$  Hz, 1H), 4.16-4.29 (m, 1H), 6.09 (d,  $J = 15.2$  Hz, 1H), 6.32 (d,  $J = 7.0$  Hz, 1H), 6.58 (dd,  $J = 15.2, 5.1$  Hz, 1H), 7.13-7.49 (m, 11H), 7.61-7.69 (m, 1H), 7.76-7.86 (m, 2H);  $^{13}\text{C NMR}$  (75 MHz,  $\text{CDCl}_3$ ) =  $\delta$ : 7.97, 32.19, 34.90, 36.25, 48.57, 51.72, 56.93, 125.16, 126.42, 126.55, 128.28, 128.76, 128.80, 128.99, 129.08, 129.43, 130.08, 130.45, 130.62, 140.04, 141.67, 142.71, 146.19, 168.44, 168.70, 170.54, 199.86; Elemental analysis: calcd for  $\text{C}_{31}\text{H}_{31}\text{N}_3\text{O}_3$ : C 75.43, H 6.33, N 8.51; found C 75.08, H 6.47, N 8.34.

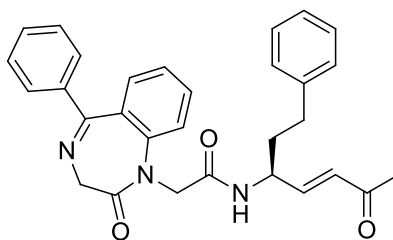


**(*S,E*)-*N*-(6-Oxo-1-phenylnon-4-en-3-yl)-2-(2-oxo-5-phenyl-2,3-dihydro-1*H*-benzo[*e*][1,4]diazepin-1-yl)acetamide (22d)**



Synthesis of compound **22d** was carried out following the procedure described for compound **22a**, using **154d** as CM partner. Yield: 84%; Consistency: white solid;  $R_f = 0.48$  (light petroleum/EtOAc, 3:2);  $^1\text{H NMR}$  (300 MHz,  $\text{CDCl}_3$ ) =  $\delta$ : 1.01 (t,  $J = 7.7$  Hz, 3H), 1.59-1.79 (m, 2H) 1.88-2.05 (m, 2H), 2.52 (t,  $J = 7.5$  Hz, 2H), 2.93-3.010 (m, 3H), 3.44 (d,  $J = 15.1$  Hz, 1H), 3.62 (d,  $J = 10.5$  Hz, 1H), 4.08 (d,  $J = 10.5$  Hz, 1H), 4.08-4.23 (m, 1H), 6.04 (d,  $J = 15.1$  Hz, 1H), 6.44 (d,  $J = 6.9$  Hz, 1H), 6.52 (dd,  $J = 15.1, 4.9$  Hz, 1H), 7.11-7.44 (m, 11H), 7.63-7.88 (m, 3H);  $^{13}\text{C NMR}$  (75 MHz,  $\text{CDCl}_3$ ) =  $\delta$ : 13.67, 18.49, 32.18, 35.77, 36.34, 48.50, 51.74, 56.88, 125.13, 126.42, 126.65, 128.34, 128.78, 128.83, 128.95, 129.03, 129.42, 130.18, 130.44, 130.62, 139.97, 141.67, 142.65, 146.55, 168.52, 168.89, 170.61, 201.30; Elemental analysis: calcd for  $\text{C}_{32}\text{H}_{33}\text{N}_3\text{O}_3$ : C 75.71, H 6.55, N 8.28; found: C 75.48, H 6.83, N 7.99.

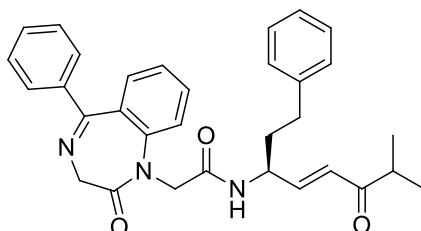
**(*S,E*)-*N*-(6-Oxo-1-phenylhept-4-en-3-yl)-2-(2-oxo-5-phenyl-2,3-dihydro-1*H*-benzo[*e*][1,4]diazepin-1-yl)acetamide (22e)**



Synthesis of compound **22e** was carried out following the procedure described for compound **22a**, using **126b** as CM partner. Yield: 91%; Consistency: white powder;  $R_f = 0.38$  (light petroleum/EtOAc, 3:2);  $^1\text{H NMR}$  (300 MHz,  $\text{CDCl}_3$ ) =  $\delta$ : 1.80-1.91 (m, 1H), 1.94-2.01 (m, 1H), 2.26 (s, 3H), 2.51 (t,  $J = 7.8$  Hz, 2H), 2.96 (d,  $J = 15.0$  Hz, 1H), 3.42 (d,  $J = 15.0$  Hz, 1H), 3.55 (d,  $J = 10.6$  Hz, 1H), 4.08 (d,  $J = 10.6$  Hz, 1H), 4.20-4.36 (m, 1H), 6.08 (d,  $J = 15.8$  Hz, 1H), 6.29 (d,  $J = 6.9$  Hz, 1H), 6.67 (dd,  $J = 15.8, 5.2$  Hz, 1H), 7.17-7.50 (m, 11H), 7.62-7.70 (m, 1H), 7.75-7.83 (m, 2H);  $^{13}\text{C NMR}$  (75 MHz,  $\text{CDCl}_3$ ) =  $\delta$ : 27.82, 32.16, 36.65, 48.55, 51.84, 56.83, 125.10, 126.47, 126.58, 128.30, 128.68, 128.75, 128.94, 129.10, 129.37, 130.21, 130.44, 130.62, 140.08, 141.66, 142.65, 145.82,

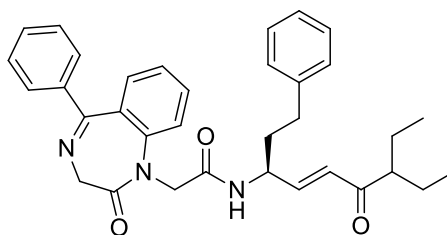
168.59, 168.82, 170.66, 197.92; Elemental analysis: calcd for C<sub>30</sub>H<sub>29</sub>N<sub>3</sub>O<sub>3</sub>: C 75.13, H 6.10, N 8.76; found C 74.89, H 5.93, N 8.99.

**(*S,E*)-*N*-(7-Methyl-6-oxo-1-phenyloct-4-en-3-yl)-2-(2-oxo-5-phenyl-2,3-dihydro-1*H*-benzo[*e*][1,4]diazepin-1-yl)acetamide (22f)**



Synthesis of compound **22f** was carried out following the procedure described for compound **22a**, using **162f** as CM partner. Yield: 84%; Consistency: white powder;  $R_f$  = 0.46 (light petroleum/EtOAc, 3:2); <sup>1</sup>H NMR (300 MHz, CDCl<sub>3</sub>) =  $\delta$ : 0.96 (d,  $J$  = 6.6 Hz, 3H), 1.01 (d,  $J$  = 6.6 Hz, 3H), 1.82-1.99 (m, 2H), 2.51 (t,  $J$  = 7.7 Hz, 2H), 3.02 (d,  $J$  = 15.0 Hz, 1H), 3.21 (m, 1H), 3.49 (d,  $J$  = 15.0 Hz, 1H), 3.66 (d,  $J$  = 10.5 Hz, 1H), 4.18 (d,  $J$  = 10.5 Hz, 1H), 4.26-4.40 (m, 1H), 6.17 (d,  $J$  = 15.5 Hz, 1H), 6.43 (d,  $J$  = 7.0 Hz, 1H), 6.83 (dd,  $J$  = 15.5, 5.6 Hz, 1H), 7.06-7.45 (m, 11H), 7.62-7.81 (m, 3H); <sup>13</sup>C NMR (75 MHz, CDCl<sub>3</sub>) =  $\delta$ : 18.87, 18.93, 32.23, 36.54, 38.96, 48.68, 51.79, 56.80, 125.17, 126.44, 126.61, 128.32, 128.74, 128.78, 129.01, 129.17, 129.43, 130.27, 130.46, 130.64, 139.98, 141.65, 142.75, 148.67, 168.31, 168.66, 170.59, 202.73; Elemental analysis: calcd for C<sub>32</sub>H<sub>33</sub>N<sub>3</sub>O<sub>3</sub>: C 75.71, H 6.55, N 8.28; found C 76.03, H 6.39, N 8.11.

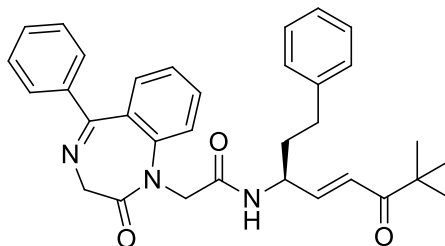
**(*S,E*)-*N*-(7-Ethyl-6-oxo-1-phenylnon-4-en-3-yl)-2-(2-oxo-5-phenyl-2,3-dihydro-1*H*-benzo[*e*][1,4]diazepin-1-yl)acetamide (22g)**



Synthesis of compound **22g** was carried out following the procedure described for compound **22a**, using **162g** as CM partner. Yield: 78%; Consistency: white powder;  $R_f$  = 0.54 (light petroleum/EtOAc, 3:2); <sup>1</sup>H NMR (300 MHz, CDCl<sub>3</sub>) =  $\delta$ : 0.84-0.97 (m, 6H), 1.26-1.42 (m, 4H), 1.83-1.95 (m, 1H), 1.99-2.12 (m, 1H), 2.31-58 (m, 3H), 3.03 (d,  $J$  = 15.0 Hz, 1H), 3.51 (d,  $J$  = 15.0 Hz, 1H), 3.56 (d,  $J$  = 10.8 Hz, 1H), 4.19 (d,  $J$  = 10.8 Hz, 1H), 4.11-4.28 (m, 1H), 6.12 (d,  $J$  = 15.3 Hz, 1H), 6.42 (d,  $J$  = 7.0 Hz, 1H), 6.74 (dd,  $J$  = 15.3, 5.2 Hz, 1H), 7.11-7.30 (m, 6H), 7.36-7.52 (m, 5H), 7.60-7.69 (m, 1H), 7.80-7.88 (m,

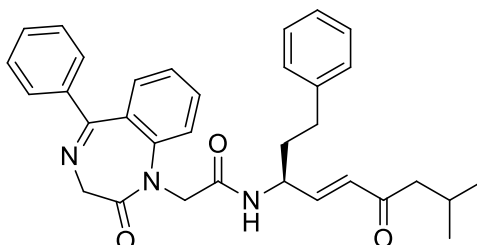
2H);  $^{13}\text{C}$  NMR (75 MHz,  $\text{CDCl}_3$ ) =  $\delta$ : 11.51, 11.54, 23.64, 23.69, 32.33, 36.40, 48.67, 51.70, 52.87, 56.94, 125.09, 126.45, 126.59, 128.27, 128.67, 128.81, 128.91, 129.07, 129.43, 130.37, 130.49, 130.63, 140.05, 141.78, 142.73, 148.70, 168.52, 168.69, 107.66, 204.37; Elemental analysis: calcd for  $\text{C}_{34}\text{H}_{37}\text{N}_3\text{O}_3$ : C 76.23, H 6.96, N 7.84; found: C 76.95, H 7.14, N 7.06.

**(*S,E*)-*N*-(7,7-Dimethyl-6-oxo-1-phenyloct-4-en-3-yl)-2-(2-oxo-5-phenyl-2,3-dihydro-1*H*-benzo[*e*][1,4]diazepin-1-yl)acetamide (22h)**



Synthesis of compound **22h** was carried out following the procedure described for compound **22a**, using **162h** as CM partner. Yield: 86%; Consistency: white powder;  $R_f$  = 0.48 (light petroleum/EtOAc, 3:2);  $^1\text{H}$  NMR (300 MHz,  $\text{CDCl}_3$ ) =  $\delta$ : 1.28 (s, 9H), 1.85-2.01 (m, 2H), 2.52 (t,  $J$  = 7.8 Hz, 2H), 2.99 (d,  $J$  = 15.0 Hz, 1H), 3.42 (d,  $J$  = 15.0 Hz, 1H), 3.64 (d,  $J$  = 10.8 Hz, 1H), 4.10 (d,  $J$  = 10.8 Hz, 1H), 4.03-4.21 (m, 1H), 6.09 (d,  $J$  = 15.2 Hz, 1H), 6.29 (d,  $J$  = 6.9 Hz, 1H), 6.82 (dd,  $J$  = 15.2, 5.1 Hz, 1H), 7.16-7.48 (m, 11H), 7.56-7.68 (m, 1H), 7.75-7.82 (m, 2H);  $^{13}\text{C}$  NMR (75 MHz,  $\text{CDCl}_3$ ) =  $\delta$ : 27.54, 32.47, 36.25, 40.51, 48.63, 51.78, 56.88, 125.19, 126.55, 126.67, 128.11, 128.64, 128.75, 128.93, 129.12, 129.42, 130.31, 130.39, 130.68, 139.97, 141.66, 142.58, 149.27, 168.53, 168.84, 170.62, 204.87; Elemental analysis: calcd for  $\text{C}_{33}\text{H}_{35}\text{N}_3\text{O}_3$ : C 75.98, H 6.76, N 8.06; found: C 76.17, H 6.54, N 8.23.

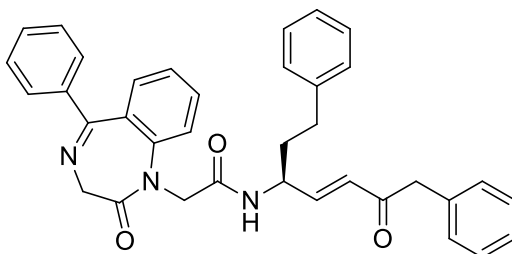
**(*S,E*)-*N*-(8-Methyl-6-oxo-1-phenylnon-4-en-3-yl)-2-(2-oxo-5-phenyl-2,3-dihydro-1*H*-benzo[*e*][1,4]diazepin-1-yl)acetamide (22i)**



Synthesis of compound **22i** was carried out following the procedure described for compound **22a**, using **162i** as CM partner. Yield: 77%; Consistency: white powder;  $R_f$  = 0.53 (light petroleum/EtOAc, 3:2);  $^1\text{H}$  NMR (300 MHz,  $\text{CDCl}_3$ ) =  $\delta$ : 0.98 (d,  $J$  = 6.7 Hz,

3H), 1.04 (d,  $J = 6.7$  Hz, 3H), 1.79-2.01 (m, 3H), 2.54 (t,  $J = 7.4$  Hz, 2H), 2.88-3.05 (m, 3H), 3.51 (d,  $J = 15.0$  Hz, 1H), 3.64 (d,  $J = 10.8$  Hz, 1H), 4.19 (d,  $J = 10.9$  Hz, 1H), 4.21-4.36 (m, 1H), 6.15 (d,  $J = 15.4$  Hz, 1H), 6.46 (d,  $J = 7.3$  Hz, 1H), 6.79 (dd,  $J = 15.4, 5.3$  Hz, 1H), 7.09-7.31 (m, 6H), 7.36-7.48 (m, 5H), 7.57-7.66 (m, 1H), 7.74-7.83 (m, 2H);  $^{13}\text{C}$  NMR (75 MHz,  $\text{CDCl}_3$ ) =  $\delta$ : 22.67, 22.73, 24.74, 32.09, 36.18, 48.50, 51.42, 51.86, 56.80, 125.10, 126.32, 126.60, 128.34, 128.75, 128.92, 129.01, 129.06, 129.37, 130.32, 130.44, 130.62, 140.14, 141.75, 142.61, 147.38, 168.49, 168.71, 170.63, 200.16; Elemental analysis: calcd for  $\text{C}_{33}\text{H}_{35}\text{N}_3\text{O}_3$ : C 75.98, H 6.76, N 8.06; found: C 75.84, H 6.92, N 7.90.

**(*S,E*)-*N*-(6-Oxo-1,7-diphenylhept-4-en-3-yl)-2-(2-oxo-5-phenyl-2,3-dihydro-1*H*-benzo[*e*][1,4]diazepin-1-yl)acetamide (22j)**



Synthesis of compound **22j** was carried out following the procedure described for compound **22a**, using **162j** as CM partner. Yield: 74%; Consistency: white solid;  $R_f = 0.41$  (light petroleum/EtOAc, 1:1);  $^1\text{H}$  NMR (300 MHz,  $\text{CDCl}_3$ ) =  $\delta$ : 1.81-1.92 (m, 1H), 1.95-2.05 (m, 1H), 2.52 (t,  $J = 7.4$  Hz, 2H), 3.00 (d,  $J = 15.0$  Hz, 1H), 3.44 (d,  $J = 15.0$  Hz, 1H), 3.66 (d,  $J = 10.8$  Hz, 1H), 4.09-4.26 (m, 4H), 6.19 (d,  $J = 15.1$  Hz, 1H), 6.29 (d,  $J = 6.7$  Hz, 1H), 6.81 (dd,  $J = 15.1, 5.2$  Hz, 1H), 7.11-7.36 (m, 11H), 7.41-7.53 (m, 5H), 7.60-7.72 (m, 1H), 7.79-7.86 (m, 2H);  $^{13}\text{C}$  NMR (75 MHz,  $\text{CDCl}_3$ ) =  $\delta$ : 32.18, 36.34, 44.75, 48.51, 51.70, 56.88, 125.12, 126.41, 126.62, 127.84, 128.30, 128.88, 128.93, 128.97, 129.09, 129.42, 129.57, 129.94, 130.22, 130.45, 130.68, 134.86, 140.02, 141.76, 142.65, 147.19, 168.53, 168.70, 170.63, 197.28; Elemental analysis: calcd for  $\text{C}_{36}\text{H}_{33}\text{N}_3\text{O}_3$ : C 77.81, H 5.99, N 7.56; found: C 78.03, H 6.18, N 7.32.

## 6.2 Biology

### Enzyme assays against rhodesain

Preliminary screening with rhodesain was performed at different inhibitor concentrations, depending on the series. It was used an equivalent amount of DMSO as negative control and E-64 as positive control. The enzyme was recombinantly expressed as reported in literature.<sup>126</sup> Product release from substrate hydrolysis (Cbz-Phe-Arg-AMC, 10  $\mu$ M) was determined continuously over a period of 30 min for irreversible inhibitors and 10 min for reversible inhibitors. Fluorescence of the product AMC of the substrate hydrolyses was measured using an Infinite 200 PRO microplate reader (Tecan, Männedorf, Switzerland) at room temperature with a 380 nm excitation filter and a 460 nm emission filter. Second-order rate constants of inhibition and  $K_i$  values were determined with 7 different inhibitor concentrations, ranging from those that minimally inhibited to those that fully inhibited the enzyme, using the program GraFit.<sup>127</sup> The assay buffer contains: 50 mM sodium acetate, pH = 5.5, 5 mM EDTA, 200 mM NaCl and 0.005 % Brij 35 to avoid aggregation and wrong-positive results. Enzyme buffer contains 5 mM DTT rather than Brij 35. The  $K_m$  value used to calculate  $K_i$  values from  $IC_{50}$  values were determined to 0.9  $\mu$ M (rhodesain).<sup>74</sup> The dissociation constants  $K_i$  were obtained from progress curves (10 min) at various concentrations of inhibitor by fitting the progress curves to the 4-parameter  $IC_{50}$  equation:<sup>128</sup>

$$y = \frac{y_{\max} - y_{\min}}{1 + \left(\frac{[I]}{IC_{50}}\right)^s} + y_{\min}$$

with  $y$  [dF/min] as the substrate hydrolysis rate,  $y_{\max}$  as the maximum value of the dose-response curve that is observed at very low inhibitor concentrations,  $y_{\min}$  as the minimum value that is obtained at high inhibitor concentrations, and  $s$  denotes the Hill coefficient,<sup>129</sup> and correction to zero substrate concentration from  $K_i = IC_{50}/(1 + [S]/K_m^{-1})$ . To determine the first-order inactivation rate constants ( $k_{obs}$ ) for the irreversible inhibition, progress curves (fluorescence vs time) were analyzed by non-linear regression analysis using the equation  $F = A (1 - \exp(-k_{obs} t)) + B$ .<sup>130</sup> Fitting of the  $k_{obs}$  values against the inhibitor concentrations to the hyperbolic equation  $k_{obs} = k_{inac} [I]/(K_{iapp} + [I])$  gave the individual values of  $K_{iapp}$  and  $k_{inac}$ .<sup>129</sup> The  $K_{iapp}$  values were corrected to zero substrate concentration by the term  $(1 + [S]/K_m)$  in equation  $K_i = K_{iapp}/(1 + [S]/K_m)$ . Inhibitor solutions were prepared

from stocks in DMSO. Each independent assay was performed twice in duplicate in 96-well-plates in a total volume of 200  $\mu$ L.

#### **Enzyme assays against hCatL and hCatB<sup>74</sup>**

Assays with hCatL and hCatB was performed as described for rhodesain, using fluorogenic substrate Cbz-Phe-Arg-AMC (5  $\mu$ M) and  $K_m$  value of 6.5  $\mu$ M for hCatL and 150  $\mu$ M for hCatB.

#### **Drug screening on *T. b. brucei* cultures**

The antitrypanosomal activity was determined using the ATPlite assay<sup>131</sup> as described previously.<sup>132</sup> This assay is based on the adenosine triphosphate (ATP) dependent light emitting reaction catalyzed by firefly luciferase. In the presence of ATP and Mg ions, the enzyme transforms D-luciferine into D-luciferine adenylate which then turns into the excited keto form of oxyluciferin. ATP can be used as a marker for cell viability. All experiments were performed in white 96-well microplates (PerkinElmer). Each well was filled with 90  $\mu$ L of medium containing 2500 cells/mL. The BSFs used in this work were of the *T. b. brucei* 449 cell line, which is a descendant of the Lister 427 strain.<sup>133</sup> Each tested compound (5 mM stock solutions, chlorhexidine: 10 mM stock solution) was then diluted in HMI-9 medium: firstly 1:3, then 1:10 and subsequently in ten 1:2 dilution steps using separate microplates. Of the final ten 1:2 dilutions, 10  $\mu$ L each were then added to the 90  $\mu$ L cell suspension, leading to an additional final 1:10 dilution for all compounds.<sup>132</sup> Addition of 10  $\mu$ L DMSO corresponding to 10% DMSO, was used as a positive control. For drug addition, highest concentration of DMSO added was 0.3% DMSO. Therefore, addition of 0.3% DMSO served as a negative control. The plates were incubated at 37 °C for 24 h and 48 h in separate triplicates. 50  $\mu$ L of ATPlite 1 step solution was added to each well of the microplate, providing luciferin and luciferase as well as initiating cell lysis, and luminescence was measured in a Victor X4 plate reader (PerkinElmer) at room temperature. A dose-response curve was obtained by plotting the measured values against the logarithmic compound concentrations and the EC<sub>50</sub> values were calculated using GraFit Vs. 5.013, Erithacus Software Ltd. Chlorhexidine, trypanothione reductase inhibitor, was used as positive control.<sup>134</sup>

#### **Enzyme assays against FP-2<sup>135,136</sup>**

Preparation of recombinant FP-2 and assessment of activity and effects of inhibitors were performed as previously described using the fluorogenic substrate Cbz-Leu-Arg-AMC (32

$\mu\text{M}$ ) and  $K_m$  values of 21.5  $\mu\text{M}$ .  $\text{IC}_{50}$  values were calculated from plots of inhibitor concentration vs. percent control activity by nonlinear regression using Graphpad Prism 6.0 software.

#### **Drug screening on *P. falciparum* cultures**<sup>137</sup>

The effects of inhibitors were studied against W2-strain *P. falciparum*, obtained from the Malaria Research and Reference Reagent Resource Center and cultured with human erythrocytes at 2% hematocrit in RPMI medium with either 10% human serum or 0.5% AlbuMAX II serum substitute. Synchrony was maintained with sorbitol. Cultures were incubated with serial dilutions of test compounds from 1000 stocks in DMSO for 48 h beginning at the ring stage. The medium was changed after 24 h, with maintenance of the appropriate inhibitor concentration. After 48 h, when control cultures contained nearly all new ring-stage parasites, parasites were fixed with 1% formaldehyde in PBS, pH 7.4, for 48h at room temperature and then labeled with YOYO-1 (1 nM; Molecular Probes) in 0.1% Triton X-100 in PBS. Parasitemias were determined from dot plots (forward scatter vs fluorescence) acquired on a FACSort flow cytometer using CELLQUEST software (Becton Dickinson).  $\text{IC}_{50}$  values for growth inhibition were determined with GraphPad Prism software from plots of percentage parasitemia compared to controls (untreated parasites) over inhibitor concentration. In each case, the goodness of curve fit was documented by R2 values of  $\geq 0.95$ .

#### **Macrophages**<sup>138</sup>

The macrophage cell line J774.1 was maintained in complete Click RPMI medium. For the experimental procedures, cells were detached from the flasks with a rubber police, washed twice with phosphate-buffered saline, and suspended at  $2 \times 10^6$  cells per mL in complete Click RPMI medium. J774.1 macrophages were plated in complete RPMI medium (200  $\mu\text{L}$ ) without phenol red in 96-well plates in the absence or presence of various concentrations of the inhibitors and incubated for 24h at 37 °C, 5%  $\text{CO}_2$  and 95% humidity. After addition of Alamar Blue (20  $\mu\text{L}$ ), the plates were further incubated under similar conditions. The plates were read after 24 and 48h. Control experiments to examine the effect of cell density, incubation time, and DMSO concentration were performed. Absorbance in the absence of compounds was set as 100% of growth control.

#### **Cell viability assay (HeLa cells)**

HeLa cells were cultured in 96 well microplates (Greiner Bio-One, Germany) at a

concentration of 15.000 cells per well and a volume of 100  $\mu\text{L}$  DMEM. All compounds were dissolved in DMSO at a concentration of 5 mM and diluted in DMEM before adding to the HeLa cells. As blank, pure DMSO was also diluted with DMEM in the same manner as the compound solutions. Cells were incubated at 37°C in 5%  $\text{CO}_2$  for 48h. A 3 mg/mL solution of MTT (3-(4,5-dimethyl-2-thiazolyl)-2,5-diphenyl-2H-tetrazolium bromide) in medium (40  $\mu\text{L}$ ) was added directly to each well, and the plate was incubated for an additional 30 min. The medium was removed and replaced by 200  $\mu\text{L}$  DMSO and 25  $\mu\text{L}$  glycine buffer (0.1 M glycine, 0.1 M NaCl, pH 10.5) followed by 15 min shaking to dissolve the purple formazan crystals. Then 50  $\mu\text{L}$  of each well was transferred to a new clear microplate containing a mixture of 17  $\mu\text{L}$  glycine buffer and 133  $\mu\text{L}$  DMSO. Finally, the absorbance was measured at 595 nm using a Victor microplate reader. Furthermore, the background was measured at 670 nm and subtracted from the data obtained from the first read out. Cell viability was normalized to the absorbance measured from the blank samples. The resulting data was analyzed with GraFit (version 5.0.13, 2006, *Erithacus Software Ltd.*,UK) using a 4 parameter logistic equation:

$$y = \frac{y_{max}}{1 + \left(\frac{[S]}{CC_{50}}\right)^s} + B$$

$y$  = cell viability,  $CC_{50}$  = cytotoxic concentration,  $[S]$  = substrate concentration,  $y_{max}$  = uninhibited value – background,  $s$  = slope factor and  $B$  = background.



### 6.3 Docking studies, molecular dynamics and computational chemistry

AD4<sup>139-140</sup> was employed for the docking calculations. In this case, as the ligands covalently bind to the target enzyme, it was necessary to employ a particular docking protocol which was recently devised by Bianco et al.<sup>141</sup> The latter requires to modify the residue which takes part in the covalent bond and to attach it to the ligand; during the docking calculation this modified residue is treated as flexible. To this end, using the Maestro suite,<sup>142</sup> we modeled the ligands with two extra atoms where the alkylation would have taken place, specifically a sulphur and a carbon atom, in order to match the corresponding atoms in the Cys25. The crystal structure of rhodesain (PDB code 2P86) was downloaded and prepared for docking using the Protein Preparation Wizard tool in Maestro. Then, with the help of the scripts provided by the AD4 website,<sup>143</sup> it was possible to overlap the ligand with the Cys25 residue. Subsequently, the receptor grid was calculated with the AutoGrid4 software thereby mapping the interaction energies of the receptor using the ligand atom types as probes. The grid of  $60 \text{ \AA} \times 60 \text{ \AA} \times 60 \text{ \AA}$  with  $0.375 \text{ \AA}$  spacing was centered on the coordinates of the ligand originally present in the 2P86 crystal.<sup>22</sup> Finally, the actual docking was run for each compound separately, keeping the remodeled residue as flexible. This allowed sampling the torsional degrees of freedom of the ligands in order to optimize the interactions of the bound ligand with the surrounding residues. For the simulations the Lamarckian Genetic Algorithm (LGA) was employed. Given the complexity of the ligands and their high number of torsional degrees of freedom, 200 runs of LGA were executed for each compound. Each docking run consisted of 25 million energy evaluations using the Lamarckian genetic algorithm local search (GALS) method. The GALS method evaluates a population of possible docking solutions and propagates the most successful individuals from each generation into the subsequent generation of possible solutions. A low-frequency local search according to the method of Solis and Wets is applied to docking trials to ensure that the final solution represents a local minimum. All dockings described in this paper were performed with a population size of 150, and 300 rounds of Solis and Wets local search were applied with a probability of 0.06. A mutation rate of 0.02 and a crossover rate of 0.8 were used to generate new docking trials for subsequent generations, and the best individual from each generation was propagated over the next generation. All the other settings were left at their default value. The docking results from each calculation were clustered on the basis of root-mean square deviation (rmsd) (solutions differing by less than  $2.0 \text{ \AA}$ ) between the Cartesian coordinates

of the atoms and were ranked on the basis of free energy of binding ( $\Delta G_{AD4}$ ). The same protocol was attained for the covalent docking on the crystal structure of FP-2 (PDB code 2OUL).<sup>100</sup>

### **Molecular Dynamics**

MD simulations were performed using the Amber14 package,<sup>144</sup> the method adopted to parameterize the modified cysteine residue was the one outlined in the Amber website and in its Reference Manual. The covalent complex consisted of the crystal structure of rhodesain bound to the compound **16b** in its lowest energy pose predicted by the docking calculations. Initially, the system was prepared for the simulation using the Protein Preparation Tool in Maestro, specifically, the missing side chains and loops were added with Prime and the C and N termini were capped with NME and ACE respectively. From this structure the modified Cys25 bound to **16b** was extracted. The AM1-BCC charges of this residue were computed with the Antechamber software, which is part of the Amber14 suite. Using the script parmchk2, the cysteine moiety of the residue was parameterized using the standard Amber protein force field (ff14SB), while for the rest of the molecule the parameters used were the ones of the General Amber Force Field (GAFF).<sup>145</sup> Subsequently, employing xLeap, the complex was then solvated in a periodic octahedral box of 10.0 Å of TIP3P<sup>146</sup> waters and then neutralized using 19 Na<sup>+</sup> ions. Finally, the parameter (.prmtop) and coordinates (.inpcrd) files could be generated for the ensuing MD simulation. The rhodesain/**16b** complex was first submitted to a stepwise minimization in which hydrogen atoms were first relaxed, then the solvent molecules were allowed to move, and finally the whole complex was minimized. Subsequently, the system was heated to 300° K in a NVT environment, followed by two phases of equilibration in NTP, using Langevin as thermostat. The production phase in a NTP ensemble lasted 80 ns. The particle mesh Ewald method<sup>147</sup> was used to evaluate the electrostatic interactions with a direct space sum cutoff of 10 Å. With the bond lengths involving hydrogen atoms kept fixed with the SHAKE algorithm,<sup>148</sup> a time step of 2 fs was employed. The analysis of the simulation was carried out using CPPTRAJ.<sup>149</sup> All the figures were rendered with the UCSF Chimera package.<sup>150</sup>

### **Computational chemistry**

A molecular model of inhibitors was constructed and energy minimized using the Schrodinger Maestro 12 program running on a Dell Precision with Fedora Core.

Minimizations were performed using the OPLS 2005 force field, an enhanced version of Jorgensen's OPLS force field, 4 with 5000 steps of steepest descent followed by conjugate-gradient energy calculations with a convergence of  $0.0005 \text{ kJ}\text{\AA}^{-1} \text{ mol}^{-1}$ . Subsequently, the several constructed of inhibitors was subjected to QikProp software calculations (QikProp, version 3.4 (2011); Schroinger, LLC, New York, NY). In addition to predicting molecular properties, QikProp provides ranges for comparing each compound's property with those of 95% of known drugs. This software was also used because it allows for flagging reactive functional groups that may cause false positives in biological assays.

## CHAPTER 7. SUPPLEMENT

### Development of fluorine-containing substrates to evaluate the biological activity of constitutive and immunoproteasome by $^{19}\text{F}$ NMR spectroscopy

#### 7.1 Introduction

During my PhD period, I spent three months at the “Faculté de Pharmacie”, “Université de Paris Sud” (Chatenay Malabry, France), supervised by Prof. Sandrine Onger, within the collaborative "Research and Mobility programme 2015" entitled "Development of novel 20S immunoproteasome-specific inhibitors for the treatment of haematological, malignancies, autoimmune and inflammatory diseases".<sup>151</sup> In this chapter, I will briefly describe the role of the proteasome, focusing my attention on the work carried out and the achieved results.

In eukaryotic cells, the ubiquitin-proteasome system (UPS) is an essential pathway, which plays a key role in the intracellular protein turnover.<sup>152</sup> In healthy cells, proteasome is responsible a major proteolytic activity in controlling the regular cell cycle progression, homeostasis and immune surveillance.<sup>153</sup> Following a defects or a malfunction in UPS, normal cells undergoes various alterations, which can lead to uncontrolled proliferation with consequent development of tumours. Commonly, the stabilization of oncoproteins/growth promoting factors, and/or the destabilization of tumour suppressors carry out to development of neoplasms and many malignancies: a classic example is the destabilization of p53 and p27 proteins, which play a role in tumour suppressor processes. At the same time, proteasome is also responsible for the degradation of many proto-oncoproteins: the incorrect operation of this process can induce cell uncontrolled proliferation.<sup>154</sup> Proteasome inhibition results in important pro-apoptotic effect in tumour cells<sup>155</sup>: therefore, the development of proteasome inhibitors is considered a valuable approach for the treatment of multiple myeloma. The 20S proteasome presents a barrel-like structure: it is composed of four stacked rings, each one of them is constituted by seven subunits (Figure 54). The two outer  $\alpha$ -rings are responsible for regulating of a gate, who allows to proteins to achieve the catalytic sites located in the two inner  $\beta$ -rings.<sup>156</sup> Each  $\beta$ -ring contains three catalytic subunits:  $\beta$ 1,  $\beta$ 2 and  $\beta$ 5, for a total of six proteolytic sites.  $\beta$ 1 is responsible for the caspase-like (C-L),  $\beta$ 2 for the trypsin-like (T-L) and  $\beta$ 5 for chymotrypsin-like (ChT-L) activities: the latter is mainly involved in proteolytic

degradation, for this reason is considered the primary target for the development of novel anticancer agents.

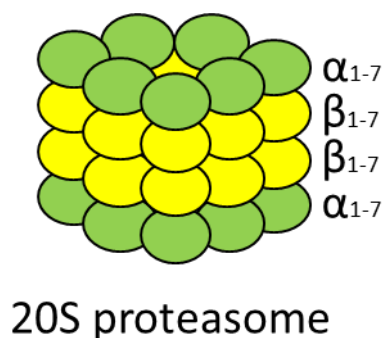
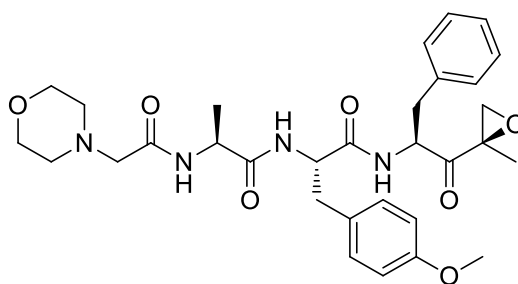


**Figure 54.** Barrel-like structure of proteasome.

It is well known from literature, that the co-inhibition of the  $\beta 5$  subunit with  $\beta 1$  or  $\beta 2$  sites, represents the ideal profile of a potential drug, as it could provide the maximal antitumor response, coupled with a reduction of cytotoxic effects.<sup>157</sup> Conversely, the inhibition of all proteasome subunits may result in cytotoxicity.<sup>158</sup> All the three subunits possess a catalytic site using the nucleophilic hydroxyl group of the *N*-terminal Thr to cleave peptide bonds.<sup>156</sup> In addition to the constitutive proteasome, vertebrate possess an immune-form of proteasome, named immunoproteasome, which is mainly expressed in monocytes and lymphocytes. The main roles played by this immuno isoform are the generation of major histocompatibility complex (MHC) ligands and the regulation of cell-mediated immunity. At present, crystal structures of murine constitutive and immunoproteasome, in the presence of peptidyl epoxyketone inhibitor PR-957 (Figure 55), also known as ONX-0914, are reported by Groll and co-workers, to explore their different subunit compositions.<sup>159</sup>



**PR-957**

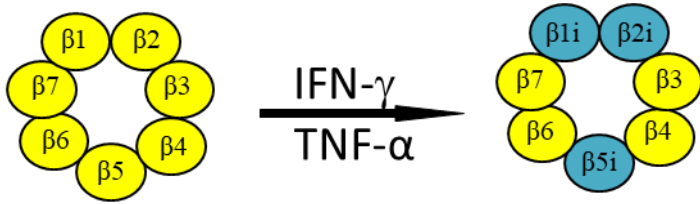
**Figure 55.** Chemical structure of potent proteasome inhibitor PR-957.

There is a high degree of homology between the catalytic subunits of the two isoform, with an identity range from 60% to 70%. The 20S core of immunoproteasome bears, in the two

inner  $\beta$ -rings, low-molecular weight proteins (LMPs): LMP2 and LMP7, expressed in response to interferon-gamma (IFN- $\gamma$ ) and tumour necrosis factor (TNF- $\alpha$ ),<sup>160</sup> in replacement of  $\beta$ 1c and  $\beta$ 5c, respectively, and multicatalytic endopeptidase complex (MECL-1), also induced by INF- $\gamma$ , in replacement of  $\beta$ 2c.<sup>161</sup> MECL-1 and LMP7, namely  $\beta$ 2i and  $\beta$ 5i, respectively, carry out the same activities of the  $\beta$ 2c and  $\beta$ 5c subunits, while the replacement of  $\beta$ 1c with  $\beta$ 1i reduces the caspase-like activity to background levels,<sup>162</sup> with a ChT-L activity,<sup>159</sup> thus cleaving peptides after hydrophobic amino acids (Table 29). It was suggested that this structural modification promotes the generation of peptides for antigen presentation. Furthermore, it was demonstrated that INF- $\gamma$  increases the proteasomes capacity to cleave small peptides after hydrophobic and basic residues, but reduces the cleavage capability after acidic amino acids.<sup>163</sup>

The proteasome forms show slight differences at the enzymatic pocket around at *N*-terminal nucleophilic threonine residue. With regard to S1 pockets of  $\beta$ 5c

**Table 29. Proteasome and immunoproteasome subunits with relative activities**



Common name	Alternative name	Activity
$\beta$ 1c	Y, delta, LMP19, <i>Pre3</i>	Caspase-like activity
$\beta$ 1i	LMP2, RING12, MC7	Chymotrypsin-like activity
$\beta$ 2c	Z, MC14, LMP9, <i>Pup1</i>	Trypsin-like activity
$\beta$ 2i	MECL-1, LMP10	Trypsin-like activity
$\beta$ 5c	X, epsilon, LMP17, MB1, <i>Pre2</i>	Chymotrypsin-like activity
$\beta$ 5i	LMP7, RING10, Y2, C13	Chymotrypsin-like activity

and  $\beta$ 5i subunits, the residues responsible for the ChT-L activity (Ala20, Met45, and Cys52) are unchanged; only amino acid Val31 of  $\beta$ 5c changes Met31 in  $\beta$ 5i, maintaining the hydrophobic character. However, a different conformation of Met45 gives rise to the formation of a larger S1 pocket, which is stabilized by van der Waals interactions with the aliphatic side chain of the residue Gln53. Therefore, the S1 pocket of  $\beta$ 5c mainly accommodates peptides with small amino acids (Ala or Val) at the P1 position, while S1 pocket of  $\beta$ 5i well fits large non-polar residues, as Tyr, Trp and Phe. In light of this,  $\beta$ 5c

and  $\beta 5i$  cleaves specific fluorogenic substrates Ac-Trp-Leu-Ala-AMC and Ac-Ala-Asn-Trp-AMC, respectively. Furthermore, another substrate which can be used for both subunits is Suc-Leu-Leu-Val-Tyr-AMC (Figure 56). Several differences were also observed between  $\beta 1c$  and  $\beta 1i$ : the substitutions T20V, T31F, R45L and T52A mainly increase the hydrophobicity of  $\beta 1i$  S1 pocket, with reduction of its dimension. As a consequence, peptide hydrolysis in immuno isoform occurs after small hydrophobic residues.

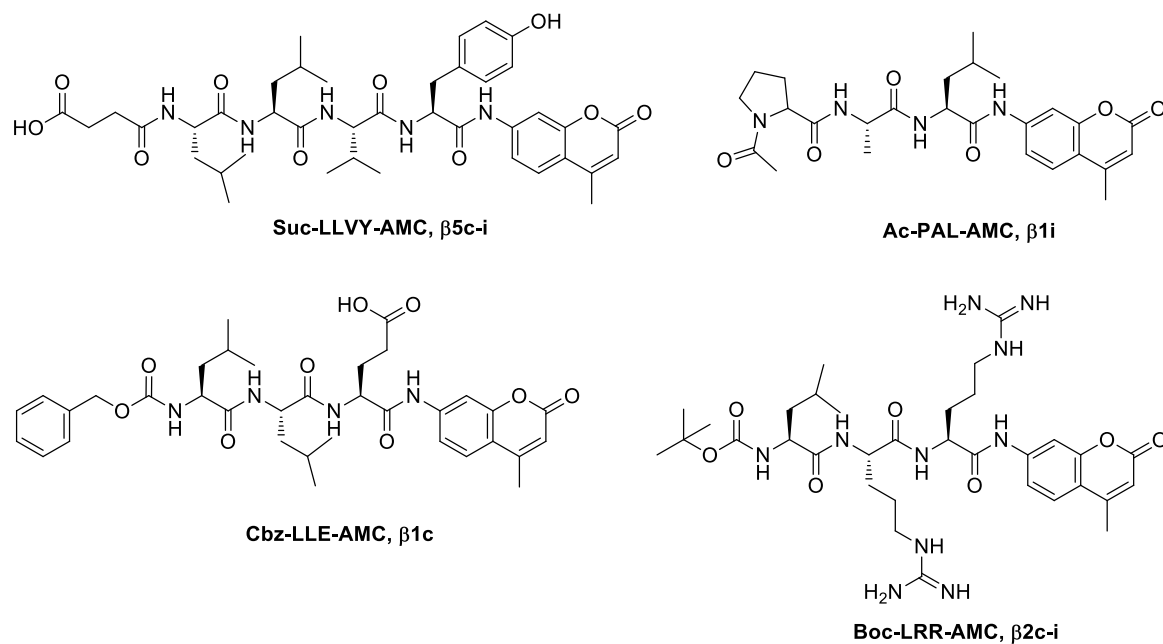


**Figure 56.** Chemical structure of substrates for constitutive and immune proteasome subunits.

On the contrary, at S3 pocket of  $\beta 1i$  subunit, the substitutions of residues T22A and A27V generally downsize and polarize the S3 pocket. Therefore,  $\beta 1c$  and  $\beta 1i$  cleaves different fluorogenic substrates, which are Z-Leu-Leu-Glu-AMC and Ac-Pro-Ala-Leu-AMC, respectively. Lastly subunit  $\beta 2i$  is was found to be identical to  $\beta 2c$  with the sole replacement of Asp53 ( $\beta 2c$ ) with Glu ( $\beta 2i$ ): their substrate fluorogenic is Boc-Leu-Arg-Arg-AMC.

The evaluation of proteasome inhibitors by fluorescence assays presents a limit, because of the unfeasibility to simultaneously monitoring the three proteolytic activities.<sup>164</sup> In 96 well-plates, the fluorescence assays are performed using only one substrate, while the complete proteolytic mechanism of proteasome is based on three different catalytic activities. Furthermore, some studies are known in literature<sup>164-165</sup> which suggest that an active site can allosterically activate or inhibit the others.

More in detail, the ChT-L activity can be regulated by T-L or C-L substrates: binding of one or both substrates at their corresponding catalytic sites might induce alterations to the structure and activity of proteasome. The role played by allosteric modulation is an essential aspect in enzyme inhibitory activity, which cannot be overlooked but accurately examined. To date, fluorescence probes with an univocal wavelength were barely described, but represent a challenge extremely hard to achieve.<sup>166</sup> For these motives, in 2014, the research group led to Prof. Ongeri developed a novel fluorine-containing substrate,<sup>167</sup> with the idea to evaluate ChT-L proteasome inhibitors by <sup>19</sup>F NMR in the presence of T-L and/or C-L substrates. <sup>19</sup>F NMR spectroscopy is characterised by high sensitivity and lack of background signal; furthermore, the FABS (Fluorine Atoms for Biochemical Screening) method uses <sup>19</sup>F NMR to detect fluorine-containing substrates, before and after enzymatic activity.<sup>168</sup> The requirements to develop novel substrates are widely described in literature: the presence of CF<sub>3</sub> group, in order to enhance the NMR signal intensity with respect to F atom;<sup>168-169</sup> the CF<sub>3</sub> group have to be introduced on the fluorescent core, in order to offer a multimodal probe; the hydrolysis of the substrate by enzyme must necessarily release the fluorine-containing core with a <sup>19</sup>F chemical shift different from that of the substrate; lastly, a quantitative monitoring of the hydrolysis is essential to determine inhibitory activity. Ongeri's group developed an analogous of Suc-LLVY-AMC (Figure 57), on which the fluorophore AMC moiety was replaced with 7-amino-4-trifluoromethylcoumarin portion (AFC).

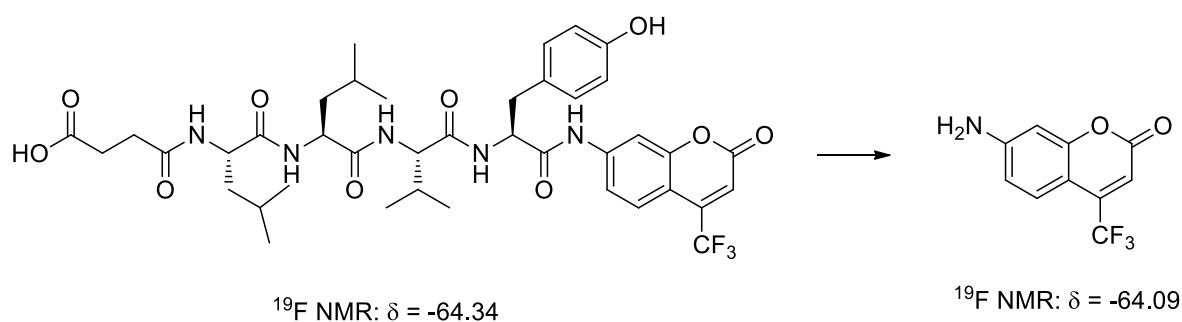


**Figure 57.** Chemical structure of fluorine-containing substrate for ChT-like activity, before and after hydrolysis with relative chemical shifts for <sup>19</sup>F NMR.

The enzymatic activity of the rabbit 20S proteasome on Suc-LLVY-AFC was evaluated, showing a chemical shift of -64.34 ppm, while amine AFC after proteolysis displayed chemical shift of -64.09 ppm.



## 7.2 Aim of the research and results and discussions

To evaluate by  $^{19}\text{F}$  NMR spectroscopy the allosteric modulation of all catalytic sites of constitutive and immunoproteasome, with and without a specific inhibitor, we decided to develop fluorine-containing substrates for  $\beta 1\text{c}$ ,  $\beta 1\text{i}$  and  $\beta 2\text{c-i}$  subunits. Our idea consists in the introduction, in the same NMR tubes, of the three different fluorinated substrates of constitutive or immuno proteasome: in so doing, we will obtain the proteasome proteolytic activities for each individual subunit in presence of three substrates. Furthermore, it is necessary a different chemical shift not only between the substrates, but also between the free amines resulting by proteolysis. Considered the amine used for the synthesis of Suc-LLVY-AFC, useful for both  $\beta 5$  subunits, we decided to introduce 4-trifluoromethyl-aniline (4FA) for  $\beta 1\text{c}$  and  $\beta 1\text{i}$ , and 3-trifluoromethyl-aniline (3FA) for both  $\beta 2$  subunits (Figure 58).

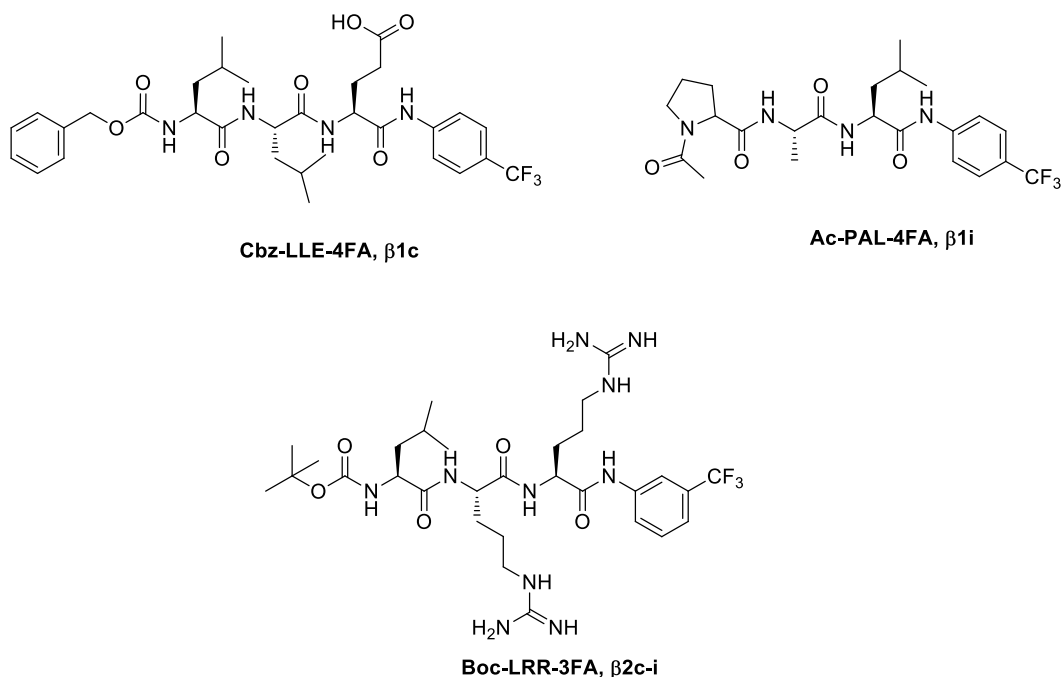
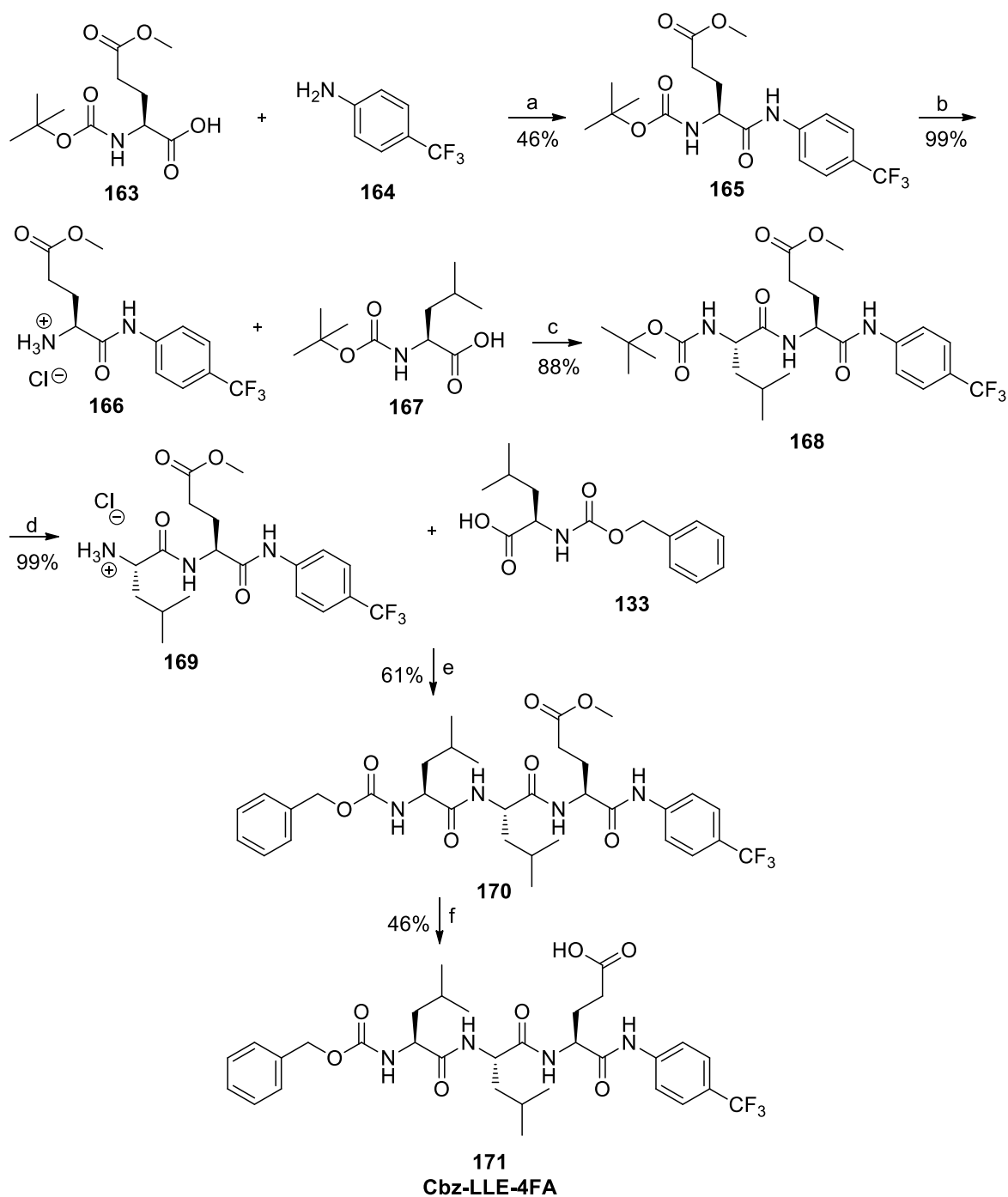


**Figure 58.** Novel fluorine-containing substrates.

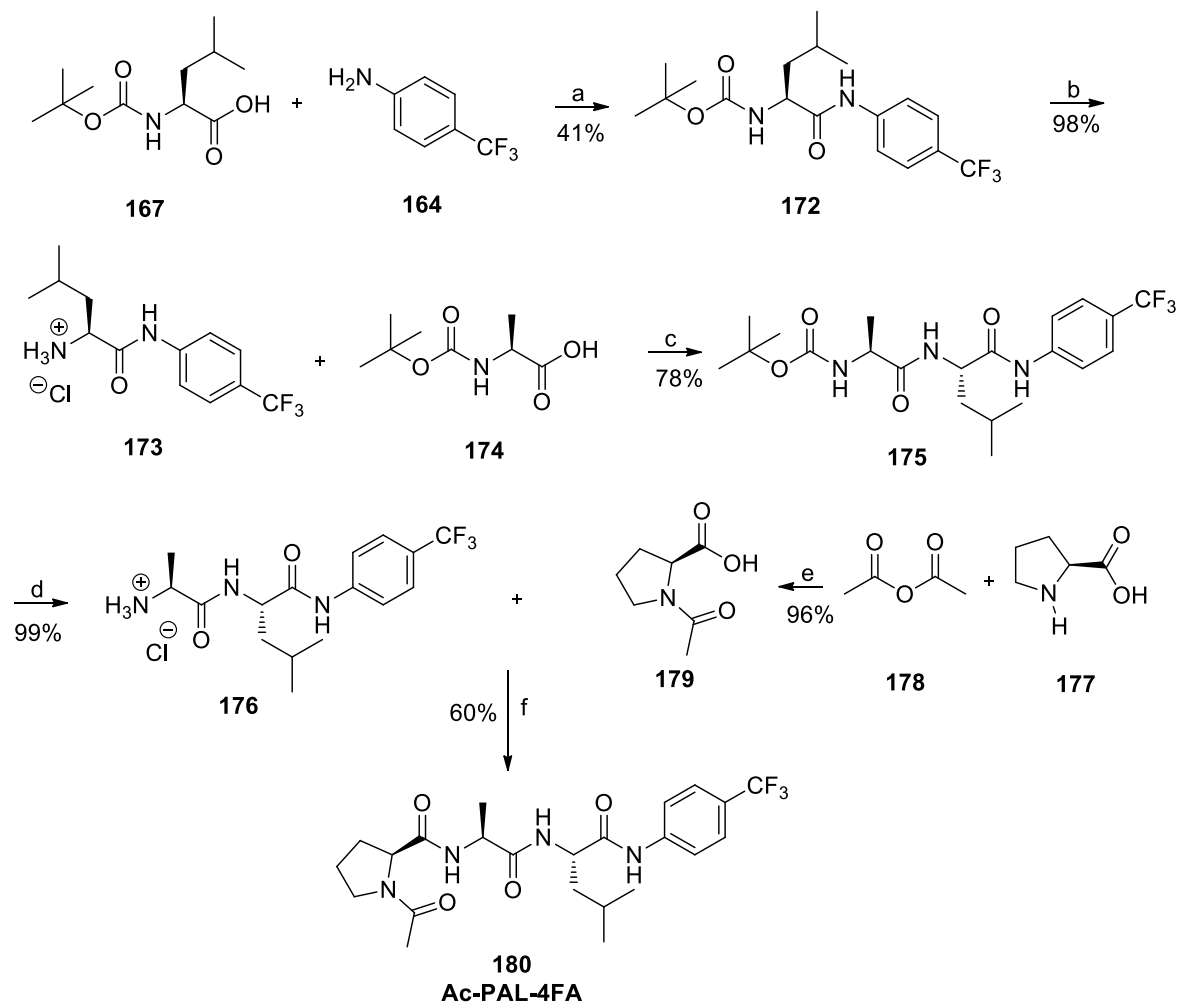
Synthesis of  $\beta 1\text{c}$  substrate (Scheme 16) was carried out starting from Boc-Glu-OH **163**, which by coupling reaction with amine **164**, gave intermediate **165**. The latter was treated with dry 4M HCl in methanol solution under nitrogen atmosphere, to obtain compound **166**. Coupling reaction with the commercially available acid Boc-Leu-OH **167**, provided compound **168**, which was deprotected to give **169**. Then, coupling reaction with Cbz-Leu-OH **133** provided intermediate **170**, which by hydrolysis in alkaline condition allowed to obtain substrate Cbz-LLE-4FA **171**.



**Scheme 16.** Reagents and conditions: a) POCl<sub>3</sub>, dry pyridine, 0°C, 15 min, then rt, 4h; b) 4 M HCl/dioxane, methanol, 0°C, N<sub>2</sub>, 10 min, then rt, 4h; c) DIPEA, EDCI, HOBT, dry DMF/CH<sub>2</sub>Cl<sub>2</sub>, N<sub>2</sub>, rt, 12 h; d) 4 M HCl/dioxane, methanol, 0°C, N<sub>2</sub>, 10 min, then rt, 4h; e) DIPEA, EDCI, HOBT, dry DMF/CH<sub>2</sub>Cl<sub>2</sub>, N<sub>2</sub>, rt, 12h; f) LiOH, MeOH/H<sub>2</sub>O/dioxane (1:1:1), 0° C, 10 min, then 12h.

To synthesise β1i substrate (Scheme 17), we started from Boc-Leu-OH **167**, which by reaction with amine **164**, gave intermediate **172**. Subsequently, Boc-deprotection provided amine hydrochlorid **173**, which by reaction with Boc-Ala-OH **174**, allowed to obtained the

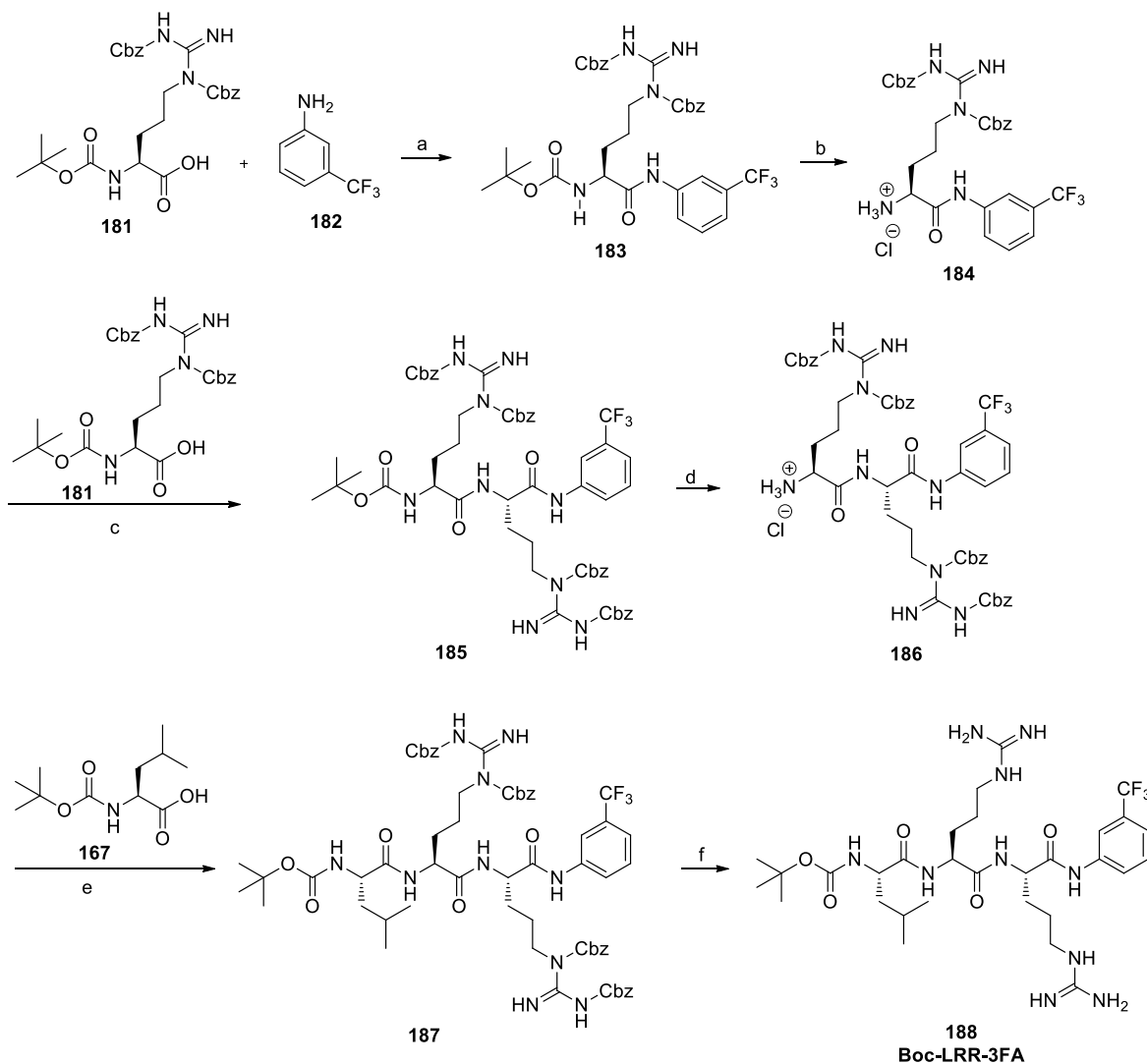
coupling product **175**. Another Boc-deprotection was performed to obtain amine hydrochlorid **176**, and coupling reaction with Ac-Pro-OH **179**, synthesized by sonication method, gave  $\beta$ li substrate **180**.



**Scheme 17.** Result and conditions: a) POCl<sub>3</sub>, dry pyridine, -15°C for 10 min, then rt for 4 h; b) 4 M HCl/dioxane, methanol, 0°C for 10 min, then rt for 4h; c) DIPEA, EDCI, HOBT, dry DMF/CH<sub>2</sub>Cl<sub>2</sub>, N<sub>2</sub>, rt, 12 h; d) 4 M HCl/dioxane, methanol, 0°C for 10 min, then rt, 4h; e) Sonication, rt, 1h; f) DIPEA, EDCI, HOBT, dry DMF/CH<sub>2</sub>Cl<sub>2</sub>, N<sub>2</sub>, rt, 12 h.

Lastly, the  $\beta$ 2c-i substrate was synthesized starting from arginine (Scheme 18) with two amino groups protected by Cbz (**181**). Initially, coupling reaction with 3-trifluoromethyl aniline **182** gave intermediate **183**, which was treated with 4 M HCl in methanol to remove Boc group (**184**). Then, coupling reaction with Cbz-protected arginine **181** provided intermediate **185**, and a new Boc-deprotection gave amine hydrochlorid **186**. The latter, by

coupling with Boc-Leu-OH **167**, allowed to obtain compound **187**. The subsequent catalytic hydrogenation using H<sub>2</sub> on Pd, to obtain substrate **188**, was not performed yet.

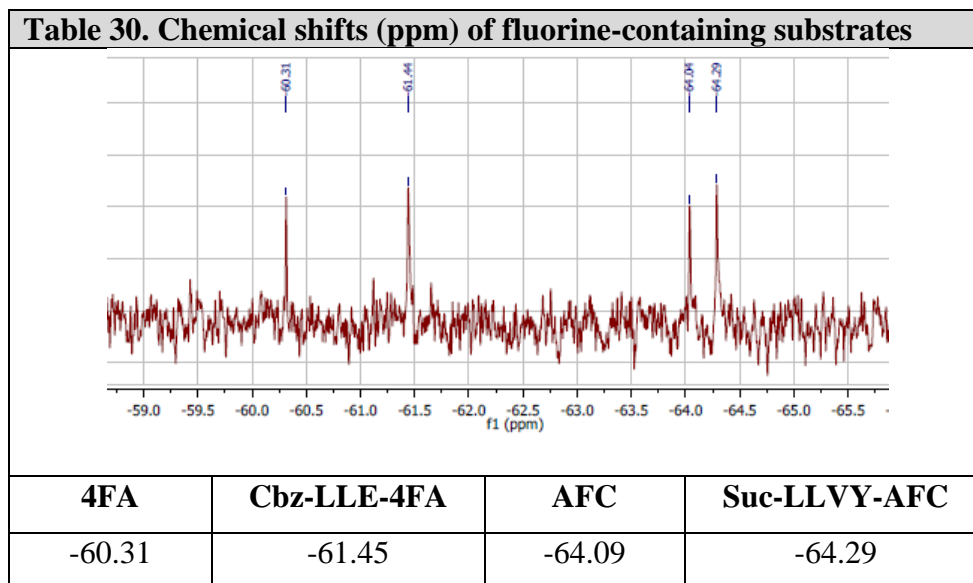


**Scheme 18.** Reagents and conditions: a) POCl<sub>3</sub>, dry pyridine, -15°C for 10 min, then rt for 4 h; b) 4 M HCl/dioxane, methanol, 0°C for 10 min, then rt for 4h; c) DIPEA, EDCI, HOBT, dry DMF/CH<sub>2</sub>Cl<sub>2</sub>, N<sub>2</sub>, rt, 12 h; d) 4 M HCl/dioxane, methanol, 0°C for 10 min, then rt for 4h; e) DIPEA, EDCI, HOBT, dry DMF/CH<sub>2</sub>Cl<sub>2</sub>, N<sub>2</sub>, rt, 12 h; f) H<sub>2</sub>, Pd/C 10%, MeOH, 2h.

Boc-LRR-3FA has not been synthesized yet (only lacking the last hydrogenation step) while synthesis of Cbz-LLE-4FA and Ac-PAL-4FA was completed.

Initially, we controlled the different chemical shift value of Cbz-LLE-4FA with respect the free amine 4FA. In a NMR tube, we inserted the buffer (392 μL), DMSO 8.8 μL, substrate (1,6 μL, 10 mM) or 4FA (1,6 μL, 10 mM): was recorded chemical shift values of -61.45 and -60.32 ppm, respectively. Then, we carried out the monitoring in presence of Cbz-

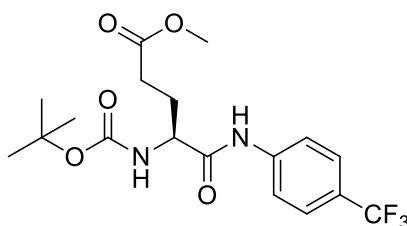
LLE-4FA and Suc-LLVY-AFC, simultaneously: the chemical shifts values recorded were perfectly distinct, as shown in table 30.



$^{19}\text{F}$  NMR spectroscopy of AcPAL-4FA was not performed yet. Further NMR analysis will be performed by Ongeri's group members when synthesis of Boc-LRR-3FA will be completed. Furthermore, the  $^{19}\text{F}$  NMR monitoring with all fluorine-containing substrates, in presence of the constitutive and immunoproteasome, will allow to evaluate their allosteric effects.

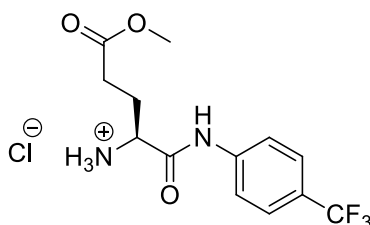
### 7.3 Experimental section

#### (S)-Methyl 4-(*tert*-butoxycarbonylamino)-5-oxo-5-((4-(trifluoromethyl)phenyl)amino)pentanoate (**165**)



To a solution of 4-(trifluoromethyl)aniline **164** (1 equiv.) and Boc-Glu-OH **163** (1. equiv.) in dry pyridine, phosphoryl chloride (1 equiv.) was added dropwise in a period of 10 min, at 0°C. The reaction mixture was stirred at rt for 2h, and after this time the solution was poured into water and the organic phase was extracted with EtOAc, washed with a saturated aqueous solution of NaHCO<sub>3</sub>, a 10% aqueous solution of citric acid, brine and dried over Na<sub>2</sub>SO<sub>4</sub>. After filtration and evaporation under reduced pressure, the crude residue was purified by silica gel column chromatography, using CH<sub>2</sub>Cl<sub>2</sub>/Et<sub>2</sub>O (4:1) as eluent mixture, to obtain compound **165**. Yield: 46%; Consistency: white powder; *R*<sub>f</sub> = 0.43 (CH<sub>2</sub>Cl<sub>2</sub>/Et<sub>2</sub>O, 4:1); <sup>1</sup>H NMR (300 MHz, CDCl<sub>3</sub>): δ = 1.47 (s, 9H), 1.95-2.10 (m, 1H), 2.17-2.32 (m, 1H), 2.44-2.56 (m, 1H), 2.58-2.71 (m, 1H), 3.73 (s, 3H), 4.27-4.41 (m, 1H), 5.46 (d, *J* = 7.2 Hz, 1H), 7.55 (d, *J* = 8.5 Hz, 2H), 7.66 (d, *J* = 8.5 Hz, 2H), 8.87-9.06 (bs, 1H); <sup>13</sup>C (300 MHz, CDCl<sub>3</sub>): δ = 27.46, 28.28, 30.45, 52.03, 54.52, 80.84, 117.72 (q, *J* = 32.0 Hz), 119.34, 124.04 (q, *J* = 271.8 Hz), 126.16, 126.21, 140.79, 156.30, 170.23, 174.10; <sup>19</sup>F NMR (200 MHz, CDCl<sub>3</sub>): δ = -60.34; M. p. = 94-96°C; ESI<sup>+</sup> ms *M/Z* = Calc 427.1457 for [C<sub>18</sub>H<sub>23</sub>F<sub>3</sub>N<sub>2</sub>O<sub>5</sub> + Na]; found 427.1463 [M+Na]<sup>+</sup>.

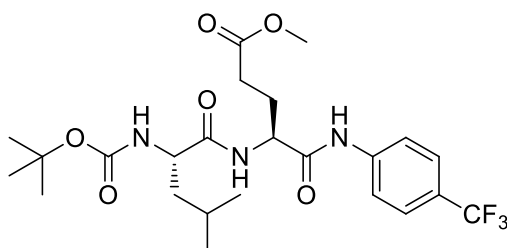
#### (S)-5-Methoxy-1,5-dioxo-1-(4-trifluoromethylphenylamino)pentan-2-aminium chloride (**166**)



A solution of compound **165** (1.0 equiv.) in of 4M HCl/dioxane (22 equiv.) was stirred for 4h at rt. Subsequently, the reaction mixture was concentrated in *vacuo* to afford the hydrochloride salt of the free amine **166**, which was used without further purification. Yield: 99%; Consistency: brown powder; *R*<sub>f</sub> = 0.08 (CH<sub>2</sub>Cl<sub>2</sub>/Et<sub>2</sub>O, 9:1); <sup>1</sup>H NMR (300

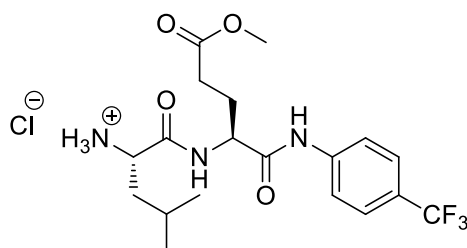
MHz, MeOD):  $\delta$  = 2.23-2.37 (m, 2H), 2.61 (t,  $J$  = 7.4 Hz, 2H), 3.66 (s, 3H), 4.17 (t,  $J$  = 6.3 Hz, 1H), 7.66 (d,  $J$  = 8.6 Hz, 2H), 7.85 (d,  $J$  = 8.5 Hz, 2H);  $^{13}\text{C}$  (300 MHz, MeOD):  $\delta$  = 30.11, 32.60, 55.02, 57.06, 117.30 (q,  $J$  = 32.0 Hz), 123.55, 124.53 (q,  $J$  = 270.1 Hz), 129.69, 129.74, 145.00, 170.94, 176.57;  $^{19}\text{F}$  NMR (200 MHz, MeOD):  $\delta$  = -60.70; M. p. = 176-178°C; ESI<sup>+</sup> ms M/Z = calc. 305.1113 for [C<sub>13</sub>H<sub>16</sub>F<sub>3</sub>N<sub>2</sub>O<sub>3</sub> + H] ; found 305.1116 [M+H]<sup>+</sup>.

**(S)-Methyl 4-((S)-2-(tert-butoxycarbonylamino)-4-methylpentanamido)-5-oxo-5-(4-trifluoromethylphenylamino)pentanoate (168)**



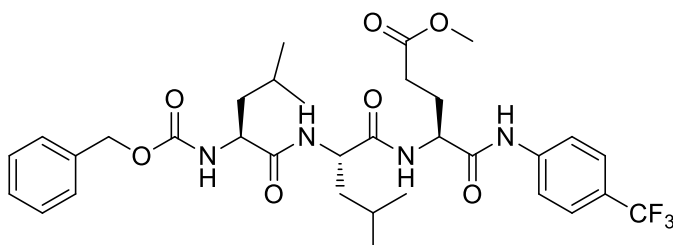
To a solution of Boc-Leu-OH **167** (1.2 equiv.) in dry DMF, at 0°C and under nitrogen atmosphere, HOBt (1.2 equiv.) and EDCI (1.2 equiv.) were added. After 10 min, DIPEA (4 equiv.) and **166** (1 equiv.) were added, and the reaction mixture was stirred for 12h. Subsequently, solvents were evaporated and the resulting residue was dissolved in EtOAc. The organic phase was washed with a 10% aqueous solution of citric acid (x 2), water, a 10% aqueous solution of K<sub>2</sub>CO<sub>3</sub> (x 2) and brine, dried over Na<sub>2</sub>SO<sub>4</sub>, filtered and concentrated *in vacuo*. The crude residue was purified by column chromatography using CH<sub>2</sub>Cl<sub>2</sub>/Et<sub>2</sub>O (9:1) as eluent mixture, to give compound **168**. Yield = 88%; Consistency: white powder;  $R_f$  = 0.29 (CH<sub>2</sub>Cl<sub>2</sub>/Et<sub>2</sub>O, 9:1)  $^1\text{H}$  NMR (300 MHz, CDCl<sub>3</sub>):  $\delta$  = 0.93-1.03 (m, 6H), 1.45 (s, 9H), 1.62-1.80 (m, 3H), 2.12-2.34 (m, 2H), 2.44-2.68 (m, 2H), 3.72 (s, 3H), 4.05-4.16 (m, 1H), 4.57-4.66 (m, 1H), 5.03 (d,  $J$  = 5.0 Hz, 1H), 7.55 (d,  $J$  = 8.5 Hz, 3H), 7.81 (d,  $J$  = 7.2 Hz, 2H), 9.14 (bs, 1H);  $^{13}\text{C}$  (300 MHz, CDCl<sub>3</sub>):  $\delta$  = 21.34, 22.68, 24.82, 26.35, 27.97, 30.27, 40.63, 51.87, 53.83, 54.29, 80.69, 117.92 (q,  $J$  = 32.0 Hz), 119.57, 124.27 (q,  $J$  = 272.0 Hz), 125.85, 125.90, 141.41, 156.36, 169.87, 173.38, 174.32;  $^{19}\text{F}$  NMR (200 MHz, CDCl<sub>3</sub>):  $\delta$  = -60.56; M. p. = 124-126°C; ESI<sup>+</sup> ms M/Z = calc for C<sub>24</sub>H<sub>34</sub>F<sub>3</sub>N<sub>3</sub>O<sub>6</sub>Na: 540.2297; found 540.2302 [M+Na]<sup>+</sup>.

**(S)-1-(((S)-5-Methoxy-1,5-dioxo-1-((4-(trifluoromethyl)phenyl)amino)pentan-2-yl)amino)-4-methyl-1-oxopentan-2-aminium chloride (169)**



A solution of compound **168** (1.0 equiv.) in of 4M HCl/dioxane (22 equiv.) was stirred for 4h at rt. Subsequently, the reaction mixture was concentrated in *vacuo* to afford the hydrochloride salt of the free amine **169**, which was used without further purification. Yield: 99%; Consistency: orange powder;  $R_f = 0.04$  ( $\text{CH}_2\text{Cl}_2/\text{Et}_2\text{O}$ , 9:1);  $^1\text{H}$  NMR (300 MHz, MeOD):  $\delta = 0.97\text{-}1.07$  (m, 6H), 1.66-1.83 (m, 3H), 2.02-2.14 (m, 1H), 2.17-2.29 (m, 1H), 2.46-2.61 (m, 2H), 3.67 (s, 3H), 3.94-4.03 (m, 1H), 4.55-4.64 (m, 1H), 7.62 (d,  $J = 8.4$  Hz, 2H), 7.79 (d,  $J = 8.4$  Hz, 2H);  $^{13}\text{C}$  (300 MHz, MeOD):  $\delta = 20.37, 21.71, 23.94, 26.90, 29.67, 40.26, 50.93, 51.53, 53.52, 118.66$  (q,  $J = 32.4$  Hz), 119.45, 124.26 (q,  $J = 271.8$  Hz), 125.62, 125.67, 141.65, 169.43, 170.22, 173.32;  $^{19}\text{F}$  NMR (200 MHz, MeOD):  $\delta = -61.74$ ; M. p. = 133-135°C; ESI<sup>+</sup> ms M/Z = calc for  $\text{C}_{19}\text{H}_{27}\text{F}_3\text{N}_3\text{O}_4$ : 418.1954; found 418.1953 [M+H]<sup>+</sup>.

(5*S*,8*S*,11*S*)-Methyl **5,8-diisobutyl-3,6,9-trioxo-1-phenyl-11-((4-(trifluoromethyl)phenyl)carbamoyl)-2-oxa-4,7,10-triazatetradecan-14-oate (170)**

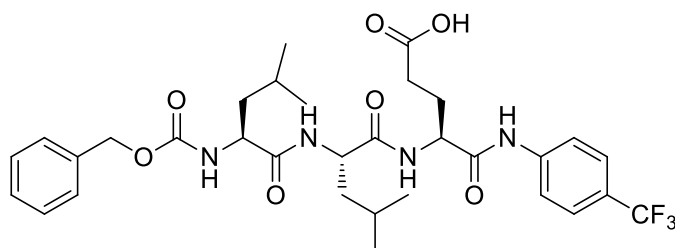


To a solution of Cbz-Leu-OH **133** (1.2 equiv.) in dry DMF, at 0°C and under nitrogen atmosphere, HOBT (1.2 equiv.) and EDCI (1.2 equiv.) were added. After 10 min, DIPEA (4 equiv.) and **169** (1 equiv.) were added, and the reaction mixture was stirred for 12h. Subsequently, solvents were evaporated and the resulting residue was dissolved in EtOAc. The organic phase was washed with a 10% aqueous solution of citric acid (x 2), water, a 10% aqueous solution of  $\text{K}_2\text{CO}_3$  (x 2) and brine, dried over  $\text{Na}_2\text{SO}_4$ , filtered and concentrated in *vacuo*. The crude residue was purified by column chromatography using cyclohexane/EtOAc (3:2) as eluent mixture, to give compound **170**. Yield: 61%; Consistency: white powder;  $R_f = 0.35$  (cyclohexane/EtOAc, 3:2);  $^1\text{H}$  NMR (300 MHz, MeOD):  $\delta = 0.93\text{-}1.05$  (m, 12H), 1.51-1.79 (m, 6H), 2.00-2.13 (m, 1H), 2.15-2.31 (m, 1H), 2.39-2.54 (m, 2H), 3.66 (s, 3H), 4.14-4.22, (m, 1H), 4.37-4.52 (m, 2H), 5.11 (s, 2H), 7.26-



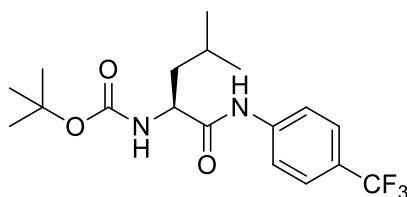
7.45 (m, 5H), 7.62 (d,  $J = 8.4$  Hz, 2H), 7.84 (d,  $J = 8.4$  Hz, 2H);  $^{13}\text{C}$  (300 MHz, MeOD):  $\delta = 23.43, 23.91, 24.93, 25.14, 27.22, 27.30, 29.19, 32.86, 42.29, 43.21, 53.55, 55.88, 56.16, 57.70, 69.10, 118.10$  (q,  $J = 32.0$  Hz), 122.11, 125.10 (q,  $J = 271.8$  Hz), 128.46, 128.50, 138.38, 130.58, 131.03, 136.04, 145.19, 159.96, 173.04, 174.81, 175.40, 177.07;  $^{19}\text{F}$  NMR (200 MHz, MeOD) =  $\delta$ : -60.22; M. p. = 219-221°C; ESI<sup>+</sup> ms M/Z = calc for  $\text{C}_{33}\text{H}_{43}\text{F}_3\text{N}_4\text{O}_7\text{Na}$ : 687.2982; found 687.2974 [M+Na]<sup>+</sup>.

**(5*S*,8*S*,11*S*)-5,8-Diisobutyl-3,6,9-trioxo-1-phenyl-11-(4-trifluoromethylphenylcarbamoyl)-2-oxa-4,7,10-triazatetradecan-14-oic acid (171)**



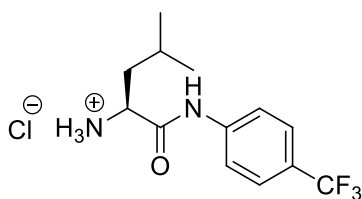
To a solution of **170** (1 equiv.) in MeOH/H<sub>2</sub>O/dioxane (1:1:1) at 0° C, LiOH powder ( 3 equiv.) was added. The reaction mixture was stirred at rt for 12h. After this time the solvents was evaporated and the residue was diluted with H<sub>2</sub>O and treated with diluted HCl until pH 2-3, with precipitate formation. Organic phase was extracted with EtOAc (x 3), dried over Na<sub>2</sub>SO<sub>4</sub> and concentrated. The crude residue was purified by column chromatography using CH<sub>2</sub>Cl<sub>2</sub>/MeOH (97:3 + 1% acetic acid) as eluent mixture, to obtain the pure carboxylic acid **171**. Yield: 46%; Consistency: white powder;  $R_f = 0.46$  (CH<sub>2</sub>Cl<sub>2</sub>/MeOH, 97:3 + 1% acetic acid);  $^1\text{H}$  NMR (300 MHz, MeOD) =  $\delta$ : 0.81-1.07 (m, 12H), 1.51-1.79 (m, 6H), 1.99-2.14 (m, 1H), 2.16-2.30 (m, 1H), 2.46 (t,  $J = 7.4$  Hz, 2H), 4.19-4.26 (m, 1H), 4.37-4.57 (m, 2H), 5.11 (s, 2H), 7.25-7.40 (m, 5H), 7.60 (d,  $J = 8.4$  Hz, 2H), 7.83 (d,  $J = 8.4$  Hz, 2H);  $^{13}\text{C}$  (300 MHz, MeOD):  $\delta = 21.93, 22.01, 23.36, 23.40, 25.88, 28.18, 31.24, 41.34, 41.87, 53.61, 54.91, 55.24, 67.82, 117.64$  (q,  $J = 32.1$  Hz), 120.98, 124.84 (q,  $J = 272.0$  Hz), 126.96, 127.00, 128.80, 129.01, 129.46, 136.11, 143.07, 158.74, 172.08, 174.90, 175.90, 176.39;  $^{19}\text{F}$  NMR (200 MHz, MeOD) =  $\delta$ : -63.99; M. p. = 224-226°C, ESI<sup>+</sup> ms M/Z = calc 673.2825 for [C<sub>32</sub>H<sub>41</sub>F<sub>3</sub>N<sub>4</sub>O<sub>7</sub> + Na]; found 673.2823 [M+Na]<sup>+</sup>.

***tert*-Butyl (S)-(4-methyl-1-oxo-1-(4-trifluoromethylphenylamino)pentan-2-yl)carbamate (172)**



To a solution of 4-(trifluoromethyl)aniline **164** (1 equiv.) and Boc-Leu-OH **167** (1. equiv.) in dry pyridine, phosphoryl chloride (1 equiv.) was added dropwise in a period of 10 min, at 0°C. The reaction mixture was stirred at rt for 2h, and after this time the solution was poured into water and the organic phase was extracted with EtOAc, washed with a saturated aqueous solution of NaHCO<sub>3</sub>, a 10% aqueous solution of citric acid, brine, and dried over Na<sub>2</sub>SO<sub>4</sub>. After filtration and evaporation under reduced pressure, the crude residue was purified by silica gel column chromatography using CH<sub>2</sub>Cl<sub>2</sub>/Et<sub>2</sub>O (4:1) as eluent mixture, to obtain compound **172**. Yield = 41%; Consistency: white powder; *R<sub>f</sub>* = 0.49 (CH<sub>2</sub>Cl<sub>2</sub>/Et<sub>2</sub>O, 4:1); <sup>1</sup>H NMR (300 MHz, CDCl<sub>3</sub>) = δ: 0.95 (d, *J* = 6.3 Hz, 3H), 0.98 (d, *J* = 6.3 Hz, 3H), 1.46 (s, 9H), 1.64-1.80 (m, 3H), 4.31-4.44 (m, 1H), 5.22 (d, *J* = 8.0 Hz, 1H), 7.41 (d, *J* = 8.0 Hz, 2H), 7.54 (d, *J* = 8.0 Hz, 2H), 9.21 (bs, 1H); <sup>13</sup>C (300 MHz, CDCl<sub>3</sub>): δ = 21.60, 23.03, 24.78, 28.34, 40.59, 54.02, 80.89, 118.27 (q, *J* = 32.2 Hz), 119.12, 124.08 (q, *J* = 272.0 Hz), 125.89, 125.93, 141.02, 156.69, 171.68; <sup>19</sup>F NMR (200 MHz, CDCl<sub>3</sub>) = δ: -62.99; M. p. = 68-70°C; ESI<sup>+</sup> ms *M/Z* = calc 397.1715 for [C<sub>18</sub>H<sub>25</sub>F<sub>3</sub>N<sub>2</sub>O<sub>3</sub> + Na]; found 397.1716 [M+Na]<sup>+</sup>.

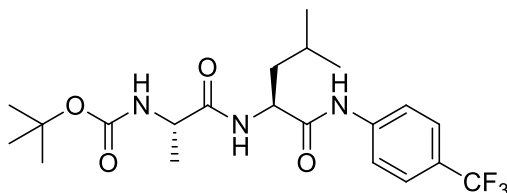
**(S)-4-Methyl-1-oxo-1-(4-trifluoromethylphenylamino)pentan-2-aminium chloride (173)**



A solution of compound **172** (1.0 equiv.) in of 4M HCl/dioxane (22 equiv.) was stirred for 4h at rt. Subsequently, the reaction mixture was concentrated in *vacuo*, to obtain the hydrochloride salt of the free amine **173**, which was used without further purification. Yield: 98%; Consistency: orange powder; *R<sub>f</sub>*: 0.07 (CH<sub>2</sub>Cl<sub>2</sub>/Et<sub>2</sub>O, 4:1); <sup>1</sup>H NMR (300 MHz, MeOD) = δ: 1.02 (d, *J* = 5.9 Hz, 3H), 1.05 (d, *J* = 5.9 Hz, 3H), 1.74-1.89 (m, 3H), 4.11 (t, *J* = 6.8 Hz, 1H), 7.66 (d, *J* = 8.5 Hz, 2H), 7.86 (d, *J* = 8.5 Hz, 2H); <sup>13</sup>C (300 MHz, MeOD): δ = 22.03, 23.28, 25.52, 41.64, 53.84, 118.57 (q, *J* = 32.1 Hz), 121.03, 123.94 (q, *J* = 271.8 Hz), 127.16, 127.21, 142.63, 169.53; <sup>19</sup>F NMR (200 MHz, MeOD) = δ: -64.10;

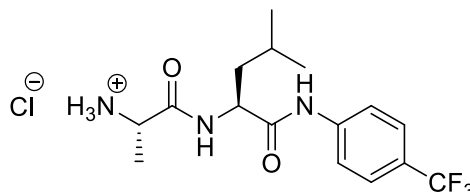
M. p. = 227-229°C; ESI<sup>+</sup> ms M/Z = calc 275.1371 for [C<sub>13</sub>H<sub>17</sub>F<sub>3</sub>N<sub>2</sub>O + H]; found 275.1369 [M+H]<sup>+</sup>.

**tert-Butyl ((S)-1-(((S)-4-methyl-1-oxo-1-(4-trifluoromethylphenylamino)pentan-2-yl)amino)-1-oxopropan-2-yl)carbamate (175)**



To a solution of Boc-Ala-OH **174** (1.2 equiv.) in dry DMF, at 0°C and under nitrogen atmosphere, HOBt (1.2 equiv.) and EDCI (1.2 equiv.) were added. After 10 min, DIPEA (4 equiv.) and **173** (1 equiv.) were added, and the reaction mixture was stirred for 12h. Subsequently, solvents were evaporated and the resulting residue was dissolved in EtOAc. The organic phase was washed with a 10% aqueous solution of citric acid (x 2), water, a 10% aqueous solution of K<sub>2</sub>CO<sub>3</sub> (x 2) and brine, dried over Na<sub>2</sub>SO<sub>4</sub>, filtered and concentrated in *vacuo*. The crude residue was purified by column chromatography using cyclohexane/EtOAc (7:3) as eluent mixture, to give compound **175**. Yield: 78%; Consistency: white powder; R<sub>f</sub>: 0.42 (cyclohexane/EtOAc, 7:3); <sup>1</sup>H NMR (300 MHz, CDCl<sub>3</sub>) = δ: 0.92 (d, J = 6.3 Hz, 3H), 0.96 (d, J = 6.3 Hz, 3H), 1.37-1.46 (m, 12H), 1.60-1.72 (m, 2H), 1.81-1.92 (m, 1H), 4.11-4.23 (m, 1H), 4.52-4.64 (m, 1H), 4.99 (d, J = 3.8 Hz, 1H), 6.76 (d, J = 7.8 Hz, 1H), 7.50 (d, J = 8.4 Hz, 2H), 7.71 (d, J = 8.4 Hz, 2H); 9.01 (bs, 1H); <sup>13</sup>C (300 MHz, CDCl<sub>3</sub>): δ = 17.58, 21.67, 22.98, 24.89, 28.21, 40.02, 51.03, 52.66, 81.15, 118.81 (q, J = 32.2 Hz), 119.52, 124.06 (q, J = 272.0 Hz), 125.94, 125.98, 141.13, 156.10, 170.48, 173.29; <sup>19</sup>F NMR (200 MHz, CDCl<sub>3</sub>) = δ: -62.55; M. p. = 167-169°C; ESI<sup>+</sup> ms M/Z = calc 468.2086 for [C<sub>21</sub>H<sub>30</sub>F<sub>3</sub>N<sub>3</sub>O<sub>4</sub> + Na]; found 468.2086 [M+Na]<sup>+</sup>.

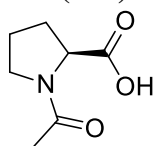
**(S)-1-(((S)-4-Methyl-1-oxo-1-(4-trifluoromethylphenylamino)pentan-2-yl)amino)-1-oxopropan-2-aminium chloride (176)**



A solution of compound **175** (1.0 equiv.) in of 4M HCl/dioxane (22 equiv.) was stirred for 4h at rt. Subsequently, the reaction mixture was concentrated in *vacuo* to obtain the hydrochloride salt of the free amine **176**, which was used without further purification.

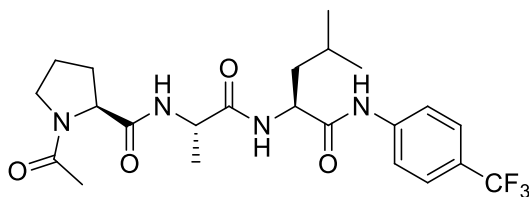
Yield: 99%; Consistency: orange powder;  $R_f$ : 0.05 (cyclohexane/EtOAc 7:3);  $^1\text{H}$  NMR (300 MHz, MeOD) =  $\delta$ : 1.01 (d,  $J$  = 3.6 Hz, 3H), 1.03 (d,  $J$  = 3.6 Hz, 3H), 1.55 (d,  $J$  = 6.8 Hz, 3H), 1.61-1.85 (m, 3H), 3.92-4.28 (m, 1H), 4.52-4.68 (m, 1H), 7.62 (d,  $J$  = 8.5 Hz, 2H), 7.80 (d,  $J$  = 8.5 Hz, 2H);  $^{13}\text{C}$  (300 MHz, MeOD):  $\delta$  = 17.72, 21.91, 23.52, 26.03, 41.94, 50.16, 54.23, 118.53 (q,  $J$  = 32.0 Hz), 120.90, 123.93 (q,  $J$  = 271.7 Hz), 127.02, 127.07, 143.25, 171.14, 173.24;  $^{19}\text{F}$  NMR (200 MHz, MeOD) =  $\delta$ : -63.19; M. p. = 154-156°C; ESI<sup>+</sup> ms M/Z = calc 346.1742 for  $[\text{C}_{16}\text{H}_{22}\text{F}_3\text{N}_3\text{O}_2 + \text{H}]$ ; found 346.1744  $[\text{M}+\text{H}]^+$ .

**(S)-1-acetylpyrrolidine-2-carboxylic acid (179)**



L-proline **177** (1 equiv.) and acetic anhydride **178** (2 equiv.) were suspended in EtOAc and sonicated for 1h at rt. After this time, the solvents were evaporated in *vacuo*, to obtain compound **179**, which was used for next step without further purification. Yield: 86%; Consistency: white powder;  $R_f$  = 0.08 (EtOAc/MeOH, 9:1);  $^1\text{H}$  NMR (300 MHz,  $\text{CDCl}_3$ ) =  $\delta$ : 1.99-2.11 (m, 3H), 2.14 (s, 3H), 2.30-2.38 (m, 1H), 3.44-3.54 (m, 1H), 3.56-3.66 (m, 1H), 4.56 (d,  $J$  = 5.3 Hz, 1H), 10.53 (bs, 1H). Spectroscopic data are in agreement to those reported in literature.<sup>170</sup>

**(S)-1-Acetyl-N-((S)-1-(((S)-4-methyl-1-oxo-1-(4-trifluoromethylphenylamino)pentan-2-yl)amino)-1-oxopropan-2-yl)pyrrolidine-2-carboxamide (180)**



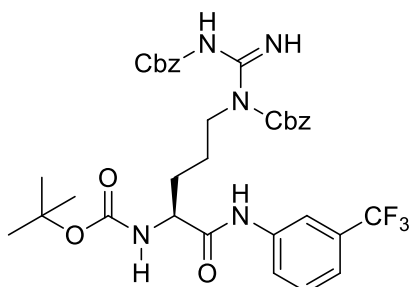
To a solution of **179** (1.2 equiv.) in dry DMF, at 0°C and under nitrogen atmosphere, HOBt (1.2 equiv.) and EDCI (1.2 equiv.) were added. After 10 min, DIPEA (4 equiv.) and **176** (1 equiv.) were added, and the reaction mixture was stirred for 12h. Subsequently, solvents were evaporated and the resulting residue was dissolved in EtOAc. The organic phase was washed with a 10% aqueous solution of citric acid (x 2), water, a 10% aqueous solution of  $\text{K}_2\text{CO}_3$  (x 2) and brine, dried over  $\text{Na}_2\text{SO}_4$ , filtered and concentrated in *vacuo*. The crude residue was purified by column chromatography using cyclohexane/EtOAc (7:3) to give compound **180**. Yield: 60%; Consistency: white powder;  $R_f$ : 0.30 (cyclohexane/EtOAc, 7:3);  $^1\text{H}$  NMR (300 MHz,  $\text{CDCl}_3$ ) =  $\delta$ : 0.92 (d,  $J$  = 6.5 Hz, 3H), 0.97

(d,  $J = 6.5$  Hz, 3H), 1.41 (d,  $J = 7.3$  Hz, 3H), 1.60-1.72 (m, 1H), 1.74-1.91 (m, 2H), 1.97-2.19 (m, 3H), 2.12 (s, 3H), 2.18-2.28 (m, 1H), 3.48-3.60 (m, 1H), 3.63-3.74 (m, 1H), 4.24-4.35 (m, 1H), 4.36-4.43 (m, 1H), 4.48-4.58 (m, 1H), 7.07 (d,  $J = 5.5$  Hz, 1H), 7.46 (d,  $J = 8.1$  Hz, 1H), 7.52 (d,  $J = 8.6$  Hz, 2H), 7.88 (d,  $J = 8.6$  Hz, 2H), 9.04 (s, 1H);  $^{13}\text{C}$  (300 MHz,  $\text{CDCl}_3$ ):  $\delta = 17.22, 21.32, 22.61, 23.06, 25.12, 25.15, 29.03, 39.98, 48.60, 50.65, 52.99, 61.32, 118.73$  (q,  $J = 32.2$  Hz), 119.63, 124.28 (q,  $J = 272.2$  Hz), 125.85, 125.90, 141.57, 171.19, 171.59, 172.51, 172.80;  $^{19}\text{F}$  NMR (200 MHz,  $\text{CDCl}_3$ ) =  $\delta$ : -62.05; M. p. = 204-206°C; ESI<sup>+</sup> ms  $M/Z = \text{calc } 507.2195$  for  $[\text{C}_{23}\text{H}_{31}\text{F}_3\text{N}_4\text{O}_4 + \text{Na}]$ ; found 507.2196  $[\text{M}+\text{Na}]^+$ .

*tert*-Butyl

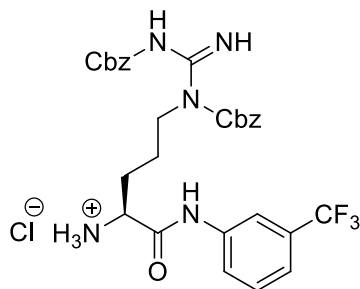
*N*-[(1*S*)-4-

{[(benzyloxy)carbonyl]({[(benzyloxy)carbonyl]amino}methanimidoyl)amino}-1-{[3-(trifluoromethyl)phenyl]carbamoyl}]butyl]carbamate (**183**)



To a solution of 3-(trifluoromethyl)aniline **182** (1 equiv.) and Boc-Arg-(di-Cbz)-OH (1 equiv.) in dry pyridine, phosphoryl chloride (1 equiv.) was added dropwise in a period of 10 min, at 0°C. The reaction mixture was stirred at rt for 2h, and after this time the solution was poured into water and the organic phase was extracted with EtOAc, washed with a saturated aqueous solution of  $\text{NaHCO}_3$ , a 10% aqueous solution of citric acid, brine, and dried over  $\text{Na}_2\text{SO}_4$ . After filtration and evaporation under reduced pressure, the crude residue was purified by silica gel column chromatography, using hexane/EtOAc,(7/3) as eluent mixture, to obtain compound **183**. Yield: 28%; Consistency: white powder;  $R_f = 0.38$  (hexane/EtOAc, 7:3),  $^1\text{H}$  NMR (300 MHz,  $\text{CDCl}_3$ ) =  $\delta$ : 1.45 (s, 9H), 1.66-1.88 (m, 4H), 3.81-3.96 (m, 1H), 4.00-4.13 (m, 1H), 4.33-4.50 (m, 1H), 5.03 (d,  $J = 12.4$  Hz, 1H), 5.16 (d,  $J = 12.4$  Hz, 1H), 5.23 (s, 2H), 5.90 (d,  $J = 8.5$  Hz, 1H), 7.24-7.30 (m, 6H), 7.31-7.38 (m, 7H), 7.71 (s, 1H), 8.84 (bs, 1H), 9.35 (bs, 1H), 9.46 (bs, 1H);  $^{13}\text{C}$  NMR (300 MHz,  $\text{CDCl}_3$ ) =  $\delta$ : 24.88, 28.30, 28.43, 44.09, 54.48, 67.38, 69.21, 80.40, 117.01 (q,  $J = 3.9$  Hz), 120.88 (q,  $J = 3.9$  Hz), 123.24, 123.90 (q,  $J = 272.8$  Hz), 128.05, 128.19, 128.48, 128.59, 128.93, 129.04, 129.32, 130.71 (q,  $J = 32.6$  Hz), 134.54, 136.25, 138.16, 155.82, 156.12, 160.98, 163.53, 171.04.

**(S)-5-(1,3-Bis((benzyloxy)carbonyl)guanidino)-1-oxo-1-((3-(trifluoromethyl)phenyl)amino)pentan-2-aminium chloride (184)**



A solution of compound **183** (1.0 equiv.) in of 4M HCl/dioxane (22 equiv.) was stirred for 4h at rt. Subsequently, the reaction mixture was concentrated in *vacuo* to obtain the hydrochloride salt of the free amine **184**, which was used without further purification. Yield: 97%; Consistency: white powder;  $R_f = 0.04$  (hexane/EtOAc, 7:3),  $^1\text{H NMR}$  (300 MHz, MeOD) =  $\delta$ : 1.75-2.10 (m, 4H), 3.87-4.01 (m, 2H), 4.15 (t,  $J = 6.2$  Hz, 1H), 5.17 (s, 2H), 5.18 (s, 2H), 7.22-7.45 (m, 11H), 7.51 (t,  $J = 7.9$  Hz, 1H), 7.77 (d,  $J = 7.9$  Hz, 1H), 8.11 (s, 1H);  $^{13}\text{C NMR}$  (300 MHz, MeOD) =  $\delta$ : 24.71, 29.07, 46.50, 54.52, 69.16, 70.78, 117.49 (q,  $J = 4.1$  Hz), 122.00 (q,  $J = 4.0$  Hz), 124.21, 125.33 (q,  $J = 271.7$  Hz), 129.41, 129.46, 129.54, 129.67, 129.70, 129.77, 130.87, 132.18 (q,  $J = 32.2$  Hz), 135.83, 137.02, 139.87, 155.46, 155.55, 160.12, 165.00, 168.69.

**tert-Butyl**

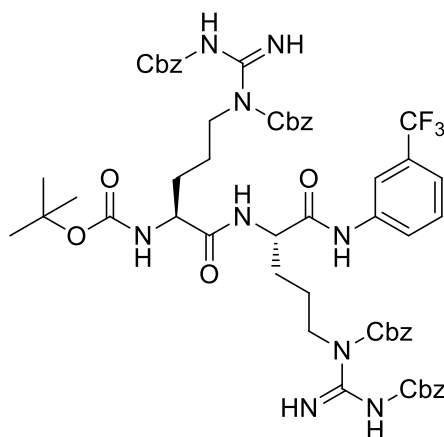
**N-[(1S)-4-**

**{[(benzyloxy)carbonyl]{[(benzyloxy)carbonyl]amino}methanimidoyl]amino}-1-**

**{[(1S)-4-**

**{[(benzyloxy)carbonyl]{[(benzyloxy)carbonyl]amino}methanimidoyl]amino}-1-{[3-**

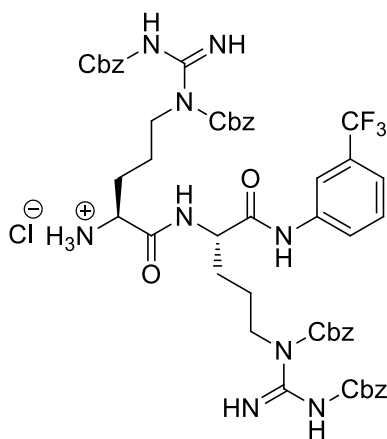
**(trifluoromethyl)phenyl]carbamoyl}butyl]carbamoyl}butyl]carbamate (185)**



To a solution of **181** (1.2 equiv.) in dry DMF, at 0°C and under nitrogen atmosphere, HOBt (1.2 equiv.) and EDCI (1.2 equiv.) were added. After 10 min, DIPEA (4 equiv.) and

**184** (1 equiv.) were added, and the reaction mixture was stirred for 12h. Subsequently, solvents were evaporated and the resulting residue was dissolved in EtOAc. The organic phase was washed with a 10% aqueous solution of citric acid (x 2), water, a 10% aqueous solution of K<sub>2</sub>CO<sub>3</sub> (x 2) and brine, dried over Na<sub>2</sub>SO<sub>4</sub>, filtered and concentrated in *vacuo*. The crude residue was purified by column chromatography using cyclohexane/EtOAc (3:2) as eluent mixture, to give compound **185**. Yield: 60%; Consistency: white powder; *R<sub>f</sub>*: 0.49 (cyclohexane/EtOAc, 3:2); <sup>1</sup>H NMR (300 MHz, CDCl<sub>3</sub>) = δ: 1.38 (s, 9H), 1.51-1.73 (m, 8H), 3.80-3.95 (m, 3H), 3.97-4.10 (m, 2H), 4.37-4.51 (m, 1H), 5.05-5.14 (m, 4H), 5.20 (s, 2H), 5.22 (s, 2H), 5.49 (d, *J* = 5.9 Hz, 1H), 7.14 (d, *J* = 6.7 Hz, 1H), 7.19-7.43, (m, 22H), 7.71 (d, *J* = 6.6 Hz, 1H), 7.82 (s, 1H), 8.89 (s, 1H), 9.18-9.54 (m, 4H); <sup>13</sup>C NMR (300 MHz, CDCl<sub>3</sub>) = δ: 24.93, 25.05, 27.74, 28.06, 28.20, 44.06, 53.63, 54.89, 67.06, 67.13, 68.99, 69.09, 80.45, 116.95 (q, *J* = 3.8 Hz), 120.62 (q, *J* = 3.8 Hz), 123.14, 123.89 (q, *J* = 273.8 Hz), 127.96, 128.03, 128.07, 128.32, 128.33, 128.44, 128.47, 128.83, 128.89, 129.24, 131.00 (q, *J* = 32.3 Hz), 134.47, 134.52, 136.26, 136.61, 138.41, 155.68, 155.75, 156.06, 160.59, 160.82, 163.47, 163.59, 169.82, 172.50.

**(10*S*,13*S*)-6,17-Bis((benzyloxy)carbonyl)-5,18-diimino-3,12,20-trioxo-1,22-diphenyl-10-((3-(trifluoromethyl)phenyl)carbamoyl)-2,21-dioxa-4,6,11,17,19-pentaazadocosan-13-aminium chloride (186)**



A solution of compound **185** (1.0 equiv.) in of 4M HCl/dioxane (22 equiv.) was stirred for 4h at rt. Subsequently, the reaction mixture was concentrated in *vacuo* to obtain the hydrochloride salt of the free amine **186**, which was used without further purification. Yield: 98%; Consistency: white powder; *R<sub>f</sub>* = 0.41 (cyclohexane/EtOAc, 3:2), <sup>1</sup>H NMR (300 MHz, MeOD) = δ: 1.68-1.97 (m, 8H), 3.80-4.03 (m, 5H) 4.39-4.50 (m, 1H), 5.15 (s, 2H), 5.17 (s, 2H), 5.19 (s, 2H), 5.22 (s, 2H), 7.27-7.47 (m, 22H), 7.68 (d, *J* = 8.4 Hz, 1H), 7.97 (s, 1H); <sup>13</sup>C NMR (75 MHz, MeOD) = δ: 23.25, 24.60, 27.82, 28.59, 45.21, 46.11,

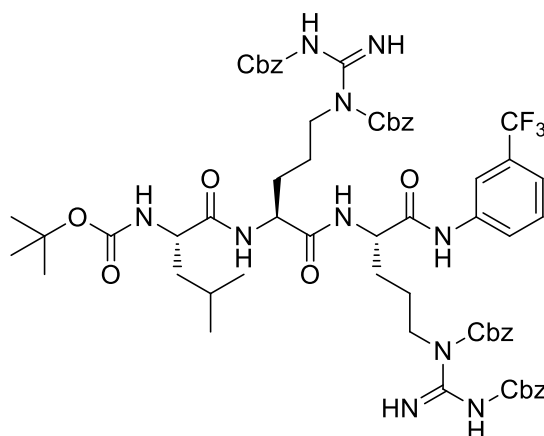
52.11, 54.07, 67.84, 68.16, 69.40, 69.48, 116.01 (q,  $J = 4.0$  Hz), 120.17 (q,  $J = 4.0$  Hz), 122.82, 124.03 (q,  $J = 271.6$  Hz), 127.94, 127.98, 128.06, 128.08, 128.18, 128.20, 128.25, 128.31, 128.33, 128.35, 128.43, 128.46, 129.41, 130.67 (q,  $J = 32.1$  Hz), 134.45, 134.50, 135.41, 135.68, 138.96, 154.01, 154.02, 158.24, 158.34, 158.66, 158.79, 168.75, 170.63.

*tert*-Butyl

*N*-[(1*S*)-1-[(1*S*)-4-

{[(benzyloxy)carbonyl]({[(benzyloxy)carbonyl]amino}methanimidoyl)amino]-1-  
 {(1*S*)-4-

{[(benzyloxy)carbonyl]({[(benzyloxy)carbonyl]amino}methanimidoyl)amino]-1-  
 {3-(trifluoromethyl)phenyl}carbamoyl}butyl]carbamoyl}-3-  
 methylbutyl]carbamate (**187**)



To a solution of **167** (1.2 equiv.) in dry DMF, at 0°C and under nitrogen atmosphere, HOBt (1.2 equiv.) and EDCI (1.2 equiv.) were added. After 10 min, DIPEA (4 equiv.) and **186** (1 equiv.) were added, and the reaction mixture was stirred for 12h. Subsequently, solvents were evaporated and the resulting residue was dissolved in EtOAc. The organic phase was washed with a 10% aqueous solution of citric acid (x 2), water, a 10% aqueous solution of K<sub>2</sub>CO<sub>3</sub> (x 2) and brine, dried over Na<sub>2</sub>SO<sub>4</sub>, filtered and concentrated in *vacuo*. The crude residue was purified by column chromatography using cyclohexane/EtOAc (7:3) as eluent mixture, to give compound **185**. Yield: 39%; Consistency: pale orange powder;  $R_f$ : 0.40 (cyclohexane/EtOAc, 7:3); <sup>1</sup>H NMR (300 MHz, CDCl<sub>3</sub>) =  $\delta$ : 0.87 (d,  $J = 5.8$  Hz, 3H), 0.91 (d,  $J = 5.8$  Hz, 3H), 1.38 (s, 9H), 1.48-1.92 (m, 11H), 3.80-4.02 (m, 4H), 4.19-4.29 (m, 1H), 4.43-4.55 (m, 1H), 4.72-4.82 (m, 1H), 5.00-5.18 (m, 4H), 5.24 (s, 4H), 7.10 (d,  $J = 4.6$  Hz, 1H), 7.19-7.43 (m, 24H), 7.91 (d,  $J = 6.2$  Hz, 1H), 8.03 (s, 1H), 8.88 (s, 1H), 9.32 (bs, 2H), 9.45 (bs, 2H); <sup>13</sup>C NMR (75 MHz, CDCl<sub>3</sub>) =  $\delta$ : 21.04, 21.69, 22.71, 24.69, 25.01, 25.42, 27.86, 28.17, 40.59, 44.05, 44.18, 53.87, 54.12, 54.24, 67.03, 67.06, 69.04, 69.09, 80.85, 116.95 (q,  $J = 3.9$  Hz), 120.37 (q,  $J = 4.0$  Hz), 123.12, 124.03 (q,  $J =$



272.3 Hz), 127.87, 127.95, 128.02, 128.17, 128.30, 128.33, 128.39, 128.59, 128.77, 128.80, 128.86, 128.90, 129.13, 130.94 (q,  $J = 32.2$  Hz), 134.54, 134.59, 136.60, 136.65, 138.92, 155.68, 155.87, 156.19, 160.72, 160.75, 163.59, 163.71, 170.02, 171.52, 174.01.

## 8. REFERENCES

1. Keating, J.; Yukich, J. O.; Sutherland, C. S.; Woods, G.; Tediosi, F. Human African trypanosomiasis prevention, treatment and control costs: a systematic review. *Acta Trop.* **2015**, *150*, 4-13.
2. Cox, F. E. History of sleeping sickness (African trypanosomiasis). *Infect Dis. Clin. N. Am.* **2004**, *18*, 231-245.
3. Kennedy, P. G. Human African trypanosomiasis of the CNS: current issues and challenges. *J. Clin. Invest.* **2004**, *113*, 496-504.
4. Kennedy, P. G. Clinical features, diagnosis, and treatment of human African trypanosomiasis (sleeping sickness). *Lancet Neurol.* **2013**, *12*, 186-194.
5. Barry, J. D.; McCulloch, R. Antigenic variation in trypanosomes: enhanced phenotypic variation in a eukaryotic parasite. *Adv. Parasitol.* **2001**, *49*, 1-70.
6. Bacchi, C. J. Chemotherapy of human African trypanosomiasis. *Interdiscip. Perspect. Infect. Dis.* **2009**, *ID 195040*, 5 pages
7. a) Mackey, Z. B.; O'Brien, T. C.; Greenbaum, D. C.; Blank, R. B.; McKerrow, J. H. A cathepsin B-like protease is required for host protein degradation in *Trypanosoma brucei*. *J. Biol. Chem.* **2004**, *279*, 48426–48433. b) Abdulla, M. H.; O'Brien, T.; Mackey, Z. B.; Sajid, M.; Grab, D. J.; McKerrow, J. H. RNA interference of *Trypanosoma brucei* cathepsin B and L affects disease progression in a mouse model. *PLoS Neglected Trop. Dis.* **2008**, *2*, e298. c) Steverding, D.; Sexton, D. W.; Wang, X.; Gehrke, S. S.; Wagner, G. K.; Caffrey, C. R. *Trypanosoma brucei*: chemical evidence that cathepsin L is essential for survival and a relevant drug target. *Int. J. Parasitol.* **2012**, *42*, 481–488.
8. a) Ettari, R.; Tamborini, L.; Angelo, I.C.; Micale, N.; Pinto, A.; De Micheli, C.; Conti, P. Inhibition of Rhodesain as a Novel Therapeutic Modality for Human African Trypanosomiasis, *J. Med. Chem.* **2013**, *56*, 5637-5658; b) Ettari, R.; Previti, S.; Tamborini, L.; Cullia, G.; Grasso, S.; Zappalà, M. The inhibition of cysteine proteases rhodesain and TbCatB: a valuable approach to treat human African trypanosomiasis. *Mini Rev. Med. Chem.* **2016**, *16*, 1374-1391.
9. Lonsdale-Eccles, J. D.; Grab, D. J. Trypanosome hydrolases and the blood–brain barrier. *Trends Parasitol.* **2002**, *18*, 17–19.
10. Overath, P.; Chaudhri, M.; Steverding, D.; Ziegelbauer, K. Invariant surface proteins in bloodstream forms of *Trypanosoma brucei*. *Parasitol. Today* **1994**, *10*, 53-58.

11. Santos, C. C.; Coombs, G. H.; Lima, A. P. C.; Mottram, J. C. Role of the *Trypanosoma brucei* natural cysteine peptidase inhibitor ICP in differentiation and virulence. *Mol. Microbiol.* **2007**, *66*, 991-1002.
12. Lecaille, F.; Kaleta, J.; Brömme, D. Human and parasitic papain-like cysteine proteases: their role in physiology and pathology and recent developments in inhibitor design. *Chem. Rev.* **2002**, *102*, 4459-4488.
13. Ettari, R.; Pinto, A.; Previti, S.; Tamborini, L.; Angelo, I. C.; La Pietra, V.; Marinelli, L.; Novellino, E.; Schirmeister, T.; Zappalà, M.; Grasso, S.; De Micheli, C.; Conti, P. Development of Novel Dipeptide-like Rhodesain Inhibitors Containing the 3-Bromoisoxazoline Warhead in a Constrained Conformation. *Bioorg. Med. Chem.* **2015**, *21*, 7053-7060.
14. Conti, P.; Pinto, A.; Wong, P. E.; Major, L. L.; Tamborini, L.; Iannuzzi, M. C.; De Micheli, C.; Barrett, M. P.; Smith, T. K. Synthesis and in vitro/in vivo Evaluation of the Antitrypanosomal Activity of 3-Bromoacivicin, a Potent CTP Synthetase Inhibitor. *ChemMedChem* **2011**, *6*, 329-333.
15. Yang, P.-Y.; Wang, M.; Li, L.; Wu, H.; He, C. Y.; Yao, S. Q. Design, synthesis and biological evaluation of potent azadipeptide nitrile inhibitors and activity-based probes as promising anti-*Trypanosoma brucei* agents. *Chem. Eur. J.* **2012**, *18*, 6528-6541.
16. Dziadulewicz, E. K.; Brown, M. C.; Dunstan, A. R.; Lee, W.; Said, N. B.; Garratt, P. J. The design of non-peptide human bradykinin B<sub>2</sub> receptor antagonists employing the benzodiazepine peptidomimetic scaffold. *Bioorg. Med. Chem. Lett.* 1999, *9*, 463-468;  
b) Lauffer, D. J.; Mullican, M. D. A practical synthesis of (S) 3-tert-Butoxycarbonylamino-2-oxo-2, 3, 4, 5-tetrahydro-1, 5-benzodiazepine-1-acetic acid methyl ester as a conformationally restricted dipeptido-Mimetic for caspase-1 (ICE) inhibitors. *Bioorg. Med. Chem. Lett.* **2002**, *12*, 1225-1227.
17. Bova, F.; Ettari, R.; Micale, N.; Carnovale, C.; Schirmeister, T.; Gelhaus, C.; Leippe, M.; Grasso, S.; Zappalà, M. Constrained peptidomimetics as antiplasmodial falcipain-2 inhibitors. *Bioor. Med. Chem.* **2010**, *18*, 4928-4938.
18. Ettari, R.; Previti, S.; Cosconati, S.; Kesselring, J.; Schirmeister, T.; Grasso, S.; Zappalà, M. Synthesis and biological evaluation of novel peptidomimetics as rhodesain inhibitors. *J. Enzyme Inhib. Med. Chem.* **2016**, *31*, 1184-1191.

19. Ettari, R.; Previti, S.; Cosconati, S.; Maiorana, S.; Schirmeister, T.; Grasso, S.; Zappalà, M. Development of novel 1, 4-benzodiazepine-based Michael acceptors as antitrypanosomal agents. *Bioorg. Med. Chem. Lett.* **2016**, *26*, 3453-3456.
20. Previti, S.; Ettari, R.; Cosconati, S.; Amendola, G.; Chouchene, K.; Wagner, A.; Hellmich, U. A.; Ulrich, K.; Krauth-Siegel, R. L.; Wich, P. R.; Schmid, I.; Schirmeister, T.; Gut, J.; Rosenthal, P. J.; Grasso, S.; Zappalà M. Development of Novel Peptide-based Michael Acceptors Targeting Rhodesain and Falcipain-2 for the Treatment of Neglected Tropical Diseases (NTDs), *J. Med. Chem.* **2017**, *60*, 6911–6923
21. Kerr, I. D.; Lee, J. H.; Farady, C. J.; Marion, R.; Rickert, M.; Sajid, M.; Pandey, K. C.; Caffrey, C. R.; Legac, J.; Hansell, E.; McKerrow, J. H.; Craik, C. S.; Rosenthal, P. J.; Brinen, L. S. Vinyl sulfones as antiparasitic agents and a structural basis for drug design. *J. Biol. Chem.* **2009**, *284*, 25697–25703.
22. Kerr, I. D.; Wu, P.; Marion-Tsukamaki, R.; Mackey, Z. B.; Brinen, L. S. Crystal structures of TbCatB and rhodesain, potential chemotherapeutic targets and major cysteine proteases of *Trypanosoma brucei*. *PLoS Neglected Trop. Dis.* **2010**, *4*, e701.
23. Mott, B. T.; Ferreira, R. S.; Simeonov, A.; Jadhav, A.; Ang, K. K.- H.; Leister, W.; Shen, M.; Silveira, J. T.; Doyle, P. S.; Arkin, M. R.; McKerrow, J. H.; Inglese, J.; Austin, C. P.; Thomas, C. J.; Shoichet, B. K.; Maloney, D. J. Identification and optimization of inhibitors of trypanosomal cysteine proteases: cruzain, rhodesain, and TbCatB. *J. Med. Chem.* **2010**, *53*, 52–60.
24. [http://www.who.int/trypanosomiasis\\_african/country/en/](http://www.who.int/trypanosomiasis_african/country/en/)
25. Matthews, K. R. The developmental cell biology of *Trypanosoma brucei*. *J. Cell Sci.* **2005**, *118*, 283-290.
26. Langousis, G.; Hill, K. L. Motility and more: the flagellum of *Trypanosoma brucei*. *Nat. Rev. Microbiol.* **2014**, *12*, 505-518.
27. Acosta-Serrano, A.; Vassella, E.; Liniger, M.; Renggli, C. K.; Brun, R.; Roditi, I.; Englund, P. T. The surface coat of procyclic *Trypanosoma brucei*: programmed expression and proteolytic cleavage of procyclin in the tsetse fly. *Proc. Natl. Acad. Sci. U. S. A.* **2001**, *98*, 1513-1518.
28. Vaughan, S.; Keith, G. Basal body structure and cell cycle-dependent biogenesis in *Trypanosoma brucei*. *Cilia* **2016**, *5*:5

29. Gluenz, E.; Povelones, M. L.; Englund, P. T.; Gull, K. The kinetoplast duplication cycle in *Trypanosoma brucei* is orchestrated by cytoskeleton-mediated cell morphogenesis. *Mol. Cell. Biol.* **2011**, *31*, 1012-1021.
30. Büscher, P.; Cecchi, G.; Jamonneau, V.; Priotto, G. Human African trypanosomiasis. *The Lancet.* **2017**, DOI:10.1016/S0140-6736(17)31510-6
31. Kennedy, P. G. Diagnostic and neuropathogenesis issues in human African trypanosomiasis. *Int. J. Parasitol.* **2006**, *36*, 505-512.
32. Brun, R.; Blum, J.; Chappuis, F.; Burri, C. Human african trypanosomiasis. *The Lancet* **2010**, *375*, 148-159.
33. Truc, P.; Lejon, V.; Magnus, E.; Jamonneau, V.; Nangouma, A.; Verloo, D.; Penchenier, L.; Büscher, P. Evaluation of the micro-CATT, CATT/ *Trypanosoma brucei gambiense*, and LATEX/T *b gambiense* methods for serodiagnosis and surveillance of human African trypanosomiasis in west and central Africa. *Bull. World Health Organ.* **2002**, *80*, 882–886.
34. Mugasa, C. M.; Adams, E. R.; Boer, K. R.; Dyserinck, H. C.; Büscher, P.; Schallig, H. D.; Leeflang, M. M. Diagnostic accuracy of molecular amplification tests for human African trypanosomiasis—systematic review. *PLoS Neglected Trop. Dis.* **2012**, *6*, e1438.
35. MacLean, L. M.; Odiit, M.; Chisi, J. E.; Kennedy, P. G.; Sternberg, J. M. Focus-specific clinical profiles in human African trypanosomiasis caused by *Trypanosoma brucei rhodesiense*. *PLoS Neglected Trop. Dis.* **2010**, *4*, e906.
36. Kennedy, P. G. Diagnosing central nervous system trypanosomiasis: two stage or not to stage? *Trans. R. Soc. Trop. Med. Hyg.* **2008**, *102*, 306-307.
37. a) Lejon, V.; Reiber, H.; Legros, D.; Djé, N.; Magnus, E.; Wouters. I.; Sindic, C. J. M.; Büscher, P. Intrathecal immune response pattern for improved diagnosis of central nervous system involvement in trypanosomiasis. *J. Infect. Dis.* **2003**, *187*, 1475–1483.  
 b) Lejon, V.; Legros, D.; Richer, M.; Ruiz, J. A.; Jamonneau, V.; Truc, P.; Doua, F.; Djè, N.; N’Siesi, F. X.; Bisser, S.; Magnus, E.; Wouters, I.; Konings, J.; Vervoot, T.; Sultan, F.; Büscher, P. IgM quantification in the cerebrospinal fluid of sleeping sickness patients by a latex card agglutination test. *Trop Med Int Health* **2002**, *7*, 685–692.
38. Grab, D. J.; Nikolskaia, O. V.; Inoue, N.; Thekisoe, O. M.; Morrison, L. J.; Gibson, W.; Dumler, J. S. Using detergent to enhance detection sensitivity of African

- trypanosomes in human CSF and blood by loop-mediated isothermal amplification (LAMP). *PLoS Neglected Trop. Dis.* **2011**, *5*, e1249.
39. Deborggraeve, S.; Büscher, P. Molecular diagnostics for sleeping sickness: what is the benefit for the patient? *Lancet Infect. Dis.* **2010**, *10*, 433–439.
40. Fairlamb, A. H.; Henderson, G. B.; Cerami, A. Trypanothione is the primary target for arsenical drugs against African trypanosomes. *Proc. Natl. Acad. Sci. USA* **1989**, *86*, 2607–2511.
41. Delespaux, V.; de Koning, H. P. Drugs and drug resistance in African trypanosomiasis. *Drug Resist. Updates* **2007**, *10*, 30–50
42. Burri, C.; Brun, R. Eflornithine for the treatment of human African trypanosomiasis. *Parasitol. Res.* **2003**, *90*, 49–52.
43. Vincent, I. M.; Creek, D.; Watson, D. G.; Kamleh, M. A.; Woods, D. J.; Wong, P. E.; Burchmore, R. J. S.; Barrett, M. P. A molecular mechanism for eflornithine resistance in African trypanosomes. *PLoS Pathog.* **2010**, *6*, e1001204.
44. Simarro, P. P.; Franco, J.; Diarra, A.; Postigo, J. A.; Jannin, J. Update on field use of the available drugs for the chemotherapy of human African trypanosomiasis. *Parasitology* **2012**, *139*, 842–46.
45. Coura, J. R.; de Castro, S. L. A critical review of Chagas disease chemotherapy. *Mem. Inst. Oswaldo Cruz* **2002**, *97*, 3–24.
46. Priotto, G.; Kasparian, S.; Mutombo, W.; Ngouama, D.; Ghorashian, S.; Arnold, U.; Ghabri, S.; Baudin, E.; Buard, V.; Kazadi-Kyanza, S.; Ilunga, M.; Mutangala, W.; Pohlig, G.; Schmid, C.; Karunakara, U.; Torreele, E.; Kande, V. Nifurtimox–eflornithine combination therapy for second-stage African *Trypanosoma brucei gambiense* trypanosomiasis: a multicentre, randomised, phase III, non-inferiority trial. *Lancet* **2009**, *374*, 56–64.
47. Mdachi, R. E.; Thuita, J. K.; Kagira, J. M.; Ngotho, J. M.; Murilla, G. A.; Ndung’u, J. M.; Tidwell, R. R.; Hall, J. E.; Brun, R. Efficacy of the novel diamidine compound 2,5-bis(4-amidinophenyl)-furan-bis-O-methylamidoxime (pafuramidine, DB289) against *Trypanosoma brucei rhodesiense* infection in vervet monkeys after oral administration. *Antimicrob. Agents Chemother.* **2009**, *53*, 953–957.
48. Chen, D.; Marsh, R.; Aberg, J. A. Pafuramidine for *Pneumocystis jiroveci* pneumonia in HIV-infected individuals. *Expert Rev. Anti-Infect. Ther.* **2007**, *5*, 921–928.

49. Jacobs, R. T.; Nare, B.; Wring, S. A.; Orr, M. D.; Chen, D.; Sligar, J. M.; Jenks, M. X.; Noel, R. A.; Bowling, T. S.; Mercer, L. T.; Rewerts, C.; Gaukel, E.; Owens, J.; Parham, R.; Randolph, R.; Beaudet, B.; Bacchi, C. J.; Yarlett, N.; Plattner, J. J.; Freund, Y.; Ding, C.; Akama, T.; Zhang, Y.-K.; Brun, R.; Kaiser, M.; Scandale, I.; Don, R. SCYX-7158, an orally-active benzoxaborole for the treatment of stage 2 human African trypanosomiasis. *PLoS Neglected Trop. Dis.* **2011**, *5*, e1151.
50. Wring, S.; Gaukel, E.; Nare, B.; Jacobs, R.; Beaudet, B.; Bowling, T.; Mercer, L.; Bacchi, C.; Yarlett, N.; Randolph, R.; Parham, R.; Rewerts, C.; Plattner, J.; Don, R. Pharmacokinetics and pharmacodynamics utilizing unbound target tissue exposure as part of a disposition-based rationale for lead optimization of benzoxaboroles in the treatment of Stage 2 Human African Trypanosomiasis. *Parasitology*, **2014**, *141*, 104-118.
51. Torreele, E.; Bourdin Trunz, B.; Tweats, D.; Kaiser, M.; Brun, R.; Mazué, G.; Bray, M. A.; Pécou, B. Fexinidazole - a new oral nitroimidazole drug candidate entering clinical development for the treatment of sleeping sickness. *PLoS Neglected Trop. Dis.* **2010**, *4*, e923.
52. <https://www.dndi.org/diseases-projects/portfolio/fexinidazole/>
53. <https://www.dndi.org/diseases-projects/hat/hat-target-product-profile/>
54. Agbo, E. C.; Majiwa, P. A.; Büscher, P.; Claassen, E.; te Pas, M. F. W. Trypanosoma brucei genomics and the challenge of identifying drug and vaccine targets. *Trends Microbiol.* **2003**, *11*, 322-329.
55. Sajid, M.; McKerrow, J. H. Cysteine proteases of parasitic organisms. *Mol. Biochem. Parasitol.* **2002**, *120*, 1-21.
56. Scory, S.; Caffrey, C. R.; Stierhof, Y. D.; Ruppel, A.; Steverding, D. Trypanosoma brucei: Killing of Bloodstream Forms in Vitro and in Vivo by the Cysteine Proteinase Inhibitor Z-Phe-Ala-CHN<sub>2</sub>. *Exp. Parasitol.* **1999**, *91*, 327-333.
57. Troeberg, L.; Morty, R. E.; Pike, R. N.; Lonsdale-Eccles, J. D.; Palmer, J. T.; McKerrow, J. H.; Coetzer, T. H. Cysteine Proteinase Inhibitors Kill Cultured Bloodstream Forms of Trypanosoma brucei brucei. *Exp. Parasitol.* **1999**, *91*, 349-355.
58. Turk, B. Targeting proteases: successes, failures and future prospects. *Nat. Rev. Drug Discovery* **2006**, *5*, 785-799.
59. Grab, D. J.; Garcia-Garcia, J. C.; Nikolskaia, O. V.; Kim, Y. V.; Brown, A.; Pardo, C. A.; Zhang, Y.; Becker, K. G.; Wilson, B. A.; de A. Lima, A.; Scharfstein, J.; Dumler, J.

- S. Protease activated receptor signaling is required for African trypanosome traversal of human brain microvascular endothelial cells. *PLoS Neglected Trop. Dis.* **2009**, *3*, e479.
60. Nikolskaia, O. V.; Lima, A. P. C. de A.; Kim, Y. V.; Lonsdale-Eccles, J. D.; Fukuma, T.; Scharfstein, J.; Grab, D. J. Blood–brain barrier traversal by African trypanosomes requires calcium signalling induced by parasite cysteine protease. *J. Clin. Invest.* **2006**, *116*, 2739–2747
61. Ferguson, M. A. The structure, biosynthesis and functions of glycosylphosphatidylinositol anchors, and the contributions of trypanosome research. *J. Cell Sci.* **1999**, *112*, 2799-2809.
62. McCulloch, R.; Rudenko, G.; Borst, P. Gene conversions mediating antigenic variation in *Trypanosoma brucei* can occur in variant surface glycoprotein expression sites lacking 70-base-pair repeat sequences. *Mol. Cell. Biol.* **1997**, *17*, 833-843.
63. Wheeler, R. J. The trypanolytic factor–mechanism, impacts and applications. *Trends Parasitol.* **2010**, *26*, 457-464.
64. Lalmanach, G.; Boulangé, A.; Serveau, C.; Lecaille, F.; Scharfstein, J.; Gauthier, F.; Authié, E. Congopain from *Trypanosoma congolense*: drug target and vaccine candidate. *Biol. Chem.* **2002**, *383*, 739–749.
65. Matsumoto, K.; Mizoue, K.; Kitamura, K.; Tse, W. C.; Huber, C. P.; Ishida, T. Structural basis of inhibition of cysteine proteases by E-64 and its derivatives. *Pept. Sci.* **1999**, *51*, 99-107.
66. Fosgerau, K.; Hoffmann, T. Peptide therapeutics: current status and future directions. *Drug discovery today* **2015**, *20*, 122-128.
67. Palmer, J. T.; Rasnick, D.; Klaus, J. L.; Bromme, D. Vinyl sulfones as mechanism-based cysteine protease inhibitors. *J. Med. Chem.* **1995**, *38*, 3193-3196.
68. Caffrey, C. R.; Hansell, E.; Lucas, K. D.; Brinen, L. S.; Hernandez, A. A.; Cheng, J.; Gwaltney II, S. L.; Roush, W. R.; Stierhof, Y.-D.; Bogyo, M.; Steverding, D.; McKerrow, J. H.; Steverding, D. Active site mapping, biochemical properties and subcellular localization of rhodesain, the major cysteine protease of *Trypanosoma brucei rhodesiense*. *Mol. Biochem. Parasitol.* **2001**, *118*, 61-73.
69. a) Choe, Y.; Leonetti, F.; Greenbaum, D. C.; Lecaille, F.; Bogyo, M.; Bromme, D.; Ellman, J. A.; Craik, C. S. Substrate Profiling of Cysteine Proteases Using a Combinatorial Peptide Library Identifies Functionally Unique Specificities. *J. Biol.*



- Chem.* **2006**, *281*, 12824-12832. b) O'Brien, T.C.; Mackey, Z.B.; Fetter, R.D.; Choe, Y.; O'Donoghue, A. J.; Zhou, M.; Craik, C. S.; Caffrey, C. R.; McKerrow, J. H. A Parasite Cysteine Protease Is Key to Host Protein Degradation and Iron Acquisition. *J. Biol. Chem.* **2008**, *283*, 28934-28943.
70. Jacobsen, W.; Christians, U.; Benet. L. Z. In vitro evaluation of the disposition of a novel cysteine protease inhibitor. *Drug Metab. Dispos.* **2000**, *28*, 1343-1351.
71. Falgueyret, J. P.; Desmarais, S.; Oballa, R.; Black, W. C.; Cromlish, W.; Lamontagne, S.; Masse, F.; Riendeau, D.; Toulmond, S.; Percival, M. D. Lysosomotropism of basic cathepsin K inhibitors contributes to increased cellular potencies against off target cathepsins and reduced functional selectivity. *J. Med. Chem.* **2005**, *48*, 7535-7543.
72. Dunny, E.; Doherty, W.; Evans, P.; Malthouse, J. P. G.; Nolan, D.; Knox, A. J. S. Vinyl Sulfone-Based Peptidomimetics as Anti-Trypanosomal Agents: Design, Synthesis, Biological and Computational Evaluation. *J. Med. Chem.* **2013**, *56*, 6638-6650.
73. Loser, R.; Frizler, M.; Schilling, K.; Gutschow, M. Azadipeptide Nitriles-Highly Potent and Proteolytically Stable Inhibitors of Papain-Like Cysteine Proteases. *Angew. Chem. Intl. Ed.* **2008**, *47*, 4331-4334.
74. Vicik, R.; Hoerr, V.; Glaser, M.; Schultheis, M.; Hansell, E.; McKerrow, J. H.; Holzgrave, U.; Caffrey, C. R.; Ponte-Sucre, A.; Moll, H.; Stich, A.; Schirmeister, T. Aziridine-2,3-dicarboxylate inhibitors targeting the major cysteine protease of *Trypanosoma brucei* as lead trypanocidal agents. *Biorg. Med. Chem. Lett.* **2006**, *16*, 2753-2757.
75. Buchold, C.; Hemberg, Y.; Heindl, C.; Weker, A.; Degel, B.; Pfeuffer, T.; Staib, P.; Schneider, S.; Rosenthal, P. J.; Gut, J.; Morschhauser, J.; Bringmann, G.; Schirmeister, T. New cis-Configured Aziridine-2-carboxylates as Aspartic Acid Protease Inhibitors. *Chem. Med. Chem.* **2011**, *6*, 141-152.
76. Nkemngu, N. J.; Grande, R.; Hansell, E.; McKerrow, H.; Caffrey, C.R.; Steverding, D. Improved trypanocidal activities of cathepsin L inhibitors. *Intl. J. Antimicrob. Agents* **2003**, *22*, 155-159.
77. a) Merchjohann, K.; Sporer, F.; Steverding, D.; Wink, M. In vitro effect of alkaloids on bloodstream forms of *Trypanosoma brucei* and *T. congolense*. *Planta Med.* **2001**, *67*, 623-627; b) Caffrey, C. R.; Schanz, M.; Nkemngu-Njinkeng, J. Brush, M.; Hansell, E.; Cohen, F. E.; Flaherty, T. M.; McKerrow, J. H.; Steverding, D. Screening of acyl

- hydrazide proteinase inhibitors for antiparasitic activity against *Trypanosoma brucei*. *Intl. J. Antimicrob. Agents* **2002**, *19*, 227-231.
78. Hruby, V. J. Prospects for peptidomimetic drug design. *Drug Discovery Today* **1997**, *2*, 165-167.
79. a) Estiarte, M.; Rich, D. H. Peptidomimetics for drug design. *Burger's Medicinal Chemistry and Drug Discovery* **2003**, *1*, 633-685 b) Ahn, J. M.; Boyle, N. A.; MacDonald, M. T.; Janda, K. D. Peptidomimetics and peptide backbone modifications. *Mini Rev. Med. Chem.* **2002**, *2*, 463-473.
80. a) Micale, N.; Kozikowski, A. P.; Ettari, R.; Grasso, S.; Zappalà, M.; Jeong, J.-J.; Kumar, A.; Hanspal, M.; Chishti, A. H. Novel Peptidomimetic Cysteine Protease Inhibitors as Potential Antimalarial Agents. *J. Med. Chem.* **2006**, *49*, 3064-3067; b) Ettari, R.; Zappalà, M.; Micale, N.; Schirmeister, T.; Gelhaus, C.; Leippe, M.; Evers, A.; Grasso, S. Synthesis of Novel Peptidomimetics as Inhibitors of Protozoan Cysteine Proteases Falcipain-2 and Rhodesain. *Eur. J. Med. Chem.* **2010**, *45*, 3228-3233.
81. Ettari, R.; Tamborini, L.; Angelo, I. C.; Grasso, S.; Schirmeister, T.; Lo Presti, L.; De Micheli, C.; Pinto, A.; Conti, P. Development of Rhodesain Inhibitors with a 3-Bromoisoxazoline Warhead. *ChemMedChem* **2013**, *8*, 2070-2076.
82. Pinto, A.; Tamborini, L.; Cullia, G.; Conti, P.; De Micheli, C. Inspired by Nature: The 3-Halo-4, 5-dihydroisoxazole Moiety as a Novel Molecular Warhead for the Design of Covalent Inhibitors. *ChemMedChem* **2016**, *11*, 10-14.
83. Ettari, R.; Pinto, A.; Tamborini, L.; Angelo, I. C.; Grasso, S.; Zappalà, M.; Capodicasa, N.; Yzeiraj, L.; Gruber, E.; Aminake, M. N.; Pradel, G.; Schirmeister, T.; De Micheli, C.; Conti, P. Synthesis and Biological Evaluation of Papain-family Cathepsin L-like Cysteine Protease Inhibitors Containing a 1,4-Benzodiazepine Scaffold as Antiprotozoal Agents. *ChemMedChem* **2014**, *9*, 1817-1825..
84. Inglese, J.; Auld, D. S.; Jadhav, A.; Johnson, R. L.; Simeonov, A.; Yasgar, A.; Zheng, W.; Austin, C. P. Quantitative high-throughput screening: a titration based approach that efficiently identifies biological activities in large chemical libraries. *Proc. Natl. Acad. Sci. U.S.A.* **2006**, *11*, 473-11478
85. Ehmke, V.; Heindl, C.; Rottmann, M.; Freymond, C.; Schweizer, W. B.; Brun, R.; Stich, A.; Schirmeister, T.; Diederich, F. Potent and selective inhibition of cysteine proteases from *Plasmodium falciparum* and *Trypanosoma brucei*. *ChemMedChem* **2011**, *6*, 273-278.

86. Ehmke V.; Winkler E.; Banner D. W.; Haap W.; Schweizer W. B.; Rottmann M.; Kaiser M.; Freymond C.; Schirmeister T.; Diederich F. Optimization of triazine nitriles as rhodesain inhibitors: structure-activity relationship, bioisosteric imidazopyridine nitriles, and X-ray crystal structure analysis with human cathepsin L. *ChemMedChem* **2013**, *8*, 967 – 975.
87. Mallari J. P.; Shelat A. A.; Obrien T.; Caffrey C. R. Kosinky A.; Connelly M.; Harbut M.; Greenbaum D.; McKerrow J. H.; Guy R. K.; Development of potent purine-derived nitrile inhibitors of the trypanosomal protease TbCatB. *J. Med. Chem.* **2008**, *51*, 545 – 552.
88. Mallari J. P.; Shelat A. A.; Kosinski A.; Caffrey C. R.; Connelly M.; Zhu F.; McKerrow J. H.; Guy R. K.; Structure-guided development of selective TbCatB inhibitors. *J. Med. Chem.* **2009**, *52*, 6489 – 6493.
89. Klayman, D. L.; Bartosevich, J. F.; Griffin, T. S.; Mason, C. J.; Scovill, J. P. 2-Acetylpyridine thiosemicarbazones. 1. A new class of potential antimalarial agents. *J. Med. Chem.* **1979**, *22*, 855–862.
90. Wilson, H. R.; Revankar, G. R.; Tolman, R. L. In vitro and in vivo activity of certain thiosemicarbazones against *Trypanosoma cruzi*. *J. Med. Chem.* **1974**, *17*, 760–761.
91. Du, X.; Guo, C.; Hansell, E.; Doyle, P. S.; Caffrey, C. R.; Holler, T. P.; McKerrow, J. H.; Cohen, F. E. Synthesis and structure–activity relationship study of potent trypanocidal thiosemicarbazone inhibitors of the trypanosomal cysteine protease cruzain. *J. Med. Chem.* **2002**, *45*, 2695–2707.
92. Greenbaum, D. C.; Mackey, Z.; Hansell, E.; Doyle, P.; Gut, J.; Caffrey, C. R.; Lehrman, J.; Rosenthal, P. J.; McKerrow, J. H.; Chibale, K. Synthesis and structure–activity relationships of parasiticidal thiosemicarbazone cysteine protease inhibitors against *Plasmodium falciparum*, *Trypanosoma brucei*, and *Trypanosoma cruzi*. *J. Med. Chem.* **2004**, *47*, 3212–3219.
93. Fujii, N.; Mallari, J. P.; Hansell, E. J.; Mackey, Z.; Doyle, P.; Zhou, Y. M.; Gut, J.; Rosenthal, P. J.; McKerrow, J. H.; Guy, R. K. Discovery of potent thiosemicarbazone inhibitors of rhodesain and cruzain. *Bioorg. Med. Chem. Lett.* **2005**, *15*, 121–123.
94. Mallari, J. P.; Shelat, A.; Kosinski, A.; Caffrey, C. R.; Connelly, M.; Zhu, F.; McKerrow, J. H.; Guy, R. K. Discovery of trypanocidal thiosemicarbazone inhibitors of rhodesain and TbCatB. *Bioorg. Med. Chem. Lett.* **2008**, *18*, 2883–2885.

95. a) Tempone, A. G.; Treiger Borborema, S. E.; de Andrade, H. F.; de Amorim Gualda, N. C.; Yogi, Á. A.; Salerno Carvalho, C.; Bachiega, D.; Lupo, F. N.; Bonotto, S. V.; Fischer, D. C. H. Antiprotozoal activity of Brazilian plant extracts from isoquinoline alkaloid-producing families. *Phytomedicine* **2005**, *12*, 382–390; b) Ma, Z.-Z.; Xu, W.; Jensen, N. H.; Roth, B. L.; Liu-Che, L.-Y.; Lee, D. Y. W. Isoquinoline alkaloids isolated from *Corydalis yanhusuo* and their binding affinities at the dopamine D1 receptor. *Molecules* **2008**, *13*, 2303–2312 c) Batra, S.; Sabnis, Y. A.; Rosenthal, P. J.; Avery, M. A. Structure based approach to falcipain-2 inhibitors: synthesis and biological evaluation of 1,6,7-trisubstituted dihydroisoquinolines and isoquinolines. *Bioorg. Med. Chem.* **2003**, *11*, 2293–2299.
96. Micale, N.; Ettari, R.; Schirmeister, T.; Evers, A.; Gelhaus, C.; Leippe, M.; Zappalà, M.; Grasso, S. Novel 2H-isoquinolin-3-ones as antiplasmodial falcipain-2 inhibitors. *Bioorg. Med. Chem.* **2009**, *17*, 6505–6511
97. Langolf, S.; Machon, U.; Ehlers, M.; Sicking, W.; Schirmeister, T.; Büchhold, C.; Gelhaus, C.; Rosenthal, P. J.; Schmuck, C. Development of antitrypanosomal and antiplasmodial nonpeptidic cysteine protease inhibitors based on N-protected-guanidino-furan and -pyrrole building blocks. *ChemMedChem* **2011**, *6*, 1581–1586
98. Bock, M. G.; DiPardo, R. M.; Evans, B. E.; Rittle, K. E.; Veber, D. F.; Freidinger, R. M.; Hirshfield, J.; Springer, J. P. Synthesis and resolution of 3-amino-1, 3-dihydro-5-phenyl-2H-1, 4-benzodiazepin-2-ones. *J. Org. Chem.* **1987**, *52*, 3232-3239.
99. Ettari, R.; Nizi, E.; Di Francesco, M. E.; Dude, M. A.; Pradel, G.; Vicik, R.; Schirmeister, T.; Micale, N.; Grasso, S.; Zappalà, M. Development of Peptidomimetics with a Vinyl Sulfone Warhead as Irreversible Falcipain-2 Inhibitors. *J. Med. Chem.* **2008**, *51*, 988-996.
100. Wang, S. X.; Pandey, K. C.; Scharfstein, J.; Whisstock, J.; Huang, R. K.; Jacobelli, J.; Fletterick, R. J.; Rosenthal, P. J.; Abrahamson, M.; Brinen, L. S.; Rossi, A.; Sali, A.; McKerrow, J. H. The Structure of Chagasin in Complex with a Cysteine Protease Clarifies the Binding Mode and Evolution of an Inhibitor Family. *Structure* **2007**, *15*, 535-543.
101. Sennyey, G. E.; Barcelo, G.; Senet, J. P. Diallyl dicarbonate. A convenient reagent for the synthesis of allyl carbamates. *Tetrahedron letters* **1987**, *28*, 5809-5810.
102. Deng, L.; Hang, J.; Tang, L. Patent US **2002**/0151744.

103. Fernández-Llamazares, A. I.; Spengler, J.; Albericio, F. The potential of N-alkoxymethyl groups as peptide backbone protectants. *Tetrahedron Letters* **2014**, *55*, 184-188.
104. Conti, P.; De Amici, M.; Pinto, A.; Tamborini, L.; Grazioso, G.; Frølund, B.; Nielsen, B.; Thomsen C.; Ebert, B.; De Micheli, C. Synthesis of 3-Hydroxy-and 3-Carboxy- $\Delta^2$ -isoxazoline Amino Acids and Evaluation of Their Interaction with GABA Receptors and Transporters. *Eur. J. Org. Chem.* **2006**, *24*, 5533-5542.
105. Zheng, Y.; Xu, J. Synthesis of enantiopure free and N-benzyloxycarbonyl-protected 3-substituted homotaurines from naturally occurring amino acids. *Tetrahedron* **2014**, *70*, 5197-5206.
106. Isidro-Llobet, A.; Guasch-Camell, J.; Álvarez, M.; Albericio, F. p-Nitrobenzyloxycarbonyl (pNZ) as a Temporary N $\alpha$ -Protecting Group in Orthogonal Solid-Phase Peptide Synthesis Avoiding Diketopiperazine and Aspartimide Formation. *Eur. J. Org. Chem.* **2005**, *14*, 3031-3039.
107. Lim-Wilby, M.; Semple, J. E.; Araldi, G. L.; Goldman, E. A.; Weinhouse, M. I. Compounds, Compositions and Methods for Treatment of Parasitic Infections. Patent WO 02/48097 PCT/US01/48032, June 20, **2002**
108. Roush, W. R.; Gwaltney II, S. L.; Cheng, J.; Scheidt, K. A.; McKerrow, J. H.; Hansell, E. Vinyl Sulfonate Esters and Vinyl Sulfonamides: Potent, Irreversible Inhibitors of Cysteine Proteases. *J. Am. Chem. Soc.* **1998**, *120*, 10994-10995
109. Tsai, J. H.; Takaoka, L. R.; Powell, N. A.; S. Nowick, J. S. Synthesis of amino acid ester isocyanates: methyl (s)-2-isocyanato-3-phenylpropanoate. *Org. Synth.* **2002**, *78*, 220.
110. Schirmeister, T.; Kesselring, J.; Jung, S.; Schneider, T. H.; Weickert, A.; Becker, J.; Lee, W.; Bamberger, D.; Wich, P. R.; Distler, U.; Tenzer, S.; Johé, P.; Hellmich, U. A.; Engels, B. Quantum Chemical-Based Protocol for the Rational Design of Covalent Inhibitors. *J. Am. Chem. Soc.* **2016**, *138*, 8332–8335
111. Spyropoulos, C.; Kokotos, C. G. One-pot synthesis of ureas from Boc-protected amines. *J. Org. Chem.* **2014**, *79*, 4477-4483.
112. Fennell, B. D.; Warren, J. M.; Chung, K. K.; Main, H. L.; Arend, A. B.; Tochowicz, A.; Götz, M. G. Optimization of peptidyl allyl sulfones as clan CA cysteine protease inhibitors. *J. Enzyme Inhib. Med. Chem.* **2013**, *28*, 468-478.

113. Tomita, K.; Oishi, S.; Ohno, H.; Fujii, N. Structure-activity relationship study and NMR analysis of fluorobenzoyl pentapeptide GPR54 agonists. *Pept. Sci.* **2008**, *90*, 503-511.
114. Draper R. W.; Hou, D.; Iyer, R.; Lee, G. M.; Liang, J. T.; Mas, J. L.; Vater, E. J. Novel Stereoselective Syntheses of the Fused Benzazepine Dopamine D1Antagonist (6aS,13bR)-11-Chloro-6,6a,7,8,9,13b-hexahydro-7-methyl-5H-benzo[d]naphth[2,1-b]azepin-12-ol (Sch 39166): 2 L-Homophenylalanine-Based Syntheses. *Org. Proc. Res. Dev.* **1998**, *2*, 186–193
115. Chen, S. J.; Lu, G. P.; Cai, C. Synthesis of Quinolines from Allylic Alcohols via Iridium-Catalyzed Tandem Isomerization/Cyclization Combined with Potassium Hydroxide. *Synthesis* **2015**, *47*, 976-984.
116. Shi, Z.; Tong, Q.; Leong, W. W. Y.; Zhong, G. [4+ 2] Annulation of Vinyl Ketones Initiated by a Phosphine-Catalyzed Aza-Rauhut–Currier Reaction: A Practical Access to Densely Functionalized Tetrahydropyridines. *Chem. - Eur. J.* **2012**, *18*, 9802-9806.
117. Bugarin, A.; Jones, K. D.; Connell, B. T. Efficient, direct  $\alpha$ -methylenation of carbonyls mediated by diisopropylammonium trifluoroacetate. *Chem. Comm.* **2010**, *46*, 1715-1717.
118. Schwertz, G., Witschel, M. C., Rottmann, M., Bonnert, R., Leartsakulpanich, U., Chitnumsub, P.; Jaruwat, A.; Ittarat, W.; Schäfer, A.; Aponte, R. A.; Charman, S. A.; Karen L. White, K. L.; Kundu, A.; Sadhukhan, S.; Lloyd, M.; Freiberg, G. M.; Srikumaran, M.; Siggel, M.; Zwysig, A.; Chaiyen, P.; Diederich Antimalarial Inhibitors Targeting Serine Hydroxymethyltransferase (SHMT) with In Vivo Efficacy and Analysis of their Binding Mode Based on X-ray Cocrystal Structures. *J. Med. Chem.* **2017**, *60*, 4840–4860
119. Lafrance, D.; Bowles, P.; Leeman, K.; Rafka, R. Mild Decarboxylative Activation of Malonic Acid Derivatives by 1, 1'-Carbonyldiimidazole. *Org. Lett.* **2011**, *13*, 2322-2325.
120. Pace, V.; Castoldi, L.; Alcántara, A. R.; Holzer, W. Highly efficient and environmentally benign preparation of Weinreb amides in the biphasic system 2-MeTHF/water. *RSC Adv.* **2013**, *3*, 10158-10162.
121. Hammen, P. D.; Braisted, A. C.; Northrup, D. L. Synthesis of vinyl and  $\beta$ -phthalimido ketones. *Synth. Commun.* **1991**, *21*, 2157-2163.

122. Schiaffo, C. E.; Rottman, M.; Wittlin, S.; Dussault, P. H. 3-Alkoxy-1, 2-dioxolanes: synthesis and evaluation as potential antimalarial agents. *ACS Med. Chem. Lett.* **2011**, *2*, 316-319.
123. Rickerby, J.; Vallet, M.; Bernardinelli, G.; Viton, F.; Kündig, E. P. Ruthenium–Lewis Acid Catalyzed Asymmetric Diels–Alder Reactions between Dienes and  $\alpha$ ,  $\beta$ -Unsaturated Ketones. *Chem. – Eur. J.* **2007**, *13*, 3354-3368.
124. Ogasawara, M.; Ge, Y.; Uetake, K.; Takahashi, T. Vinyl Ketones to Allenes: Preparation of 1, 3-Dien-2-yl Triflates and Their Application in Pd-Catalyzed Reactions with Soft Nucleophiles. *Org. Lett.* **2005**, *7*, 5697-5700.
125. Satoh, T.; Kumagawa, T.; Sugimoto, A.; Yamakawa, K.  $\alpha$ ,  $\beta$ -Epoxy Sulfoxides as Useful Intermediates in Organic Synthesis. IX. A Novel Synthesis of Alkyl Vinyl Ketones and Divinyl Ketones from Carbonyl Compounds and 1-Chloro-3-phenylthiopropyl Phenyl Sulfoxide as a Three-Carbon Homologating. *Agent. Bull. Chem. Soc. Jpn.* **1987**, *60*, 301-310.
126. Latorre, A.; Schirmeister, T.; Kesselring, J.; Jung, S.; Johé, P.; Hellmich, U. A.; Heilos, A.; Engels, B.; Krauth-Siegel, R. L.; Dirdjaja, N.; Bou-Iserte, L.; Rodríguez, S.; González, F.V. Dipeptidyl Nitroalkenes as Potent Reversible Inhibitors of Cysteine Proteases Rhodesain and Cruzain, *ACS Med. Chem. Lett.* **2016**, *7*, 1073–1076.
127. GraFit, Version 5.0.1.3; Erithacus Software Ltd.: London, **2006**.
128. Cheng Y.; Prusoff, W. H. Relationship between the inhibition constant ( $K_i$ ) and the concentration of inhibitor which causes 50 per cent inhibition ( $I_{50}$ ) of an enzymatic reaction. *Biochem. Pharmacol.* **1973**, *22*, 3099–3108.
129. Ludewig, S.; Kossner, M.; Schiller, M.; Baumann, K.; Schirmeister, T. Enzyme kinetics and hit validation in fluorimetric protease assays. *Curr. Top. Med. Chem.* **2010**, *10*, 368-382.
130. Tian, W. X.; Tsou, C. L. Determination of the Rate Constant of Enzyme Modification by Measuring the Substrate Reaction in the Presence of the Modifier. *Biochemistry* **1982**, *21*, 1028–1032.
131. Crouch, S. P.; Kozlowski, R.; Slater, K. J.; Fletcher, J. The Use of ATP Bioluminescence as a Measure of Cell Proliferation and Cytotoxicity. *J. Immunol. Methods* **1993**, *160*, 81-88.

132. Schirmeister, T.; Schmitz, J.; Jung, S.; Schmenger, T.; Krauth-Siegel, R. L.; Gütschow, M. Evaluation of Dipeptide Nitriles as Inhibitors of Rhodesain, a Major Cysteine Protease of *Trypanosoma brucei*. *Bioorg. Med. Chem. Lett.* **2016**, *27*, 45-50.
133. Cunningham, M. P.; Vickerman, K. Antigenic Analysis in the *Trypanosoma brucei* Group, Using the Agglutination Reaction. *Trans. R. Soc. Trop. Med. Hyg.* **1962**, *56*, 48-59.
134. Beig, M.; Oellien, F.; Garoff, L.; Noack, S.; Krauth-Siegel, R. L.; Selzer, P. M. Trypanothione Reductase: A Target Protein for a Combined In Vitro and In Silico Screening Approach. *PLoS Neglected Trop. Dis.* **2015**, *9*, e0003773.
135. Shenai, B. R.; Sijwali, P. S.; Singh, A.; Rosenthal, P. J. Characterization of Native and Recombinant Falcipain-2, a Principal Trophozoite Cysteine Protease and Essential Hemoglobinase of *Plasmodium falciparum*. *J. Biol. Chem.* **2000**, *275*, 29000-29010.
136. Rosenthal, P. J.; Olson, J. E.; Lee, G. K.; Palmer, J. T.; Klaus, J. L.; Rasnick, D. Antimalarial Effects of Vinyl Sulfone Cysteine Proteinase Inhibitors. *Antimicrob. Agents Chemother.* **1996**, *40*, 1600-1603.
137. Coterón, J. M.; Catterick, D.; Castro, J.; Chaparro, M. J.; Díaz, B.; Fernández, E.; Ferrer, S.; Gamo, F. J.; Gordo, M.; Gut, J.; de las Heras, L.; Legac, J.; Marco, M.; Miguel, J.; Muñoz, V.; Porras, E.; de la Rosa, J. C.; Ruiz, J. R.; Sandoval, E.; Ventosa, P.; Rosenthal, P. J.; Fiandor, J. M. Falcipain Inhibitors: Optimization Studies of the 2-Pyrimidinecarbonitrile Lead Series. *J. Med. Chem.* **2010**, *53*, 6129–6152.
138. Ahmed, S. A.; Gogal, R. M.; Walsh, J. E. A new rapid and simple non-radioactive assay to monitor and determine the proliferation of lymphocytes: an alternative to [3H] thymidine incorporation assay. *J. Immunol. Methods* **1994**, *170*, 211-224.
139. Morris, G. M.; Huey, R.; Lindstrom, W.; Sanner, M. F.; Belew, R. K.; Goodsell, D. S.; Olson, A. J. Autodock4 and AutoDockTools4: Automated Docking with Selective Receptor Flexibility. *J. Comput. Chem.* **2009**, *16*, 2785-2791.
140. Cosconati, S.; Forli, S.; Perryman, A. L.; Harris, R.; Goodsell, D. S.; Olson, A. J. Virtual Screening with AutoDock: Theory and Practice. *Expert Opin. Drug Discovery* **2010**, *5*, 597-607.
141. Bianco, G.; Forli, S.; Goodsell, D. S.; Olson, A. J. Covalent Docking Using Autodock: Two-Point Attractor and Flexible Side Chain Methods. *Protein Sci.* **2016**, *25*, 295-301.
142. Schrödinger Release 2016-3: Maestro, Schrödinger, LLC, New York, NY, **2016**.



143. <http://autodock.scripps.edu/>. (January 13, **2016**).
144. <http://ambermd.org/>. (June 03, **2014**).
145. Wang, J.; Wolf, R. M.; Caldwell, J. W.; Kollman, P. A.; Case, D. A. Development and Testing of a General Amber Force Field. *J. Comp. Chem.* **2004**, *25*, 1157–1173.
146. Jorgensen, W. L.; Chandrasekhar, J.; Madura, J. D.; Impey, R. W.; Klein, M. L. Comparison of Simple Potential Functions for Simulating Liquid Water. *J. Chem. Phys.* **1983**, *79*, 926-935.
147. Darden, T.; York, D.; Pedersen, L. Particle Mesh Ewald: An N·log(N) Method for Ewald Sums in Large Systems. *J. Chem. Phys.* **1993**, *98*, 10089-10092.
148. Ryckaert, J. P.; Ciccotti, G.; Berendsen, H. J. C. Numerical Integration of the Cartesian Equations of Motion of a System with Constraints: Molecular Dynamics of n-Alkanes. *J. Comp. Phys.* **1977**, *23*, 327–341.
149. Roe, D. R.; Cheatham, T. E. PTRAJ and CPPTRAJ: Software for Processing and Analysis of Molecular Dynamics Trajectory Data. *J. Chem. Theory Comput.* **2013**, *9*, 3084-3095.
150. <http://www.rbvi.ucsf.edu/chimera/>. (September 13, **2016**).
151. Ettari, R.; Previti, S.; Bitto, A.; Grasso, S.; Zappalà, M. Immunoproteasome-selective inhibitors: a promising strategy to treat hematologic malignancies, autoimmune and inflammatory diseases. *Curr. Med. Chem* **2016**, *23*, 1217-1238.
152. Micale, N.; Scarbaci, K.; Troiano, V.; Ettari, R.; Grasso, S.; Zappalà, M. Peptide-based proteasome inhibitors in anticancer drug design. *Med. Res. Rev.* **2014**, *34*, 1001-1069.
153. a) DeMartino, G. N.; Gillette, T. G. Proteasomes: machines for all reasons. *Cell* **2007**, *129*, 659–662; b) Weissman, A. M.; Shabek, N.; Ciechanover, A. The predator becomes the prey: regulating the ubiquitin system by ubiquitylation and degradation. *Nat. Rev. Mol. Cell Biol.* **2011**, *12*, 605–620.
154. Ciechanover, A.; Schwartz, A. L. The ubiquitin system: pathogenesis of human diseases and drug targeting. *Biochim Biophys Acta* **2004**, *1695*, 3-17
155. Kisselev, A. F.; van der Linden, W. A.; Overkleeft, H. S. Proteasome inhibitors: an expanding army attacking a unique target. *Chem. Biol.* **2012**, *19*, 99–115.
156. Groll, M.; Ditzel, L.; Lowe, J.; Bochtler, M.; Bartunik, H. D.; Huber, R. Structure of 20S proteasome from yeast at 2.4 Å resolution. *Nature* **1997**, *386*, 463–471.

157. a) Kisselev, A. F.; Callard, A.; Goldberg, A. L. Importance of different active sites in protein breakdown by 26S proteasomes and the efficacy of proteasome inhibitors varies with the protein substrate. *J Biol Chem* **2006**, *281*, 8583–8590; b) Oberdorf, J.; Carlson, E.J.; Skach, W.R. Redundancy of mammalian proteasome beta subunit function during endoplasmic reticulum associated degradation. *Biochemistry* **2001**, *40*, 13397–13405; c) Mirabella, A. C.; Pletnev, A. A.; Downey, S. L.; Florea, B. I.; Shabaneh, T. B.; Britton, M.; Verdoes, M.; Filippov, D. V.; Overkleeft, H. S.; Kisselev, A. F. Specific cell-permeable inhibitor of proteasome trypsin-like sites selectively sensitizes myeloma cells to bortezomib and carfilzomib. *Chem. Biol.* **2011**, *18*, 608–618.
158. Parlati F.; Lee, S. J.; Aujay, M.; Suzuk, E.; Levitsky, K.; Lorens J. B.; Micklem, D. R.; Ruurs, P.; Sylvain, C.; Lu, Y.; Shenk, K. D.; Bennett, M. K. Carfilzomib can induce tumour cell death through selective inhibition of the chymotrypsin-like activity of the proteasome. *Blood* **2009**, *114*, 3439–3447.
159. Huber, E. M.; Basler, M.; Schwab, R.; Heinemeyer, W.; Kirk, C. J.; Groettrup, M.; Groll, M. Immuno- and constitutive proteasome crystal structures reveal differences in substrate and inhibitor specificity. *Cell* **2012**, *148*, 727-738.
160. Ferrington, D. A.; Gregerson, D. S. Immunoproteasome: structure, function, and antigen presentation. *Prog. Mol. Biol. Transl. Sci.* **2012**, *109*, 75-112.
161. a) Groettrup, M.; Kraft, R.; Kostka, S.; Standera, S.; Stohwasser, R.; Kloetzel, P. M. A third interferon-gamma-induced subunit exchange in the 20S proteasome. *Eur. J. Immunol.* **1996**, *26*, 863-869; b) Hayashi, M.; Ishibashi, T.; Tanaka, K.; Kasahara, M.. The mouse genes encoding the third pair of beta-type proteasome subunits regulated reciprocally by IFN-gamma: structural comparison, chromosomal localization, and analysis of the promoter. *J. Immunol.* **1997**, *159*, 2760–2770; c) Nandi, D.; Jiang, H.; Monaco, J. J. Identification of MECL-1 (LMP-10) as the third IFN-gamma inducible proteasome subunit. *J. Immunol.* **1996**, *156*, 2361–2364.
162. Basler, M.; Lauer, C.; Moebius, J.; Weber, R.; Przybylski, M.; Kisselev, A. F.; Tsu, C.; Groettrup, M. Why the structure but not the activity of the immunoproteasome subunit low molecular mass polypeptide 2 rescues antigen presentation. *J. Immunol.* **2012**, *189*, 1868-1877.
163. Gaczynska, M.; Rock, K. L.; Goldberg, A. L.  $\gamma$ -Interferon and expression of MHC genes regulate peptide hydrolysis by proteasomes. *Nature* **1993**, *365*, 264-267

164. a) Kessler, B. M.; Tortorella, D.; Altun, M.; Kisselev, A. F.; Fiebiger, E.; Hekking, B. G.; Ploegh, H. L.; Overkleeft, H. S. Extended peptide-based inhibitors efficiently target the proteasome and reveal overlapping specificities of the catalytic  $\beta$ -subunits. *Chem. Biol.* **2001**, *8*, 913–929; b) Kisselev, A. F.; Goldberg, A. L. Monitoring activity and inhibition of 26S proteasomes with fluorogenic peptide substrates. *Methods Enzymol.* **2005**, *398*, 364–378; c) Wakata, A.; Lee, H. M.; Rommel, P.; Toutchkine, A.; Schmidt, M.; Lawrence, D. S. Simultaneous fluorescent monitoring of proteasomal subunit catalysis. *J. Am. Chem. Soc.* **2010**, *132*, 1578–1582.
165. Kisselev, A. F.; Akopian, T. N.; Castillo, V.; Goldberg, A. L. Proteasome active sites allosterically regulate each other, suggesting a cyclical bite-chew mechanism for protein breakdown. *Mol. Cell* **1999**, *4*, 395–402.
166. Śledź, P.; Förster, F.; Baumeister, W. Allosteric effects in the regulation of 26S proteasome activities. *J. Mol. Biol.* **2013**, *425*, 1415–1423.
167. Keita, M.; Kaffy, J.; Troufflard, C.; Morvan, E.; Crousse, B.; Ongeri, S.  $^{19}\text{F}$  NMR monitoring of the eukaryotic 20S proteasome chymotrypsin-like activity: an investigative tool for studying allosteric regulation. *Org. Biomol. Chem.* **2014**, *12*, 4576–4581.
168. a) Dalvit, C. Ligand- and substrate-based  $^{19}\text{F}$  NMR screening: principles and applications to drug discovery. *Prog. Nucl. Magn. Reson. Spectrosc.* **2007**, *51*, 243–271; b) Dalvit, C.; Ardini, E.; Fogliatto, G. P.; Mongelli, N.; Veronesi, M. Reliable high-throughput functional screening with 3-FABS. *Drug discovery today* **2004**, *9*, 595–602; c) Chen, H.; Viel, S.; Ziarelli, F.; Peng, L.  $^{19}\text{F}$  NMR: a valuable tool for studying biological events. *Chem. Soc. Rev.* **2013**, *42*, 7971–7982.
169. Dalvit, C.; Ardini, E.; Flocco, M.; Fogliatto, G. P.; Mongelli, N.; Veronesi, M. A general NMR method for rapid, efficient, and reliable biochemical screening. *J. Am. Chem. Soc.* **2003**, *125*, 14620–14625.
170. Challis, B. C.; Milligan, J. R.; Mitchell, R. C. Synthesis and characterisation of some new N-nitrosodipeptides. *J. Chem. Soc. Perkin Transactions 1* **1990**, *11*, 3103–3108.